

**Methane and nutrient dynamics in a tidal flat
area of the Southern North Sea:
Time-series and budgets**

Dynamik von Methan und Nährstoffen im
Wattenmeer der Südlichen Nordsee:
Zeitreihen und Budgets

An der
Fakultät für Mathematik und Naturwissenschaften
der Carl von Ossietzky Universität Oldenburg
angenommene

Dissertation zur Erlangung des Grades
Doktor der Naturwissenschaften
(Dr. rer. nat.)

von

Maik Grunwald
geboren am 02.06.1972 in Cloppenburg

Erstreferent: Prof. Dr. H.-J. Brumsack

Koreferent: Prof. Dr. J. Rullkötter

Eingereicht am: 03.06.2009

Disputation am: 08.07.2009

Abstract

To investigate the dynamics of biogeochemical processes in temperate tidal flat ecosystems a time-series station was established in the tidal inlet between the islands of Spiekeroog and Langeoog (NW Germany). Realisation of this station was carried out within the scope of the DFG Research Group "Biogeochemistry of tidal flats" which was established in 2001 at the "Institute for Chemistry and Biology of the Marine Environment" in Oldenburg. Among others, one major goal of this Research Group was to investigate exchange processes of dissolved and particulate matter between the tidal flat area and the open North Sea.

The time-series station provides the opportunity to determine continuously physical, chemical, and metrological parameters in a high resolution throughout the year, even during storms and ice winters. Inside the pole of the station, sensor tubes are installed at different water depth in direction of the prevailing tidal currents. The tubes are equipped with sensors to determine temperature, conductivity, and pressure. Furthermore, the uppermost sensor tube allows retrieval of surface water for nutrient analysis. In order to study the dynamics of nutrients (silica, phosphate, nitrite, and nitrate) and methane, a setup for continuous determination of these metabolites of organic matter degradation has been established. Nutrients were determined hourly from April 2006 by autonomous nutrient analysers, whereas methane was measured during several months in 2005 by a sensor mounted outside the pole.

In addition to measurements at the station, methane was detected during several sampling campaigns in the German Bight, the River Weser, in pore waters of tidal flat sediments, tidal creeks, and in the freshwater contributed to the study area via a flood-gate in Neuharlingersiel. The resulting spatial distribution of methane demonstrated a clear trend of decreasing concentrations with increasing distance from the coast, which points towards a source for dissolved methane in the coastal areas. This assumption was supported by high resolution measurements of methane at the time-series station revealing distinctly higher concentrations during low tide. Pore water concentrations down to 4.5 m depth emphasised deep sediments to be the loci for enhanced methane production. Mathematical modelling showed that pore waters of deeper sediment layers are transported advectively to the tidal flat margin and finally into the open water column of the back barrier area. Two further model approaches, which estimated export budgets from the study area into the open North Sea, resulted in a net export of dissolved methane in an order of magnitude between the Wash estuary and River Elbe. Therefore, it can be concluded from this study, that methane

contributed by tidal flat areas has to be considered in budget calculations for the southern North Sea.

Concentrations of the nutrients silica, phosphate, and nitrite plus nitrate (NO_x) determined at the time-series station revealed different seasonal patterns as well as alternating tidal dependencies. Silica concentrations were highest during winter months with a pattern seemingly influenced by zooplankton grazing pressure leading to a more plateau-shaped or peak-shaped development, respectively. High winter levels decrease drastically in spring due to elevated diatom growth. However, the onset of the diatom blooms varied between the years as indicated by the silica development. Low concentrations during summer increase again towards autumn and winter due to both decreasing assimilation by diatoms and pore water contribution. In contrast, phosphate concentrations are highest in late summer, which is governed by both phytoplankton assimilation/degradation and coupling of phosphate to the iron-oxyhydroxide cycle in sediments. On the other hand, NO_x follows a general seasonal pattern with highest concentrations in winter and lowest during the vegetation period. On a tidal scale, the nutrient patterns of the open water column are predominantly controlled by pore water contributions as organic particulate matter is imported into the Wadden Sea and is remineralised especially in the sediments.

It could have been shown, that decomposition of phytoplankton affects the dynamics of redox-sensitive trace metals. In addition to elevated release of nutrients to the open water column, breakdowns of algae blooms favour aggregation due to intense release of transparent exopolymer particles (TEP) thus leading to formation of large organic-rich aggregates. Deposition of such aggregates enhances microbial activity within the surface sediments and the release of dissolved organic carbon, nutrients and trace metals like Mn, Mo, or V.

The investigation of pore waters, enriched in silica and phosphate, reveal a diffusive as well as advective transport to the open water column, which leads to a seasonal and tidal periodicity in the study area. In contrast, the freshwater contribution via the flood-gate is identified to be of minor importance in terms of nutrient budgets of the back barrier area and the German Bight. This study highlights the role of tidal flat sediments concerning nutrient contribution to the German Bight. It could have been demonstrated, that the entire tidal flat areas of the German Bight Wadden Sea contribute dissolved silica and phosphate in the same order of magnitude as the sum of Rivers Elbe, Weser, and Ems, while NO_x is exported in one order of magnitude lower. Thus, tidal flat areas act as a 'bio-reactor' and contribute largely to the nutrient budget of the German Bight ecosystem, as organic particulate matter is degraded and subsequently exported as dissolved nutrients to the open North Sea.

Kurzfassung

Um die Dynamik biogeochemischer Prozesse in Wattgebieten gemäßigter Zonen zu untersuchen, wurde eine Messstation im Seegatt zwischen den Inseln Spiekeroog und Langeoog (NW Deutschland) errichtet. Diese Station wurde im Rahmen der im Jahr 2001 am „Institut für Chemie und Biologie des Meeres“ in Oldenburg gegründeten DFG-Forschergruppe „Biogeochemie des Watts“ realisiert. Eine Hauptzielsetzung dieser Forschergruppe war, Austauschprozesse gelöster und partikulärer Stoffe zwischen dem Watt und der offenen Nordsee zu untersuchen.

Die Messstation bieten die Möglichkeit, kontinuierlich physikalische, chemische und meteorologische Daten in einer hohen zeitlichen Auflösung über das ganze Jahr, auch bei Stürmen oder Eisgang, zu erheben. Im Pfahlrohr der Station sind Querrohre in verschiedenen Wassertiefen in vorherrschender Strömungsrichtung der Tide installiert. Diese Querrohre sind mit Sensoren ausgestattet, die Temperatur, Leitfähigkeit und Druck messen. Zusätzlich befindet sich am obersten dieser Querrohre eine Wasserentnahmestelle zur Nährstoffanalyse. Um die Dynamik von Nährstoffen (Kieselsäure, Phosphat, Nitrit, Nitrat) und Methan zu untersuchen, wurde ein Messsystem entwickelt, das diese Metaboliten, die beim Abbau organischen Materials freigesetzt werden, kontinuierlich erfasst. Seit April 2006 werden Nährstoffe durch automatisierte Analysatoren im stündlichen Intervall gemessen. Methanmessungen erfolgten während mehrerer Monate im Jahr 2005 durch einen Sensor, der außerhalb des Pfahlrohres angebracht war.

Neben Messungen an der Station wurde Methan während verschiedener Schiffseinsätze in der Deutschen Bucht und der Weser, sowie im Porenwasser von Wattsedimenten, in Tiderinnen und im Süßwasser, das über das Siel in Neuharlingersiel in das Untersuchungsgebiet gelangt, untersucht. Die sich daraus ergebende räumliche Verteilung von in Wasser gelöstem Methan zeigte eine deutliche Tendenz abnehmender Konzentrationen in Richtung offene Nordsee, was auf eine Methanquelle in den Küstengebieten hinweist. Diese Annahme wurde durch zeitlich hoch aufgelöste Methanmessungen an der Messstation unterstützt, die merklich höhere Konzentrationen während der Niedrigwasserphase aufwiesen. Porenwasserkonzentrationen, die bis zu einer Sedimenttiefe von 4,5 m gemessen wurden, brachten hervor, dass tiefere Sedimentregionen Orte erhöhter Methanproduktion sind. Eine mathematische Modellierung zeigte, dass Porenwässer dieser tieferen Sedimente advektiv zu den Platenrändern der Wattsedimente und schließlich in die Wassersäule der Rückseitenwatten transportiert werden. Zwei weitere Modellansätze, die den Methanexport des Untersuchungsgebietes in die offene Nordsee abschätzten, ergaben einen Nettoexport von

Methan, der in der Größenordnung zwischen dem Wash-Ästuar und der Elbe liegt. Es kann daher aus diesen Untersuchungen geschlussfolgert werden, dass der Methaneintrag aus den Rückseitenwatten in die Nordsee bei Budgetberechnungen berücksichtigt werden muss.

Die auf der Messstation gemessenen Nährstoffe Kieselsäure, Phosphat und Nitrit + Nitrat (NO_x) wiesen sowohl Unterschiede im saisonalen wie auch im tidalen Konzentrationsverlauf auf. Kieselsäure zeigte die höchsten Konzentrationen während der Wintermonate. Die Form des Konzentrationsverlaufes im Winter schien durch den von Zooplankton ausgeübten Fraßdruck beeinflusst zu sein, was sich in einer eher abgeflachten oder eher spitz verlaufenden Verlaufsform widerspiegelte. Diese hohen Winterwerte nahmen im Frühjahr, bedingt durch die Diatomeenblüte, stark ab. Dabei variierte jedoch der Beginn der Frühjahrsblüte zwischen den Jahren, was durch die unterschiedlichen Verläufe der Kieselsäurekonzentration angezeigt wurde. Niedrige Sommerkonzentrationen stiegen zum Herbst und Winter wieder an, was durch Eintrag von Porenwasser in die Wassersäule und verringerte Kieselsäureaufnahme durch Diatomeen bedingt war. Phosphat wies demgegenüber die höchsten Konzentrationen im Sommer auf, was durch eine Kombination aus sowohl der Aufnahme durch Phytoplankton sowie deren Abbau, als auch der Kopplung von Phosphat an den Eisen-Oxidhydroxid-Kreislauf, beruhte. Im Gegensatz dazu wiesen die Konzentrationen von NO_x einen generellen saisonalen Verlauf mit Maxima im Winter und Minima während der Wachstumsperioden auf. Betrachtet man die Konzentrationsverläufe in der Wassersäule des Rückseitenwatts auf einer tidalen Zeitskala, zeigt sich, dass die Nährstoffkonzentrationen durch den Porenwassereintrag kontrolliert werden, da partikuläres organisches Material aus der Nordsee in das Rückseitenwatt importiert und dort in den Sedimenten remineralisiert wird.

Es konnte weiterhin gezeigt werden, dass der Abbauprozess von Phytoplankton die Dynamik von redox-sensiblen Spurenmetallen beeinflusst. Zusätzlich zu erhöhter Freisetzung von Nährstoffen in die Wassersäule, begünstigen Zusammenbrüche von Algenblüten Aggregationsprozesse. Durch die Abgabe von transparenten exopolymeren Partikeln (TEP) werden große, organikreiche Aggregate gebildet. Die Ablagerung solcher Aggregate führt zu verstärkter mikrobieller Aktivität in den Oberflächensedimenten und dadurch bedingt zur Freisetzung von gelöstem organischen Kohlenstoff, Nährstoffen und Spurenmetallen wie Mn, Mo, oder V.

Die Untersuchung von Porenwässern, ergab, dass diese an Kieselsäure und Phosphat angereicherten Wasser sowohl diffusiv als auch advektiv in die Wassersäule transportiert werden. Dies führt zu tidal und saisonal wiederkehrenden Mustern im Konzentrationsverlauf. Demgegenüber erwies sich der Süßwasserbeitrag des Siels im Untersuchungsgebiet, in

Hinsicht auf Nährstoffbilanzen des Rückseitenwatts und der Deutschen Bucht, als vernachlässigbar. Die Untersuchungen dieser Arbeit konnten die große Bedeutung der Wattsedimente auf den Nährstoffeintrag in die Deutsche Bucht herausstellen. Es konnte gezeigt werden, dass die Gesamtfläche der Rückseitenwatten des Wattenmeeres in der Deutschen Bucht Nährstoffe in der gleichen Größenordnung in die Nordsee exportieren, wie die Summe der Einträge aus Elbe, Weser und Ems, während der NO_x -Eintrag der Watten um eine Größenordnung geringer ist. Demzufolge fungieren Rückseitenwatten als eine Art „Bioreaktor“, in dem partikuläres organisches Material abgebaut und als gelöste Nährstoffe exportiert wird und somit in hohem Maße zur Nährstoffbilanz des Ökosystems Deutsche Bucht beitragen.

Table of contents

Abstract.....	I
Kurzfassung	III
Table of contents	VII
Figure legends.....	IX
Table legends.....	XIV
1 Introduction	1
1.1 The North Sea.....	1
1.2 Organic matter remineralisation.....	5
1.3 The time-series station	10
1.4 Objectives of the thesis	11
1.5 Outline of the author's contribution	13
2 A novel time-series station in the Wadden Sea (NW Germany): First results on continuous nutrient and methane measurements	17
3 Methane in the southern North Sea: Sources, spatial distribution and budgets	33
4 Nutrient dynamics in a back barrier tidal basin of the Southern North Sea: Time-series, model simulations, and budget estimates	61
5 Sulphate, dissolved organic carbon, nutrients and terminal metabolic products in deep pore waters of an intertidal flat	87
6 Trace metal dynamics in the water column and pore waters in a temperate tidal system: Response to the fate of algae derived organic matter.....	113
7 General conclusions and perspectives	139
8 References	143
Acknowledgements	175
Curriculum vitae.....	177

Figure legends

(abbreviated)

Fig. 1.1. The North Sea with connections to the Atlantic Ocean and the Baltic Sea, amphidromes (orange points; Pethick, (1984), and the Dogger Bank (grey area with dashed line). Picture modified from Google Maps (www.maps.google.com).....	1
Fig. 1.2. Spatial extension of Wadden Sea ecosystem of the southern North Sea. Picture modified after Marencic et al. (2005).....	2
Fig. 1.3. Map of the study area showing the tidal channel system, the time-series station in the main tidal inlet, the pore water sampling site JS1 on the sandy tidal flat Janssand, and the flood-gate in Neuharlingersiel.	5
Fig. 1.4. Sketch of the time-series station. Green labelled sensor tube openings are equipped with sensor tubes.....	10
Fig. 2.1. Map of the study area in the German Bight. The detailed map shows Spiekeroog Island, the backbarrier tidal flats, the position of the time-series station in the tidal inlet (Otzumer Balje), and the pore water sampling site Janssand (JS).	19
Fig. 2.2. Photograph of the time-series station.....	20
Fig. 2.3. Sketch of the time-series station. White sensor tube openings are equipped with sensor tubes, black ones are not.	21
Fig. 2.4. Sketch of nutrient measurement hardware arrangement located in the upper part of the pole.....	23
Fig. 2.5. Methane measurements of sensor vs. GC.	25
Fig. 2.6. Nutrient concentrations at the time-series station from April to July 2006 (a-e). The grey bar indicates the time period shown in f-j, where the tidal resolution of the individual parameter is shown. The dots mark the hourly measurements and the tidal gauge is given by the dashed line.	27
Fig. 2.7. Methane concentrations at the time-series station from September to November 2005 (a).Methane concentrations (black) and corresponding wind speed data (grey). (b) Tidal pattern from 17 th to 21 st of September 2005. The dashed line denotes the tidal gauge.....	29
Fig. 3.1. (a) Map of the study area in the German Bight. Black dots denote sampling sites. The detailed map (b) shows Spiekeroog and Langeoog Island, the	

transect in front of the islands, the back barrier tidal flats, the position of the time-series station and the sampling site OB9 in the tidal inlet (Otzumer Balje), the pore water sampling sites Janssand (JS) and Neuharlingersieler Nacken (NN), and the position of tidal creek measurements. White areas in Fig. 3.1b indicate tidal flats emerging during low tide. Map (c) shows the transect of River Weser. Map (d) shows the classification of boxes used in the Euler-Lagrangian model including averaged water depths of the boxes.35

Fig. 3.2. CH₄ concentrations in the German Bight, coastal areas, and River Weser. Data originate from cruises HE188 in May 2003 (squares), HE238 in September 2005 (circles), HE243 in November 2005 (diamonds), and from time-series station data obtained in October to November 2005 (triangles).42

Fig. 3.3. High tide and low tide CH₄ concentrations along the west-east-transects beyond the Islands Langeoog and Spiekeroog in May 2003 (solid line) and September 2005 (dashed line). ‘A’ (53.8 °N, 7.56 °E) and ‘B’ (53.82 °N, 7.7 °E) indicate start and end points of the transects.43

Fig. 3.4. CH₄ concentrations (a), wind speed (ws; b), and cross-correlations (xcov) with time lag (τ) of CH₄ and wind speed (c) in October to November 2005.44

Fig. 3.5. CH₄ concentrations (solid line) and tidal gauge (dashed line) at the time-series station in 2005 (a) and at OB9 (b) in August 2003 (black line) and January 2005 (solid grey line).45

Fig. 3.6. CH₄ and SO₄²⁻ pore water measurements at site Janssand (JS) in 2006. SO₄²⁻ data are average values of February, March, April, June, and July. Horizontal lines in SO₄²⁻ data denote the annual min/max.47

Fig. 3.7. Comparison of model data (black line) and data from the time-series station (grey line) for different model boundary conditions.48

Fig. 3.8. Data of the River Weser transect in May 2003 with CH₄ (solid line), salinity (dotted line), and SPM (dashed line with circles).50

Fig. 4.1. Map of the study area. (a) German Bight position where North Sea samples were analysed which were used as boundary conditions in the model setup. The close-up view (b) shows the sampling sites in the back barrier area of Spiekeroog Island: Time-series station, JS1, and the flood-gate in Neuharlingersiel. (c) Classification of boxes used in the Euler-Lagrangian model simulations with corresponding average water depths.63

Fig. 4.2. Silica, phosphate, and nitrite plus nitrate in the years 2006-2008 determined at the time-series station in the tidal inlet of the Island of Spiekeroog. Single measurements are shown as grey points. The black line represents running average concentrations (dashed segments: no data are available) and open circles indicate monthly averages. Total cell counts in 2008 (grey line) are given in a logarithmic axis scale.....	69
Fig. 4.3. Tidal dynamics of silica, phosphate, and nitrite plus nitrate in winter, spring, summer, and autumn 2007. Note the different scales for silica (winter) and nitrite plus nitrate. Grey lines indicate the tidal state.....	74
Fig. 4.4. Monthly freshwater contribution of silica, phosphate, and nitrite plus nitrate via the flood-gate in Neuharlingersiel to the tidal flat area of Spiekeroog (columns). Data are averaged for the years 2002-2004. For comparison, averaged freshwater discharge rates (Rupert et al., 2004) via the flood-gate are given (circles).	77
Fig. 4.5. Pore water concentrations of silica and phosphate in 2008 at site JS1 (columns). For comparison, monthly averages of water column concentrations (circles) and total cell counts (squares) are indicated.	79
Fig. 4.6. Model simulation for silica, phosphate, and nitrite plus nitrate (black line) compared with data determined at the time-series station (grey circles) in 2007.....	82
Fig. 4.7. Annual pattern of silica, phosphate, and nitrite plus nitrate in 2007 as simulated by the reference run (run1, black line), the run without additional import of POM (run3, dark grey line), and enhanced import of POM (run4, light grey line) compared to measurement data from the time-series station (black dots).	84
Fig. 5.1. (A) Study site in an intertidal sand flat (Janssand) in the backbarrier area of Spiekeroog Island, Wadden Sea, Germany. (B) Tidal flat topography.....	90
Fig. 5.2. Sketch of model sediment column. The upper part is free of organic matter (OM). The lower part contains 1 % total organic carbon (TOC), most of which is refractory (grey), however, there is a layer of labile OM around 2.8 m depth. Advection is indicated by arrows. The division into 20 boxes is indicated by lines.	95
Fig. 5.3. Organic matter degradation scheme of the integrated sediment model. POC quality classes are converted to DOC classes according to the distribution vectors. Upon hydrolysis, nutrients are released according to the specific	

C:N:P ratios. The distribution scheme may be extended by further POC classes (grey and dashed arrows). DOC is separated into high and low molecular weight DOC (DOC-H and DOC-L). Larger molecules (DOC-H) can only be degraded by aerobic heterotrophs or must be converted to smaller units (DOC-L) by fermenting bacteria. All heterotrophic functional groups can use DOC-L for catabolic processes.96

Fig. 5.4. Depth profiles of parameters characterising the lithology at the sampling site in an intertidal sand flat. The continuous lines in Ti/Al and Zr/Al figures indicate the geogenic background (Wedepohl 1971). The grey bars highlight the clay rich layers of the sediment profile. Depths of about 1.5 to 2.5 m are marked with a hatched area because the lithological description shows that the sediment is predominantly sandy, with very thin clay layers.99

Fig. 5.5. Pore water profiles of Cl^- , pH, NO_3^- , SO_4^{2-} , H_2S , CH_4 , H_4SiO_4 , TA, NH_4^+ , PO_4^{3-} , and DOC at the sampling site in an intertidal sand flat of the backbarrier area of Spiekeroog Island (April 2006; CH_4 March 2006). DIC concentrations were calculated using TA and pH.100

Fig. 5.6. Modelled (continuous line) and measured (points) pore water profiles. Same samples as in Figure 5.3. To test to sensitivity of the pore water profiles to organic matter composition, simulations were conducted with Redfield ratios increased and decreased by 50% (dashed lines).102

Fig. 5.7. Ratios of DOC, TA, NH_4^+ , and PO_4^{3-} concentrations to $(\text{SO}_4^{2-})_{\text{Dep}}$ concentrations. Best-fit linear regressions are calculated for samples from April 2006 separately (A) and for all samples taken from May 2005 till June 2006 (B).105

Fig. 5.8. Sea water PO_4^{3-} and H_4SiO_4 concentrations determined at a monitoring station in the backbarrier area of Spiekeroog Island in May 2006. The dashed line indicates the tidal variations of the sea water level.109

Fig. 6.1. Map of the study area showing the backbarrier tidal flats of Spiekeroog island, Wadden Sea (NW Germany). The detailed map presents sampling sites in the tidal inlet (Otzumer Balje, OB) and on the Janssand tidal flat (JS).117

Fig. 6.2. Silica concentrations and diatom cell counts in the water column of the Spiekeroog island backbarrier area in 2007.120

Fig. 6.3. Concentrations of a) DOC, TA, ammonium, phosphate, and silica, and b) hydrogen sulphide and sulphate in the pore waters at site JS in 2007.....	121
Fig. 6.4. Seasonal variations of dissolved U and Mo in the water column of the Spiekeroog island backbarrier area in 2002. Data presented in blue colour are normalized to offshore salinity. The grey line denotes the North Atlantic value; the vertical grey lines mark high tide (HT) and the dashed line low tide (LT).....	123
Fig. 6.5. Seasonal variations of dissolved U, Mo, V, and Mn in pore waters and tidal creek waters in 2002.....	125
Fig. 6.6. Concentrations of dissolved U, Mn, V, and Mo in the water column of the Spiekeroog island backbarrier area from April to September 2007. The grey line denotes the North Sea value.	126
Fig. 6.7. Seasonal variation of enrichment factors (EFS) for particulate organic matter (POC), P, U, Mo, V, and Mn of suspended particulate matter in 2002.	127
Fig. 6.8. Concentrations of dissolved a) U and HS ⁻ , b) Fe (please note the different scale for Fe _{diss.} in April) and HS ⁻ , c) Mn and V, and d) Mo and HS ⁻ in the pore waters of site JS from April to October 2007. The grey lines mark the North Sea values of the trace metals.	129
Fig. 6.9. Phosphate concentrations in the water column of the Spiekeroog island backbarrier area in 2007 (monthly average).....	130
Fig. 6.10. Seasonal variations of dissolved Mn and V in the water column of the Spiekeroog island backbarrier area in 2002. The vertical grey line marks high tide (HT) and the dashed line low tide (LT). The horizontal grey lines in the V plots denote the North Atlantic value.	131
Fig. 6.11. Conceptual model (modified after Dellwig et al., 2007b) showing Mn and Mo dynamics in the water column and pore waters resulting from a pronounced benthic-pelagic coupling. Seasonal fluctuations of phytoplankton growth significantly influence the trace metal budget in the water column and shallow pore waters. Schematic water column trends and pore water profiles illustrate the seasonal variations of Mn (black lines) and Mo (dark grey lines) dynamics due to pelagic and benthic coupling. The general pore water trends are adapted to the scale of the present investigations.	136

Table legends

Table 1.1. Standard free energy (SFE) gain by organic matter remineralisation modified from Froelich (1979), with SFE presented as $\Delta G_0'$ in kJ per mole of glucose (C ₆ H ₁₂ O ₆).....	6
Table 2.1. Measuring principles and parameters of nutrient determination.	24
Table 2.2. Mean concentrations of ship-based measurements in the tidal inlet at time-series station position.	26
Table 3.1. Parameter variation of the mean CH ₄ concentration (m) at the North Sea boundary, the tidal amplitude of the CH ₄ concentration (a) at the North Sea boundary, the pore water discharge (d), and the resulting export out of the back barrier area.	39
Table 3.2. CH ₄ concentrations and saturations of tidal flats and coastal tributaries.	41
Table 3.3. Estimation of freshwater and pore water CH ₄ contribution to the back barrier are of Spiekeroog Island.	49
Table 3.4. Summary of European rivers discharging into the German Bight.	57
Table 4.1. Summary of monthly averaged concentrations for silica, phosphate, and nitrite plus nitrate for the years 2006 – 2008. Corresponding ranges (min – max) are given in brackets. ‘n’ denote the number of measurements used for averaging. Values indicated by ‘*’ are below detection limit.	70
Table 4.2. Results of Euler-Lagrangian model simulations. Export of dissolved inorganic silica, phosphate and nitrite plus nitrate from the back barrier area as well as the impact of freshwater contribution via the flood-gate are given for different runs of model calculations (see text). Values in brackets indicate the percentage in comparison to the reference run (run1).	81
Table 4.3. Nutrient export from the whole back barrier area of the Wadden Sea in the German Bight compared with riverine nutrient load.	85
Table 5.1. Parameters of the model setup.	97
Table 5.2. Stoichiometry during organic matter degradation estimated from slopes of pore water concentrations of total alkalinity TA and sulphate depletion (SO ₄ ²⁻) _{Dep} against NH ₄ ⁺ and PO ₄ ³⁻ concentrations for samples of April 2006 and for all samples taken form May 2005 till June 2006. The ratios of suspended particulate matter and the ratios derived from modelling pore water profiles are further displayed.	106

Table 6.1. Average values and range (in parentheses) of salinity, SPM, POC, and dissolved and particulate trace metals in the Wadden Sea and in freshwater flowing into the backbarrier area via flood-gates in Neuharlingersiel in 2002. 124

1 Introduction

1.1 The North Sea

The North Sea, as a semi-enclosed marginal sea of the Atlantic Ocean, covers an area of 575,000 km² with an average water depth of 70 m and a resulting volume of 41,000 km³ (Becker, 1990). The borders are given by the coastlines of England, Scotland, Norway, Sweden, Denmark, Germany, Netherlands, Belgium, and France. The connection to the Atlantic Ocean is given through the English Channel in the south and between Scotland and Norway in the north. The connection to the Baltic is represented by the Skagerrak/Kattegat in the east. The connection to the Baltic is represented by the Skagerrak/Kattegat in the east.

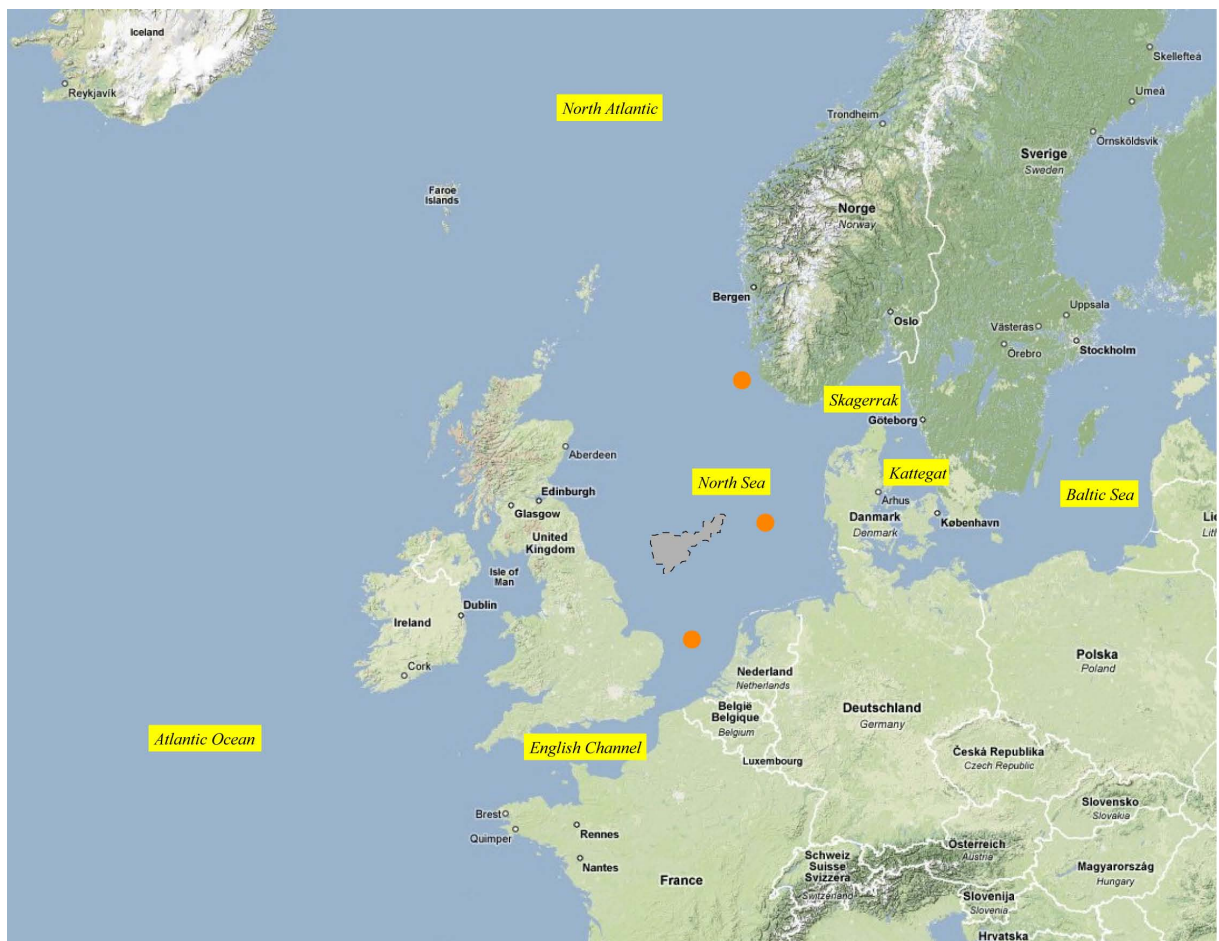


Fig. 1.1. The North Sea with connections to the Atlantic Ocean and the Baltic Sea, amphidromes (orange points; Pethick, 1984), and the Dogger Bank (grey area with dashed line). Picture modified from Google Maps (www.maps.google.com).

The formation of the present North Sea started after the Weichselian Glacial maximum some 18,000 years BP when the sea level was 110 - 130 m below the present level (Cameron et al., 1987; Long et al., 1988; Reise, 2005). At this time, the coastline was located between the mid of England and the south of Sweden, with a vegetation characterized by tundra and boreal forest. In the following time the sea-level rose with an average rate of about 2.1 m 100 a⁻¹ due to climate warming (Streif, 1990). From approximately 8500 years BP the sea level rise led to the formation of the Holocene sedimentary wedge and the formation of the present day coastal landscape with its barrier islands, tidal flats, and coastal marshland (Hoselmann and Streif, 2004).

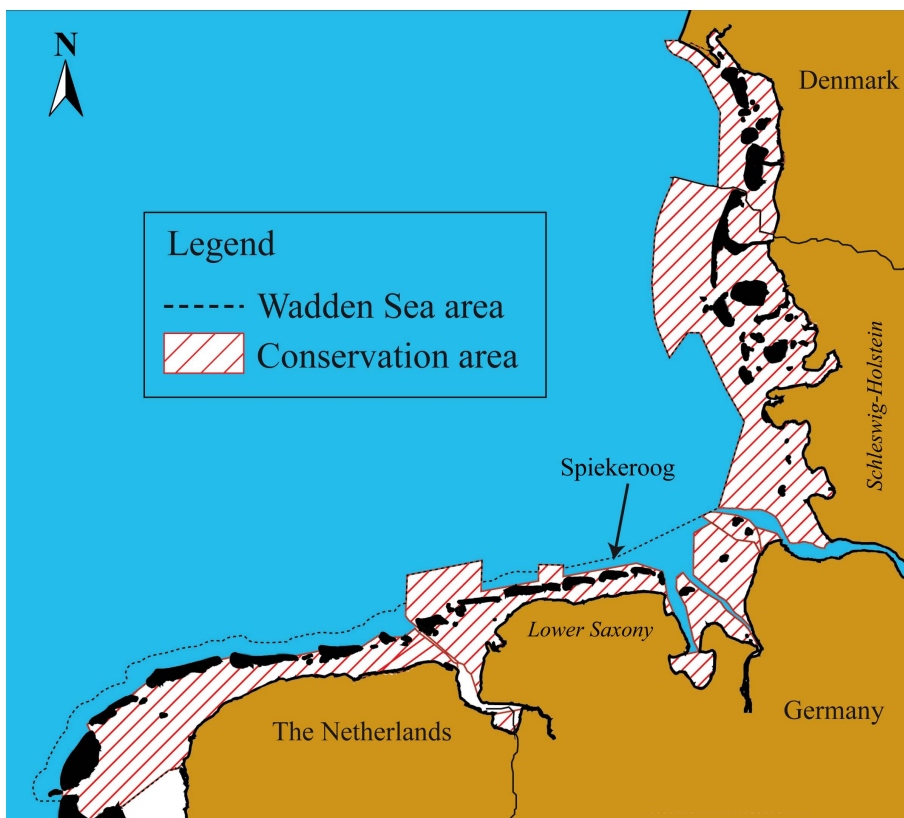


Fig. 1.2. Spatial extension of Wadden Sea ecosystem of the southern North Sea. Picture modified after Marencic et al. (2005).

Overall, this process created one of the world's largest connected Wadden Sea system amounting for about 60% of Wadden Sea areas of entire Europe and northern Africa (Umweltbundesamt, 2004). The Wadden Sea stretches from Den Helder (Netherlands) to Skallingen (Denmark) with an extent of about 450 km (Essink et al., 2005). While the chain of barrier islands off the coasts of The Netherlands, Lower Saxony, and south-western Denmark forms part of the Holocene sedimentary wedge, the islands off Schleswig-Holstein are relicts of former Pleistocene land masses (Streif, 1990).

Since about 1000 years BP land reclamation and dike building influenced dramatically the development of the Wadden Sea (Streif, 1990). Dike construction leads to decreasing deposition of fine grained particles and consequently fine to medium sand dominate the sediments of the intertidal German Wadden Sea (Flemming and Nyandwi, 1994; Flemming and Ziegler, 1995; Dellwig et al., 2002; Hinrichs et al., 2002) and largely determines the morphology of the coastline (Dellwig et al., 2007b).

1.1.1 Water circulation

The water circulation in the North Sea is mainly controlled by the bottom topography, since currents follow the relief and flows tend to be concentrated in areas where slopes are steepest. Generally, the seabed of the North Sea reveals a structure shaped during glacial periods when the sea level was lower as indicated for instance by glacial river valley systems (OSPAR Commission, 2000). The depth of the central North Sea increases towards the Atlantic Ocean until about 200 m at the edge of the continental shelf southeast of Great Britain and France. However, the English Channel has a relatively shallow depth of about 30 m in the Strait of Dover increasing gradually to a depth of 100 m in the west. In contrast, the Norwegian Trench in the north with a sill depth of about 270 m plays a major role in steering large inflows of Atlantic water into the North Sea. In the area between The Netherlands and Great Britain average water depths are between 20 and 30 m, while at the Dogger Bank (compare Fig. 1.1), a shallow area in the central North Sea, depths can be less than 20 m leading to a significant impact on the circulation in the southern North Sea. This topography governs the inflow of Atlantic Ocean water of about $55,000 \text{ km}^3 \text{ a}^{-1}$ from the North Atlantic and $4900 \text{ km}^3 \text{ a}^{-1}$ through the English Channel, while the net inflow from the Baltic Sea accounts for about $500 \text{ km}^3 \text{ a}^{-1}$, whereas the main outflow from the North Sea along the Norwegian coast amounts for $57,000 \text{ km}^3 \text{ a}^{-1}$ (Becker, 1990).

The general pattern in the North Sea follows an anti-clockwise (cyclonal) circulation, which has first been determined by Böhnecke (1922) on the basis of salinity distributions. This circulation pattern has been generally supported by measurements of Cs-137 discharged from nuclear reprocessing plants in Sellafield (England) and La Hague (France) in the 1980s (Nies, 1990). One has to keep in mind that the aforementioned cyclonal circulation is an idealised average which is valid just for long-time examination of several months. On a smaller temporal scale the currents are also influenced by metrological forces (wind, insolation), inflow from the Northern Atlantic and the Baltic as well as freshwater contribution.

Tides in the North Sea

Tides in the North Sea are affected by the tides of the Atlantic Ocean. Accordingly, the tide in the North Sea is characterized by a semidiurnal principal lunar tide (M_2) with a periodicity of 12.4 hours (12h 25min) and a superposing quarter-diurnal lunar tide (M_4) with a periodicity of 6.21 hours (6h 13min). Due to the periodically horizontal displacement of water masses by tides, horizontal as well as vertical mixing of waters occurs.

The tidal gauges of the Wadden Sea in the German Bight (Southern North Sea, Fig. 1.2) are affected in different extents. The tide wave in the German Bight emanates circularly from the south-western amphidrome, a site with no tidal gauge, towards the coasts (Flemming and Davis, 1994). Thus, in the western part at the Belgian and Dutch Wadden Sea, as well as in the northern part of the Danish Wadden Sea the tidal range accounts only for 1.5 – 2 m whereas 3 – 4 m are in the mouth of the Rivers Elbe and Weser.

Tidal flat areas

Lateral exchange of major water masses between tidal flat areas occurs at high tide, while a system of major and smaller tidal channels crossing the individual tidal flats facilitates a minor lateral water exchange during low tide. Water of this channel system flows into a main channel, the tidal inlet between the islands, which forms the connection of each back barrier area to the German Bight and the pathway for tidally driven water exchange with the North Sea (Fig. 1.3). Pronounced tidal currents cause elevated loads of suspended particulate matter (SPM) and intense sedimentation and resuspension (Flemming and Nyandwi, 1994; Flemming and Ziegler, 1995; Chang et al., 2006a; Lunau et al., 2006). Coastal zones as intertidal flats and estuaries have a considerable impact on the biogeochemical processes of the oceans, due to water column/sediment interaction and estuarine mixing (Shiller and Boyle, 1991; Shiller, 1996; Brasse et al., 1999). Tidal flat areas are usually net-heterotrophic and act as a sink for organic matter (Postma, 1981), which underlies intense remineralisation when entering. Thus, tidal flats play an important role in global biogeochemical cycles, as they are the most productive natural ecosystems and provide the nursery for many marine organisms.

In the context of preserving and assessing the quality status of the marine environment, sustained joint efforts are undertaken, which are e.g. the “OSPAR commission” and the “Trilateral Cooperation on the Protection of the Wadden Sea”. Despite substantial studies, participants of these ventures emphasise, the necessity of further investigations concerning tidal circulations and the balance of primary production and biomass recycling.

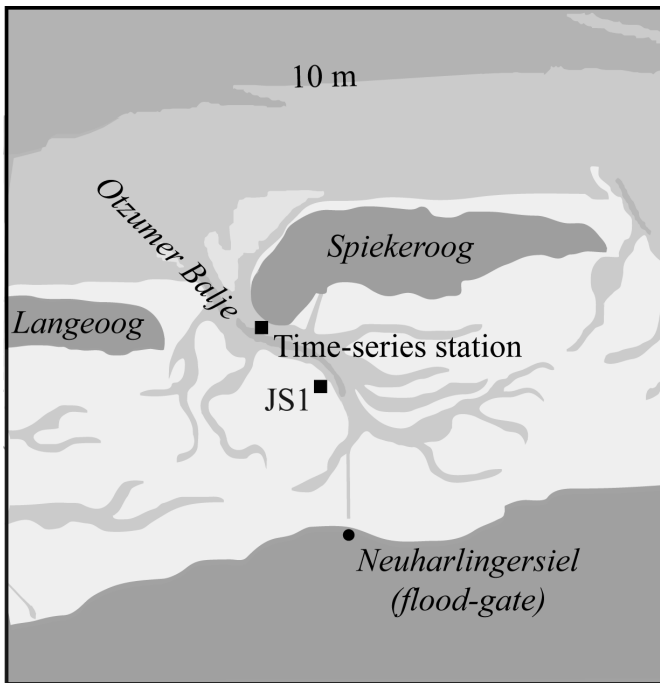


Fig. 1.3. Map of the study area showing the tidal channel system, the time-series station in the main tidal inlet, the pore water sampling site JS1 on the sandy tidal flat Janssand, and the flood-gate in Neuharlingersiel.

1.2 Organic matter remineralisation

The generalized composition of organic matter is given by $(\text{CH}_2\text{O})_x(\text{NH}_3)_y(\text{H}_3\text{PO}_4)_z$, with values of x , y , and z depending on the age and origin of the material. For fresh marine phytoplankton Redfield (1958) proposed a molar stoichiometry of $x = 106$, $y = 16$, and $z = 1$, whereas the composition of altered marine organic matter can partly differ from these C:N:P ratios (Atkinson and Smith, 1983).

High amounts of organic matter are imported from the North Sea into the Wadden Sea (van Beusekom and de Jonge, 2002) and are remineralised aerobically and anaerobically by microorganisms and benthic fauna in the tidal flat sediments (Böttcher et al., 2000; Werner et al., 2006; Al-Raei et al., 2009). The availability of the electron acceptors oxygen, nitrate, manganese oxides, iron oxides, or sulphate governs the pathway dominating organic matter mineralisation. Furthermore, mineralisation is controlled by a catabolic succession, which is based on the standard free energy gain of oxidation using different oxidants. Table 1.1 provides an overview about the molar standard free energy gains taken from Froelich (1979).

Table 1.1. Standard free energy (SFE) gain by organic matter remineralisation modified from Froelich (1979), with SFE presented as ΔG^0 in kJ per mole of glucose ($C_6H_{12}O_6$).

Pathway of organic matter oxidation	ΔG^0 [kJ mole ⁻¹]
1. Oxic respiration (CH ₂ O) ₁₀₆ (NH ₃) ₁₆ (H ₃ PO ₄) + 138 O ₂ → 106 CO ₂ + 16 HNO ₃ + H ₃ PO ₄ + 122 H ₂ O	- 3190 (Glucose)
2. Manganese (IV) reduction (CH ₂ O) ₁₀₆ (NH ₃) ₁₆ (H ₃ PO ₄) + 236 MnO ₂ + 472 H ⁺ → 106 CO ₂ + 236 Mn ²⁺ + 8 N ₂ + H ₃ PO ₄ + 366 H ₂ O	- 3090 (Birnessite) - 3050 (Nsutite) - 2920 (Pyrolusite)
3. Nitrate reduction (CH ₂ O) ₁₀₆ (NH ₃) ₁₆ (H ₃ PO ₄) + 94.4 HNO ₃ → 106 CO ₂ + 52.2 N ₂ + H ₃ PO ₄ + 177.2 H ₂ O	- 3030
(CH ₂ O) ₁₀₆ (NH ₃) ₁₆ (H ₃ PO ₄) + 84.8 HNO ₃ → 106 CO ₂ + 42.4 N ₂ + H ₃ PO ₄ + 148.4 H ₂ O	- 2750
4. Iron (III) reduction (CH ₂ O) ₁₀₆ (NH ₃) ₁₆ (H ₃ PO ₄) + 212 Fe ₂ O ₃ (or 424 FeOOH) + 848 H ⁺ → 424 Fe ²⁺ + 106 CO ₂ + 16 NH ₃ + H ₃ PO ₄ + 530 H ₂ O (or 742 H ₂ O)	- 1410 (Fe ₂ O ₃) - 1330 (FeOOH)
5. Sulphate reduction (CH ₂ O) ₁₀₆ (NH ₃) ₁₆ (H ₃ PO ₄) + 53 SO ₄ ²⁻ → 106 CO ₂ + 16 NH ₃ + 53 S ²⁻ H ₃ PO ₄ + 106 H ₂ O	- 380
6. Methanogenesis (C-reduction) (CH ₂ O) ₁₀₆ (NH ₃) ₁₆ (H ₃ PO ₄) → 53 CO ₂ + 53 CH ₄ + 16 NH ₃ + H ₃ PO ₄	- 350

The thermodynamically most favoured process is represented by oxic respiration, which is limited to the uppermost millimetres to centimetres, dependent on oxygen penetration depth. Despite the catabolic succession listed in Table 1.1, which is valid only in diffusion dominated sediments, oxidation pathways can overlap vertically. Permeable sediments operate as biocatalytical filters where metabolites of organic matter decomposition are contributed via pore water exchange to the open water column (Rusch et al., 2006).

Pore waters entering the open water column during ebb tide are controlled by both advective and diffusive transport (Huettel et al., 1996; Huettel and Rusch, 2000; Huettel et al., 2003; Precht and Huettel, 2004). The main driving force for advective exchange, which exceeds molecular diffusion by at least 3 orders of magnitude, is the pressure gradient generated by the interaction of oscillating boundary flows and sediment wave ripples. These

gradients produce a pore-water flow field, with a regular pattern of intrusion and release zones that migrates with ripple propagation (Precht and Huettel, 2003).

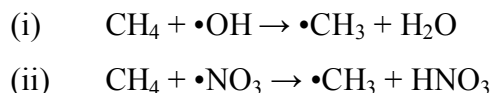
In comparison to the open water column, pore waters are highly enriched in metabolic endmembers as methane, silica, ammonium, and phosphate (Huettel et al., 1998; Billerbeck et al., 2006b; Wilms et al., 2007). In contrast, concentrations of nitrite and nitrate are influenced by aforementioned reduction processes and are depleted and absent in pore waters, respectively. Thus, the influence of the processes within the sediments on the concentrations of metabolites in the water column as well as the subsequent exchange between the Wadden Sea and the open North Sea forms an important scientific challenge.

1.2.1 Methane

Methane (CH₄), as the most abundant organic compound in the atmosphere, contributes largely to the earth's greenhouse effect by absorption of infrared radiation and affecting tropospheric photochemical reactions (Cicerone and Oremland, 1988; Crutzen and Zimmermann, 1991; Lelieveld et al., 1993). The global molar radiative forcing of methane in the atmosphere is stronger, when compared to the likely best-known greenhouse gas CO₂. In 2005, CO₂ concentration accounts for 379 ppm and leads to a radiative forcing of +1.66 (±0.17) W m⁻², while methane concentrations of 1774 ppb contributing +0.48 (±0.05) W m⁻² (Forster et al., 2007). Sources for methane are various: Beside methane production in stomachs of ruminants and by termites, major amounts of biogenic methane originates from bacterial anaerobic decomposition of organic matter in swamps, rice fields, wetlands, and landfills (Sass et al., 1990; Fung et al., 1991; Bartlett et al., 1992; Roulet et al., 1992a). Marine methane contribution is estimated to account for about 10 % of global atmospheric methane budget (Sass et al., 1990; Fung et al., 1991; Bartlett et al., 1992; Roulet et al., 1992b). Minor methane contributors in the marine environment are given by bacterial production in zooplankton digestive tracks (Bianchi et al., 1992; Marty, 1993), whereas most of marine methane originates from deeper sediment layers of productive coastal areas (Scranton and McShane, 1991; Hovland et al., 1993), continental river runoff (de Angelis and Lilley, 1987; Middelburg et al., 2002), and groundwater discharge (Bugna et al., 1996; Kim and Hwang, 2002).

Methane producing archaea are in competition for substrates with sulphate reducing bacteria, however, they can avoid this competition by using different types of substrates (e.g. methylamines, dimethyl sulphides), which are not utilized by sulphate reducers (Madigan et al., 2003). Thus, methanogenesis can occur parallel to bacterial sulphate reduction.

Sinks for methane are manifold. In the atmosphere methane is reduced by radical reactions:



Dissolved methane in the water column, which has not been exhaled to the atmosphere, is oxidized aerobically using dissolved oxygen, whereas in sediments different processes of methane oxidation occur. The most common process is aerobic oxidation by methanotrophic bacteria, while aerobic oxidation by ammonium oxidizing bacteria and oxidation by a consortium of archaea and sulphate reducing bacteria (Boetius et al., 2000) is rather rare.

1.2.2 Nutrients

Nutrients are organic or inorganic substances, which are essential for any kind of organism. Nutrients can be divided into (i) micronutrients (e.g. manganese, iron, copper, zinc, molybdenum), which are needed by phytoplankton in minor amounts, and (ii) the macronutrients silica, ammonium, nitrite, nitrate, and phosphate. In the North Sea micronutrients are available in sufficient amounts for phytoplankton, whereas macronutrients can be a limiting factor due to depletion. While silica is used by diatoms for their shell formation (Helmcke, 1954; Lewin, 1962; Antia et al., 1963; Grant, 1971; Paasche, 1973), nitrogen and phosphorus are used by any kind of phytoplankton for synthesis of enzymes and nucleotides for DNA, phospholipids for cell membranes, and the generation of ATP for energy buffering (Schlesinger, 1997).

In the marine environment the distribution of nutrients exhibits a horizontal as well as vertical pattern. Vertical nutrient concentration profiles in the oceans exhibit a surface minimum with increasing values with depth, due to microbial decomposition of organic matter and subsequent release of nutrients in the water column (Bruland et al., 1978b, a). The horizontal pattern in the oceans is characterized by increasing concentrations towards the coasts, which is governed by riverine inputs, upwelling, and enhanced remineralisation processes in coastal areas (Brockmann et al., 1990; Bruland et al., 2005). In addition to concentration gradients with depth and towards the coasts, an ocean-ocean-fractionation is induced by the global thermohaline water transport (Broecker and Peng, 1982). North Atlantic Deep Water (NADW) formed in high latitudes between Greenland, Iceland, and Norway flows through the Atlantic towards Antarctica and finally to the Indian and Pacific Ocean, where nutrient enriched water reaches surface areas due to upwelling. Thus, nutrient

concentrations are higher in the Pacific and the Indian Ocean, when compared with the Atlantic (Broecker and Peng, 1982).

Nutrient budgets in the North Sea are affected by both riverine supply and remineralisation processes. It is known, that rivers export nutrients to the North Sea (Hickel et al., 1993) and thus contribute to the eutrophication of coastal regions. The primary task of the 'Common Wadden Sea Secretariat' (CWSS), established in 1987, is to support, initiate, facilitate and coordinate the activities of the trilateral collaboration program of The Netherlands, Germany, and Denmark with regard to a comprehensive Wadden Sea protection (The Common Wadden Sea Secretariat (CWSS), 2009). Many efforts have been undertaken to understand processes occurring in the Wadden Sea, which affect the coastal zones and the Southern North Sea (van Beusekom et al., 2001). However, information about the significance of the Wadden Sea - and in particular the tidal flat areas - with respect to nutrient budgets is still lacking. To overcome this, continuous measurements of nutrient concentrations are needed, since they are a useful tool to verify mathematical models for budget calculations. Outcomes of the combination of measurements and model results can provide implications in the concern of human impact discussion on eutrophication in the German Bight.

1.3 The time-series station

Concerning the need of continuous data sets for budget calculation a time-series station (Fig. 1.4) was installed within the scope of the DFG Research Group “Biogeochemistry of tidal flats” the tidal inlet of the Island of Spiekeroog in August 2002.

In addition to meteorological parameters (wind speed, wind direction, air pressure, air temperature, air humidity, irradiance; Reuter et al., 2009), the station is equipped with 10 sensor tube openings below sea level for recording oceanographic parameters.

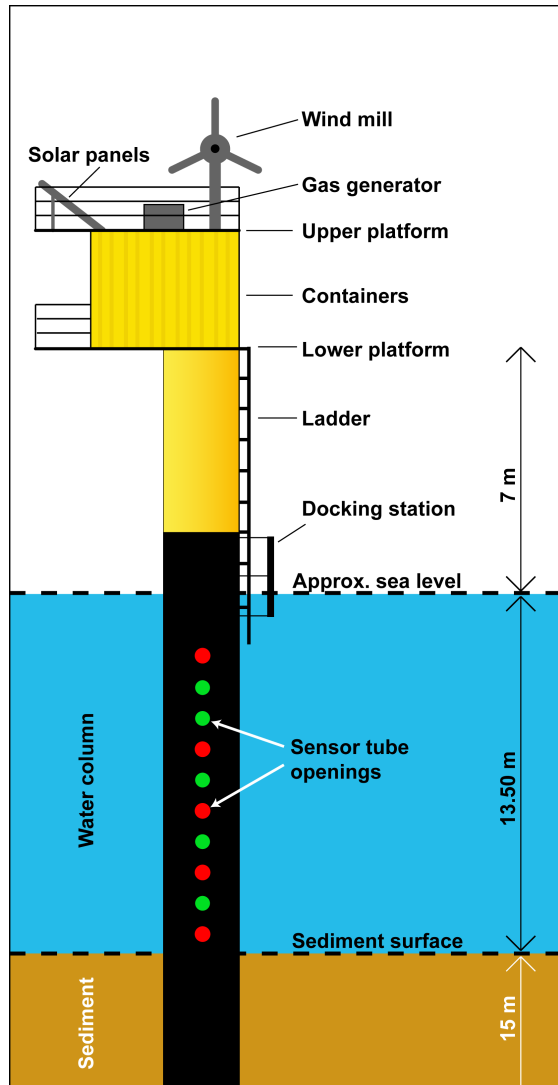


Fig. 1.4. Sketch of the time-series station. Green labelled sensor tube openings are equipped with sensor tubes.

At five openings sensor tubes are installed which are equipped with sensors for water temperature and conductivity in every tube and a pressure sensor in the lowest tube. Outside the station an acoustic doppler current profiler (ADCP) for determining currents and surface waves, a multispectral transmissometer (MST) for detecting suspended particulate matter, and

a methane sensor were installed. Due to its design, the station is operable throughout the year, even during storms and ice winters. Power generators (wind mill, solar panels, and gas generator) on top of the upper platform of the station ensure an autonomous electrical energy management without cable connection to the Island of Spiekeroog. After initiation of the station in October 2002 the first meteorological and oceanographical parameters were measured continuously (Grunwald et al., 2007; Reuter et al., 2009).

In order to record tidal and seasonal nutrient variations in the study area, a system of autonomous nutrient analysers has been established on the station in April 2006 (Grunwald et al., 2007). This system provides the opportunity of continuous measurements of silica, phosphate, nitrite, and nitrate in surface waters on an hourly interval. As the water column of the back barrier area is well mixed (Stanev et al., 2007; Lemke et al., 2009) and stratification is only observed during short periods after high tide, measurements of surface waters are assumed to be representative for the system.

1.4 Objectives of the thesis

This thesis forms part of the interdisciplinary DFG Research Group “Biogeochemistry of Tidal Flats”, established in 2001 at the Institute for Chemistry and Biology of the Marine Environment (ICBM), University of Oldenburg. The major goals of the Research Group comprise biogeochemical transformation processes in the open water column, at the water-sediment boundary layer, and within the deeper parts of the sediments. Furthermore, the fate and budgets of material and compounds entering and leaving the study area should be investigated by continuous measurements and modelling approaches (e.g. Kohlmeier and Ebenhöh, 2007). The main objective of this thesis was to design and maintain a system for continuous measurements of dissolved nutrients and methane at the time-series station in order to record tidal and seasonal variations of these parameters and to calculate their budgets.

Thus, chapter 2 describes the development of such system for continuous measurements of nutrients and methane in the surface waters entering and leaving the back barrier area of Spiekeroog Island. After a time-intensive planning phase, the nutrient analyser system has been installed on the time-series station in November 2005. After eliminating start-up problems comprising sample and rinse water supply, the analysers produce continuous nutrient data since April 2006. Methane measurements were conducted using a commercial sensor, which was mounted outside the pole in 2003. The sensor had to be modified, since previous measurements during a cruise with R/V “Heincke“ revealed a thitherto strong dependence on the incident flow of water to the membrane surface.

Installation of a pump, which ensured a constant flow, solved this problem and additionally reduced the response time of measurement. However, due to persistent sensor problems as instability of sensor performance, leakage, and electrical malfunctions of the sensor, methane measurements were aborted in November 2005. However, the obtained data base was sufficient for budget estimations by model calculations, which are presented in chapter 3.

For studying methane sources in the Wadden Sea pore water samples originating from tidal flat sediments down to 5 m depth were analysed by conventional GC techniques (Niewöhner et al., 1998) as methanogenesis in deeper sediments is supposed to contribute significantly to methane budgets (Røy et al., 2008). The pore water samples were obtained by using permanently installed pore water lances from the Janssand tidal flat (Fig. 1.3; Beck et al., 2007). As the freshwater entering the study area via flood-gates in Neuharlingersiel (Fig. 1.3.) may also form an important source these waters as well as the connected small coastal tributaries were investigated by using the methane sensor. Based on the resulting data, model calculations show that the pore waters reflect the ultimate source for methane in the Wadden Sea, whereas the freshwater plays only a minor role. Furthermore, the methane distribution in the river Weser, the German Bight, and the open North Sea was investigated during several cruises with R/Vs “Senckenberg” and “Heincke”. Along with methane data from the time-series station, model approaches reveal a significant contribution of the back barrier tidal flats on the methane budget of the southern North Sea.

Chapter 4 is focussed on nutrient dynamics in the back barrier area of Spiekeroog Island. Time-series station measurements of an almost 3 year period are presented to evaluate tidal and seasonal dynamics. Pore water and freshwater measurements again identify the tidal flat sediments as the major source in the back barrier area. Correspondingly, mathematical model simulations by using the ecosystem model EcoTiM (Kohlmeier and Ebenhöf, 2007) provide export budget estimations, which are comparable to riverine nutrient inputs into the German Bight. These results justify the term “bio-reactor Wadden Sea” as particulate organic matter imported from the open North Sea is remineralised within the back barrier tidal flat systems.

The study presented in chapter 5 addresses biogeochemical processes within deeper pore waters of a permeable intertidal sand flat. The vertical distributions of sulphate, hydrogen sulphide, dissolved organic carbon, nutrients, methane, and alkalinity were studied down to 5 m sediment depth to identify the dominant terminal metabolic pathways of organic matter degradation. A sediment model setup is used to estimate the impact of advective transport within the sediment on pore water concentration profiles. Furthermore, hourly

determined nutrients at the time-series station help to investigate the significance of pore water contribution on the water column tidal pattern.

In chapter 6, the trace metal dynamics in the water column and pore waters and their response to algae blooms are presented. As postulated by Dellwig et al. (2007b), the molybdenum cycle in the back barrier area is strongly influenced by reduction in oxygen-depleted micro zones of aggregates, which are formed during breakdown of algae blooms (Passow, 2002; Bhaskar et al., 2005). Thus, the comparison of diatom cell counts with silica concentrations determined at the time-series station should be assessed in terms of whether continuous nutrient data can be used as an indicator for both the onset and breakdown of diatom blooms. Accordingly, continuous nutrient data are a useful tool to schedule sampling campaigns for investigation of dynamics related to the development and breakdown of algae blooms.

1.5 Outline of the author's contribution

The thesis comprises five manuscripts presented in chapters. The author's contribution to the included studies is detailed below.

Chapter 2

A novel time-series station in the Wadden Sea (NW Germany): First results on continuous nutrient and methane measurements

A setup for continuous measurements of nutrients and methane at the time-series station in the tidal inlet of the back barrier area of Spiekeroog Island was developed.

The concept of continuous nutrient analysis was developed by the author, the co-authors, and the company 4-H Jena engineering. Adaption and maintenance of nutrient analyser setup was done by the author himself. Methane sensor adaption and improvement by installing a pump, as well as maintenance work was done by the author himself. All data presented in the manuscript were analysed by the author himself, except ship-based nutrient measurements and methane comparison measurements by GC. The concept of the manuscript, the interpretation, evaluation, and discussion of the results as well as the preparation and editorial handling of the manuscript was developed by the author, who was supported by suggestions of Olaf Dellwig, Bernhard Schnetger, and Hans-Jürgen Brumsack.

The manuscript has been published 2007 in *Marine Chemistry* 107, 411-421.

Chapter 3

Methane in the southern North Sea: Sources, spatial distribution and budgets

This study addresses methane distribution in the Southern North Sea. Results of measurements at the time-series station, in the German Bight, the River Weser, pore waters of the tidal flat Janssand, and freshwater concentrations at the flood-gate in Neuharlingersiel were investigated in terms of sources of methane for the water column of the back barrier area and the German Bight. Two model approaches were used to estimate export budgets of the back barrier area to the German Bight.

The concept of this study was developed by the author who also conducted all measurements of the sampling campaigns. Correlation calculations were done by Jan A. Freund. Budget estimations using the EcoTiM model were conducted by Cora Kohlmeier. Joachim W. Dippner provided hydrodynamical data for a further approach of budget estimations, which were calculated by the author. Interpretation, evaluation, and discussion of the results as well as writing of the manuscript were done by the author, who was supported by suggestions of Olaf Dellwig, Cora Kohlmeier, Melanie Beck, Joachim W. Dippner, and Hans-Jürgen Brumsack. Editorial handling was done by the author.

The manuscript has been published 2009 in *Estuarine, Coastal and Shelf Science* 81, 445-456.

Chapter 4

Nutrient dynamics in a back barrier tidal basin of the Southern North Sea: Time-series, model simulations, and budget estimates

This study focuses on nutrient dynamics in the back barrier area of Spiekeroog Island. Nutrient measurements and analyser maintenance at the time-series station were conducted by the author. Since November 2007, Melanie Beck and Waldemar Siewert continued operating the setup. Pore water sampling was conducted by Nicole Kowalski, who also analysed the samples with support by Olaf Dellwig. Total algae cell counts were done by the company 'Aqua ecology', while freshwater samples were collected by Gerd Liebezeit and analysed by Heike Rickels. Model calculations and budget estimations were performed by Cora Kohlmeier. The concept of the manuscript, the interpretation, evaluation and discussion of results was done by the author, who was supported by Olaf Dellwig. Writing of the manuscript was done by the author, Olaf Dellwig, and Cora Kohlmeier, who were supported by comments of Melanie Beck and Hans-Jürgen Brumsack.

The manuscript has been submitted to *Journal of Sea Research*.

Chapter 5

Sulphate, dissolved organic carbon, nutrients and terminal metabolic products in deep pore waters of an intertidal flat

This study addresses biogeochemical processes in deep pore waters of a permeable intertidal sand flat in the back barrier area of Spiekeroog Island. Results of deep pore water studies are shown and organic matter degradation pathways were identified at one sampling site. The concept of the study was developed by Melanie Beck, who also conducted all sampling campaigns. All samples were analyzed by Melanie Beck except for nutrient and total alkalinity analyzes as well as sediment analyzes, which were carried out by our lab assistants Carola Lehnert, Eleonore Gründken, and Martina Wagner. Methane concentrations in pore water were analyzed by Maik Grunwald, who further contributed sea water phosphate and silica data determined at the time-series station in the back barrier area of Spiekeroog Island. Interpretation of the results and writing was done by Melanie Beck with help of all co-authors. The modelling part was contributed by Jan Holstein.

The manuscript has been published 2008 in *Biogeochemistry* 89, 221–238.

Chapter 6

Trace metal dynamics in the water column and pore waters in a temperate tidal system: response to the fate of algae-derived organic matter

In this study, the tidal and seasonal response of redox-sensitive trace metal dynamics in the water column and pore waters on algae blooms is investigated. Water column sample collection was done by Olaf Dellwig and Nicole Kowalski. Water column nutrient concentrations were determined by Maik Grunwald. Phytoplankton cell counts were performed by Maike Piepho. Pore water sampling and analysis was conducted by Nicole Kowalski, who also developed the concept of the manuscript and did the writing with support of all co-authors.

This manuscript has been published 2009 in *Ocean Dynamics* 59, 333–350.

2 A novel time-series station in the Wadden Sea (NW Germany): First results on continuous nutrient and methane measurements

M. Grunwald, O. Dellwig, G. Liebezeit, B. Schnetger, R. Reuter, H.-J. Brumsack

This chapter has been published 2007 in *Marine Chemistry* 107, 411-421.

Abstract

In autumn 2002 a time-series station was installed in the tidal inlet between the Islands of Langeoog and Spiekeroog (Southern North Sea, NW Germany) to continuously measure physical, chemical, and meteorological parameters, even during extreme weather conditions (gale-force storms, drifting ice). Inside the pole of the station sensor tubes are installed in direction of the prevailing tidal currents. The tubes are equipped with hydrographic sensors (pressure, temperature, conductivity) and allow retrieval of water for nutrient analysis by automated instruments located inside the pole. Dissolved methane and the nutrients ammonia, nitrite, nitrate, phosphate, and silicate are measured at the station.

Nutrient patterns obtained during spring and summer 2006 reflect the development of nutrient concentrations during the annual spring phytoplankton bloom. Methane measurements showed a tidal dependence with maxima at low tide, which emphasizes the tidal flat sediments as the dominating source for methane in the open coastal water column.

2.1 Introduction

The Wadden Sea is a highly dynamic environment due to physical and biological forcing. In addition to eutrophication, human activities (e.g. dike building, land reclamation) and freshwater contribution influence this coastal system (e.g. Flemming and Davis, 1994; Flemming and Nyandwi, 1994; Dellwig et al., 2000; Hinrichs et al., 2002; Colijn and van Beusekom, 2004). While the Wadden Sea of the Southern North Sea is mainly controlled by physical forcing in autumn and winter, biological processes dominate the system during spring and summer (e.g. Lunau et al., 2006; Dellwig et al., 2007b). Biomass formation in tidal flat areas is dominated by phytoplankton and microphytobenthos production (Reid et al., 1990), with production rates depending on nutrient availability and light regime (Colijn, 1982). Seasonal as well as tidal changes in aggregate composition and concentration affect the light attenuation coefficient. These changes depend on tidal current velocities, shear rates, and

aggregate formation processes (Behrends and Liebezeit, 1999; Grossart et al., 2004; Lunau et al., 2006; Dellwig et al., 2007b). Wadden Sea data for dissolved nutrients are predominantly available at an annual or seasonal resolution (de Jonge and Postma, 1974; Helder, 1974; van Bennekom et al., 1974; Martens, 1989; van Beusekom and de Jonge, 2002). Nutrient time-series on a tidal resolution are essentially lacking. According to Langner-van Voorst and Höpner (1996), Villbrandt et al. (1999), Billerbeck et al. (2006a,b), and recent pore water measurements (Beck et al., pers. comm.), tidal flat sediments presumably are an important source for dissolved nutrients and dissolved inorganic and organic carbon, and may contribute to the budget of the open water column. Despite of rather small bacterial numbers and low organic matter contents (Bergamaschi et al., 1997; Llobet-Brossa et al., 1998; Rusch et al., 2003) the sandy sediments dominating the investigated area are characterized by a high organic carbon mineralization rates (Cammen, 1991; D'Andrea et al., 2002; Huettel et al., 2003).

In coastal zones values of dissolved methane may be orders of magnitudes higher than in open ocean waters (e.g. Scranton and McShane, 1991; Bugna et al., 1996). Methane is generated within the tidal flat sediments by archaea (e.g., *Methanomicrobiales* and *Methanosarcinales*, spp.: Wilms et al., 2006a) and is transported by diffusion and advection (Hovland et al., 1993) into the open water column. While methane data for European rivers, estuaries, and the North Sea are available (Scranton and McShane, 1991; Rehder et al., 1998; Upstill-Goddard et al., 2000; Middelburg et al., 2002), information for the Wadden Sea is still scarce.

In spring 2001 a research group was established to investigate biogeochemical processes in the Wadden Sea of Spiekeroog Island (NW Germany). One major aim of this project is to evaluate, whether the Wadden Sea system presently is in a steady state or whether it is subject to a net loss or gain of material and compounds. Modelling, which forms an integral part of the research group, also relies on continuous data sets to tune model parameters and to verify model results. Especially the online availability of nutrient data allows monitoring the biological state of the tidal flat system. The time-series station provides the unique opportunity to obtain data sets over extended time periods at high temporal resolution.

2.2 Geographical settings

Figure 2.1 shows the study area in the Southern North Sea and the position of the time-series station between Langeoog and Spiekeroog Islands in the main tidal inlet (Otzumer Balje) of the back barrier area of Spiekeroog Island. The water depth (below mean sea level)

is 13.5 m at position 53°45'01.00" N and 007°40'16.30" E. The back barrier tidal flat area is characterized by semidiurnal tides under mesotidal conditions (tidal range 2.2-2.8 m) and encompasses an area of about 74 km² (Walther, 1972). During low tide, the area of dry-falling tidal flat sediments amounts to 46 km² during spring tide and 30 km² during neap tide. The tidal flat sediments are dominated by sands in the western part while in the eastern part mixed and muddy deposits prevail. The permeable sandy sediments may significantly influence the geochemical budgets of the Wadden Sea water column owing to draining pore waters during ebb tide (e.g. Dellwig et al., 2007a).

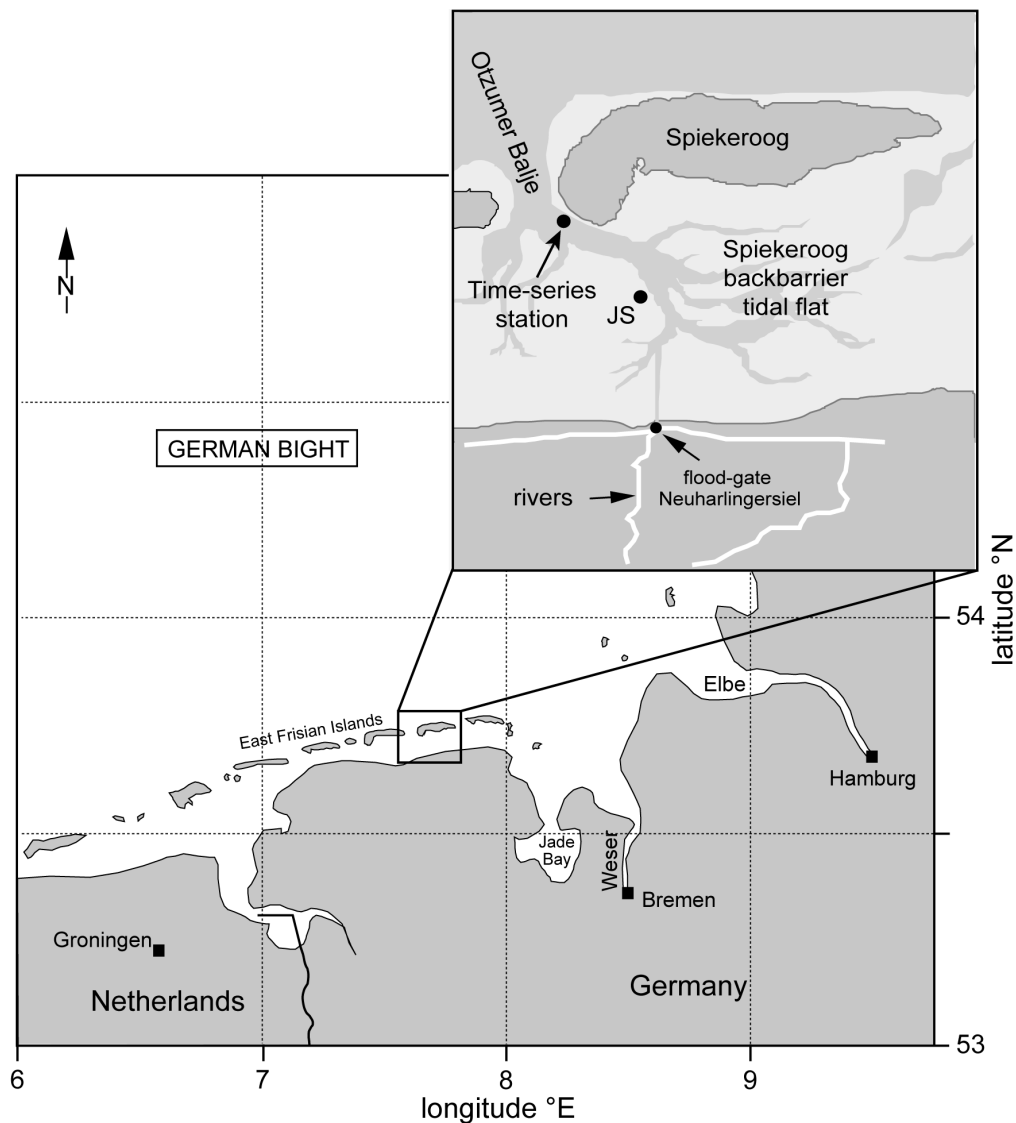


Fig. 2.1. Map of the study area in the German Bight. The detailed map shows Spiekeroog Island, the back barrier tidal flats, the position of the time-series station in the tidal inlet (Otzumer Balje), and the pore water sampling site Janssand (JS).

2.3 Materials and methods

2.3.1 Time-series station

The time-series station (Fig. 2.2 and Fig. 2.3) consists of a 35.5 m long steel-pole with a diameter of 1.6 m. About 15 m of the pole are grounded in the sediment to resist tidal currents, wind, and floating ice sheets. The water column covers 13.5 m of the pole at mean sea level and the remaining 7 m are above the water line. This station is designed for operation throughout the year, even during heavy storms and ice winters.



Fig. 2.2. Photograph of the time-series station

On top of the pole a platform houses two containers, one for the electrical system, containing storage batteries, fuse boxes, battery charging equipment, and a PLC (Programmable Logic Controller), with the latter controlling the electrical equipment. The second container houses a station computer for data storage, power management, and sensor control. A wind generator, solar panels, and a gas generator (in case of insufficient wind and sun) are located on an upper platform for electric power supply. The whole station has a self-sufficient electrical system and does not require any connection to onshore electricity networks.

Ladders provide access to the station, the platforms, and the inner pole. The submerged part of the pole contains ten flanges and sensor tube openings, ranging from 0.5 m to 11.5 m above sea floor (Fig. 2.3). These openings serve to install sensor tubes in the prevailing tidal current direction. Five openings are equipped with exchangeable sensor tubes (inner diameter 22 cm) at 1.5 m, 3.5 m, 5.5 m, 7.5 m, and 9.0 m above the seafloor. This setup enables measurement of several physical parameters (temperature, pressure in the lowermost tube, and conductivity) at different depths to identify possible vertical gradients.

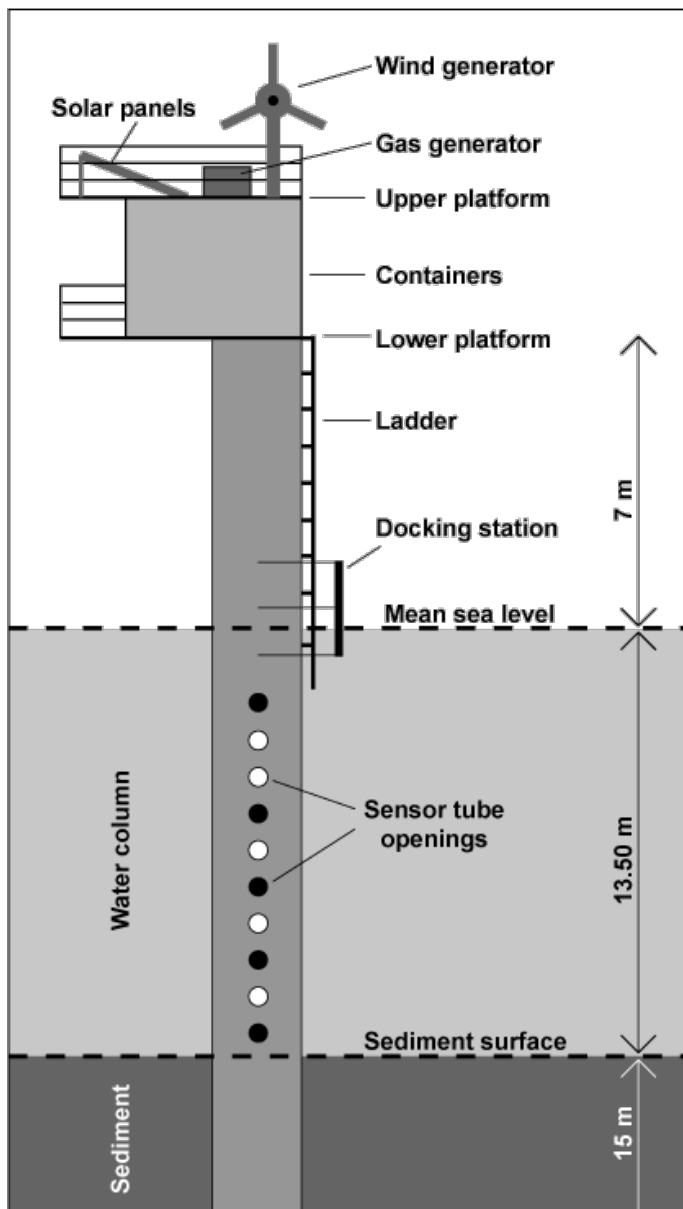


Fig. 2.3. Sketch of the time-series station. White sensor tube openings are equipped with sensor tubes, black ones are not.

For nutrient measurements, water from the sensor tube 9.0 m above seafloor is used. The sensor for methane measurements is attached at the exterior pole at a fixed position about 0.5 m below low-tide water level.

The entire system described above is controlled by a land-based computer station located at the University of Oldenburg. It is possible to connect to the time-series station via modem and wireless LAN (local area network). Special remote software enables to manage the whole measuring and controlling equipment. Data stored on the time-series station computer are transferred automatically every four hours to the land station. If required, data transmission can be initiated manually.

2.3.2 Nutrient analyses

Figure 2.4 shows a sketch of the hardware set-up of the nutrient analysers. The belt filter and the analysers are mounted to the uppermost ladder at the inside of the pole. While the filter system is unmovable fixed, the nutrient analysers and a container (20 L) with imidazole buffer solution for nitrate measurements are situated on swivel-mounted racks. All racks are attached by hinge joints to a stainless steel pipe. This concept allows maintenance of the analysers without dismounting. De-ionized (DI) water is stored in three fibre reinforced polyethylene (PE) bags (total volume 150 L).

At the 9.0 m sensor tube a water-inlet device is installed, consisting of a ball valve, a self-closing corrosion-free magnetic valve (Bürkert, Fluid Control System Type 0121, Germany), and a sediment trap. A water volume of approx. 7 L min^{-1} is transported by a membrane pump (Johnson, Aqua Jet, WPS 2.4, 24V, Germany) to the belt filter (Metrohm, Series 01.12, Germany). If the water flow falls below an alarm threshold, the entire system is stopped to prevent damage. The cellulose filter belt (length 100 m; Schleicher & Schuell, No. 1574, Germany) has a pore size of 7 to 12 μm . Prior to analysis the entire tubing from the inlet via the belt filter towards the outlet is rinsed for three minutes, followed by a five minutes rinse of the nutrient analysers with filtered water. After nutrient analysis the analysers are cleaned with 75 mL DI-water from the PE bags. The supply of DI-water lasts for about two weeks when measurements are performed once every hour.

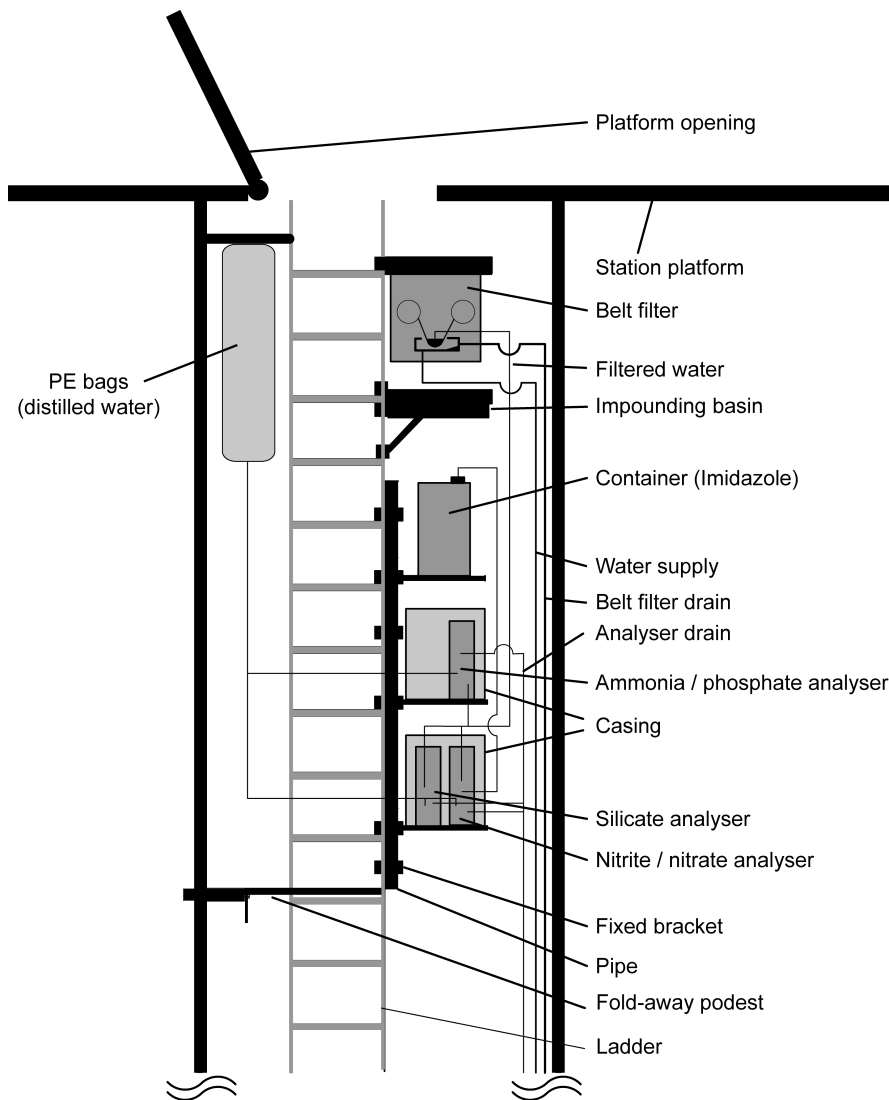


Fig. 2.4. Sketch of nutrient measurement hardware arrangement located in the upper part of the pole.

Controlling and monitoring of nutrient analyses, including pump, valve, and flow meter, is assured via Soft-PLC software (-4H-Jena, Germany). The Soft-PLC is subdivided into four main sub-programmes: 'wait for start', 'operate', 'stop water', and 'error water'. Continuous nutrient measurements for ammonia, nitrite, nitrate, phosphate, and silicate are performed by Systea μ Mac1000 analysers (Systea, Italy). These analysers are based on a loop-flow reactor (LFR) and loop flow analysis (LFA) technology. The filtered sample is pumped into the analysers and the required reagents are added automatically by negative pressure. Determination of nutrients is performed by conventional photometry.

Three analysers are installed on the station for ammonia and phosphate, nitrite and nitrite + nitrate, and silicate. Analysers for two parameters operate in sequential mode. After each measurement a wash cycle with DI-water is performed automatically. If concentrations

exceed the calibration range by a given percentage (Table 2.1, 'Full range'), the analysers automatically dilute the sample and repeat the measurement (dilution factor approx. 10). An overview of determination methods, calibration ranges, cuvette lengths, and wave lengths is given in Table 2.1. Reagents used for nutrient measurements have a shelf life of about two to three weeks, depending on the ambient temperature inside the pole. Approximately 330 to 500 analyses of each parameter are performed in-between maintenance intervals. Despite of the temperature-depending durability of reagents, no interference of measurements with temperature or humidity of the inner pole was recognized. Calibration and reproducibility measurements are performed with solutions containing $11.1 \mu\text{mol L}^{-1}$ ammonia, $2.1 \mu\text{mol L}^{-1}$ phosphate, $60 \mu\text{mol L}^{-1}$ nitrite + nitrate ($6.5 \mu\text{mol L}^{-1}$ as nitrite), and $50 \mu\text{mol L}^{-1}$ silicate (see Table 2.1).

Table 2.1. Measuring principles and parameters of nutrient determination.

Parameter	Reference	Cuvette length (mm)	λ (nm)	Calibration range ($\mu\text{mol L}^{-1}$)	SD*	Full range** (%)	Remarks
Ammonia	Patton and Crouch (1977)	50	660	0.01 – 11.1	0.4	350	Trisodium citrate and disodium EDTA are added to prevent precipitation of Ca and Mg hydroxides or carbonates.
Phosphate	Murphy and Riley (1962)	50	660	0.01 – 2.1	0.1	500	
Nitrite	Shinn (1941) Bendschneider and Robinson (1952)	15	530	0.01 – 6.5	0.3	266	
Nitrite + Nitrate	Morris and Riley (1963) Strickland and Parsons (1968)	15	530	0.17 – 60	1.85	184	Internal copper-coated cadmium granule column (operation time ~1000 samples) to reduce nitrate to nitrite
Silicate	Chow and Robinson (1953)	15	850	0.38 – 50	1.01	208	

* Standard deviation of calibration solution measurements

** % excess of maximum calibration concentration measured without dilution

2.3.3 Methane measurement

For the measurement of dissolved methane (CH_4) in surface water, a sensor (Capsum Technologies, Germany) is installed at the exterior pole at 10.5 m above the seafloor. The measuring principle of the sensor is based on the adsorption of hydrocarbon molecules (mainly CH_4) on a tin dioxide semiconductor detector, which results in resistance variation as reported by Garcia and Masson (2004) and Marinaro et al. (2004). During operation, hydrocarbon molecules diffuse through a silicone membrane into the detector chamber. The detection limit of the sensor is $0.02 \mu\text{mol L}^{-1}$. As the measurement is diffusion-controlled, the sensor has been modified by adding a pump (Rule, 360 GPh, 23 L h^{-1} , USA), which ensures a constant flow of water to the membrane surface and reduces equilibration time. Furthermore, the constant jet of water protects the membrane from fouling.

For data verification methane was determined in water samples by gas chromatographic headspace analysis as described by Niewöhner et al. (1998). Sampling was done with a FreeFlow sampler (Hydro-Bios, Germany) at the time-series station. The water was immediately transferred into serum flasks, crimped, and frozen upside down in dry ice. The results (Fig. 2.5) generally show a reasonable agreement between both techniques with a mean sensor deviation of +11%, most likely caused by the inaccuracy of sensor calibration.

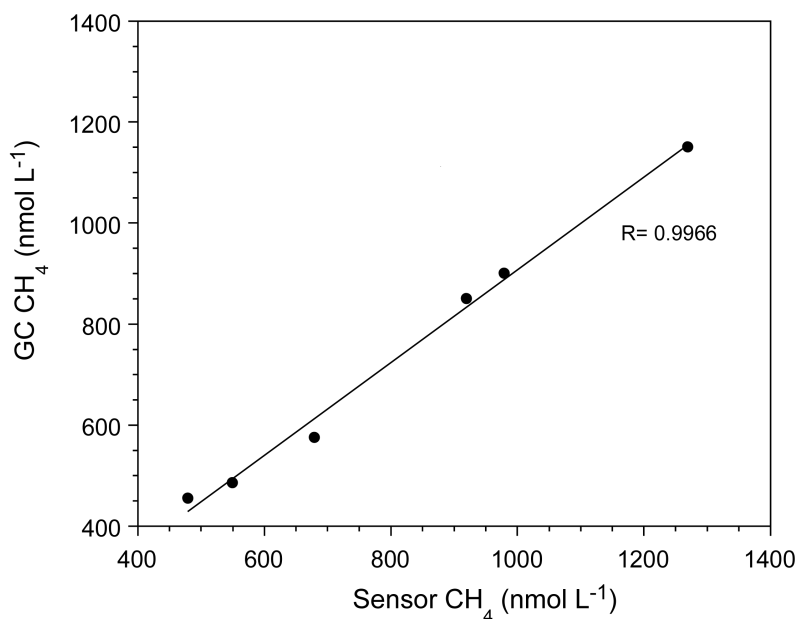


Fig. 2.5. Methane measurements of sensor vs. GC.

2.4 Results and discussion

2.4.1 Nutrients

Concentrations of silicate, phosphate, nitrate, nitrite, and ammonia measured from April to July 2006 at our time-series station are shown Figure 2.6. In Table 2.2 mean values of ship-based measurements from previous years are shown for comparison.

Decreasing concentrations of silicate in April (from about 20 $\mu\text{mol L}^{-1}$ to minimum values of on average 0.26 $\mu\text{mol L}^{-1}$) reflected the development of the spring diatom bloom (Fig. 2.6a). The subsequent breakdown of this algal bloom in late April to early May led to a moderate increase in silicate of up to 5 $\mu\text{mol L}^{-1}$, due to decomposition of diatom frustules within the water column of the back barrier area. Such processes may be accelerated by high shear stress due to tidal forces. Maximum concentrations were observed at low tide (Fig. 2.6f), which suggests the tidal flats to be an essential source for dissolved silicate. Pore water measurements from a sand flat site (Janssand (JS), Fig. 2.1b) between March and June 2006 revealed an average concentration of 60 $\mu\text{mol L}^{-1}$ in the upper 10 cm of the sediment (M. Beck, pers. comm.). In contrast, during high tide silicate remained extremely low, caused by the influx of silicate-low North Sea water. Additionally to the above mentioned mineralization processes a distinctly lower consumption of dissolved silicate by diatoms after breakdown of the spring bloom must be taken into account. Thus, the pore water discharging at low tide will impact silicate water column signals. Due to the lack of silicate mineralization rates as well as pore water fluxes, we cannot assess the importance of these two processes at this point of time.

Table 2.2. Mean concentrations of ship-based measurements in the tidal inlet at time-series station position.

Month	Year, day	Silicate ($\mu\text{mol L}^{-1}$)	Phosphate ($\mu\text{mol L}^{-1}$)	Nitrite ($\mu\text{mol L}^{-1}$)	Nitrate ($\mu\text{mol L}^{-1}$)	n
April	2000, 19 - 20	13.6 (7.4/32.2)	0.5 (0.2/0.8)	1.0 (0.5/1.8)	30 (24.6/34.9)	48
	2003, 23 - 26	2.9 (0.1/9.1)	0.2 (0.02/1.0)	0.5 (0.3/1.0)	10.0 (6.9/13.4)	82
	2005, 27	1.7 (0.6/2.9)	0.4 (0.1/0.8)	0.4 (0.3/0.5)	5.1 (3.9/9.2)	25
May	2000, 17	8.6 (1.2/16.1)	0.5 (0.1/1.1)	0.5 (0.1/1.8)	2.0 (0.4/5.0)	21
July	2005, 20 - 22	2.9 (0.6/9.3)	0.5 (0.0/1.1)	0.05 (0.0/0.2)	0.7 (0.0/2.4)	55

Values in brackets show concentration ranges (min/max). The numbers of analysed samples are given by 'n'. Nutrient measurements are performed according to Liebezeit et al. (1996).

The minor decrease in silicate in early May might be due to a further, less pronounced onset of diatom growth, followed by another breakdown at the end of May. The subsequent increase in distinct amplitudes with higher values at low tide point towards recycling processes within the Wadden Sea system.

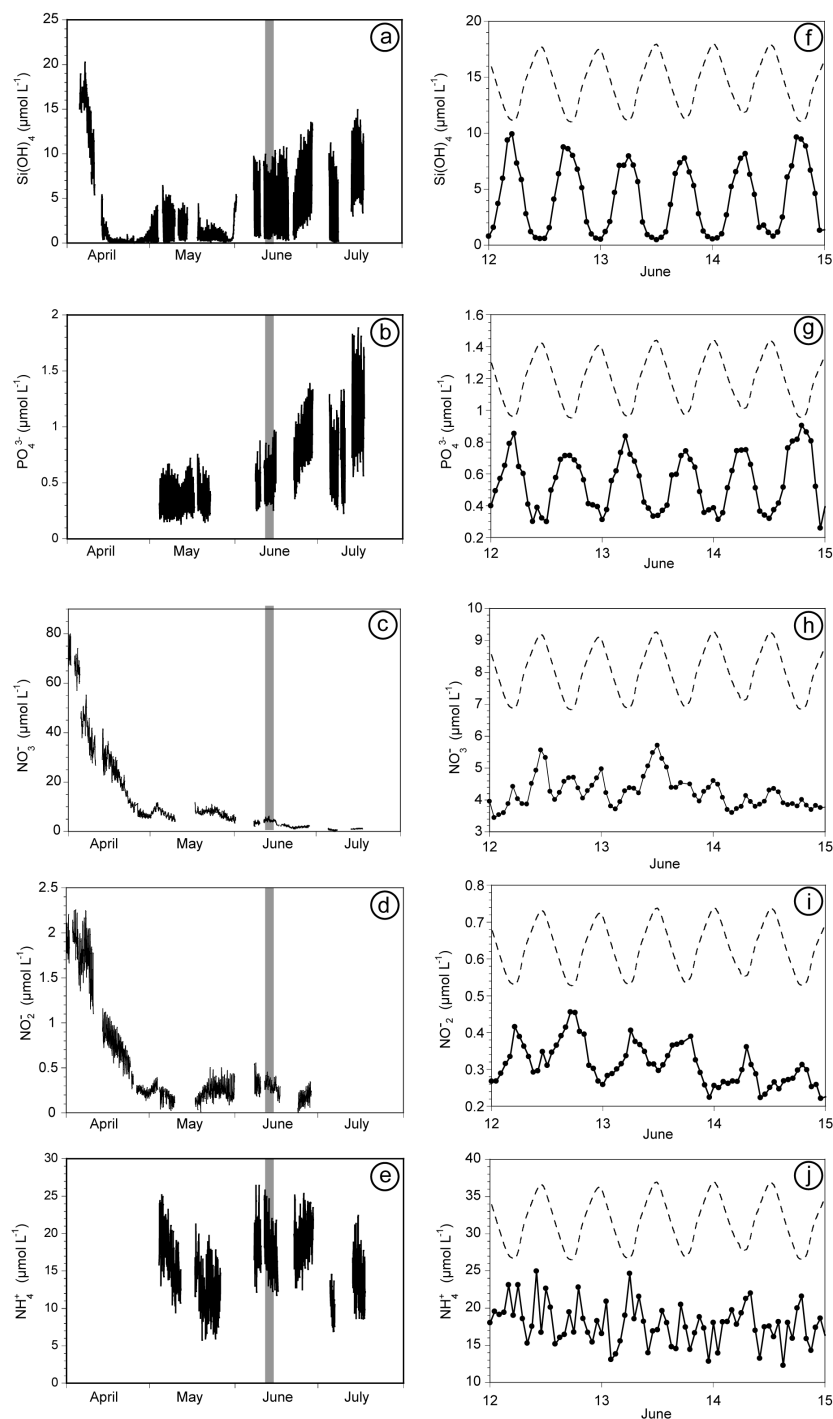


Fig. 2.6. Nutrient concentrations at the time-series station from April to July 2006 (a-e). The grey bar indicates the time period shown in f-j, where the tidal resolution of the individual parameter is shown. The dots mark the hourly measurements and the tidal gauge is given by the dashed line.

Phosphate showed a general increase during the time interval, with a tidal signal similar to that of silicate (Figs. Fig. 2.6b and g). This behaviour was most likely caused by release of phosphate from the tidal flat sediments as well as re-mineralisation processes within the water column. During winter phosphate is scavenged by ferric oxyhydroxides within the sediments. More pronounced reducing conditions during warmer periods lead to reduction of iron compounds and release of phosphate (Gunnars and Blomqvist, 1997). A further source during low tide is the decomposition of particulate phosphate imported from the North Sea, as described by DeJonge and Postma (1974). Because of technical problems, April data were not available. However, time-series station data combined with ship based measurements of previous years (2000, 2003, and 2005) showed a mean value in April of about $0.4 \mu\text{mol L}^{-1}$, which supports the trend of increasing concentrations from spring to summer.

Nitrite and nitrate showed a general decrease from April to July (Figs. Fig. 2.6c and d) due to consumption by phytoplankton, where nitrate is used for biomass formation. In contrast to nitrite, which showed the typical tidal pattern with maxima at low tide, nitrate revealed an indifferent behaviour (Figs. Fig. 2.6h and i). In April maximum concentrations occurred during high tide (not shown), which is supported by elevated North Sea values. Raabe et al. (1997) reported concentrations of about $10 \mu\text{mol L}^{-1}$ for the German Bight. However, in July the pattern changes to high nitrate values (on a generally low level) at low tide (not shown), possibly caused by re-mineralisation processes within the upper sediment layer of the tidal flats. The pattern of nitrate in June (Fig. 2.6h) showed no distinct tidal dependence, which may be caused by enhanced bacterial ammonia oxidation during high and low tide. In contrast, tidal behaviour of nitrite (Fig. 2.6i) reflected the release of nitrite enriched pore waters during low tide.

Ammonia (Fig. 2.6e) in general revealed almost no coupling to other nutrient patterns. Fig. 2.6j shows a tendency towards lower values occurring during high tide and low tide in parallel to higher nitrate concentrations, probably caused by bacterial ammonia oxidation. Ammonia may have two different sources. Enhanced bacterial activity after algal bloom breakdown within the water column may lead to ammonification of proteins and amino acids (Herbert, 1999) and corresponding increases in ammonia concentration. Bacteria cell counts (J. Stone, unpubl. data) of up to $6 \cdot 10^6$ cells mL^{-1} in May 2006 support the assumption of high bacterial activity, when compared to cell counts with at maximum $2 \cdot 10^6$ cells mL^{-1} in January 2005. The second source is the pore water, which is enriched in ammonia (up to $100 \mu\text{mol L}^{-1}$, M. Beck, pers. comm.), when compared to the Wadden Sea water column. Both, microbial production within the water column and the pore water signal seem to impact the water column signal, thus obscuring tidal variation (Fig. 2.6j).

2.4.2 Methane

Figure 2.7a shows surface concentrations of dissolved methane from September to November 2005. The concentration ranges between 0.12 and 0.54 $\mu\text{mol L}^{-1}$ (mean 0.29 $\mu\text{mol L}^{-1}$). Such values correspond well to concentrations reported for estuaries and rivers of the German Bight (Scranton and McShane, 1991; Upstill-Goddard et al., 2000; Middelburg et al., 2002).

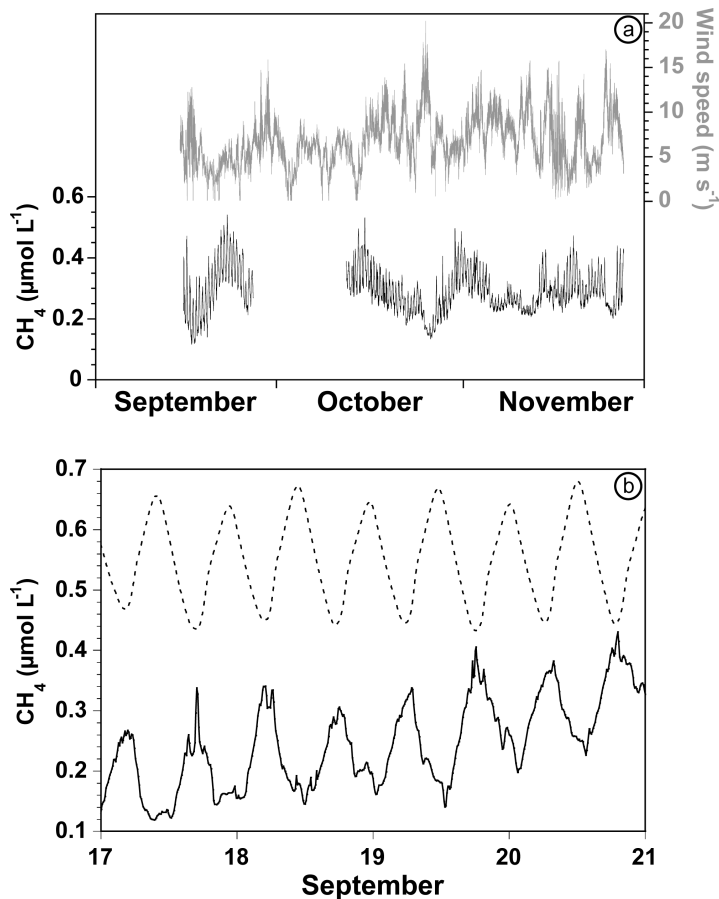


Fig. 2.7. Methane concentrations at the time-series station from September to November 2005 (a).Methane concentrations (black) and corresponding wind speed data (grey). (b) Tidal pattern from 17th to 21st of September 2005. The dashed line denotes the tidal gauge.

The concentration pattern shows a tidal dependence with maxima at low tide (Fig. 2.7b), which indicates the Wadden Sea to be a source for methane. Pore water draining from tidal flats seems to be the main source for dissolved methane in this system. Pore water methane concentrations of up to 180 $\mu\text{mol L}^{-1}$ at 4.0 m and 90 $\mu\text{mol L}^{-1}$ at 1.0 m sediment depth and additional measurements of tidal creek waters with concentrations up to 3.7 $\mu\text{mol L}^{-1}$ support this assumption.

The development and spontaneous change in concentration, like in late October 2005 (Fig. 2.7), was apparently caused by variation of wind speed and direction (data not shown). As described by Scranton and McShane (1991) increasing wind speed ($>10 \text{ m s}^{-1}$) leads to enhanced degassing of methane from the water column, whereas long-term changes are a consequence of changes in the variation of the tidal water level. The larger the amplitude from low tide to high tide, the more pore water is released from the sediments, and vice versa. This effect additionally supports the assumption that tidal flat pore waters form the main source for dissolved methane in the Wadden Sea.

2.4.3 Maintenance of the instrumentation

Larger data gaps are due to different reasons, like insufficient electrical power supply owing to low production by the wind generator and solar panels, clogging/breakdown of the water supply pump, and severe weather conditions preventing maintenance work. The latter reasons are in most cases responsible for malfunctions and data loss. Continuous measurements in the study area require intensive maintenance efforts, due to pronounced bio-fouling of sensor components and tubes. The sensor tubes have to be cleaned or replaced manually. If necessary, anti-fouling paint has to be applied. Analyser tubings are preferentially made of silicone for inhibition of fouling. Despite of this precaution tubings need to be cleaned and/or exchanged approx. every four months, since bio-films might be a source for ammonia and phosphate as well as a sink for ammonia by nitrifying bacteria.

We will try to reduce these effects by applying new anti-fouling techniques (e.g. electrochemical). Additionally to bio-fouling, high SPM concentrations complicate the operation of a continuous and autonomous time-series station. High SPM concentrations alter the durability of the belt filter. The life-time of a 100 m filter belt varies between three weeks and two months, depending on the SPM load.

The pump of the methane sensor is treated with commercial anti-fouling paint which protects it from fouling for more than two months, but the silicone membrane of the sensor has to be changed every four to six weeks due to abrasion by the water-jet of the pump. However, this abrasion protects the membrane against bio-film formation

The analysers perform wash cycles with distilled water after each measurement. This largely inhibits fouling inside of the analysers. But on the longer term they are affected by (bio-) film formation and residua of analysis solutions. Therefore the analysers have to be periodically removed and cleaned on-shore.

2.5 Summary

It has been demonstrated that a continuous nutrient and methane analysis of surface waters by a time-series station is feasible in a highly dynamic area, the NW German Wadden Sea. The direct measurements do not require sample storage or treatment such as preservation. Hourly sampling frequencies of nutrient measurements allow resolving tidal, diurnal and seasonal variability. Such a time-series station can provide the necessary data for long-term monitoring of processes in coastal waters, e.g. the development of toxic plankton blooms. We have used the data of the times-series station for the planning of ship-based sampling campaigns focussed on questions related to the development and breakdown of plankton blooms. The combination of meteorological and oceanographic parameters with nutrient data (and methane) allows new insights into the dominant driving forces of the bioreactor Wadden Sea. The impact of events like heavy storms, ice winters or other extreme weather conditions can be evaluated.

Besides the on-line availability these data may help to verify mathematical models describing the complex Wadden Sea system, and to perform balance calculations for specific compounds like nutrients. In summary, the operation of the station helps to answer one of the key questions whether the Wadden Sea system is in a steady state regarding import/export from or to the German Bight and to the North Sea.

Acknowledgements

The authors thank A. Braun, B. Wachowicz, and I. Ötken for maintenance of the time-series station. We are also grateful to M. Beck (ICBM, University of Oldenburg) for providing unpublished pore water nutrient data. We wish to thank K. Enneking (University of Bremen) for methane GC measurements. Thanks to -4H- JENA engineering GmbH (Jena, Germany) for participating in planning meetings and establishing the station and the crew of R/V Senckenberg for support during sampling. Three anonymous reviewers are thanked for their constructive comments. This study was funded by the Deutsche Forschungsgemeinschaft (DFG) through grants FOR 432/1-1, BR 775/14, and RE 624/5.

3 Methane in the southern North Sea: Sources, spatial distribution and budgets

Maik Grunwald, Olaf Dellwig, Melanie Beck, Joachim W. Dippner, Jan A. Freund, Cora Kohlmeier, Bernhard Schnetger, Hans-Jürgen Brumsack

This chapter has been published 2009 in *Estuarine, Coastal and Shelf Science* 81, 445-456.

Abstract

Measurements of methane (CH₄) so far have always shown supersaturation in the entire North Sea relative to the atmospheric partial pressure and the distribution of surface CH₄ reveals a distinct increase towards the shore. Since North Sea sediments presumably are an insignificant source for CH₄ the coastal contribution via rivers and tidal flats gains in importance.

In this work, CH₄ data from the River Weser, the back barrier tidal flats of Spiekeroog Island (NW Germany), and the German Bight are presented. Results from the River Weser are compared to other rivers draining into the German Bight. Measurements in the tidal flat area of Spiekeroog Island highlight this ecosystem as an additional contributor to the overall CH₄ budget of the southern North Sea. A tidally driven CH₄ pattern is observed for the water column with maximum values during low tide. Tidal flat sediments turn out to be the dominating source because pore waters discharged during low tide are highly enriched in CH₄. In contrast, the freshwater contribution to the tidal flats by small coastal tributaries has almost no impact on water column CH₄ concentrations. The CH₄ level seems to be disturbed irregularly by wind forcing due to elevated degassing and prevention of advective flow when tidal flats remain covered by water.

Based on our data, two model calculations were used to estimate the impact of tidal flats on the CH₄ budget in the German Bight. Our results demonstrate that the back barrier tidal flats of the east Frisian Wadden Sea contribute CH₄ in an order of magnitude between the Wash estuary and River Elbe and thus have to be considered in budget calculations.

3.1 Introduction

Methane (CH₄) is the most abundant organic compound in the Earth's atmosphere. It contributes largely to the greenhouse effect by absorption of infrared radiation and photochemical reactions (Crutzen and Zimmermann, 1991; Lelieveld et al., 1993). CH₄ affects tropospheric ozone, hydroxyl radicals, and carbon monoxide concentrations as well as stratospheric chlorine. Principal atmospheric reactions of CH₄ are described in detail by e.g. Cicerone and Oremland (1988). Methane is produced in stomachs of ruminant mammals and by termites, but most biogenic CH₄ originates from bacterial production under anaerobic conditions in wetlands, swamps, rice fields, and landfills (Cicerone and Oremland, 1988; Sass et al., 1990; Fung et al., 1991; Bartlett et al., 1992; Roulet et al., 1992a; Roulet et al., 1992b). Marine environments may account for up to 10% of the global atmospheric CH₄ budget (Oremland et al., 1987; Cicerone and Oremland, 1988; Bange et al., 1994). Marine CH₄ produced within the water column originates from bacterial production in the digestive tracts of zooplankton (Bianchi et al., 1992; Marty, 1993; de Angelis and Lee, 1994) and from sinking organic particles (Karl and Tilbrook, 1994). However, the highest amount of CH₄ is produced by methanogenesis in deeper sediment layers of productive coastal areas (Scranton and McShane, 1991; Hovland et al., 1993). Further sources are river runoff (de Angelis and Lilley, 1987; Scranton and McShane, 1991; Middelburg et al., 2002) and ground water discharge (Bugna et al., 1996; Kim and Hwang, 2002). Besides microbial oxidation (Ward et al., 1987; Jones, 1991), removal of dissolved CH₄ occurs mainly via sea-air flux by both diffusive and turbulent transfer as well as bubble effervescence (Upstill-Goddard, 2006). Increasing atmospheric CH₄ concentrations during the last two centuries (Ehhalt et al., 2001) document that production by above mentioned processes is higher than removal.

Although shelves and estuaries represent only a small part of the world's ocean area they contribute about 75% to the global oceanic CH₄ flux (Bange et al., 1994). In this contribution we focus on the CH₄ distribution pattern in the German Bight (southern North Sea) and the adjacent coastal environment. Riverine input is regarded as a major coastal source (Scranton and McShane, 1991; Upstill-Goddard et al., 2000; Middelburg et al., 2002; Bange, 2006), while the contribution of intertidal flats has not been studied so far. In this contribution we present data for the water column and pore water from the back barrier tidal flats of Spiekeroog Island. On the basis of tidal CH₄ patterns, two different model approaches are used to estimate the CH₄ exchange between the tidal flat area and the German Bight. The resulting annual CH₄ discharge is compared with riverine CH₄ input from literature in order to assess the relevance of tidal flat areas for the coastal CH₄ cycle.

3.2 Geographical setting

The Wadden Sea of the southern North Sea covers an area of about 9300 km² and stretches along a 500 km long coastline from Den Helder in The Netherlands to Esbjerg in Denmark (Ehlers, 1994). The semi-enclosed East Frisian Wadden Sea with its barrier islands amounts to about 15% of the entire area, which is connected to the German Bight by tidal inlets. The system is characterized by semidiurnal tides with a tidal range of 2.2-2.8 m. The dominant M₂ tide has a period of 12 hours and 25 minutes and the S₂ tide of 12 hours forms a spring-neap tide cycle of app. 14.8 days. The main study site of this contribution is the back barrier tidal flat area of Spiekeroog Island, which covers about 74 km² (Walther, 1972). Freshwater is contributed in irregular intervals to the back barrier tidal flats via a flood-gate in Neuharlingersiel (Fig. 3.1b).

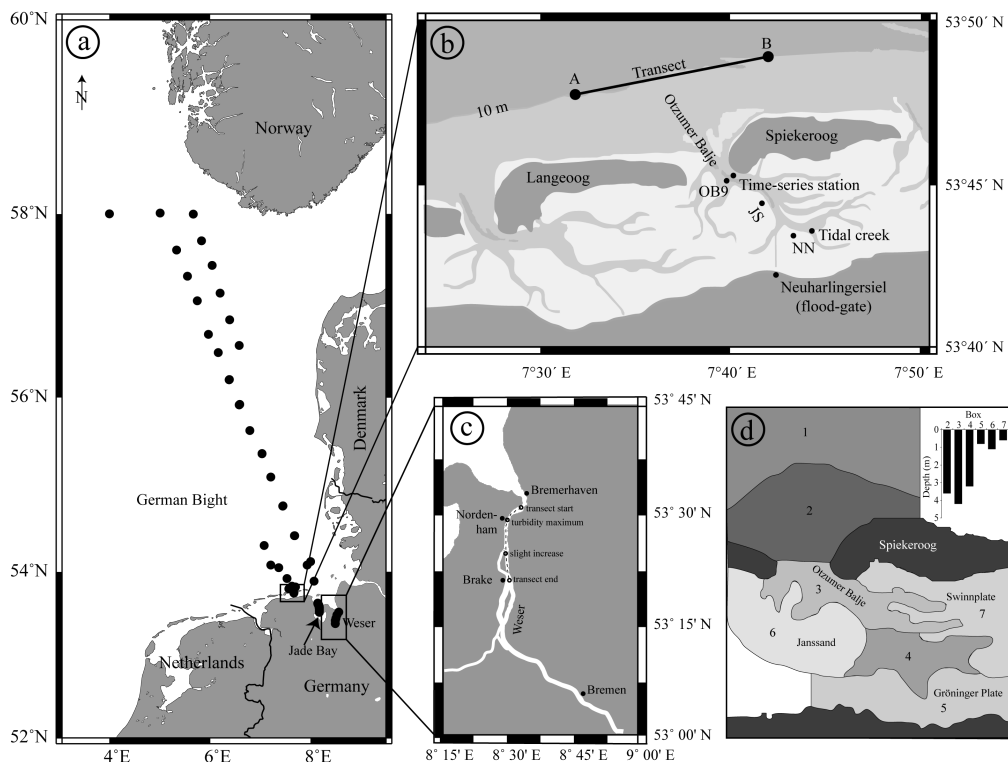


Fig. 3.1. (a) Map of the study area in the German Bight. Black dots denote sampling sites. The detailed map (b) shows Spiekeroog and Langeoog Island, the transect in front of the islands, the back barrier tidal flats, the position of the time-series station and the sampling site OB9 in the tidal inlet (Otzumer Balje), the pore water sampling sites Janssand (JS) and Neuharlingersiel Nacken (NN), and the position of tidal creek measurements. White areas in Fig. 3.1b indicate tidal flats emerging during low tide. Map (c) shows the transect of River Weser. Map (d) shows the classification of boxes used in the Euler-Lagrangian model including averaged water depths of the boxes.

The catchment area of the flood-gate encompasses about 125 km² and is characterized by marsh soils in the north and fen peats and forests in the south. The amount of freshwater discharge depends on precipitation in autumn and winter, while during the vegetation growth period in late spring and summer the freshwater contribution is distinctly lower (Dellwig et al., 2007a).

3.3 Material and methods

3.3.1 Methane measurements

Dissolved CH₄ was determined by using a sensor (Franatech, formerly: Capsum Technologies, Germany) for continuous measurements during pre-defined time intervals. Hydrocarbon molecules diffuse through a silicone membrane into the detector chamber. As the measurement is diffusion-controlled we modified the sensor by installing a pump (Rule, 360 GPh, 27.3 L min⁻¹) to ensure a constant flow of water to the membrane surface. The measuring principle of the sensor is based on the adsorption of hydrocarbon molecules (mainly CH₄) on a tin dioxide semiconductor detector. This leads to changes in resistance proportional to the gas concentration (Garcia and Masson, 2004; Marinaro et al., 2004). The calibrated concentration range of the sensor is 20 – 10,000 nM. Sensor accuracy was checked by head space gas chromatographic (GC) measurements with a flame ionisation detector (Varian CX-3400 equipped with a capillary column, plot-fused silica column No.7517, 25 m by 0.53 mm, Al₂O₃/KCl coated; Chromopack) according to the setup described in Niewöhner et al. (1998). Accuracy (2.9%) and precision (13.9%) of GC measurements were controlled using a 100 ppmv standard of CH₄. The deviation of sensor data to GC measurements is +11%, most likely due to inaccuracy of sensor calibration (Grunwald et al., 2007).

Data from the time-series station (Grunwald et al., 2007) were determined in intervals of 10 minutes. The sensor was fixed in the water column about 11 m above seafloor. The immersion depth of the sensor varies from 0.5 to 3.5 m depending on the state of the tidal cycle.

During ship-based measurements the sensor was fixed at app. 2 m water depth and the measurement interval was 1 min. During transects off the islands of Langeoog and Spiekeroog (Fig. 3.1b) ship speed was 5 kn in east-west direction. Each transect took about one hour. The River Weser transect started 4 hours after local high tide and lasted until about 2.5 hours before low tide.

Pore water samples were taken by an in-situ sampler (Beck et al., 2007), which consists of a permanently installed polyethylene pipe with 20 sampling ports down to 5 m. Each port is connected via Teflon tubes to the sediment surface where pore water from

different depths can be extracted by syringes. Pore waters were transferred into serum flasks, sealed, and immediately frozen upside down in dry ice. Methane was determined by GC head space measurements in the laboratory.

Freshwater measurements at the flood-gate in Neuharlingersiel (Fig. 3.1b) were performed by using the sensor at a depth of 1 m with a recording interval of 10 min.

3.3.2 Sulphate analysis

Pore water samples for sulphate analysis were taken from in-situ samplers. All samples were filtered immediately using Whatman glass microfibre filters GF/C (1.2 μm) which were pre-combusted at 400 °C. Samples were stored in PE vials which were pre-rinsed with purified water (18.2 M Ω). Sulphate was analysed by ion chromatography (Dionex DX 300) at 250-fold dilution. Precision and accuracy were 3% and -5.3%, respectively.

3.3.3 Suspended particulate matter

Samples for suspended particulate matter (SPM) were taken from surface water in the River Weser. Depending on SPM load, 200 to 400 mL of water were filtered through pre-weighed Whatman glass microfibre filters GF/F (0.7 μm), rinsed with 60 mL purified water, dried at 60 °C for 48 h, and re-weighed for determination of total SPM.

3.3.4 Saturation calculations

Methane percent saturations were calculated using the solubility equilibration of Wiesenburg and Guinasso (1979). For North Sea and Wadden Sea saturation calculations, salinity and temperature data of a calibrated CTD (Model OTS 1500, ME Meerestechnik-Elektronik, Germany) were used. For freshwater calculations salinity and temperature were recorded using a WTW LF196 conductivity meter (WTW, Germany).

3.3.5 Correlation calculations

Wind speed was measured using a wind sensor (Type 14576, Lambrecht, Germany) installed at the top of the time-series station at about 10 m above mean sea level. While CH₄ was determined in intervals of 10 minutes with only few irregularities (<1.7%), the interval of wind speed measurements was 1 minute with hardly any irregularities (<0.05%). The use of an automatic outlier removal procedure (iterated removal of points that exceeded five standard deviations until convergence was reached) removed less than 0.5% of CH₄ raw data, while wind speed data remained unaffected. Data sets were smoothed and standardised by averaging segments of 30 min which results in equidistant data points. Remaining gaps,

caused by the outlier removal procedure, were finally closed by cubic spline interpolation. From the equidistant pre-processed data we estimated a cross-correlation function by using Matlab's built-in function `xcov` (CH_4 , windspeed, 'coeff'). It renders a normalized and advantageously biased estimator, while statistically unreliable estimates at larger lags are suppressed. The null hypothesis of uncorrelated data series was tested with 600 pairs of surrogate data series that were constructed from the measured methane and wind speed series by randomising their related Fourier phases, thus preserving mean, variance and auto-covariance structure of the original series.

3.3.6 Modelling CH_4 dynamics of the back barrier area by a coupled Euler-Lagrangian model

The Euler-Lagrangian model is an extension of the complex ecosystem model EcoTiM (Ecological Tidal Model; Kohlmeier and Ebenhöf, 2007) to CH_4 . EcoTiM considers tracers moving along a 2D velocity field. Every tracer holds the CH_4 concentration. Due to the 2D approach, each tracer has a variable contact area to the sediment with changing water levels. These contact areas represent the interface to the sediment. The water movement as well as the processes concerning the CH_4 concentrations are calculated with a fixed time step of 1/100 day. The number of Lagrangian tracers amounts to 200, while each tracer describes a volume of $2.22 \cdot 10^6 \text{ m}^3$.

The area used for model calculations stretches from the water shed behind Langeoog Island to the water shed behind Spiekeroog Island in west-east direction. In north-south direction the area is bordered by the 5 m water depth line during high tide and the coastline. The back barrier area in the model is subdivided into five boxes (No. 3-7) plus one box (No. 2) between the North Sea (No.1) and the back barrier area (Fig. 3.1d). This subdivision is based on a combination of the underlying depth profile (adopted from nautical charts) and the different emerging tidal flats (compare Fig. 3.1b). The mean depth of the boxes is given in Fig. 3.1d.

Water transport in the back barrier system is modelled using a surface velocity field from a general circulation model (Stanev et al., 2003). A detailed description of the implementation is given in Kohlmeier and Ebenhöf (2007). The here presented model extension describes the cycling of CH_4 , which is assumed to have a parameterized efflux out of the sediment into the water column. The model is designed to describe the cycling of CH_4 within the back barrier area and focuses on general interactions at the North Sea boundary and the sediment-water interface. The results give an averaged estimation of the budgets between

the back barrier area and the adjacent open sea. Variations due to riverine input are included in the synthetic boundary conditions.

3.3.6.1 Initial conditions, boundary conditions and forcing

The boundary conditions at the North Sea boundary are derived from transect data beyond the islands of Langeoog and Spiekeroog in May 2003 and September 2005 (Fig. 3.1b). It is assumed that the CH₄ concentration follows roughly the tidal signal. Hence, it has been derived by a functional correlation of the tide amplitude. The resulting signal for the North Sea boundary conditions of CH₄ reflects the tidal cycle as well as the variation due to the spring-neap cycle. Changes in concentration due to degradation and degassing of CH₄ have been neglected in this calculation. The impact of model parameterization on CH₄ concentration is estimated by a reference run (run 1), which is compared to runs with modifications of the North Sea boundary and sediment conditions. Varied parameters are the North Sea boundary mean concentration of CH₄ (m), the North Sea boundary concentration amplitude (a), and the pore water discharge (d). The parameter sets for the different runs are given in Table 3.1. In an additional run, the relevance of freshwater input through the flood-gate has been considered.

Table 3.1. Parameter variation of the mean CH₄ concentration (m) at the North Sea boundary, the tidal amplitude of the CH₄ concentration (a) at the North Sea boundary, the pore water discharge (d), and the resulting export out of the back barrier area.

Parameter	run 1	run 2	run 3	run 4	run 5
m [nM]	130	100	150	130	130
a [nM]	50	30	70	50	50
d [$\mu\text{mol m}^{-2} \text{d}^{-1}$]	120	120	120	60	180
Export [10^6 mol a^{-1}]	3.2	3.2	3.2	1.6	4.8

3.3.6.2 Benthic-pelagic-coupling

Since the model is 2D, the total exchange of one box (Fig. 3.1d) with the underlying sediment area is calculated by summing up the exchange of all single moving water bodies within the considered box at the actual time. It is assumed that every water body (with fixed volume) has a certain depth depending on the actual water level at its position. This depth determines an estimation of the area of interaction which is related to the geographical area of

the box. The efflux of CH₄ is calculated for every area of interaction, where a constant pore water discharge according to Table 3.1 is assumed.

3.3.7 Budget calculations based on hydrodynamical model data

The tidal circulation model of the inner part of the German Bight is based on the Reynolds equation of motion and the equation of continuity in a vertically integrated form:

$$\frac{\partial U}{\partial t} + u \frac{\partial U}{\partial x} + v \frac{\partial U}{\partial y} - fV = -gH \frac{\partial \zeta}{\partial x} - \tau_B^{(x)} \quad (1)$$

$$\frac{\partial V}{\partial t} + u \frac{\partial V}{\partial x} + v \frac{\partial V}{\partial y} + fU = -gH \frac{\partial \zeta}{\partial y} - \tau_B^{(y)} \quad (2)$$

$$\frac{\partial \zeta}{\partial t} = - \frac{\partial U}{\partial x} - \frac{\partial V}{\partial y} \quad (3)$$

where u and v are the west-east and south-north component of the velocity, h is the undisturbed water depth, ζ the water elevation, f the Coriolis parameter, g the gravity, and τ_B a quadratic bottom stress. The vertically integrated transports are defined by:

$$U = \int_{-h}^{\zeta} u dz, \quad V = \int_{-h}^{\zeta} v dz, \quad \text{and} \quad H = h + \zeta.$$

The boundary conditions at closed boundaries are 1) the normal component of the velocity is zero, and 2) half slip conditions at the coast. On the open boundary 1) the spatial derivatives of the velocities are zero and 2) the sea level is prescribed as $\zeta_{\text{boundary}} = \zeta(x, y, t)$.

The equations are discretized in a staggered Arakawa C-grid (Arakawa and Lamb, 1977) and solved with a semi-implicit scheme for the pressure gradient in the equations of motion and the divergence of the transport in the continuity equation using a successive over-relaxation method which has been modified for the physics of flooding and falling dry in the Wadden Sea area with the technique of moving boundaries (Duwe and Hewer, 1982). The non-linear advection terms are discretised with a vector upstream scheme (Lillington, 1981). The model has a grid size of one nautical mile and the time step is 300 s. A detailed description of the model and a model validation with respect to observations from tide gauges and current meters is given in Dippner (1984).

The model needs a spin-up time of three periods of an M₂ tide to reach a periodic steady state. For this paper, two simulations are performed and the northward transport between the islands of Spiekeroog and Langeoog is calculated. In the first simulation the

model is forced at the open boundary with an M_2 tide only and integrated over a single M_2 period. In the second simulation the influence of an S_2 tide is considered. The model is forced with an $M_2 + S_2$ tide at the open boundary and integrated over their beat period of 14.8 days.

For CH_4 transport calculation, 94 tidal cycles of the CH_4 dataset (September – November 2005) were taken into account, while data obtained during extreme events like gale-force winds were omitted. The water volume transport of the $M_2 + S_2$ tide is multiplied with the corresponding CH_4 concentration for each time step resulting in CH_4 transport over a tidal cycle. By summing up these data net CH_4 transport is calculated for each of the 94 tidal cycles.

3.4 Results

A summary of both CH_4 concentrations and saturations of CH_4 at the flood-gate (Neuharlingersiel), in the back barrier area, on transects off the islands of Langeoog and Spiekeroog, in the Jade Bay, and in the River Weser is given in Table 3.2. A detailed consideration of each site is given in the following sections.

Table 3.2. CH_4 concentrations and saturations of tidal flats and coastal tributaries.

Location	Month / year	CH_4 (nM; range)	CH_4 saturation (%; range)
Neuharlingersiel (flood-gate)	12 / 2003	5850 (2760–7970)	n.d.*
Neuharlingersiel (flood-gate)	09 / 2004	4400 (2130–8490)	n.d.*
Neuharlingersiel (flood-gate)	10 / 2004	1350 (830–2440)	n.d.*
Time-series station	10-11 / 2005	280 (140–570)	12,052 (6246–24,066)
OB9	08 / 2003	170 (20–270)	10,550 (1374–17,243)
OB9	01 / 2005	260 (190–340)	11,010 (7970–14,520)
Coastal area transect (10 m depth line)	05 / 2003	155 (70–270)	5519 (3337–7325)
Coastal area transect (10 m depth line)	09 / 2005	144 (40–237)	7940 (2213–13,114)
Jade Bay transect	11 / 2005	416 (23–583)	18,468 (1042–25,719)
River Weser transect	03 / 2003	1135 (367–1860)	49,116 (16,099–81,990)

* not determined

3.4.1 North Sea

The concentration level of the southern North Sea is low, when compared to adjacent coastal areas and rivers (Fig. 3.2). Generally, CH_4 decreases further offshore and shows highest concentrations in the estuary of the River Weser. Transects north of 55.5 °N reveal concentrations <20 nM (sensor detection limit) in September 2005 and are omitted in Fig. 3.2. According to Rehder et al. (1998), who observed a distinct patchiness along an east-west transect at ~58 °N, values range between 4 and 30 nM. Additionally, the same authors

observed elevated concentrations along $\sim 58^\circ\text{N}$ due to gas release from abandoned boreholes and natural CH_4 vents (e.g. Dando et al., 1991). Such enrichments were not detected during the cruise presented here.

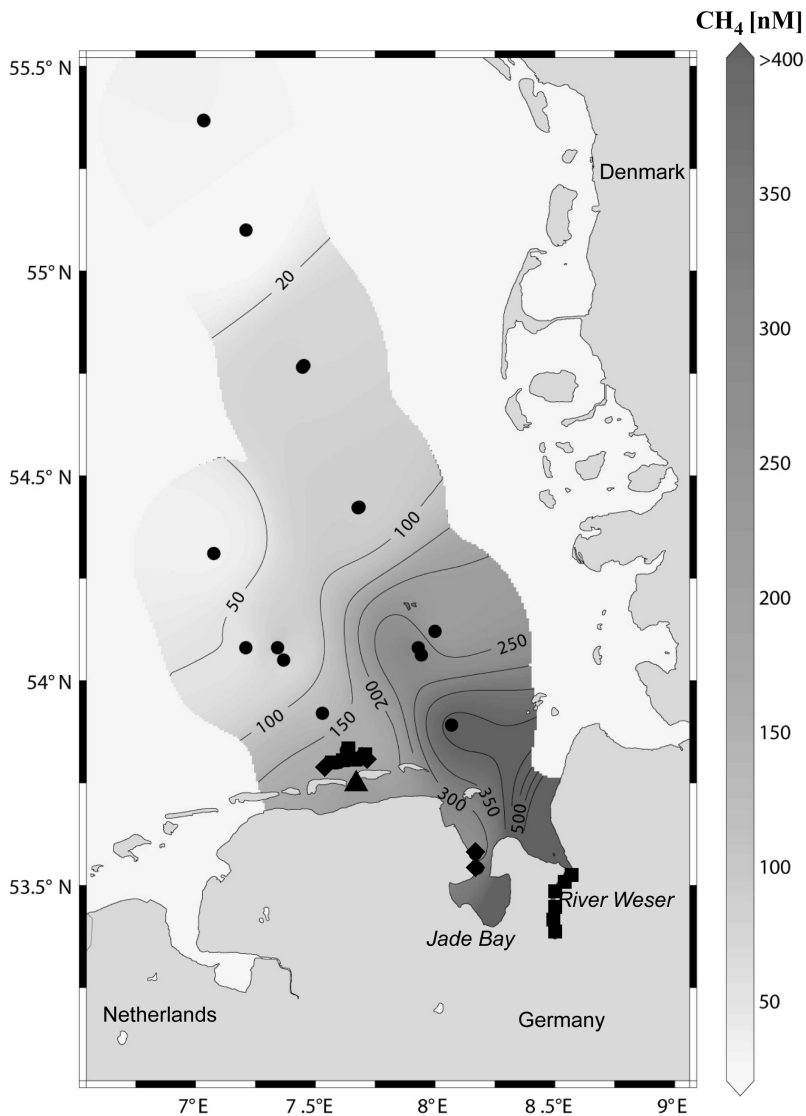


Fig. 3.2. CH_4 concentrations in the German Bight, coastal areas, and River Weser. Data originate from cruises HE188 in May 2003 (squares), HE238 in September 2005 (circles), HE243 in November 2005 (diamonds), and from time-series station data obtained in October to November 2005 (triangles).

3.4.2 Wadden Sea

Transects off the islands Langeoog and Spiekeroog close to the 10 m water depth line (Fig. 3.1b) show differences between high tide and low tide CH_4 concentrations (Fig. 3.3). During high tide transect median concentrations are 86 nM (70 – 111 nM) in May 2003 and 79 nM (40 – 91 nM) in September 2005. In contrast, during low tide elevated values with a

median of 201 nM (142 – 252 nM) in May 2003 and 208 nM (160 – 237 nM) in September 2005 were detected. Maximum concentrations are observed in the main efflux region in the tidal inlet, while minima are located in front of the islands.

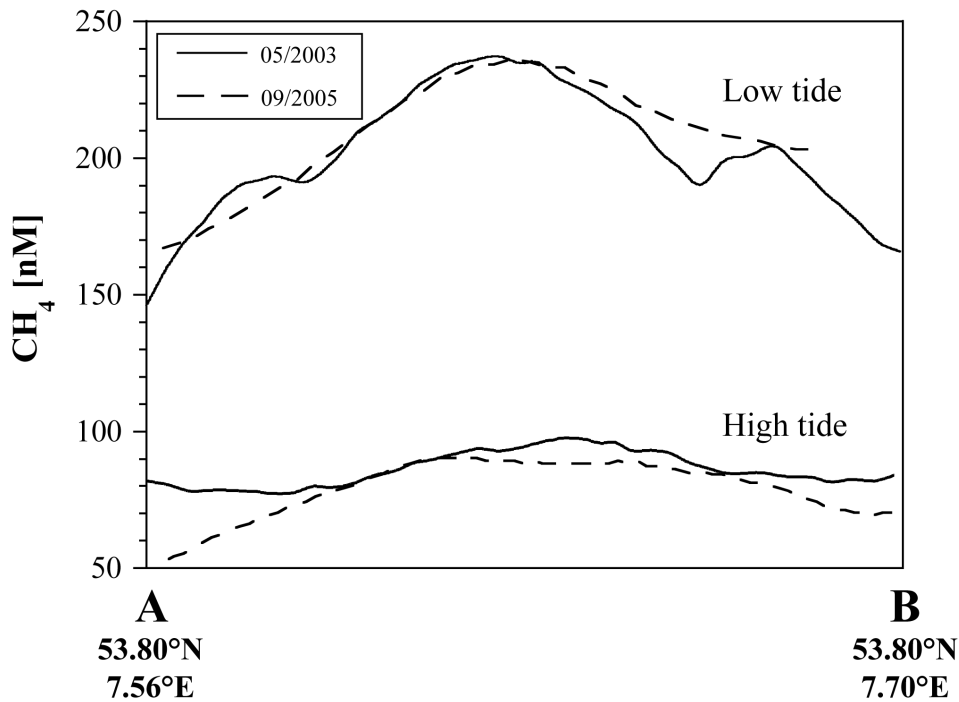


Fig. 3.3. High tide and low tide CH_4 concentrations along the west-east-transects beyond the Islands Langeoog and Spiekeroog in May 2003 (solid line) and September 2005 (dashed line). ‘A’ (53.8°N , 7.56°E) and ‘B’ (53.82°N , 7.7°E) indicate start and end points of the transects.

3.4.2.1 Back barrier area

CH_4 concentrations determined at the time-series station in October and November 2005 (Fig. 3.4a) range from 140 to 570 nM (median: 280 nM) with minima at high tide and maxima at low tide. Increasing concentrations coincide with ebb tide and decreasing values with flood current (Fig. 3.5a). Additionally, ship based measurements at the tidal inlet (OB9, Fig. 3.5b) reveal a median concentration of 170 nM (20 – 270 nM) in August 2003, whereas concentrations of 260 nM (190 – 340 nM) were observed in January 2005. These data show the variability of both average concentration and concentration range in this area. Wind speed and CH_4 concentrations seem to show a certain correspondence (Fig. 3.4). In order to substantiate this, cross-correlation calculations between both time-series data sets of October to November 2005 were performed.

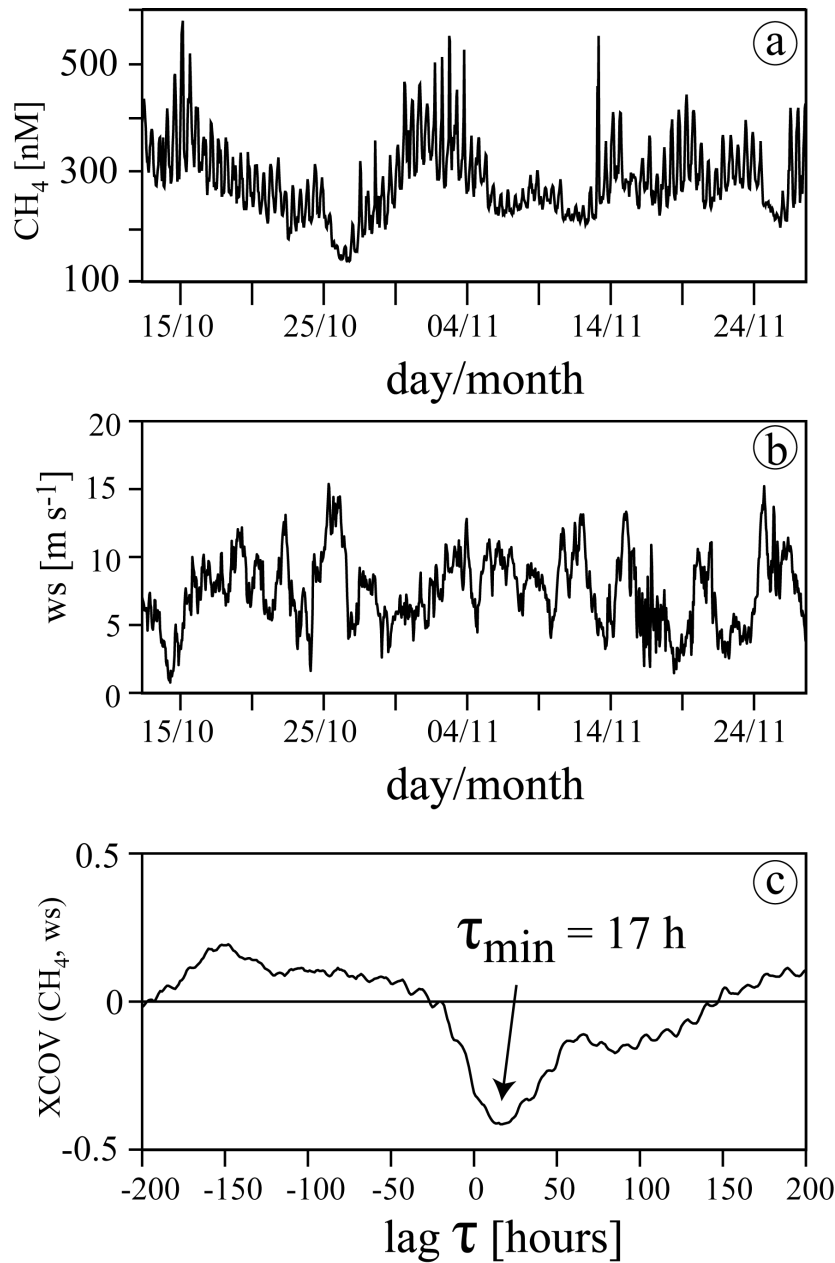


Fig. 3.4. CH_4 concentrations (a), wind speed (ws; b), and cross-correlations (xcov) with time lag (τ) of CH_4 and wind speed (c) in October to November 2005.

The result is shown in Fig. 3.4c for lag parameters ranging between -200 hours (CH_4 advancing wind speed) and $+200$ hours (wind speed advancing CH_4). The most pronounced signature is a minimum at the lag $\tau_{\min}=17$ hours with a value of $C(\tau_{\min}) = -0.41$ which indicates a significant ($p < 0.01$) anti-correlation between CH_4 concentration and wind speed.

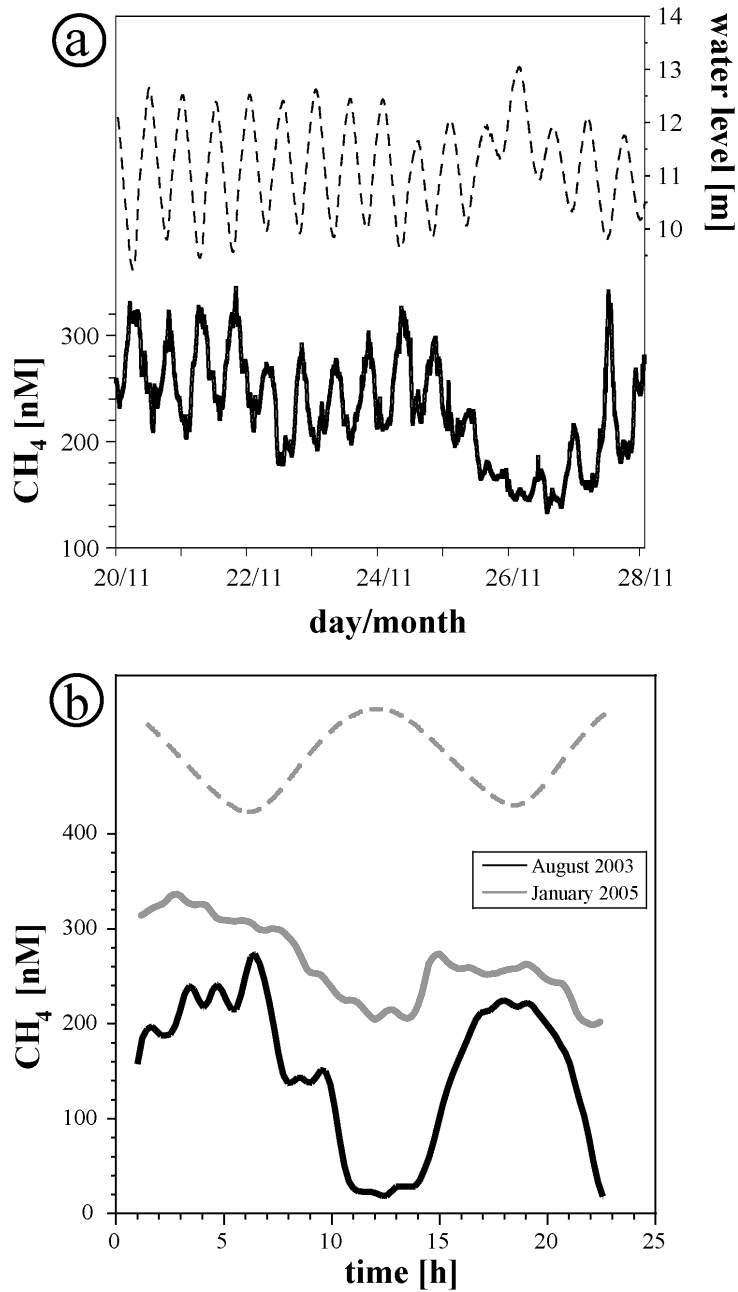


Fig. 3.5. CH_4 concentrations (solid line) and tidal gauge (dashed line) at the time-series station in 2005 (a) and at OB9 (b) in August 2003 (black line) and January 2005 (solid grey line).

3.4.2.2 Freshwater

CH_4 concentrations in freshwater (Table 3.2, flood-gate Neuharlingersiel) show no concentration pattern with mean concentrations of 5850 nM (December 2003), 4400 nM (September 2004), and 1350 nM (October 2004). Freshwater concentrations vary by one order

of magnitude (830 to 8490 nM). Large variations are related to the opening of the flood-gate with subsequent increases in concentration, whereas during slack times concentrations decrease. On average CH₄ concentration increases continuously by 2800 nM within 2.4 hours after opening the flood-gate, while the decrease by 1300 nM within 9.5 hours is seen directly after closing the flood-gate. Freshwater CH₄ contribution to the back barrier area can be assessed by using an average of the determined concentrations (3870 nM) and the annual freshwater discharge. In 2003 and 2005 (no data available for 2004) water discharges were 17.4 and 18.5 · 10⁶ m³ a⁻¹ (Rupert et al., 2004; L. Aden, pers. comm.), which results in an annual freshwater CH₄ contribution of 6.7 · 10⁴ mol a⁻¹ (2003) and 7.2 · 10⁴ mol a⁻¹ (2005).

3.4.2.3 Sediments and pore water

Measurements in a tidal creek (Fig. 3.1b) in February 2005 showed exponentially increasing values during ebb tide with up to 3700 nM two hours before low tide. At the adjacent tidal flat Neuharlingersieler Nacken (NN, Fig. 3.1) Wilms et al. (2006a) reported pore water concentrations of up to 125 µM in the sulphate minimum zone at 100 - 200 cm depth. Seasonal pore water measurements on the Janssand tidal flat (JS) (Fig. 3.1b) show no systematic seasonal behaviour, but increasing CH₄ concentrations with depth from below 10 µM in the upper 50 cm to maximum concentration at 4 m depth (Fig. 3.6). Sulphate concentrations generally decrease with depth with a stronger depletion in the summer months (Beck et al., 2008c).

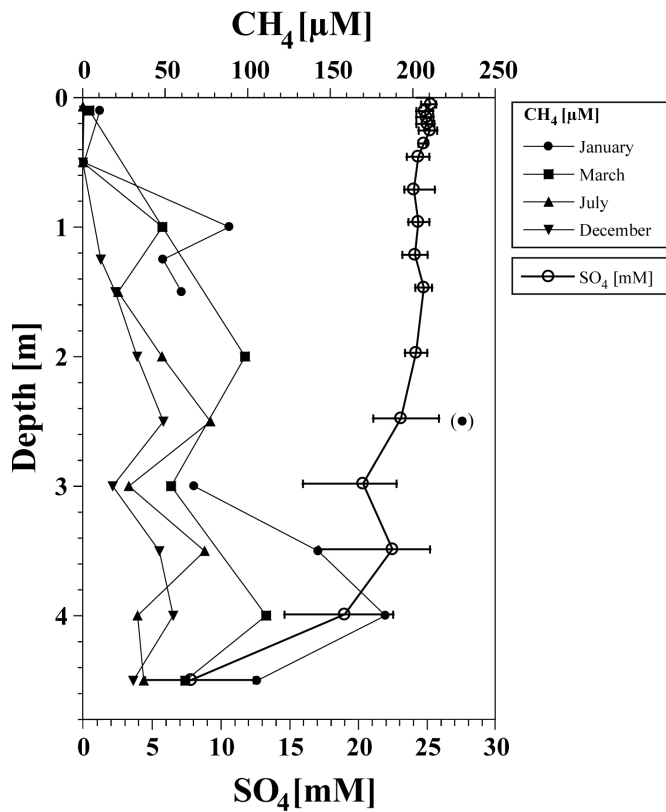


Fig. 3.6. CH_4 and SO_4^{2-} pore water measurements at site Janssand (JS) in 2006. SO_4^{2-} data are average values of February, March, April, June, and July. Horizontal lines in SO_4^{2-} data denote the annual min/max.

3.4.3 Budget calculations

3.4.3.1 Coupled Euler-Lagrangian model

A coupled Euler-Lagrangian model is used to estimate whether the back barrier area forms a zone of import or export of CH_4 to the German Bight or whether it is in a steady state. The resulting exports from the back barrier area to the German Bight through the main tidal inlet varies from 2250 mol per tide for an estimated pore water contribution of $60 \mu\text{mol m}^{-2} \text{d}^{-1}$ up to 6750 mol per tide for $180 \mu\text{mol m}^{-2} \text{d}^{-1}$. The mean annual tidal export out of the back barrier area at the border of boxes 2 and 3 (Fig. 3.1d) for the different runs are summarised in Table 3.1.

3.4.3.1.1 The reference run

The reference run (run 1) reveals an annual mean CH_4 concentration of 314 nM (range 287 to 354 nM) within the back barrier area (mean of boxes 3 to 7). The mean value in the northern part of the tidal inlet (box 3) is 300 nM (range 266 to 351 nM). On the eastern part of the tidal flats (box 7) the annual mean is 341 nM (range from 250 to 500 nM). Single events range from 217 nM to 661 nM. The results for boxes 3 and 7 for the time interval of one month are compared to the data from the time-series station (Fig. 3.7). The mean annual tidal back barrier efflux (from box 3 to box 2) amounts to 4500 mol CH_4 per tide resulting in a net efflux of app. $3.2 \cdot 10^6$ mol a^{-1} . The flood-gate contribution is of minor importance and enhances the total CH_4 efflux to $3.3 \cdot 10^6$ mol a^{-1} , which is equivalent to about 3% freshwater CH_4 contribution.

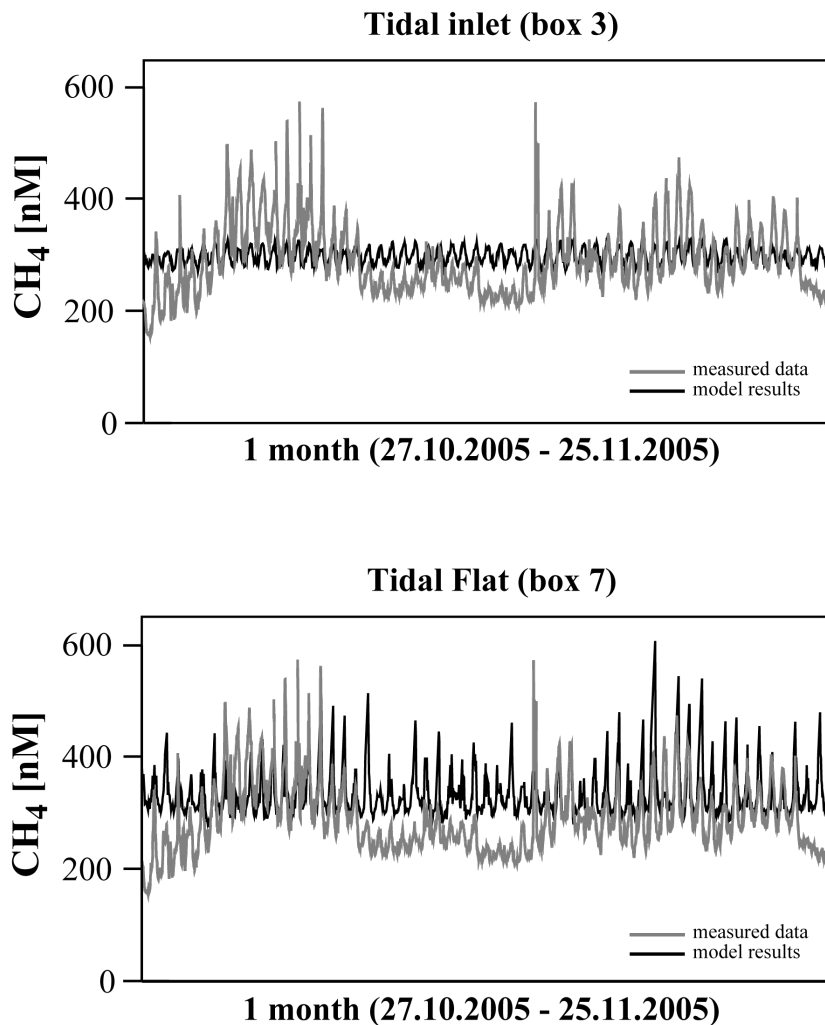


Fig. 3.7. Comparison of model data (black line) and data from the time-series station (grey line) for different model boundary conditions.

3.4.3.2 Hydrodynamical model

In a second approach to assess the CH₄ contribution of the back barrier area to the German Bight a tidal circulation model is used. The M₂ + S₂ water volume transport has a mean amplitude of 11,228 m³ s⁻¹ and a net residual offshore transport of 325 m³ s⁻¹. By averaging transport data of 94 calculated tidal transports (September – November 2005) a CH₄ export of $3.6 \cdot 10^6$ ($\pm 0.39 \cdot 10^6$) mol a⁻¹ into the German Bight is estimated for the tidal flat area of Spiekeroog Island.

3.4.3.3 Estimation of CH₄ sources for the back barrier area

To identify the dominating source for CH₄ in the back barrier area, calculations based on salinity differences between the German Bight and the back barrier area are performed (Dellwig et al., 2007a). These calculations are based on the assumption that differences in salinity are caused by rainfall as well as by freshwater contribution via the flood-gate. The percentage of total freshwater volume input can be calculated on the basis of salinity differences between the German Bight and the back barrier area (2.0 in September and 2.1 in October 2004). Thus, freshwater has an amount of 6.0 % (September) and 6.2 % (October) of the water volume in the back barrier area.

Table 3.3. Estimation of freshwater and pore water CH₄ contribution to the back barrier are of Spiekeroog Island.

	September 2004	October 2004
Mean salinity German Bight	33.1	33.1
Salinity back barrier area	31.1 (29.5-32.4)	31.0 (29.2-32.2)
Δ Salinity	2.0	2.1
% total freshwater (flood-gate + rain)	6.0	6.2
% Rainfall of % total freshwater	95	74
% Flood-gate input of % total freshwater	5	26
% Freshwater (only flood-gate)	0.3	1.6
Freshwater CH ₄ (nM)	4400	1350
Back barrier area CH ₄ (nM)	170	280
% CH ₄ via freshwater (flood-gate)	8	8
% CH ₄ via porewater	92	92

We derived the percentage of input only via the flood-gate by taking the ratios of rainfall and flood-gate discharge of total freshwater input into account. The results reveal that a percentage of 0.3 % (September) and 1.6 % (October) of back barrier area freshwater is contributed via the flood-gate. Based on freshwater concentration at the flood-gate the CH₄

contribution can be calculated. The results show that 8 % of back barrier area CH_4 origins from freshwater contribution via the flood-gate both in September and October 2004. Hence, an amount of 92 % of back barrier area CH_4 is contributed via pore water. Data of these calculations are summarized in Table 3.3.

3.4.4 Riverine input to the German Bight

In River Weser (Fig. 3.1c) CH_4 concentrations increase upstream (Fig. 3.8). Single measurements in the estuary at salinity 6.1 (not shown) reveal CH_4 concentration of 500 nM. This value is used for discharge calculations as the effective CH_4 input concentration.

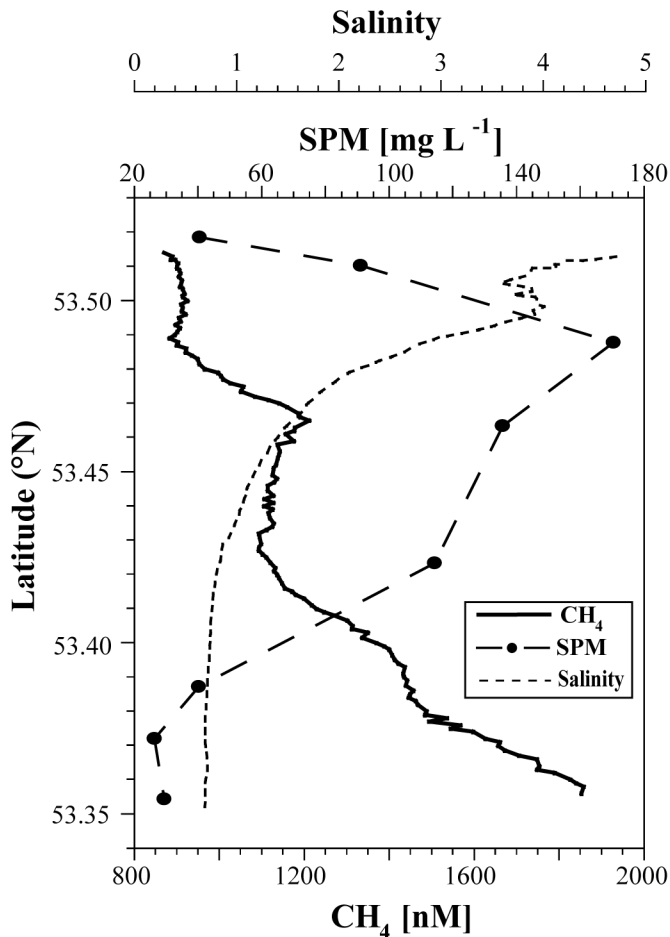


Fig. 3.8. Data of the River Weser transect in May 2003 with CH_4 (solid line), salinity (dotted line), and SPM (dashed line with circles).

The increase south of 53.49 °N may be related to the presence of elevated amounts of suspended particulate matter (SPM). At salinity 0.7 (end of transect) CH_4 reaches maximum

concentrations of 1860 nM. The water discharge varies over a large scale both monthly and annually (Engel, 1995; FGG-Weser, 2008). The 'Flussgebietsgemeinschaft Weser' (FGG-Weser) indicates a discharge of $339 \text{ m}^3 \text{ s}^{-1}$ ($10.7 \cdot 10^9 \text{ m}^3 \text{ a}^{-1}$) as an annual average in 2003. Based on the effective input concentration of 500 nM in the estuary, we estimate a River Weser CH_4 discharge of $5.4 \cdot 10^6 \text{ mol a}^{-1}$ (Table 3.4).

3.5 Discussion

3.5.1 Methane distribution in the southern North Sea and in the coastal environment

The distribution of dissolved CH_4 in any environment represents a balance of CH_4 sources and sinks. In the North Sea, CH_4 is generally consumed by microbial oxidation and removed from the water column due to degassing. Additionally, Atlantic Ocean inflow is a diluting component due to its concentration of 2.5 – 3.5 nM CH_4 in surface waters (Rehder et al., 1998). The sandy sediments of the North Sea are not assumed to be an important source for CH_4 (Scranton and McShane, 1991). The two dominating sources of CH_4 in the German Bight are the Wadden Sea environment and riverine input. The concentration pattern in the southern North Sea shows distinctly higher values in the mouth of the River Weser and in the coastal areas (Fig. 3.2).

3.5.1.1 Wadden Sea

CH_4 concentrations in the tidal inlet between Spiekeroog and Langeoog islands reveal a tidal periodicity with maximum values observed during low tide (Fig. 3.4 and Fig. 3.5). Reasons for lower CH_4 concentrations at high tide are (i) dilution with CH_4 depleted offshore waters, (ii) CH_4 degassing from the water column, and (iii) CH_4 oxidation within the water column. Degassing of CH_4 presumably occurs when water in the tidal inlet passes a shoal with enhanced turbulence and wave activity off the islands leading to degassing processes. Biological oxidation within the water column is strongly dependent on temperature (Pulliam, 1993) and salinity. Only very low oxidation rates are observed at salinities above 6 (de Angelis and Scranton, 1993). Scranton and McShane (1991) determined CH_4 oxidation rates with minor impact on CH_4 loss in comparison to high sea-to-air emissions. Thus, we assume that CH_4 oxidation is of minor importance in our investigation area since the residence time of back barrier area water is comparatively low.

Since the tidal pattern is disturbed irregularly and the level of CH₄ concentration changes, a further driving force has to affect CH₄ concentration besides the tide. Turbulence at the air-water interface regulates gas transfer processes (Jähne et al., 1987). Layer stability, surfactants, bubbles, and bottom driven turbulence may be further influencing factors, as suggested by Broecker et al. (1978), Merlivat and Memery (1983), Broecker and Siems (1984), Goldman et al. (1988), Kourtidis et al. (2006), and Upstill-Goddard (2006). However, they have not been considered in this study due to lack of data. As wind speed has a major effect on gas transfer (Wanninkhof, 1992) we performed correlation calculations between wind speed and CH₄ concentrations. The median wind speed of 6.9 m s⁻¹ in the investigated time period represents the average wind situation in the study area. Wind data in 2005 and 2006, covering about 95,000 measurements, reveal an average wind speed of 6.6 m s⁻¹ (prevailing 31% of the time). A special wind situation occurred in October 25th – 26th 2005 when the wind direction was changing from SE to NW and wind speed was increasing to 16 m s⁻¹ with a median of 12.6 m s⁻¹. This led to a low tide water level only 0.6 m below the preceding high tide. Due to the elevated low water level, the tidal flat sediments were completely covered by water, thus suppressing deep advective flow at tidal flat margins. The resulting decrease in CH₄ concentration supports our assumption, that tidal flats represent the major source for CH₄.

Correlation calculations of wind speed and CH₄ concentration show a prominent maximum in anti-correlation with a time lag of 17 hours, which demonstrates that CH₄ concentrations decrease while wind speed increases and vice versa. The time lag of 17 hours only represents the maximum in anti-correlation. As figure 3.4c shows, this anti-correlation can also be observed both without any time shift before the maximum emerges and after the time lag of 17 hours. Thus, the influence of wind speed resulting in decreasing CH₄ concentration arises immediately after increase of wind speed. The enhanced wave activity triggered by wind force may as well have caused higher degassing of CH₄ from the water column.

3.5.1.1.1 CH₄ sources for the back barrier area

Apart from possible groundwater discharge from shore as well as from the adjacent islands, which is not in the focus of this study, elevated CH₄ values during low tide may be caused by two major sources: (i) pore waters draining from the tidal flat sediments during ebb tide and (ii) freshwater contributed to the back barrier area via the flood-gate at Neuharlingersiel (Fig. 3.1b).

Tidal flat sediments are a source of anaerobically produced CH₄ (Kelley et al., 1995; Middelburg et al., 1996; Van der Nat and Middelburg, 2000) since they form a zone of intense organic matter remineralisation (Billerbeck et al., 2006b; Wilms et al., 2006a; Wilms et al., 2007; Beck et al., 2008a; Beck et al., 2008c). Fresh marine organic compounds are transferred into the anaerobic zone due to enhanced advective pore water exchange with the water column as described for tidal flat margin sediments by Howes and Goehring (1994), Billerbeck et al. (2006a,b), and Wilson and Gardner (2006). For our investigation area Beck et al. (2008b) and Gittel et al. (2008) emphasize the importance of the margins of the tidal flat Janssand as loci of enhanced microbial activity due to their lithological and hydrological conditions favouring advection down to several meters sediment depth. The significance of heterotrophic as well as autotrophic activity in different sediment types of our investigation area is pointed out in several publications (Grossart et al., 2004; Stevens et al., 2005; Billerbeck et al., 2006b; Wilms et al., 2007). Generally, Rusch et al. (2006) reported that sandflats with low organic carbon contents have remineralisation rates comparable to those of organic-rich muds since higher permeability of sandflats enables enhanced pore water advection and exchange of components. Enhanced permeability also favours release of CH₄ to the open water column (Røy et al., 2008). On the tidal flat Janssand CH₄ pore water concentrations increase with sediment depth which point towards enhanced methanogenesis by methylothrophic archaea in deeper parts of the sediment (Wilms et al., 2006a; Wilms et al., 2007). This coincides with decreasing sulphate concentrations below 2 m since methanogens are in direct substrate competition with sulphate reducers. However, according to Wilms et al. (2007) and Madigan et al. (2003) methanogens can escape this competition by utilization of certain methylated substrates (e.g. methylamines, dimethyl sulphides) which are not utilized by sulphate reducers. Concerning our investigation area we postulate CH₄ production within the entire sediment with the main production zone below 5 m depth, as indicated by the depletion in SO₄²⁻. Elevated CH₄ concentrations above 5 m, coexisting to sulphate concentrations of almost seawater level, may be caused by upwards diffusing CH₄. Based on the lack of seasonality in CH₄ concentration profiles (Fig. 3.6) we assume that the annual CH₄ contribution to the open water column via pore water is almost constant.

In contrast to pore water contribution freshwater is discharged irregularly. Thus, the tidal pattern of CH₄ in the back barrier area seems not to be formed by this source. To estimate the impact of freshwater discharge in comparison to pore water contribution we used different approaches. Calculations of a coupled Euler-Lagrangian model result in a freshwater contribution which is responsible for 3 % of back barrier area CH₄. Additionally, estimations based on salinity differences between the German Bight and the back barrier area show that

freshwater contributes 8 % of CH₄ in the tidal flat area. In a third approach to identify the main source for CH₄ in this system we compared the calculated freshwater CH₄ discharge via the flood-gate in 2003 ($6.7 \cdot 10^4 \text{ mol a}^{-1}$) and 2005 ($7.2 \cdot 10^4 \text{ mol a}^{-1}$) with the total export of the back barrier area. Since the export amounts to $3.3 \cdot 10^6 \text{ mol a}^{-1}$ (Euler-Lagrangian model) and $3.6 \cdot 10^6 \text{ mol a}^{-1}$ (hydrodynamical model) freshwater accounts for only up to 2 % as a source for CH₄ in this area.

Hence, despite the enrichment of freshwater in CH₄ the impact on the back barrier area water column budget may be regarded as minor (less than 10%). In contrast, all our budget estimations point out that the sediment pore water system forms the major source providing at least 90% of Wadden Sea CH₄.

3.5.1.2 Riverine input to the German Bight

Estuarine and river water concentrations of CH₄ along with their inputs to the southern North Sea are reported in several publications (e.g. Scranton and McShane, 1991; Upstill-Goddard et al., 2000; Middelburg et al., 2002; Bange, 2006). Both river concentrations and contributions to the North Sea encompass a wide range due to varying discharge rates and different properties of the catchment areas. According to de Angelis and Lilley (1987) surface CH₄ in rivers is not only produced in underlying sediments. The authors measured both surface and bottom water samples of different Oregon rivers and observed no consistently higher bottom CH₄ concentration as it would be expected if sediments would represent the major source. Since even rivers with rocky bottoms or little sediment cover contain elevated CH₄ concentrations, the authors postulate that most of the CH₄ originates from lateral diffusion from stream banks and runoff from forests and agricultural soils. In this study we do not consider the importance of groundwater discharge for the CH₄ budget, which remains largely unknown.

During a River Weser transect, CH₄ values increase stepwise upstream (Fig. 3.8). The first prominent increase south of 53.49 °N is associated with the onset of the turbidity maximum, while the slight increase in the CH₄ profile south of 53.43 °N is most likely caused by local contributions of small tributaries, channels, and flood-gates. Upstill-Goddard et al. (2000) postulated that especially in the turbidity maximum elevated amounts of CH₄ are released from the underlying anoxic sediments during active particle resuspension. Furthermore, they assumed bacterial in-situ CH₄ production in the water column on suspended particles, similar to N₂O production in the Humber as reported by Barnes and Owens (1998). Morris et al. (1978) pointed out that the turbidity maximum is a region of

intense biogeochemical activity and O₂ depletion, where bacteria attached to tidally trapped suspended particles provide the basis for enhanced nitrification, which forms the source for N₂O.

3.5.2 Budget calculations

3.5.2.1 Coupled Euler-Lagrangian model

The coupled Euler-Lagrangian model as a part of the ecological tidal model EcoTIM (Kohlmeier and Ebenhöf, 2007) is used to estimate the net CH₄ import or export of the back barrier area to the German Bight. To review the reliability of the reference run (compare 4.3.1) a sensitivity analysis is applied, which shows that the modification of the North Sea boundary conditions do not lead to a significant change in the mean CH₄ concentration. The reduction of pore water discharge leads not only to a reduced mean concentration of CH₄ in the back barrier area, but also to lower amplitudes during the tidal cycle. An enhanced discharge leads to both, a higher mean concentration and higher tidal amplitudes. Variation of pore water discharge has a comparably larger influence on CH₄ concentrations in the pelagic part of the back barrier area than changing conditions at the North Sea boundary.

In our coupled Euler-Lagrangian model approaches the temporal variability of CH₄ concentrations, beside the tidal signal, differs from the measurements (Fig. 3.7) because no special wind forcing for the simulated time range is assumed. The simulation results for the tidal flats of box 7 show a better accordance with the field data than the results for the tidal inlet (box 3). This is a consequence of the 2D-setup of the model. The concentrations as simulated for box 3 are mean values for the total water column. Additionally, box 3 may extend too far northwards, when compared with the position of the time-series station. It is not consistent with measured tidal variations, due to dilution processes with lower concentrated offshore water. Thus, model results of box 7 obviously better reproduce the concentration pattern measured at the time-series station. Despite the mentioned uncertainties, the resulting CH₄ export of the back barrier area to the German Bight ($3.3 \cdot 10^6 \text{ mol a}^{-1}$) represents a realistic estimate for the tidal flat CH₄ budget.

3.5.2.2 Hydrodynamical modelling

In a second attempt to estimate the annual back barrier area CH₄ contribution to the German Bight we used data from a hydrodynamical model combined with CH₄ concentrations

measured late in 2005. This approach is strongly simplified because all water transport data are based on one mean tidal cycle. Thus, no differences in tide situation like spring and neap tide were taken into account, in contrast to the Euler-Lagrangian data. However, despite this uncertainty the results of $3.6 \cdot 10^6 (\pm 0.39 \cdot 10^6)$ mol a⁻¹ differ only slightly from those obtained from the coupled Euler-Lagrangian approach ($3.3 \cdot 10^6$ mol a⁻¹). To evaluate this way of estimation one has to take into account that (i) freshwater contribution only plays a minor role in this system, (ii) biological degradation is negligible, (iii) pore water shows no significant seasonality, and (iv) the wind situation in the considered period represents the annual mean. Thus, the main influencing factors can be assumed to be almost constant or having a minor impact. Therefore, we suspect that our estimates of the CH₄ contribution from the back barrier area to the German Bight are reasonable.

3.5.2.3 Rivers

Table 3.4 provides a summary of European rivers discharging into the southern North Sea. The discharge volume of riverine freshwater varies over a large scale, depending on their catchment area. However, when riverine CH₄ contribution is regarded, it is obvious that river size and runoff are not the only crucial factors. Upstill-Goddard et al. (2000) reported that the rivers Rhine, Humber, Wash, and Tyne are responsible for about 71% of the total annual discharge to the southern North Sea (ca. $99 \cdot 10^9$ m³ a⁻¹; Howarth et al., 1994). Based on the data presented in Table 3.4 the rivers mentioned before including the Rivers Weser and Elbe contribute a water discharge of $108 \cdot 10^9$ m³ a⁻¹. Radach and Pätsch (2007) calculated an annual continental discharge of European rivers of $133 \cdot 10^9$ m³ a⁻¹ ($\pm 26 \cdot 10^9$ m³ a⁻¹). Thus, freshwater discharge via rivers as listed in Table 3.4 represents about 81% of the annual riverine freshwater discharge to the southern North Sea. The differences in volumes and percentage of discharge represent the variability of freshwater contribution to the North Sea, depending on the years considered. We wanted to assess the CH₄ contribution of the River Weser to the German Bight. Upstill-Goddard et al. (2000) corrected the low salinity end member data of their studied estuaries for losses (oxidation and gas loss), whereas Rehder et al. (1998) present uncorrected data for the River Elbe since they found no losses affecting the advective transport of CH₄. In the budget calculation for River Weser we use the effective CH₄ input data derived from estuarine measurements at salinity >5, where removal by oxidation and gas loss is essentially completed (Upstill-Goddard et al., 2000). At our time of survey (May 2003) the water discharge of river Weser was about average over the last 10 years (FGG-Weser, 2008). Our estimation of $5.4 \cdot 10^6$ mol a⁻¹ CH₄ underlines the high impact

of this river in comparison to the River Elbe ($2.2 \cdot 10^6 \text{ mol a}^{-1}$), i.e. the River Weser contributes CH_4 in the same order of magnitude with about one third discharged water volume. This emphasises the River Weser as a considerable source of CH_4 for the German Bight.

Table 3.4. Summary of European rivers discharging into the German Bight.

River	Mean water discharge ($10^9 \text{ m}^3 \text{ a}^{-1}$)	Low salinity end member CH_4 (nM)	Low salinity end member CH_4 (% Saturation)	Effective CH_4 input (nM)	CH_4 contribution to southern North Sea (10^6 mol a^{-1})	Reference
Rhine	59.8	7099	$2.3 \cdot 10^3$	354	21.2	Upstill-Goddard et al. (2000)
Weser	10.7	1860	$7.9 \cdot 10^4$	500	5.4	This paper
Wash	1.6	47,000	$1.6 \cdot 10^4$	2400	3.8	Upstill-Goddard et al. (2000)
Elbe	27	80	n.n.	80	2.2	Rehder et al. (1998)
Humber	7.9	439	$1.4 \cdot 10^4$	33	0.3	Upstill-Goddard et al. (2000)
Tyne	1.3	650	$2.2 \cdot 10^4$	113	0.1	Upstill-Goddard et al. (2000)
Total	108.3				32.9	

3.5.3 Assessment of the significance of back barrier areas

Compared to the CH_4 contribution of the rivers Rhine, Wash, Weser, Humber, Elbe, and Tyne to the German Bight the back barrier area of Spiekeroog Island forms a significant source of CH_4 . Staneva et al. (2009; J. Staneva, pers. comm.) calculated an area of the entire back barrier tidal flats from Den Helder to Esbjerg of about 3364 km^2 (including estuaries) and 1688 km^2 without estuaries. The back barrier area from Norderney to Wangerooge (East Frisian Wadden Sea) encompasses an area of about 197 km^2 . Based on water volume transport data provided by the here presented hydrodynamical model and by assuming that our study area is representative for the entire tidal flat area of the East Frisian Wadden Sea we extrapolate the CH_4 export of the Spiekeroog Island back barrier area. Hence, with a net offshore water transport of $700 \text{ m}^3 \text{ s}^{-1}$ the East Frisian back barrier areas contribute $7.8 \cdot 10^6$

mol a^{-1} CH_4 to the southern North Sea which is between the magnitude of the rivers Rhine and Weser (Table 3.4). Therefore we conclude that tidal flat systems play a significant role in the CH_4 budget of the German Bight.

3.6 Summary and concluding remarks

Methane measurements in the southern North Sea reveal a general supersaturation with respect to the atmospheric partial pressure. CH_4 shows elevated concentrations in the coastal areas, while values are decreasing offshore. Thus, estuaries, rivers, and tidal flats seem to be a source of CH_4 for the German Bight. Methane concentrations of River Weser reveal stepwise increases due to the turbidity maximum and the contribution by small tributaries. In general, water discharge does not seem to be the governing factor of riverine CH_4 contribution.

The concentration pattern of Wadden Sea CH_4 shows a tidal periodicity with maximum values during low tide. Lower concentrations at high tide are mainly caused by dilution with CH_4 -poor offshore waters as well as degassing processes. Biological CH_4 degradation is of minor importance in our investigation area due to short residence time of the corresponding water masses within the back barrier area. Rough estimates show that freshwater contributed via the flood-gate represents a minor fraction of the tidal flat CH_4 budget. In contrast, pore water forms the major source for Wadden Sea CH_4 generated by biogeochemical remineralisation processes in anaerobic sediments. Since pore water CH_4 concentrations show no distinct seasonality the amount of interstitially produced CH_4 presumably is almost constant. Despite the recurrent tidal forces the periodical pattern as well as the concentration level of CH_4 in the back barrier area is heavily influenced by strong winds. Cross-correlation calculations reveal an anti-correlation of wind speed and CH_4 concentration.

Two different approaches of model based calculations show that CH_4 contribution of the tidal flat systems to the German Bight is in the same order of magnitude as those of major rivers. We conclude that the back barrier tidal areas have to be taken into account for the CH_4 budget of marine systems.

Acknowledgements

The authors wish to thank the crews of R/V Senckenberg and R/V Heincke for support during cruises. Helmo Nicolai (ICBM) is thanked for invaluable assistance during several sampling campaigns. Further thanks are due to Thomas H. Badewien (Marine Physics, University of Oldenburg) for providing salinity, temperature, water level, and wind speed

data. Joanna Staneva (GKSS Research Centre) is thanked for providing coastline and area estimates for the entire tidal flat area. We are grateful to thank K. Enneking (University of Bremen) for methane GC measurements. Carsten Frank (GKSS Research Centre) is thanked for support in data assimilation. Two anonymous reviewers are thanked for their constructive comments. This study was funded by the Deutsche Forschungsgemeinschaft (DFG) through grants FOR 432/1-1 and BR 775/14.

4 Nutrient dynamics in a back barrier tidal basin of the Southern North Sea: Time-series, model simulations, and budget estimates

Maik Grunwald, Olaf Dellwig, Cora Kohlmeier, Melanie Beck, Stephan Kotzur, Nicole Kowalski, Gerd Liebezeit, and Hans-Jürgen Brumsack

This chapter has been submitted for publication to *Journal of Sea Research*.

Abstract

In the tidal inlet of the back barrier area of Spiekeroog Island (Southern North Sea), nutrient concentrations (silica, phosphate, Σ nitrite + nitrate) were determined hourly by an autonomously analysing system on a permanently installed time-series station from April 2006 to December 2008. The high frequency of analyses provides the opportunity to study nutrient dynamics on annual, seasonal, and tidal time scales. By comparing the nutrient input to the tidal flat area via freshwater through the flood-gate and pore water discharge from tidal flat sediments, we conclude that nutrients are primarily supplied to the water column by pore waters, while the freshwater contribution is negligible. To assess the annual nutrient contribution of our study area to the German Bight, we used a numerical Euler-Lagrangian model (EcoTiM) to calculate annual budgets of silica, phosphate, and Σ nitrite+nitrate. The model indicates that the back barrier area of Spiekeroog Island exports inorganic silica, phosphate, and Σ nitrite+nitrate to the North Sea (silica: $128 * 10^6 \text{ mol a}^{-1}$; phosphate: $3 * 10^6 \text{ mol a}^{-1}$; Σ nitrite plus nitrate: $29 * 10^6 \text{ mol a}^{-1}$). Extrapolating our data to the whole Wadden Sea along the southern North Sea reveals that the back barrier areas export silica and phosphate in the same order of magnitude and nitrite plus nitrate in one order of magnitude lower than the sum of the rivers Elbe, Weser, and Ems.

4.1 Introduction

The Wadden Sea as part of the Southern North Sea forms the transition zone between the terrestrial and open marine realm. This dynamic system is influenced by freshwater inputs via rivers and small coastal tributaries from the hinterland as well as by the exchange with offshore waters. Since eutrophication has been recognized as a global challenge (Nixon,

1990), many studies focus on sources and sinks of nutrients in coastal areas (de Jonge and Postma, 1974; van Raaphorst and Kloosterhuis, 1994; van Beusekom et al., 1999; van Beusekom and de Jonge, 2002; van Raaphorst and de Jonge, 2004; van Beusekom, 2005; Soetaert et al., 2006; Withers and Jarvie, 2008). Tidal systems, such as the Wadden Sea with its chain of barrier islands, are of special interest since they are characterised by intensive production and mineralization of organic matter.

High amounts of particulate organic matter are imported from the North Sea (van Beusekom and de Jonge, 2002) and after bacterial mineralization (Böttcher et al., 2000; Böttcher et al., 2004; Werner et al., 2006; Al-Raei et al., 2009) dissolved species are exported from the Wadden Sea, thus justifying the idea of the “bio-reactor Wadden Sea” (de Jonge and Postma, 1974; van Beusekom et al., 1999; van Beusekom et al., 2001; van Beusekom and de Jonge, 2002; van Beusekom, 2005). Generally, about 70% of the coastal remineralisation of organic matter (OM) takes place in the water column (Smith and Hollibaugh, 1993). In contrast, in more shallow areas benthic processes gain in importance and can account for 50-60% of the total carbon mineralization (Heip et al., 1995). Algae and (cyano-)bacteria contribute significantly to these benthic transformation processes (Colijn and de Jonge, 1984; de Jonge and Colijn, 1994).

Once nutrients are produced by OM degradation in surface sediments, their release to the open water column is governed by several factors, i.e. sediment permeability (Rusch and Huettel, 2000; Rusch et al., 2000), tidal pumping (Billerbeck et al., 2006b; Beck et al., 2008b,c), and bioturbation (Volkenborn et al., 2007). As shown by Fong et al. (1993), consumption by benthic organisms also influences the amount of released nutrients. The authors observed growth limitation of pelagic algae due to consumption of nutrients by benthic primary producers.

So far little is known about the importance of back barrier tidal areas for the nutrient budget of the Southern North Sea. In this contribution, we present nutrient dynamics in the surface waters of the back barrier tidal flat area of Spiekeroog Island (Southern North Sea) which were determined continuously by a time-series station between 2006 and 2008 (Grunwald et al., 2007). The numerical model “EcoTiM” (Kohlmeier and Ebenhöf, 2007) was used to simulate the nutrient variations and to estimate the outflow of nutrients from the Wadden Sea to the open North Sea. In order to assess potential nutrient sources in the Wadden Sea, we also analyzed pore waters of surface tidal flat sediments and small coastal tributaries.

4.2 Geographical setting

The Wadden Sea in the Southern North Sea (Fig. 4.1) stretches from Den Helder (The Netherlands) to Esbjerg (Denmark) and encompasses an area of about 9500 km². A chain of barrier islands forms the boundary between the Wadden Sea and the open North Sea. The entire Wadden Sea system is characterised by semidiurnal tides with a tidal range between 1.5 m in the most westerly part and 4 m in the estuaries of the rivers Weser and Elbe. The main study site of this contribution is the back barrier area of the Island of Spiekeroog, which covers about 74 km² (Walther, 1972). Depending on water level, freshwater contribution to the back barrier tidal flat occurs generally about 2 h before low tide via a flood-gate in Neuharlingersiel (Fig. 4.1b). The catchment area of the flood-gate is about 125 km² and is composed of marsh soils in the north and fens as well as forests in the south.

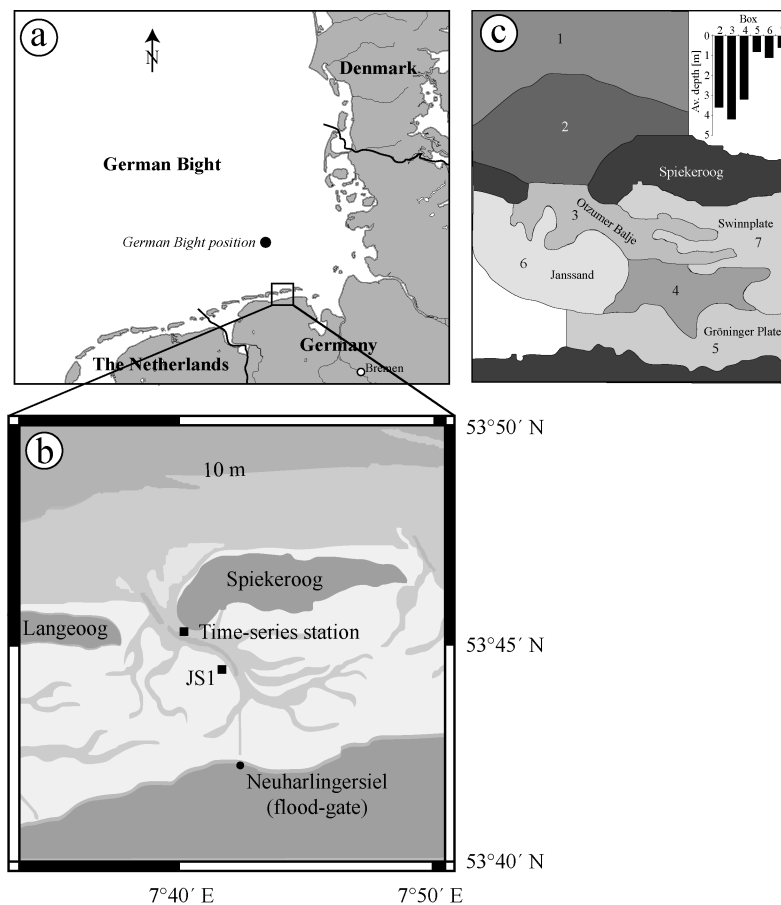


Fig. 4.1. Map of the study area. (a) German Bight position where North Sea samples were analysed which were used as boundary conditions in the model setup. The close-up view (b) shows the sampling sites in the back barrier area of Spiekeroog Island: Time-series station, JS1, and the flood-gate in Neuharlingersiel. (c) Classification of boxes used in the Euler-Lagrangian model simulations with corresponding average water depths.

Nutrient dynamics are studied at a time-series station (Grunwald et al., 2007) located at 53°45.02' N and 7° 40.27' E in the tidal inlet between the Islands of Spiekeroog and Langeoog. Pore waters samples were obtained by using permanently installed lances located on a sandy tidal flat Janssand (site JS1, 53° 44.18' N, 7° 41.9' E; Beck et al., 2007). During high tide the JS tidal flat is covered by 1 - 2 m of water, while it is subaerially exposed for approximately 6 hours around low tide.

4.3 Materials and methods

Time-series station

In surface waters of the back barrier area of Spiekeroog Island, nutrients were determined by automated nutrient analyzers (Systea, μ Mac1000) mounted on a permanent time-series station in the tidal inlet (Fig. 4.1). At the study site, the average water depth of 13.5 m (below mean sea level) varies due to semidiurnal tides with a range of 2.6 m (Flemming and Davis, 1994). Samples were taken from a through-flow tube which crosses the time-series station at 9 m above seafloor. Nutrients were measured hourly after automated filtration by a belt filter (Metrohm, Series 01.12) of 7 – 12 μ m pore size (Schleicher & Schuell, No. 1574). The time-series station and the analyzer setup is described in detail by Grunwald et al. (2007) and Reuter et al. (2009). Detection limits are 0.38 μ M (silica), 0.01 μ M (phosphate), and 0.17 μ M (nitrite plus nitrate). The agreement of analyser and laboratory spectrophotometer (Spekol 1100, Analytik Jena) measurements according to methods described by Grasshoff et al. (1999) were 3.6% for phosphate, 11.3% for silica, and 6.0% for nitrite plus nitrate.

Total algae cell counts

Samples for the analysis of total algae cell counts (phytoplankton abundance of a size class $>3\mu$ m) were collected at the position of the time-series station in 2008. Surface water was sampled at low tide in an at least monthly interval. Each sample of 100 mL was treated with 2 – 3 drops of Lugol's solution (aqueous iodine / potassium iodide solution) and stored at 4°C in brown glass bottles until analysis. Using the Utermöhl method (Utermöhl, 1958), a sample aliquot of 25 mL was counted under an inverted microscope (Zeiss Axiovert 25).

Pore water

Pore waters were sampled at position JS1 (Fig. 4.1) in a monthly interval from January – October 2008. Samples were taken using a permanently installed in-situ sampler (Beck et al., 2007). The samples were filtered through 0.45 μm SFCA syringe filters into pre-cleaned PE-bottles and acidified to 1 % (v/v) with HNO_3 (supra pure, Merck). For phosphate and silica analysis, a 5-fold diluted aliquot was measured using ICP-OES (iCAP 6300 Duo, Thermo Fisher). Accuracy and precision were controlled by a spiked seawater standard Cass-4 solution (National Research Council, Canada) containing 16 μM phosphate and 890 μM silica. Accuracy / precision were 3% / 7% for silica and 6% / 5% for phosphate. A comparison to concentrations determined using a spectrophotometer shows a deviation of 9% for silica and 10% for phosphate.

Freshwater

In freshwater, nutrients were analysed in a monthly interval from February 2002 to April 2004 at the flood-gate in Neuharlingersiel. Nutrients were determined according to Grasshoff et al. (1999).

Modelling nutrient dynamics in the back barrier area

The ecological tidal model (EcoTiM) is a semi-Lagrangian model describing water transport by tracers moving along a velocity field (Kohlmeier and Ebenhöf, 2007; Kohlmeier and Ebenhöf, 2009). The tracers are assumed to have a finite volume and represent the real volume in this system at any time. Water transport in the back barrier system is included using a surface velocity field from a general circulation model (Stanev et al., 2003). North Sea boundary conditions are taken into account by (i) equating box 1 with the North Sea conditions and (ii) tracers entering box 1 become mixed with North Sea water. Turbulent diffusion is considered by a randomized offset of water bodies. Diffusive exchange processes between different water bodies are further implemented. Conditions at the North Sea boundary for state variables were taken from the COCOA-model, a Continental Coastal Application of ERSEM (Lenhart et al., 1997). For inorganic silica, phosphate, and nitrite plus nitrate the boundary conditions were derived from measurements in 2002 (MARNET, 2008) determined in the German Bight at 54.17°N and 7.45°E (Fig. 4.1a). Nutrient input via the flood-gate in Neuharlingersiel is based on concentrations determined during this study and freshwater discharge rates published by Rupert et al. (2004). Atmospheric interaction is not considered in the model.

The model is treated as a 2D-model. The total exchange of a box (Fig. 4.1c) with the underlying sediment area is calculated by summing up the exchange of all single moving water bodies within the box at the actual time. Every water body (with fixed volume) has a certain depth depending on the actual sea level at its position. The model is forced by temperature and irradiance (Photosynthetically Active Radiation, PAR) measured at the time-series station.

The basis of the ecological model is the European Regional Seas Ecosystem Model (ERSEM), which is a biomass based differential equation model describing the cycling of carbon and nutrients within a marine ecosystem (Baretta-Bekker and Baretta, 1997). According to the ERSEM-philosophy of a top-down approach, the food web consists of functional groups and not of single species. The food web is built with respect to trophic position, size, and function. The model describes the main metabolic processes within and the predation processes between the functional groups. These processes are: carbon assimilation, nutrient uptake and lysis of primary producers, grazing processes of secondary producers, and respiration, mortality excretion, and exudation of all organisms. As an extension to the original benthic food web of ERSEM (Ebenhöh et al., 1995), benthic silica dependent algae and non-silica dependent algae are added, following the description of Blackford (2002).

The benthic system is segmented into three layers, an oxic, a nitrate dominated, and an anoxic layer. The separating horizons of these layers are variable and depend on the concentrations and distribution of oxygen and nitrate in the sediment. The benthic nutrient model (Ebenhöh et al., 1996; Kohlmeier, 2004) governs the nutrients nitrate, phosphate, and silica as well as their exchange with the pelagic system depending on the nutrient gradients at the sediment surface. Fluxes are determined by pre-calculated equilibrium profiles. The vertical extension of the modelled benthic system is limited to 30 cm. Transport of benthic organic particulate material as postulated by van Beusekom and de Jonge (2002) is included as exchange process between adjacent sediment areas (Ebenhöh et al., 2004).

Furthermore, the model is implemented in CEMoS (*C Environment for Model Simulation*; Hamberg, 1996). The water movement is calculated with a fixed time step of 1/100 day. Ecological processes are calculated with a Runge-Kutta method with time step adaption and a maximum time step of 1/100 day. The number of Lagrangian tracers amounts to 200. Each tracer describes a volume of $2.22 \cdot 10^6 \text{ m}^3$. A more detailed description of the model is given in Kohlmeier and Ebenhöh (2007).

Calculations comprise the period of the first to the last low tide in 2007 (364.82 days). Different scenarios (run1 - run4) are investigated, which are used as a sensitivity analysis. The reference run (run1) is parameterised according to Kohlmeier and Ebenhöh (2007). In a

second run (run2), the contribution via the flood-gate in Neuharlingersiel is excluded to calculate the freshwater impact on nutrient budgets of the back barrier area. In runs3 and 4 the influence of benthic organic particulate matter import is estimated. While in run3 the benthic sedimentary import of particulate matter into the back barrier area is excluded, the amount is doubled in calculations of run4.

4.4 Results and discussion

4.4.1 Seasonal dynamics in surface waters of the Wadden Sea

Since April 2006 dissolved nutrients (silica, phosphate, and nitrite plus nitrate) were determined by automated nutrient analysers mounted on a time-series station (Grunwald et al., 2007) in the tidal inlet of the back barrier area of Spiekeroog Island (Fig. 4.1). The time-series station provides the opportunity to measure dissolved nutrients hourly throughout the year, even during gale-force winds or ice winters.

Silica

Silica shows a pronounced seasonal cycling in surface waters of the back barrier area of Spiekeroog Island (Fig. 4.2), with highest values determined during late autumn and winter (December – March). Silica median concentrations in autumn/winter of the years 2006/2007 were about 23 μM . Measurements of the same period in 2007/2008 exhibit a similar level at 21 μM . Although, there are some data gaps (dashed lines in Fig. 4.2), the silica pattern during the winter period reveals distinct differences for the investigated years. While in winter 2006/2007 (December - March) the silica pattern has a plateau-like shape, data from winter 2007/2008 are characterized by a steeper slope with maximum values being reached in January 2008 (Table 4.1).

Subsequent to elevated winter levels, a rapid decrease is seen in early spring due to the onset of the spring diatom bloom in the North Sea, as diatoms use silica for their shell formation (Lewin, 1962; Antia et al., 1963; Grant, 1971; Ryther et al., 1971; Paasche, 1973). In 2007, silica concentration decrease within 25 days from a value of 28.8 μM (18th March) to 0.4 μM (11th April) resulting in an average loss of 1.1 $\mu\text{M d}^{-1}$. In 2008, concentrations decrease from 30.1 μM to 1.7 μM (2nd March - 15th April) with a gradient of 0.63 $\mu\text{M d}^{-1}$ within 45 days. Additionally, the spring diatom bloom starts later in 2007 when compared with 2008. Typically, the spring bloom starts in the shallow waters of the German Bight between week 6 and 14 (Wiltshire et al., 2008) with inter-annual variations (Townsend et al., 1994). Wiltshire and Manly (2004) postulated that a delay of the early spring bloom may be

related to a longer persistence of zooplankton grazers in autumn and early winter (Beare et al., 2002) thereby reducing the crucial biomass stock necessary to initiate a phytoplankton bloom. A further reason for a delay in spring bloom is insufficient insolation under disadvantageous weather conditions (cloudiness, wave action), which is especially important in the turbid waters of the study area (Smetacek and Passow, 1990; Townsend et al., 1994; Tillmann et al., 2000; Colijn and Cadee, 2003; Billerbeck et al., 2007; Loebl et al., 2009).

Due to silica consumption by diatoms, silica concentrations reach a minimum in May 2006 as well as 2007 and in late June 2008 indicating silica limitation. In 2006 and 2007, the diatom growth seems to be limited solely by silica availability. In contrast, phosphate as a further essential nutrient (Philippart et al., 2007) also reaches a minimum in May 2008 (Fig. 4.2), which probably limited diatom growth and led to a decrease in silica uptake. Generally, silica concentrations are lowest during spring and summer (April – September) with median values of 0.41 – 5.48 μM (Table 4.1). This level is below or at least close to the threshold of 2 μM where diatoms compete with dinoflagellates, which leads to a change in the phytoplankton community with increasing abundance of dinoflagellates (Egge and Aksnes, 1992; Egge, 1998). Due to the breakdown of the summer bloom, silica concentrations increase rapidly from an average level of about 2 μM at the end of August to a first maximum in November (about 14 μM). During November and December the silica increase comes to a halt which is probably caused by a weakly developed bloom in autumn. Insufficient insolation in autumn and winter further reduces the phytoplankton population and thus silica uptake by phytoplankton (Hagmeier and Bauerfeind, 1990; van Bennekom and Wetsteijn, 1990; Peeters et al., 1991), which leads to a second maximum in January (about 25 μM).

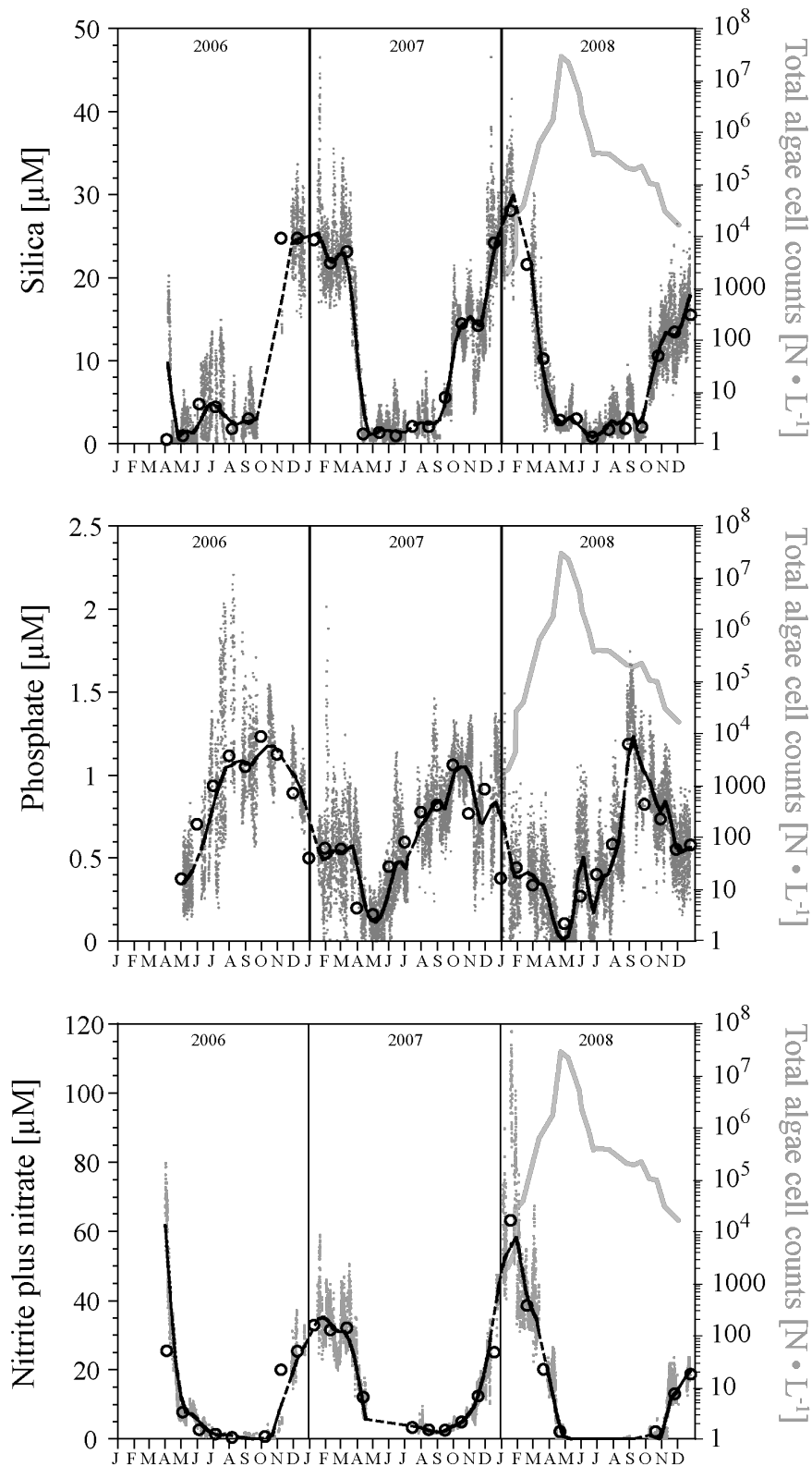


Fig. 4.2. Silica, phosphate, and nitrite plus nitrate in the years 2006-2008 determined at the time-series station in the tidal inlet of the Island of Spiekeroog. Single measurements are shown as grey points. The black line represents running average concentrations (dashed segments: no data are available) and open circles indicate monthly averages. Total algae cell counts in 2008 (grey line) are given in a logarithmic axis scale.

Table 4.1. Summary of monthly averaged concentrations for silica, phosphate, and nitrite plus nitrate for the years 2006 – 2008. Corresponding ranges (min – max) are given in brackets. ‘n’ denote the number of measurements used for averaging. Values indicated by ‘*’ are below detection limit.

	Silica [μM]		
	2006		2007
	Median	(min - max; n)	Median (min - max; n)
January			24.4 (17.0 - 46.6; 267)
February			21.7 (16.4 - 35.6; 503)
March			23.1 (8.8 - 34.4; 524)
April	0.4	(<0.38* - 20.3; 521)	1.1 (<0.38* - 12.2; 445)
May	0.9	(<0.38* - 6.4; 590)	1.3 (<0.38* - 4.7; 648)
June	4.7	(<0.38* - 13.5; 465)	0.9 (<0.38* - 7.7; 592)
July	4.4	(<0.38* - 15.0; 358)	2.0 (<0.38* - 5.1; 145)
August	1.7	(<0.38* - 8.2; 278)	2.0 (<0.38* - 8.7; 363)
September	2.9	(0.6 - 9.3; 328)	5.5 (0.7 - 16.6; 429)
October	n.d.	(- ; 0)	14.4 (9.9 - 21.5; 615)
November	24.7	(13.4 - 30.7; 83)	14.2 (3.6 - 22.1; 592)
December	24.7	(15.3 - 33.7; 345)	24.1 (11.1 - 46.6; 572)

	Phosphate [μM]		
	2006		2007
	Median	(min - max; n)	Median (min - max; n)
January			0.5 (0.01 - 0.79; 261)
February			0.6 (0.01 - 2.01; 476)
March			0.6 (0.01 - 1.24; 520)
April			0.2 (<0.01* - 0.72; 408)
May	0.4	(0.1 - 0.8; 438)	0.2 (<0.01* - 0.59; 588)
June	0.7	(0.3 - 1.4; 311)	0.4 (0.01 - 1.14; 612)
July	0.9	(0.2 - 2.0; 405)	0.6 (0.23 - 1.05; 224)
August	1.1	(0.7 - 2.2; 269)	0.8 (0.24 - 1.46; 504)
September	1.0	(0.6 - 1.7; 316)	0.8 (0.50 - 1.19; 609)
October	1.2	(0.8 - 1.6; 237)	1.1 (0.79 - 1.33; 611)
November	1.1	(0.7 - 1.3; 74)	0.8 (0.19 - 1.36; 544)
December	0.9	(0.6 - 1.3; 207)	0.9 (0.29 - 1.37; 347)

	Nitrite plus nitrate [μM]		
	2006		2007
	Median	(min - max; n)	Median (min - max; n)
January			32.5 (23.1 - 59.0; 260)
February			31.3 (20.0 - 46.0; 500)
March			31.8 (12.4 - 50.6; 547)
April	25.2	(5.3 - 79.9; 584)	11.8 (5.9 - 21.3; 299)
May	7.4	(4.1 - 11.7; 557)	n.d. (- ; 0)
June	2.4	(0.6 - 6.2; 508)	n.d. (- ; 0)
July	1.2	(<0.17* - 2.3; 402)	3.1 (1.8 - 7.3; 69)
August	0.2	(<0.17* - 1.9; 129)	2.4 (1.8 - 9.6; 316)
September	0.6	(<0.17* - 1.8; 162)	2.3 (1.5 - 4.4; 580)
October	0.5	(<0.17* - 4.3; 173)	4.6 (2.7 - 9.1; 520)
November	19.7	(2.1 - 31.2; 100)	12.1 (4.3 - 20.4; 621)
December	25.1	(16.7 - 37.3; 106)	24.8 (5.8 - 47.4; 337)

n.d.: not determined

The pattern and concentration levels found in our study area are comparable to findings in the Belgian coastal area (western Wadden Sea, southern North Sea) in 1993 and 1994 (Schoemann et al., 1998) and in 2002 (van der Zee and Chou, 2005) as well as in the List tidal basin (northern Wadden Sea, German Bight) in 2004 and 2005 (Loebl et al., 2007; van Beusekom and Diel-Christiansen, 2009). The authors determined highest silica concentrations in February with up to 30 μM for the Belgian coast and 35 μM for the List tidal basin. A subsequent strong decrease in March due to assimilation by diatoms is observed at all study sites. Similar to our results, Schoemann et al. (1998) also observed some variation in diatom bloom onset between the years 1993 and 1994. While in 1993 the bloom started in late March, in 1994 a decrease in silica already occurs in late February. Additionally, the slopes of concentration decrease differ between the years with a steeper gradient in 1994. This is in good agreement with our data, where a delayed onset of diatom bloom is accompanied by a less steep gradient in concentration decrease, which is assumed to be governed by inter-annual variation of persistence of zooplankton grazers, as mentioned before. Consequently, low concentrations during summer with increasing levels towards autumn also have been reported for both, the Belgian coast (Schoemann et al., 1998; van der Zee and Chou, 2005) and the northern part of the Wadden Sea (Loebl et al., 2007; van Beusekom and Diel-Christiansen, 2009), with similar levels when compared to the back barrier area of Spiekeroog Island.

Phosphate

Phosphate is an essential nutrient for any organism, since phosphorus is needed for synthesis of e.g. nucleotides for DNA, phospholipids for cell membranes, and the generation of ATP for energy buffering (Schlesinger, 1997). Thus, the concentration of dissolved phosphate in marine environments is strongly affected by primary production. In the water column of the back barrier area, phosphate shows seasonal cycling, however the annual pattern is different when compared with silica (Fig. 4.2) as maximum levels are observed in late summer and early autumn. The phosphate level increases to a maximum value of on average 1.0 μM in September - October, whereas minima of below 0.2 μM are reached between April and May (Table 4.1). This seasonal pattern is in good agreement with the behaviour of phosphate reported for the Southern North Sea and the adjacent Wadden Sea areas (Postma, 1954; de Jonge and Postma, 1974; Brockmann et al., 1990; Hickel et al., 1993).

As described for the silica cycle, maximum phosphate concentrations are seen at a different point in time in the years 2006 – 2008. The autumn maxima change from a plateau-like shape in 2006 to a more peak-like profile in 2008, probably due to different consumption

and remineralisation conditions. Although phosphate is consumed by phytoplankton, decomposition of produced biomass prevails over consumption from early summer onwards, thereby replenishing the pelagic phosphate pool (van Beusekom and Diel-Christiansen, 2009). The predominance of decomposition over consumption occurs until September/October, when the annual maximum concentrations are reached. Afterwards, the phosphate level decreases in autumn and winter, which can be hardly attributed to phytoplankton activity, as supported by decreasing total algae cell counts (Fig. 4.2). As the phosphorus cycle is not only governed by bioproductivity and organic matter decomposition, adsorption and desorption processes by ferric oxyhydroxides in the sediments have to be considered as well (Einsele, 1938; Berner, 1973; Slomp et al., 1996; van Beusekom and de Jonge, 1998). The connection between dissolved phosphate and the sedimentary iron cycle probably causes lower average winter concentrations when compared to autumn values. This aspect will be discussed in detail below.

Nitrite plus nitrate (NO_x)

According to van Beusekom et al. (2001), nitrogen input to the coastal zone is dominated by dissolved inorganic fractions, responsible for about 80% of the total N input. The authors point out that ammonia is of minor importance (about 5%), while nitrate forms the major component by accounting for about 75% of the total N import.

The seasonal pattern of nitrite plus nitrate, here referred to as NO_x, in 2006 - 2008 is comparable to that of silica (Fig. 4.2) with highest values in winter and the lowest level during spring and summer. However, the inter-annual variability in winter concentrations is much more pronounced for NO_x when compared with silica and phosphate. In January – March 2007, we determined almost uniform plateau-like average concentrations of about 32 μM, whereas in the same period of 2008 monthly average concentrations varied from about 63 μM (January) to 17 μM in March (Table 4.1). Although, there is a small data gap, Figure 4.2 indicates that NO_x winter concentrations in 2005/2006 were similar to those in 2008. The inter-annual variation of winter NO_x concentration levels in the study area is likely governed by both, varying NO_x contribution by large rivers and denitrification processes within tidal flat sediments, as described van Beusekom et al. (2008) for the northern Wadden Sea of the German Bight. This assumption is supported by findings of e.g. Lacroix et al. (2007) and Johannsen et al. (2008) who reported highest NO_x loads of rivers in winter, while river concentrations can vary by a factor of 2 between succeeding years (e.g. Lacroix et al., 2007).

Low concentrations in spring and summer denote the direct coupling to primary production, which is supported by the almost coincident decrease of NO_x and silica during

spring bloom in 2007 and 2008. The pattern as well as concentration levels of NO_x observed in the study area are in good agreement with data for the Dutch Wadden Sea (van Beusekom et al., 2001) and the List tidal basin of the northern Wadden Sea (Loebl et al., 2007; van Beusekom and Diel-Christiansen, 2009). However, the NO_x cycle is not only affected by phytoplankton assimilation but by nitrogen recycling processes as well, which occur in both, the water column (Caperon et al., 1979; Glibert, 1982; Christensen, 1994; Soetaert et al., 2006; Pätsch and Kühn, 2008) and the sediments (Nixon et al., 1976; Lohse et al., 1993; van Beusekom et al., 1999; Ehrenhauss et al., 2004; Murray et al., 2006). Especially during spring and summer, decomposition of organic material leads to enhanced oxygen consumption in sediments and thus to elevated denitrification (Christensen, 1994; Jensen et al., 1996; Seitzinger and Giblin, 1996; van Beusekom and Reise, 2008). The concurrent processes of both, enhanced assimilation by phytoplankton and elevated denitrification are assumed to be the driving forces for low NO_x concentration during the growing season in our system.

4.4.2 Tidal dynamics in the Wadden Sea

The tidal patterns of silica, phosphate, and NO_x are exemplarily discussed using data determined at the time-series station in 2007 (Fig. 4.3).

Silica

Silica shows a uniform tidal pattern in every season, with maximum concentrations at low tide. Since literature data for silica concentration of tidal systems and estuaries are scarce on a tidal scale, we compare our data to the data set obtained by Liebezeit et al. (1996). These authors determined dissolved silica in the study area in May 1993, April 1994, and February 1995. However, no tidally driven dynamics could be observed due to exceptional wave action and high currents leading to these irregularities (Liebezeit et al., 1996).

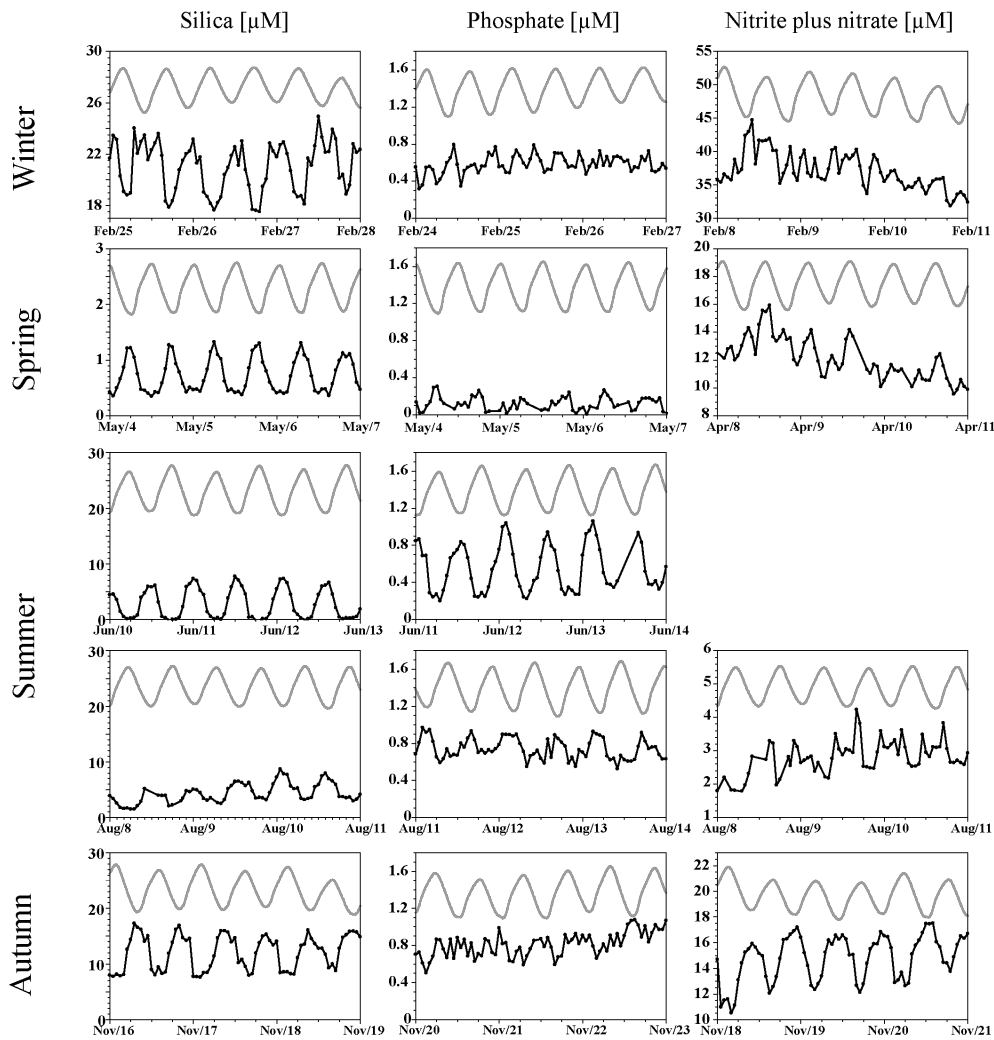


Fig. 4.3. Tidal dynamics of silica, phosphate, and nitrite plus nitrate in winter, spring, summer, and autumn 2007. Note the different scales for silica (winter) and nitrite plus nitrate. Grey lines indicate the tidal state.

In our study, differences in amplitude, i.e. concentration range between low and high tide, and concentration level are observed on a seasonal scale. The winter amplitude in February 2007 of $6 \mu\text{M}$ at a high concentration level of about $22 \mu\text{M}$ decreases towards spring (May) to an amplitude and concentration level of below $1 \mu\text{M}$. For example in June, high tide silica is depleted while low tide concentrations increase to values of up to $7.7 \mu\text{M}$. This reveals that release of remineralised silica prevails over consumption in the back barrier area. Furthermore, reduced levels at high tide are due to dilution with nutrient-poor waters from the German Bight. Hence, decreasing assimilation towards August results in slightly elevated high tide concentrations of about $2 \mu\text{M}$. The gain in silica concentration continues during autumn by gradual replenishment of the water column towards winter.

Phosphate

During winter (February, Fig. 4.3), phosphate shows no clear tidal-induced pattern. During spring (May), a slight tidal dependence with decreasing concentrations during high tide (about 0.2 μM) develops, which is due to elevated phosphate assimilation by phytoplankton in the German Bight. Towards June, tidal cyclicity is high with amplitudes of 0.6 μM . This points towards increased phosphate release within the back barrier area in June, which compares well with other back barrier tidal flats and estuaries in the Southern North Sea (Rutgers van der Loeff et al., 1981; Jensen et al., 1995; Dick et al., 1999). In August, the tidal pattern is similar to that observed in May. However, the tidal amplitude is smaller in August compared to June, reaching about 0.3 μM at a concentration level of 0.8 μM . From November, no tidally-driven pattern can be observed.

The tidal dynamics of phosphate and silica are different since the biogeochemistry of both nutrients differs. Besides assimilation by phytoplankton, phosphate dynamics are influenced by adsorption to FeOOH in the tidal flat sediments (see below).

NO_x (Nitrite plus nitrate)

The tidal pattern of NO_x is different to those of silica and phosphate. In winter, NO_x in general does not reveal tidally-driven dynamics, but during certain days higher concentrations can be observed at low tide. This tidal dependence only lasts for up to 4 days and seems to be caused by random contribution of freshwater via the flood-gate. In spring, concentrations are slightly higher at high tide compared to low tide. The lower concentrations at low tide may reflect lower assimilation rates in the back barrier area compared to the German Bight. Enhanced denitrification processes in tidal flat sediments may further lead to depleted concentrations at low tide. As phytoplankton is able to store nitrate in its vacuoles (Dortch, 1982; Stolte et al., 1994), the deposition of intact cells may result in accumulation in the sediment (Cadée, 1996) followed by release of nitrate and thus to an enhancement of denitrification rates (Lomstein et al., 1990).

In summer (August, Fig. 4.3), a coupling to the tidal signal can be seen which is inverse to the pattern observed in April. Higher NO_x concentrations tend to appear during low tide with an amplitude of 1.2 μM which points towards remineralisation occurring in the back barrier area. This is in accordance with investigations in the Dutch Wadden Sea (Helder, 1974), where decomposition of organic matter dominates over assimilation in late summer and autumn. The slight accordance with the tidal state observed in summer (August) becomes more pronounced in autumn (November), when an amplitude of about 4 μM is observed.

4.4.3 Nutrient sources in the back barrier area

For the back barrier area of Spiekeroog Island the potential sources for dissolved inorganic nutrients are freshwater discharge via the flood-gate in Neuharlingersiel, pore waters draining out of the tidal flat sediments, and precipitation as a source for atmospheric nitrogen input. Here we focus on the contributions via freshwater and pore water, due to lack of information about the amount of atmospheric deposition.

4.4.3.1 Freshwater

In the study area, freshwater discharge via the flood-gate in Neuharlingersiel to the back barrier area changes seasonally due to rainfall and vegetation periods in the hinterland. The freshwater contribution is based on averaged water discharge of the years 1996 to 2006 (Rupert et al., 2004) and nutrient concentrations determined at the flood-gate in 2002 – 2004 (Fig. 4.4). High water discharge rates from November to March are directly coupled to precipitation. In contrast, during the vegetation period freshwater contribution is distinctly lower and not related to precipitation. The inter-monthly variation of averaged discharge encompasses a range from $0.4 * 10^6 \text{ m}^3$ in June to $3.4 * 10^6 \text{ m}^3$ in January (Rupert et al., 2004).

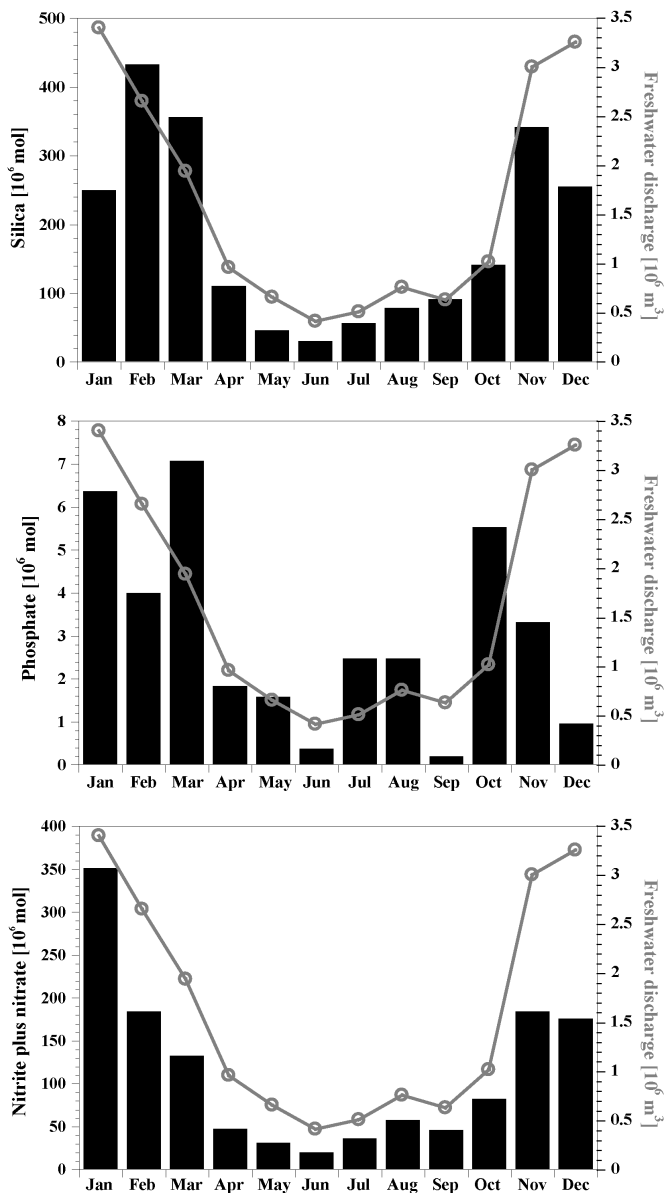


Fig. 4.4. Monthly freshwater contribution of silica, phosphate, and nitrite plus nitrate via the flood-gate in Neuharlingersiel to the tidal flat area of Spiekeroog (columns). Data are averaged for the years 2002-2004. For comparison, averaged freshwater discharge rates (Rupert et al., 2004) via the flood-gate are given (circles).

Monthly amounts of nutrient discharge by freshwater to the tidal flat area reveal different patterns for silica, phosphate, and nitrite plus nitrate (Fig. 4.4). While silica and nitrite plus nitrate obeys roughly the freshwater discharge, phosphate contribution seems to be decoupled, which may be due to different kinds of sources. For dissolved silica weathering processes of soil minerals (Turner et al., 2003) within the catchment area are the main source,

while freshwater phosphate as well as nitrite plus nitrate concentration is strongly dependent on land use and fertilizer application (Turner et al., 2003).

The annual pattern of silica and nitrite plus nitrate discharge via freshwater is comparable to the one observed at the time-series station (compare to Fig. 4.2), while phosphate shows no similarities. Silica contribution is directly coupled to the amount of discharged water volume (Fig. 4.4) and varies between $0.3 * 10^8$ (June) to $4.2 * 10^8$ mol per month (February). For phosphate, no seasonal pattern is found and contribution via freshwater is irregular with a range of $0.2 - 8 * 10^6$ mol per month. The seasonal pattern of nitrite plus nitrate is directly coupled to freshwater discharge volume and reveal a contribution of $0.2 * 10^8$ (June) - $3.5 * 10^8$ (January) mol per month.

Freshwater is discharged irregularly to the back barrier area, only at around two hours before low tide depending on the level in the flood-gate basin. Therefore, the tidal nutrient pattern determined at the time-series station, with the exception of random events for NO_x in winter, cannot be explained by freshwater contribution. Further, the highest discharge volume of $3.4 * 10^6 \text{ m}^3$ per month is one order of magnitude smaller than the water volume of the back barrier area of about $39 * 10^6 \text{ m}^3$ at neap tide low water (Stanev et al., 2003). Thus, despite the enrichment of silica and phosphate in freshwater compared to the water column in the back barrier area, the volume of freshwater released to the back barrier area is too small to produce remarkable signals, even during winter. Consequently, the nutrient discharge via the flood-gate in Neuharlingersiel is of minor importance, which is supported by results of our model simulations (see below).

4.4.3.2 Pore water

A further nutrient source are pore waters draining from tidal flat sediments during low tide. Nutrients and dissolved organic carbon (DOC) dynamics in tidal flat sediments have been intensively studied (Howes and Goehring, 1994; Böttcher et al., 1998, 2000, 2004; de Beer et al., 2005; Billerbeck et al., 2006a; Beck et al., 2008b,c; Kowalski et al., 2009). Intertidal sediments are characterised by enhanced degradation of organic matter with subsequent release of dissolved nutrients to the interstitial waters. Jansen et al. (2009) studied pore water dynamics in the upper few centimetres at site Janssand. They emphasized the high variability in oxygen penetration and solute exchange in this layer.

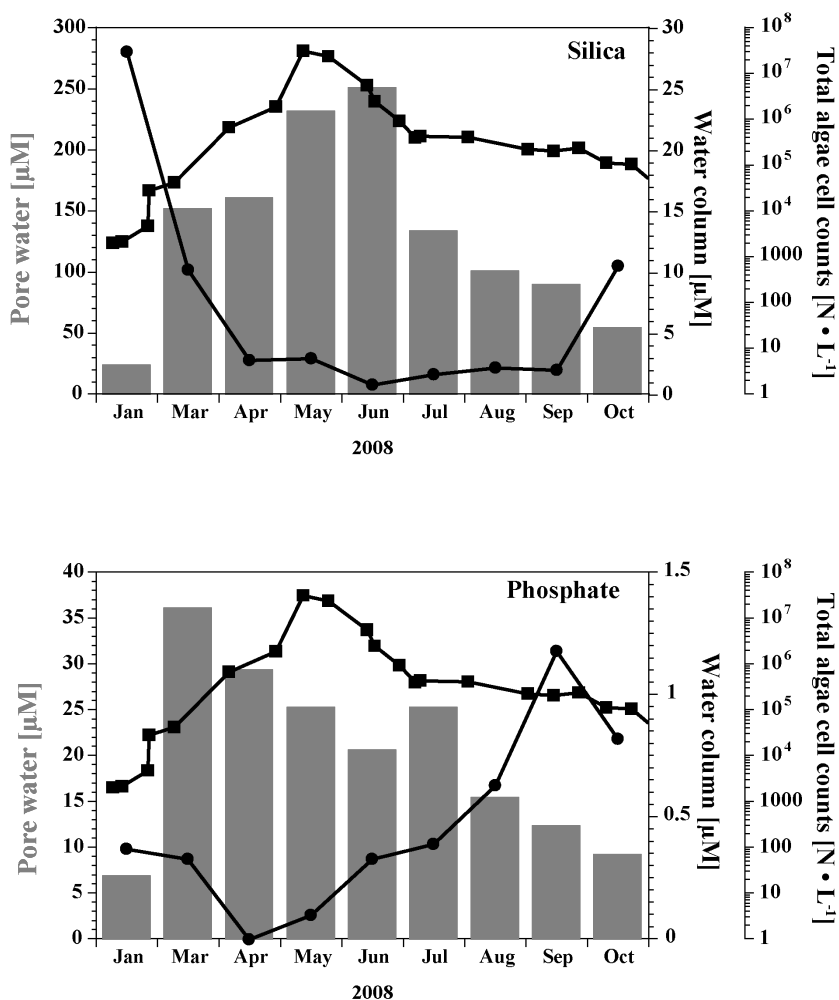


Fig. 4.5. Pore water concentrations of silica and phosphate in 2008 at site JS1 (columns). For comparison, monthly averages of water column concentrations (circles) and total algae cell counts (squares) are indicated.

In the upper 10 cm sediment at site JS1, pore water concentrations change seasonally. Silica pore water concentrations are highest during the growth season (March – September), while during autumn and winter concentrations are lower (Fig. 4.5). Concentrations vary from 25 µM (January) up to 250 µM (June). The pattern of pore water silica seems to be influenced directly by the diatom succession in the water column. After the onset of the annual diatom spring bloom in February, silica concentration in pore water increase due to sedimentation, burial and subsequent decomposition of diatom frustules. Dissolution rates of diatom walls depend on temperature as well as pH, i.e. dissolution increases at higher temperatures or at higher pH (Lewin, 1961; Kamatani and Riley, 1979; Kamatani, 1982; Nelson et al., 1995; Cheng et al., 2009). The decrease in pore water silica towards autumn is due to decreasing supply of diatom frustules to the sediments.

For phosphate, the seasonal pattern in pore water differs from that of silica. Similar to silica, highest phosphate concentrations are observed in March. However, concentrations decrease more or less linearly in spring and summer towards autumn and winter. Besides the direct coupling to biological assimilation, phosphate underlies a further source/sink process as mentioned above. Phosphate from both, organic matter decomposition and the open water column can be trapped during precipitation of ferric oxyhydroxides in oxic surface sediments. This process is most pronounced in autumn and winter when decreasing microbial activity due to lower temperatures (Vosjan, 1974) results in an expansion of the oxic surface layer. In contrast, both, increased deposition of organic material on sediment surfaces and microbial activity in summer results in a migration of the anoxic layer towards the sediment surface. The subsequent reduction of ferric oxyhydroxides leads to a release of dissolved iron (Fe^{2+}) and phosphate to interstitial waters (van Beusekom et al., 2001). Upwards migrating Fe^{2+} and phosphate can reprecipitate to some extent when reaching the oxic zone, while part of the dissolved iron can already precipitate in the anoxic zone in presence of H_2S as sulphide. Phosphate, which is not retained in the sediments, can be released to the water column. Thus, during spring and summer pore waters are highly enriched in phosphate. Jensen et al. (1995) figured out a low molar Fe/P ratio of 2 in the sediments of Aarhus Bay. At this level the buffer capacity of the sediment for P is exhausted. For comparison, the authors found maximum molar Fe/P-ratios of about 10 in winter and early spring, when the sediments are well oxygenated and thus still possess capacity for phosphate fixation. Therefore, sediments act as phosphate sinks during winter (van Beusekom et al., 2001).

Especially in the Wadden Sea, iron-bound phosphate is of the same importance like particulate organic phosphorous (van Beusekom and de Jonge, 1997; van Beusekom and de Jonge, 1998). Thus, during summer pore waters can contribute phosphate notably to the back barrier area water column.

4.4.4 Nutrient budgets

The Euler-Lagrangian model EcoTiM describes the cycling of silica, phosphate and nitrite plus nitrate in the back barrier area of Spiekeroog Island. The study focusses on the budgets at the tidal inlet at the boundary between model boxes 2 and 3 (Fig. 4.1c). An estimation of dissolved inorganic nutrient export as well as the impact of nutrient supply via freshwater is summarized in Table 4.2.

Table 4.2. Results of Euler-Lagrangian model simulations. Export of dissolved inorganic silica, phosphate and nitrite plus nitrate from the back barrier area as well as the impact of freshwater contribution via the flood-gate are given for different runs of model calculations (see text). Values in brackets indicate the percentage in comparison to the reference run (run1).

Silica [10^6 mol a^{-1}]	run1	run2	run3	run4
Dissolved export	127.7	125.2 (98 %)	38.0 (30 %)	206.4 (162 %)
Freshwater input	2.6	0.0 (0 %)	2.6 (100 %)	2.6 (100 %)

Phosphate [10^6 mol a^{-1}]	run1	run2	run3	run4
Dissolved export	3.06	3.0 (98 %)	2.7 (89 %)	3.5 (114 %)
Freshwater input	0.05	0.00 (0 %)	0.05 (100 %)	0.05 (100 %)

Nitrite plus nitrate [10^6 mol a^{-1}]	run1	run2	run3	run4
Dissolved export	28.9	27.2 (94%)	33.9 (117%)	26.5 (92%)
Freshwater input	1.9	0.0 (0%)	1.9 (100%)	1.9 (100%)

The comparison of reference run (run1) and data determined at the time-series station in 2007 shows that the seasonal pattern is reproduced by the model (Fig. 4.6). However, calculated winter concentrations of silica and nitrite plus nitrate are too low compared to time-series station data. This may be due to the applied boundary conditions, which were not available for 2007 but have been derived from data in 2002. Thus, winter values at the North Sea boundary as well as assumed particulate matter import into the back barrier area in autumn and winter might be underestimated in the model study. Nevertheless, the strong concentration decrease due to the annual spring bloom is reproduced very well. The annual simulated phosphate pattern reproduces measured values, with the exception that in summer (June – October) the model results are too low. This may be caused by an underrated contribution of phosphate-rich pore waters to the pelagic system or by overestimated assimilation by phytoplankton. In agreement with the measurements, model results of run2 reveal that nutrient contribution via the flood-gate is of minor importance and accounts for only 2% (silica), 2% (phosphate), and 6% (nitrite plus nitrate) of the total nutrient budget of the study area, respectively.

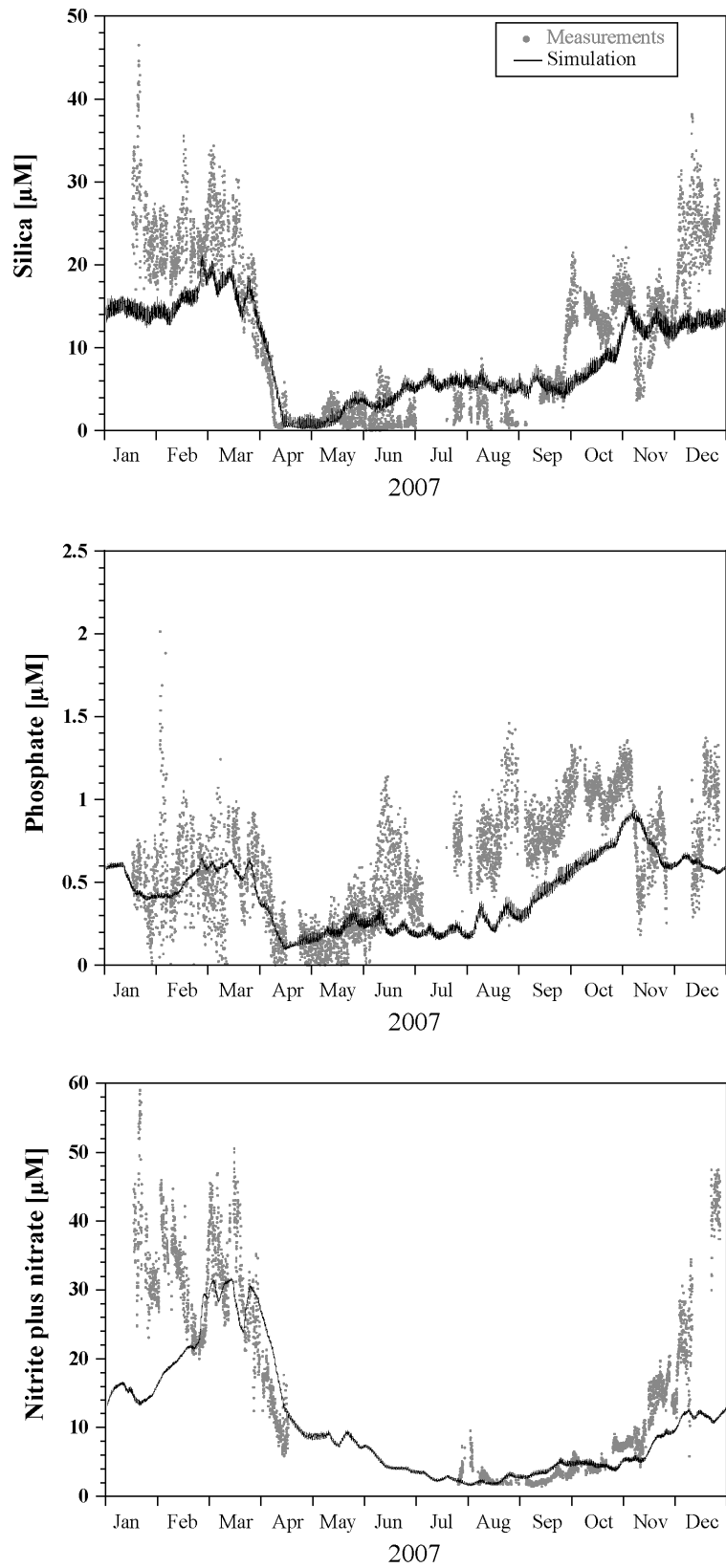


Fig. 4.6. Model simulation for silica, phosphate, and nitrite plus nitrate (black line) compared with data determined at the time-series station (grey circles) in 2007.

Particulate organic matter (POM) is probably the least studied parameter which is included in the model. According to van Beusekom and de Jonge (2002) who emphasise the import of POM into the Wadden Sea, this is implemented in the model calculations. Nutrient gradients occurring within back barrier areas (Ebenhöh et al., 2004) can only be reproduced by the model if an additional sedimentary import of organic matter is implemented (Postma, 1961). To analyse the importance of sedimentary import of organic matter, this import is omitted in run3, whereas in a further scenario (run4) the import is doubled.

While phosphate and nitrite plus nitrate budgets are quite similar for all scenarios, silica concentrations show significant differences (Fig. 4.7). Without import of additional sedimentary organic matter, the model underestimates silica winter values within the back barrier area. The scenario with doubled import (run4) is in good agreement with measured data in winter, whereas summer values are overestimated.

Since the reference run (run1) is the run most suitable to reproduce the annual pattern observed by measurements, these data are used for budget estimations. Results of model calculations indicate that dissolved inorganic silica, phosphate, and nitrite plus nitrate are exported from the back barrier area of Spiekeroog Island towards coastal waters of the North Sea. Amounts of $128 * 10^6 \text{ mol a}^{-1}$ dissolved inorganic silica, $3 * 10^6 \text{ mol a}^{-1}$ dissolved inorganic phosphate, and $29 * 10^6 \text{ mol a}^{-1}$ nitrite plus nitrate are estimated to be supplied to the North Sea.

The model results indicate that particulate nutrients are imported from the North Sea to tidal flat areas. In the semi-enclosed tidal flat areas, settling and degradation of the imported organic material may be faster than in the open North Sea. The tidal flat 'bioreactor' accelerates remineralisation processes and thus the release of dissolved inorganic nutrients, which are partly exported to coastal waters of the North Sea.

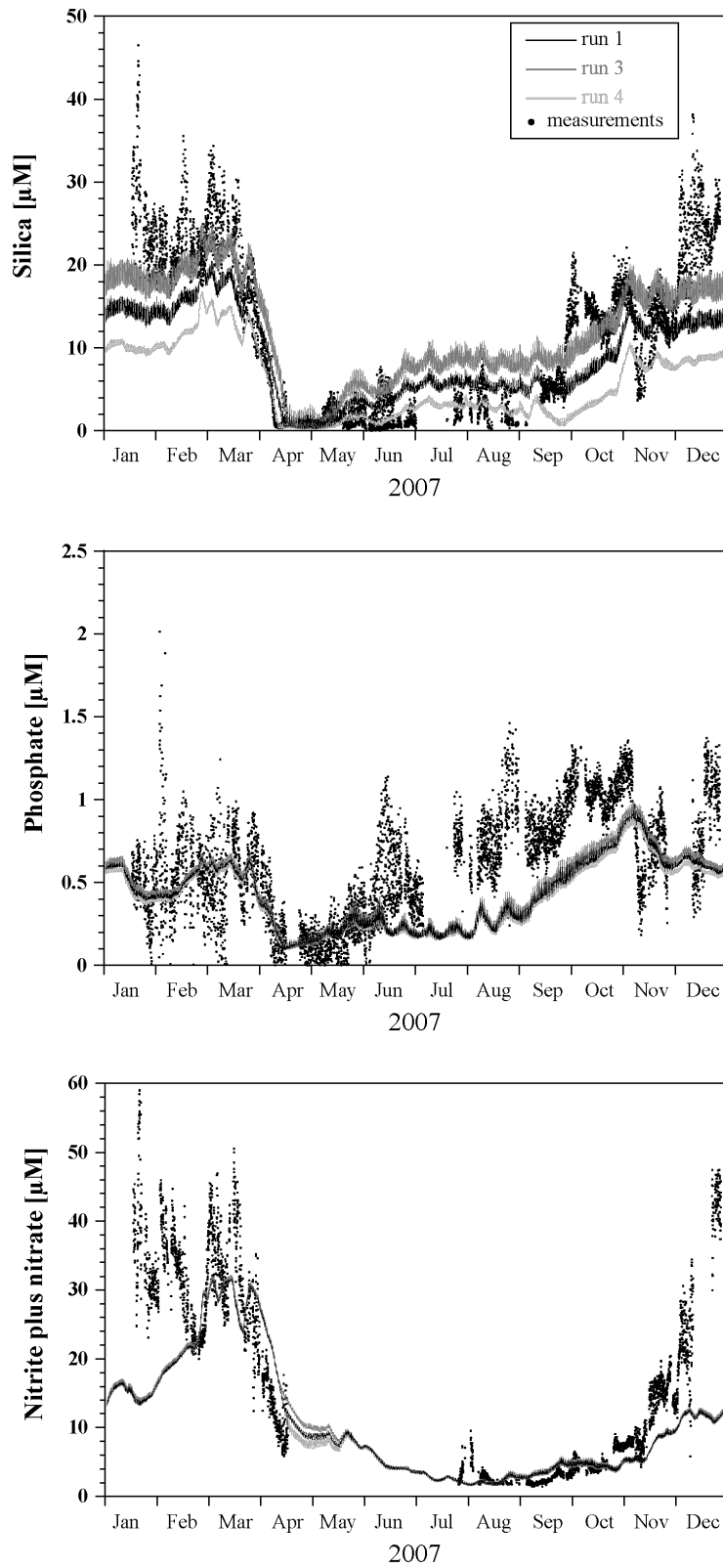


Fig. 4.7. Annual pattern of silica, phosphate, and nitrite plus nitrate in 2007 as simulated by the reference run (run1, black line), the run without additional import of POM (run3, dark grey line), and enhanced import of POM (run4, light grey line) compared to measurement data from the time-series station (black dots).

The entire tidal flat area of the Wadden Sea comprises about 1688 km² (Grunwald et al., 2009) excluding estuaries, which is about 23 times larger than the back barrier area of Spiekeroog Island. An extrapolation of the export values from our study area to the entire back barrier area of the German Bight denote the significance of tidal flat areas in the line of nutrient contribution to the German Bight (Table 4.3). The sum of net dissolved export of silica and phosphate is in the same order of magnitude like the sum of the major German rivers Elbe, Weser, and Ems (Lenhart and Pätsch, 2001) discharging into the German Bight, while nitrite plus nitrate (NO_x) export is one order of magnitude lower than riverine contribution. Therefore, nutrient recycling in the tidal flat areas has to be taken into account when budget calculations for the North Sea are performed.

Table 4.3. Nutrient export from the whole back barrier area of the Wadden Sea in the German Bight compared with riverine nutrient load.

		Σ Wadden Sea	Σ rivers (Elbe, Weser, Ems)*	Elbe*	Weser*	Ems*
Silica	[10 ⁸ mol a ⁻¹]	30	20	7	10	3
Phosphate	[10 ⁶ mol a ⁻¹]	70	25	17	7	1
NO_x	[10 ⁸ mol a ⁻¹]	7	23	13	7	3

*: Lenhart and Pätsch (2001)

4.5 Conclusions

Silica, phosphate, and nitrite plus nitrate concentrations of surface water were determined hourly since April 2006 by automated nutrient analysers mounted on a time-series station in the tidal inlet of the back barrier area of Spiekeroog Island. The high frequency of measurements provides the opportunity to identify dynamics on annual, seasonal, and tidal scales. Silica concentrations are governed by assimilation by diatoms leading to low concentrations in spring and summer. Due to the subsequent remineralisation of diatom frustules within the sediments, silica concentrations increase towards autumn with highest values in winter. Phosphate is not only affected by biological dynamics, but may be trapped by ferric oxyhydroxides in oxygenated sediments as well. When sediments become anoxic, phosphate is desorbed from ferric oxyhydroxides and released into the open water column. NO_x concentrations are highest in winter months, mainly controlled by river discharge. Interannual variation in concentration levels are governed by fluctuating river loads as well as denitrification processes within the sediments.

Nutrient patterns at a tidal resolution reveal a different behaviour for silica, phosphate, and NO_x. Silica reveals a consistent relation to the tidal state with higher concentrations at low tide throughout the year. However, the tidally driven pattern of phosphate is most pronounced in summer and only a slight dependence to the tidal state can be observed in the remaining seasons. For NO_x a distinct tidal pattern can be observed in autumn, while the remaining seasons reveal a slight or even no coupling to the tide.

Measured data are used to verify model simulations which are used for budget calculations. Freshwater contribution to the back barrier area from the hinterland via the flood-gate is negligible for the nutrient budget, whereas pore waters form the main source of nutrients, as revealed by both, measurements and numerical modelling. The back barrier area forms a “bio-reactor” where nutrients are assimilated and remineralised. Modelling indicates that dissolved inorganic nutrients are exported from the tidal flat area. Thus, tidal flat areas play a major role in supplying nutrients to the German Bight and have to be considered in budget calculations besides riverine nutrient discharge.

Acknowledgements

The authors are indebted to W. Siewert for his help in operating the nutrient analysers. H. Nicolai as well as A. Braun are thanked for their assistance in maintaining the time-series station. We thank C. Lehnert, E. Gründken, M. Schulz, and H. Rickels for their assistance during laboratory work and F. Schoster for analyser maintenance. Furthermore, we wish to thank C.-D. Dürselen for total algae cells count data and T.H. Badewien for providing water temperature and PAR data of the time-series station. B. Schmetger is thanked for his valuable help in nutrient analyser maintenance. L. Aden and J. Meinen-Hieronimus are thanked for providing data of freshwater contribution via the flood-gate in Neuharlingersiel. This work was funded by the Deutsche Forschungsgemeinschaft through grant FOR 432.

5 Sulphate, dissolved organic carbon, nutrients and terminal metabolic products in deep pore waters of an intertidal flat

Melanie Beck, Olaf Dellwig, Jan M. Holstein, Maik Grunwald, Gerd Liebezeit, Bernhard Schnetger & Hans-Jürgen Brumsack

This chapter has been published 2008 in *Biogeochemistry* 89, 221-238.

Abstract

This study addresses deep pore water chemistry in a permeable intertidal sand flat at the NW German coast. Sulphate dissolved organic carbon (DOC), nutrients, and several terminal metabolic products were studied down to 5 m sediment depth. By extending the depth domain to several meters, insights in the functioning of deep sandy tidal flats were gained. Despite the dynamic sedimentological conditions in the study area, the general depth profiles obtained in the relatively young intertidal flat sediments of some metres depth are comparable to those determined in deep marine surface sediments. Besides diffusion and lithology which control pore water profiles in most marine surface sediments, biogeochemical processes are influenced by advection in the studied permeable intertidal flat sediments. This is supported by the model setup in which advection has to be implemented to reproduce pore water profiles. Water exchange at the sediment surface and in deeper sediment layers converts these permeable intertidal sediments into a “bio-reactor” where organic matter is recycled, and nutrients and DOC are released. At tidal flat margins a hydraulic gradient is generated which leads to water flow towards the creekbank. Deep nutrient-rich pore waters escaping at tidal flat margins during low tide presumably form a source of nutrients for the overlying water column in the study area. Significant correlations between the inorganic products of terminal metabolism (NH_4^+ and PO_4^{3-}) and sulphate depletion suggest sulphate reduction to be the dominant pathway of anaerobic carbon remineralisation. Pore water concentrations of sulphate, ammonium, and phosphate were used to elucidate the composition of organic matter degraded in the sediment. Calculated C:N and C:P ratios were supported by model results.

5.1 Introduction

It has been demonstrated that sandflats with low organic carbon contents have rates of organic matter remineralisation comparable to those of organic rich muds (Rusch et al., 2006).

The permeability of sand facilitates advective pore water transport in contrast to diffusion-controlled muddy sediments. Rapid exchange between pore water and the overlying water column has been identified as the most important process responsible for enhanced remineralisation rates and carbon cycling in sands. In both sandy and muddy sediments water exchange in the upper sediment layers is facilitated by bioturbation. In sand flats pore water flow in the upper decimetres of permeable sandy sediments is further enhanced due to pressure gradients which are generated during inundation by the interaction of bottom currents with sediment topography like ripples (Huettel et al., 1996; Huettel and Rusch, 2000; Precht and Huettel, 2004). The induced pore water flow at the sediment surface is an effective mechanism for rapid exchange of oxygen (Ziebis et al., 1996; Precht et al., 2004; Rusch et al., 2006), dissolved and particulate organic matter (Huettel et al., 1996; Huettel and Rusch, 2000; Rusch and Huettel, 2000; Rusch et al., 2001), and nutrients (Caetano et al., 1997; Huettel et al., 1998) in permeable sediments. Consequently, advective pore water exchange at the sediment surface leads to fast recycling of organic matter and the removal of metabolic products within a time range of hours and/or days.

Processes of organic matter mineralisation were described in numerous studies concerning deep marine and coastal sediments. The dominant organic matter mineralisation pathways vary depending on the availability of the electron acceptors oxygen, nitrate, manganese oxides, iron oxides or sulphate. Nitrate reduction is of minor importance (< 10%) for C oxidation in coastal sediments (Sørensen et al., 1981; Canfield et al., 1993b). The contributions of manganese and iron reduction to C oxidation are less frequently determined. In many sediments their contribution is small, however, gain importance in Mn or Fe rich sediments (Canfield et al., 1993a; Thamdrup and Canfield, 1996). Determinations of sulphate reduction rates in sediments are numerous and have shown that this pathway accounts for 10-90% of the C oxidation in coastal sediments (Jørgensen, 1982; Thamdrup and Canfield, 1996; Gribsholt and Kristensen, 2003).

In tidal flat sediments nutrients and dissolved organic carbon (DOC) were examined by several authors (Howes and Goehring, 1994; Böttcher et al., 1998, 2000; Jahnke et al., 2003; Kuwae et al., 2003; de Beer et al., 2005; Billerbeck et al., 2006a; Magni and Montani, 2006; Murray et al., 2006; Weston et al., 2006). However, there are few studies which focused on these species in sediment depths exceeding 1 m. Charette and Sholkovitz (2006) determined nutrients and DOC down to about 8 m depth in a subterranean estuary of Waquoit Bay, USA, but focused on trace elements. Concerning tidal flat sediments, there is thus little knowledge about biogeochemical processes occurring in pore waters from below the sediment surface. It is not known whether in relatively young tidal flat sediments of some metres depth

similar biogeochemical processes occur than in surface sediments of deep marine environments.

In this study, sulphate, DOC, nutrients, and several terminal metabolic products were for the first time determined in pore waters down to 5 m depth in an intertidal flat from the NW German coast. Pore water analyses were complemented by a geochemical characterisation of the sedimentary column required to understand pore water profiles. In contrast to previous studies which focus on surface sediments, we try to decipher biogeochemical processes and organic matter remineralisation pathways in deep intertidal flat sediments. Biogeochemical processes deduced from pore water results were verified by a model setup.

5.2 Materials and Methods

5.2.1 Study area

The Wadden Sea, located in the Southern North Sea, forms one of the largest tidal flat areas extending for almost 500 km between Den Helder (Netherlands) and Skallingen (Denmark). In Northwest Germany the tidal flat area is located between the coastline and a chain of barrier islands, which are separated by tidal inlets. These inlets connect the tidal flat areas with the open North Sea. The tidal flat area itself is divided by a tidal channel system consisting of large main channels and smaller secondary channels. Sampling was carried out on the Eastern margin of the intertidal sand flat Janssand, located in the back barrier area of the Island of Spiekeroog (53° 44.183' N; 007° 41.904' E; Fig. 5.1). The study area is characterised by semi-diurnal tides and a tidal range of 2.6 m (Flemming and Davis, 1994). During high tide the Janssand tidal flat is covered by 1 - 2 m of water. It becomes exposed to the atmosphere for approximately 6 hours, depending on tidal range and wind direction. The Janssand tidal flat surface is almost horizontal, except for the margin where the sediment surface slopes towards the main tidal creek. At low tide the distance between the sampling location and the water line is approximately 70 m and the difference in altitude amounts to about 1.5 m.

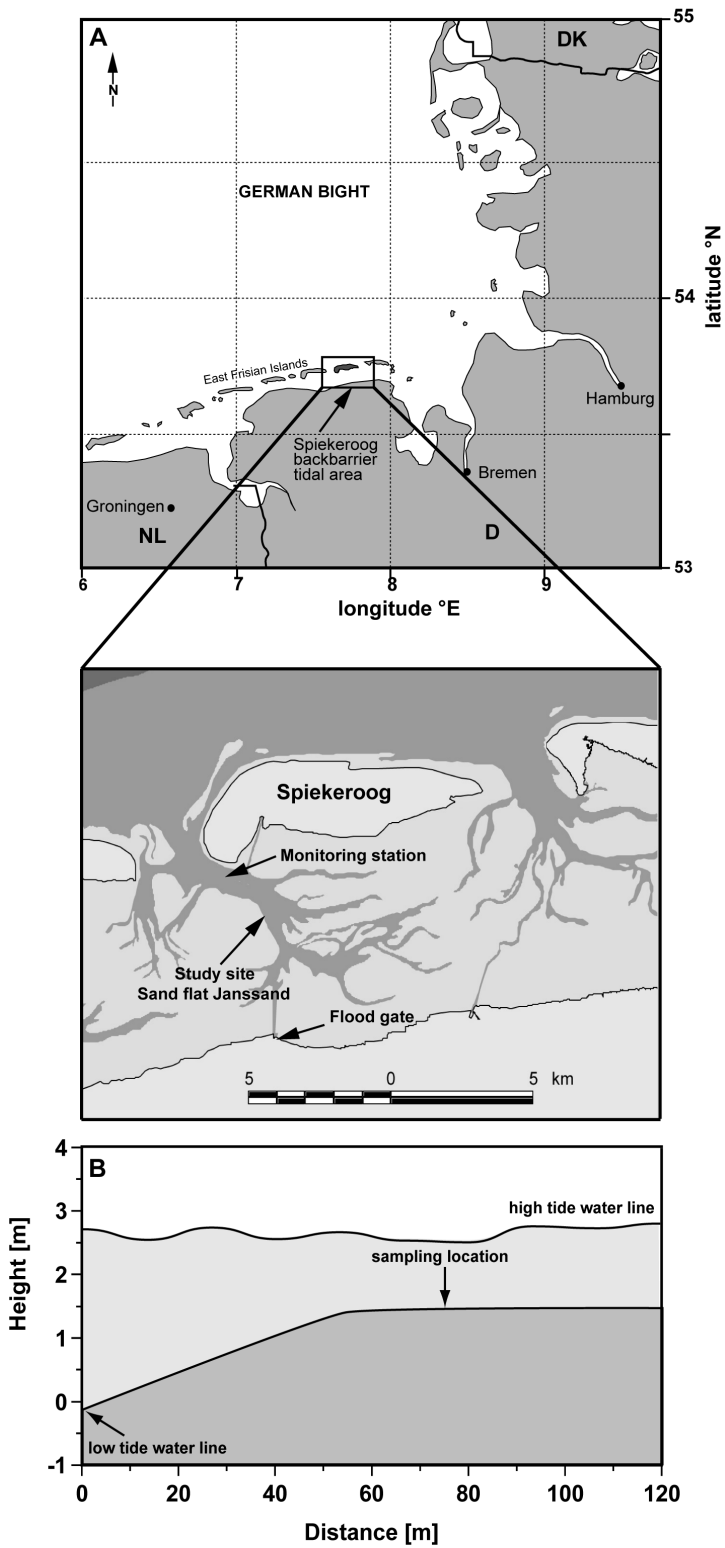


Fig. 5.1. (A) Study site in an intertidal sand flat (Janssand) in the back barrier area of Spiekeroog Island, Wadden Sea, Germany. (B) Tidal flat topography.

5.2.2 Sample collection

Pore water – Pore water sampling was carried out using in situ samplers described in more detail in Beck et al. (2007). Each sampler is composed of a polyethylene (PE) pipe with sampling ports at different depths down to 5 m. Teflon tubings link the sampling orifice to sampling devices located at the sediment surface. Each in situ pore water sampling system consists of two samplers. The short sampler (1 m length) has 11 sampling ports at 0.05 m, 0.07 m, 0.10 m, 0.15 m, 0.20 m, 0.25 m, 0.30 m, 0.40 m, 0.50 m, 0.75 m and 1.0 m sediment depth. The long sampler (5 m length) has 10 sampling ports located at 1.0 m, 1.25 m, 1.5 m, 2.0 m, 2.5 m, 3.0 m, 3.5 m, 4.0 m, 4.5 m, and 5.0 m sediment depth. At the top of the sampler PE syringes can be connected to the sampling system to extract pore water from the sediment. Depending on sampling depth and diameter of the teflon tubes, different volumes of pore water were discarded before taking samples for analyses. All samples were pre-filtered through nylon gauzes of 100 and 50 μm pore size located in front of the sampling orifices and immediately filtered through 1.2 μm GF/C filters after extraction.

Pore water samples were taken on April 25th 2006 except for methane samples which were retrieved on March 22nd 2006. To elucidate organic matter composition, data from May 2005 till June 2006 are further used. Samples were analysed for nutrients (NH_4^+ , PO_4^{3-} , H_4SiO_4 , NO_3^-), sulphate (SO_4^{2-}), sulphide (H_2S), methane (CH_4), dissolved organic carbon (DOC), total alkalinity (TA) and chloride (Cl^-). Furthermore, the pH value was measured on site using an aliquot of the sample (pH/Cond 340i, WTW, Weilheim, Germany). Samples for the analysis of nutrients, TA, SO_4^{2-} , and Cl^- were stored in PE vials. Samples for DOC analyses were acidified by adding 1 ml HCl (6 M) to 40 ml sample and stored in glass bottles. All PE vials were pre-rinsed with ultrapure water prior to use, while all glass bottles were acid washed and rinsed with ultrapure water. All samples were stored at 4-6°C until analysis. The determination of nutrients was conducted the day after sampling.

For the determination of H_2S a certain volume of sample, depending on the expected H_2S concentration, was added to 5 ml of a 10 mM Cd-acetate solution immediately after sampling. The addition of sample was stopped when yellow fluffs of CdS started to precipitate. Samples for CH_4 analysis were filled from the syringe into headspace vials with rubber septa and aluminium crimp seal, and immediately frozen in the field. Degassing of the sample has to be taken into account because of pore water extraction by vacuum. However, analyses of CH_4 in sediment cores taken close to the pore water sampling site showed similar results suggesting that degassing is rather limited.

Sediment core – Within a distance of some metres to the pore water samplers a sediment core was collected in April 2005. An aluminium tube with a diameter of 8 cm was driven into the sediment by a vibration corer to a depth almost equivalent to the length of the sampler. Sampling of the sediment core was carried out depending on changes in lithology.

5.2.3 Pore water analysis

Nutrients – Nutrient concentrations (NH_4^+ , PO_4^{3-} , H_4SiO_4 , NO_3^-) were determined photometrically by methods described in Grasshoff et al. (1999) using a spectrophotometer (Spekol 1100, Analytik Jena). Samples containing high concentrations of sulphide were diluted to reduce the effect of sulphide on the formation of coloured complexes, especially for the determination of PO_4^{3-} and H_4SiO_4 . Total alkalinity was determined by a spectroscopic method proposed by Sarazin et al. (1999). Solutions containing known concentrations of the analytes were used to check precision and accuracy of the measurements. Precision / accuracy were 5.6% / -2.5% for alkalinity (at 2.5 mM), 5.1% / -3.0% for NH_4^+ (at 1 mM), 4.8% / 1.2% for PO_4^{3-} (21 μM), and 4.1% / 2.7% for H_4SiO_4 (at 142 μM).

Sulphate – SO_4^{2-} was analysed by ion chromatography (Dionex DX 300) in a 250-fold dilution, with standard Atlantic Seawater (Salinity 35.0 (\pm 0.2%); OSIL, UK) used to control the precision (3.0%) and accuracy (-5.3%) of the measurements.

Sulphide – For the analysis of H_2S the solution containing the yellow CdS precipitate was filtered through a 0.2 μm syringe filter. The filter was washed with 5 ml 1% (v/v) formic acid and 10 ml ultrapure water to dissolve Cd carbonates also retained on the filter and to remove any excess Cd that did not react with H_2S . The yellow precipitate on the filter was dissolved by adding 10% HCl (v/v), and the filtrate was made up to a constant volume. Cd was analysed by FAAS (Perkin Elmer AAS 4100) and the H_2S concentration in the samples was calculated based on the Cd concentrations measured as well as CdS stoichiometry.

Dissolved organic carbon – DOC was analysed by high temperature catalytic oxidation using a multi N/C 3000 analyser (Analytik Jena, Jena, Germany). Prior to the determination of DOC, the acidified samples were purged by synthetic air to remove any dissolved inorganic carbon. Potassium hydrogen phthalate solutions were used for external calibration and to control precision and accuracy of the measurements. Precision was better than 2.4% and accuracy better than 1.9%.

Chloride – Cl^- was determined by micro titration using a 0.1 mM AgNO_3 solution to titrate a solution composed of 100 μl sample, 5 ml ultrapure water and 100 μl of a K-chromate/-dichromate solution (4.2 g and 0.7 g, respectively, dissolved in 100 ml ultrapure

water). Standard sea water of salinity 30.005 (OSIL, UK) was used to control the precision (0.41%) and accuracy (-0.11%) of the measurements.

Methane – For measuring methane concentrations, gas from the headspace of the bottles was injected into a CX-3400 gas chromatograph (Varian, Darmstadt, Germany) equipped with a capillary column (plot-fused silica column no. 7517, 25 m by 0.53 mm, Al₂O₃/KCl coated; Chromopack, Middelburg, The Netherlands) and measured by a flame ionisation detector. Accuracy (2.9%) and precision (13.9%) were controlled by a 100 ppmv standard of methane.

5.2.4 Sediment analysis

XRF – Sediment samples were freeze dried and homogenised in an agate mill. All samples were analysed for the elements Si, Al, Ti, and Zr by XRF using a Philips PW 2400 X-ray spectrometer. 600 mg of sample were mixed with 3600 mg of a mixture of dilithiumtetraborate/lithiummetaborate (50% Li₂B₄O₇/50% LiBO₂), pre-oxidised at 500°C with NH₄NO₃ (p.a.), and fused to glass beads. Analytical precision and accuracy were better than 5% for all elements.

Bulk parameters – Total carbon (TC) and total sulphur (TS) were determined using an CS 500 IR analyser (Eltra, Neuss, Germany), while total inorganic carbon (TIC) was analysed coulometrically by a CM 5012 CO₂ coulometer coupled to a CM 5130 acidification module (UIC, Joliet, USA). Total organic carbon (TOC) was calculated as the difference between TC and TIC. Total nitrogen (TN) was analysed by an Carlo Erba Element Analyser EA 1108. Precision and accuracy of TC and TIC analyses were better than at least 3% and 1%, respectively.

5.2.5 Calculation of sulphate depletion, C:N, and C:P ratios

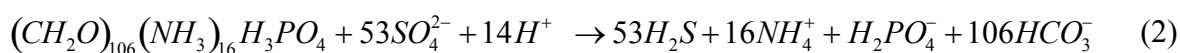
Sulphate depletion – The SO₄²⁻ depletion in pore waters was calculated using the concentrations determined for the specific sediment depths (Sholkovitz, 1973; Weston et al., 2006). The depletion in SO₄²⁻ reflects the net amount of SO₄²⁻ consumption, presumably via bacterial SO₄²⁻ reduction, and was calculated according to

$$(SO_4^{2-})_{Dep} = \left[(Cl^-)_{PW} \cdot (R_{SW})^{-1} \right] - (SO_4^{2-})_{PW} \quad (1)$$

where (SO₄²⁻)_{Dep} is the SO₄²⁻ depletion, (Cl⁻)_{PW} and (SO₄²⁻)_{PW} are the pore water concentrations of Cl⁻ and SO₄²⁻, and R_{SW} is the molar ratio of Cl⁻ to SO₄²⁻ in surface sea water

($R_{SW} = 19.33$). A hypothetical SO_4^{2-} concentration at a specific depth interval is calculated by using Cl⁻ data. Slight changes in salinity due to rain or fresh water input are thus compensated. The difference between the hypothetical and the measured SO_4^{2-} concentration forms an estimate for the metabolic amount of SO_4^{2-} reduction.

Ratios – Carbon to nitrogen (C:N) and carbon to phosphorus (C:P) stoichiometry of the organic matter degraded was estimated by regression analysis of $(SO_4^{2-})_{Dep}$ against NH_4^+ and PO_4^{3-} and multiplying the ratios of $(SO_4^{2-})_{Dep}$ to NH_4^+ and PO_4^{3-} by a factor of 2. This estimation is based on the assumption that the ratio of C to SO_4^{2-} is 2:1 if the oxidation of organic matter is coupled to sulphate reduction according to the equation



where organic matter composition follows the Redfield relationship. Using the Redfield formula represents an approximation. The formula is based on living marine phytoplankton and is thus uncertain in buried organic matter (Sholkovitz, 1973). A further approximation is the estimation of the C: SO_4^{2-} ratio in the pore water samples by a regression analysis of $(SO_4^{2-})_{Dep}$ against TA. Dissolved inorganic carbon (DIC) should be used for the determination of the C: SO_4^{2-} ratio. Calculating DIC concentrations by using a program developed for CO₂ system calculations (Lewis and Wallace, 1998) revealed that TA equals DIC except at 5 m depth where a slight pH decline is observed (Fig. 5.5). The use of TA instead of DIC has thus only very minor implications on the results. TA concentrations are used for regression analyses because of missing pH values for some sampling campaigns. All ratios were further corrected by the appropriate diffusion coefficients described by Boudreau (1997) for HCO_3^- , SO_4^{2-} , NH_4^+ and PO_4^{3-} . The C:N ratio of the organic matter being mineralised was estimated from the linear regression of TOC against TN determined in sediment samples of April 2005.

5.2.6 Model setup and pore water modelling

Pore water modelling was conducted to study the impact of advective flow on the observed pore water profiles. The applicability of the regression technique for sites with advective lateral exchange should further be evaluated by comparing the respective C:N:P ratios with those of in situ decomposing organic matter in the model setup. For modelling the pore water profiles, the generic computer model ISM (integrated sediment model) was used (Wirtz, 2003). It is a partial differential equation model describing diffusive transport and biogeochemical processes in aquatic porous media. The redox processes are conducted by functional groups of bacteria and bacterial growth is simulated. The model description is

confined to the capabilities of the model that have been applied in this study. The model is implemented in C++ and solved using a 3rd order Runge Kutta integration method.

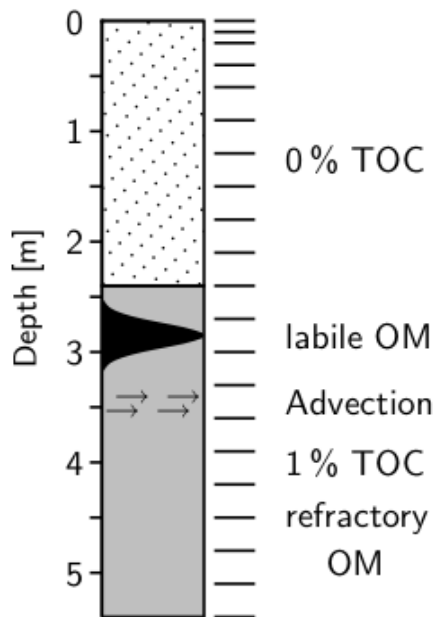


Fig. 5.2. Sketch of model sediment column. The upper part is free of organic matter (OM). The lower part contains 1 % total organic carbon (TOC), most of which is refractory (grey), however, there is a layer of labile OM around 2.8 m depth. Advection is indicated by arrows. The division into 20 boxes is indicated by lines.

In the model setup an idealised sediment column is considered, which is free of organic matter in the upper part (0 - 2.5 m) and contains 1% TOC in the lower part (2.5 - 5 m) (Fig. 5.2). The model column is composed of 20 boxes with slightly higher resolution near the surface (Fig. 5.2). At 3.5 m depth horizontal advection is simulated. Above the advective layer is a zone rich in labile organic matter. Apart from this zone, organic matter is refractory. The shapes of the pore water profiles are controlled by organic matter degradation and subsequent nutrient release to pore waters, by diffusion and advective flow. The model was calibrated to fit the observed pore water profiles by varying advection intensity, rate of decay, and C:N:P ratios of labile and refractory organic matter. Model fitness was evaluated after the model reached its steady-state.

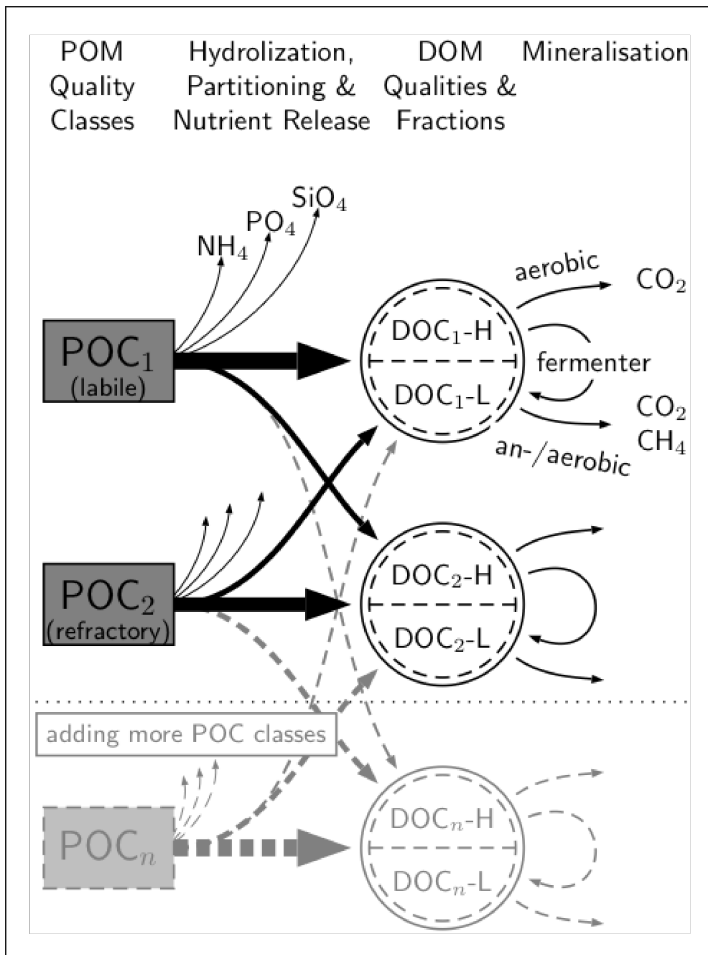


Fig. 5.3. Organic matter degradation scheme of the integrated sediment model. POC quality classes are converted to DOC classes according to the distribution vectors. Upon hydrolysis, nutrients are released according to the specific C:N:P ratios. The distribution scheme may be extended by further POC classes (grey and dashed arrows). DOC is separated into high and low molecular weight DOC (DOC-H and DOC-L). Larger molecules (DOC-H) can only be degraded by aerobic heterotrophs or must be converted to smaller units (DOC-L) by fermenting bacteria. All heterotrophic functional groups can use DOC-L for catabolic processes.

Special emphasis was put on the organic matter remineralisation process (Fig. 5.3). According to Boudreau (1992), particulate organic carbon (POC) exists in two qualities (POC₁ is labile and POC₂ is refractory). POC hydrolysis is implemented as a first order decay process depending on ambient temperature T via the nonlinear Q_{10} temperature term after van't Hoff's rule. Upon hydrolysis, NH_4^+ , PO_4^{3-} , and H_4SiO_4 are released according to the quality-class specific C:N:P ratios. The carbon is distributed to the DOC pools (labile and refractory) according to the distribution vectors. The effect on cross distribution is indicated

in light grey dashed arrows. Each DOC quality class is split into high and low molecular weight DOC (DOC-H and DOC-L) by a global fractioning coefficient. DOC-H can be degraded by aerobic heterotrophs to CO₂ or by fermenting bacteria to DOC-L. DOC-L acts as an electron donor for all six heterotrophic functional groups of bacteria $Abac_m$ (m=1-6) for catabolic processes according to the scheme of Froelich et al. (1979). The POC hydrolysis rate is proportional to the POC mass to the power of 2/3 because enzymatic processes depend on the surface of organic particles, which is simplified as sphere. POC hydrolysis is further enhanced by enzymatic activity that relates to the abundances of active bacteria $Abac_m$ and their specific yield factor on DOC. The POC hydrolysis rate of concentration C_{POC} with the quality j is

$$\dot{C}_{POC,j} = -\frac{(1-\phi)}{\phi} \cdot Q_{10}^{(T-TS)/10} \cdot C_{POC,j}^{2/3} \cdot r_j \cdot (1 + h \cdot \sum_{m=1}^6 y_m \cdot Abac_m) \quad (3)$$

where f is the porosity, r_j the specific rate constant (1/d) for quality j, and h the enzymatic enhancement coefficient. Further parameters are summarised in Table 5.1. Due to the steady-state requirement, bacterial biomass only shows small variations resulting from the annual temperature cycle. Thus, the enzymatic enhancement term in equation 3 (in brackets) becomes nearly constant. In the zone of labile organic matter, approximately 30% of the POC hydrolysis rate relates to enzymatic enhancement, while in the organic matter free zone there is no enhancement.

Table 5.1. Parameters of the model setup.

Parameter	Symbol	Value
Sediment temperature	T	time series (Beck et al., 2008c)
Standard temperature	TS	294 Kelvin
Temperature increase reaction factor	Q_{10}	2
Specific rate constant for labile organic matter	r_1	$8.0 \cdot 10^{-6}$ 1/d
Specific rate constant for refractory organic matter	r_2	$1.9 \cdot 10^{-6}$ 1/d
Porosity	f	0.5

Diffusion is implemented according to Fick's second law. Diffusion coefficients are used according to Boudreau (1997). Since horizontal chemical gradients as well as horizontal flow velocities at the study site are unknown, a one dimensional column setup was chosen to limit uncertainties in model calibration. In this setup, advective flow is realised by a surrogate process. Non-local transport is a suitable substitute for advection since it connects a box

directly to a pool of water which exhibits the concentrations C_0 of the species i . Instead of flow velocity, the controlling parameter is the dilution coefficient b .

$$\dot{C}_i = \beta(C_{0,i} - C_i). \quad (4)$$

The best fit to the field data was obtained by using a dilution coefficient of 0.005 1/d, which implies a turnover of the zone of pseudo-advection in 200 days. The model, however, is fairly insensitive to the dilution coefficient. A variation by one order of magnitude resulted in no principal change of profile shapes (not shown). The concentrations of introduced water were derived from pore waters of central parts of the tidal flat because pore water presumably flows from the central parts towards the margins of tidal flats. The concentrations applied in the model are average pore water concentrations determined at 17 different depths down to 3.5 m at a location in the central part of the tidal flat (23 mM SO_4^{2-} , 1.0 mM H_2S , 0.4 mM DOC, 0.4 mM NH_4^+ , 0.5 mM PO_4^{3-} and 0.2 mM H_4SiO_4). Seasonal sea water concentrations measured in the back barrier area of Spiekeroog are used as upper boundary conditions for the modelled column stem (unpublished data). At the lower boundary, concentrations are kept constant reflecting the quasi-linear gradients of pore water species in the lower part of the column.

5.3 Results

5.3.1 Sediment geochemistry

Higher amounts of coarse-grained quartz are reflected by enrichments in SiO_2 , whereas higher clay contents are characterised by enrichments in Al_2O_3 . At the sampling site the SiO_2 content of the sediment exceeds 80% down to 1.8 m depth, whereas below SiO_2 contents vary between 60 and 90% (Fig. 5.4). In depths exceeding 1.8 m the Al_2O_3 content ranges from about 3 to 9%. The lithology is thus composed of sandy sediment intermingled by clay lenses down to 3 m depth, a clay layer at 3 m depth, a sandy layer below and clayey sediments at depths exceeding 4 m depth. Additional Al_2O_3 rich intervals shown in Figure 5.4 reflect very thin clay layers or lenses. Due to lithological inhomogeneity in the sampling area, the lithology of the sediment core presumably differs slightly from the lithology at the pore water sampling site. The lithological structure of the sediment core, however, reproduces well the general sequence of sediment layers typically found in the sampling area.

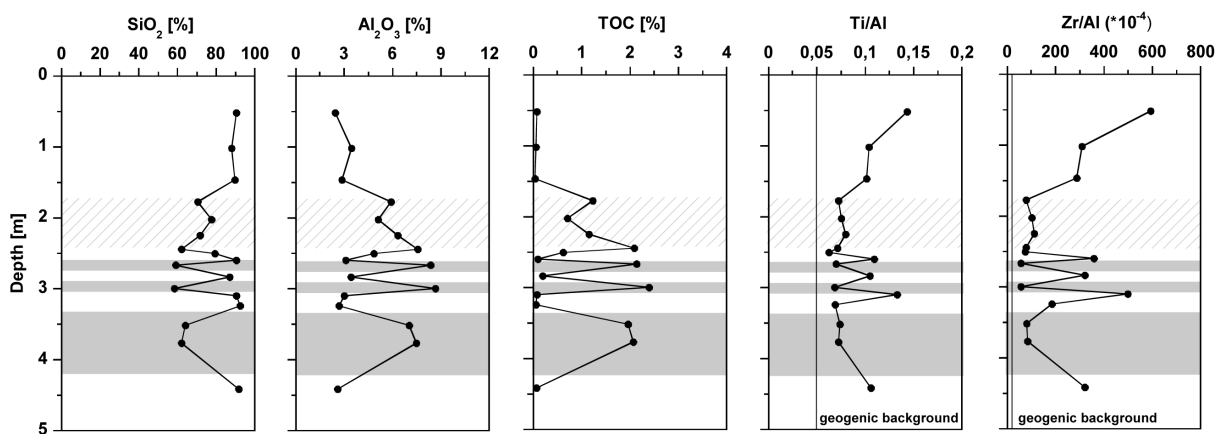


Fig. 5.4. Depth profiles of parameters characterising the lithology at the sampling site in an intertidal sand flat. The continuous lines in Ti/Al and Zr/Al figures indicate the geogenic background (Wedepohl 1971). The grey bars highlight the clay rich layers of the sediment profile. Depths of about 1.5 to 2.5 m are marked with a hatched area because the lithological description shows that the sediment is predominantly sandy, with very thin clay layers.

The content of total organic carbon (TOC) varies between 0.04 and 2.4% with the highest values found in clay-rich layers (Fig. 5.4). These TOC contents are typical for sediments in the study area (Dellwig et al., 2000). TOC shows positive correlations with increasing clay content indicating the importance of organic matter sorption onto clay particles for preservation of both marine and terrestrial organic matter (Mayer, 1994; Delafontaine et al., 1996; Baldock et al., 2004).

The elements Ti and Zr are indicators of the energetic conditions prevailing during the deposition of the sediment. In Figure 5.2 Ti/Al and Zr/Al ratios are displayed instead of Ti and Zr contents. Normalisation to Al eliminates dilution effects caused by quartz, carbonates, and organic matter. Any deviation from average shale composition (Wedepohl, 1971) is easily recognised in element/Al ratios. High Ti/Al and Zr/Al ratios point towards elevated heavy mineral contents (e.g. ilmenite, rutile, zircon), which are found in layers deposited during high current velocities. Clay minerals in contrast are deposited during low energy conditions. At our sampling site the depth profiles of Ti/Al and Zr/Al show that the depositional conditions changed frequently, in accordance with the very dynamic nature of the back barrier tidal flat area. The time span needed for the sedimentation of such layers may differ significantly. For instance, sediment redistribution may occur due to wave action during storms (Chang et al., 2006b,c; Christiansen et al., 2006).

5.3.2 DOC, sulphate, and metabolic products in pore waters

The depth trends of sulphate, DOC, nutrients, several metabolic products, chloride, and pH (Fig. 5.5) are typical for the sampling site and were chosen as representative example for the sampling period from May 2005 to June 2006. Concentrations change to some extent within the sampling period of one year, however the trends with depth remain the same.

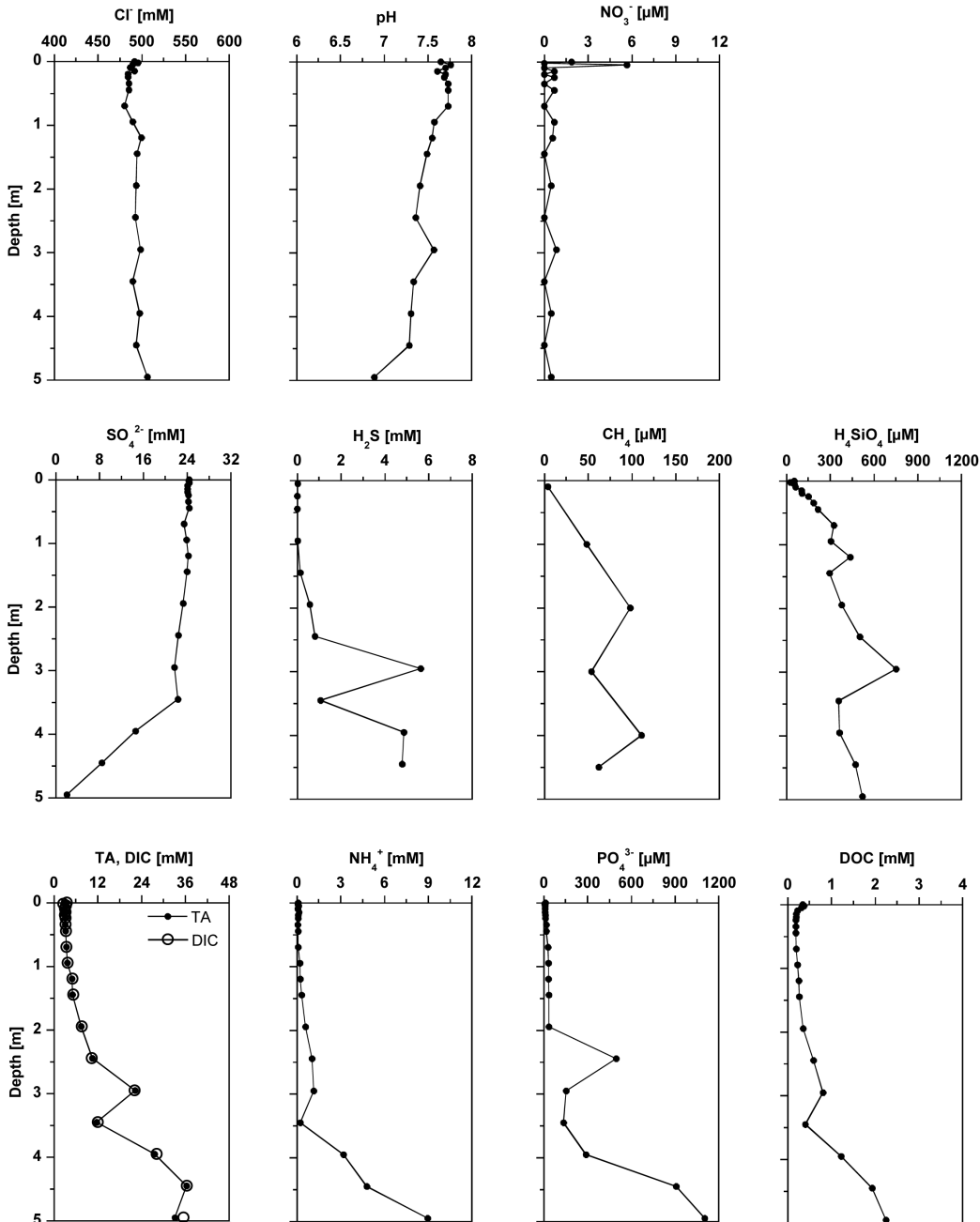


Fig. 5.5. Pore water profiles of Cl^- , pH, NO_3^- , SO_4^{2-} , H_2S , CH_4 , H_4SiO_4 , TA, NH_4^+ , PO_4^{3-} , and DOC at the sampling site in an intertidal sand flat of the back barrier area of Spiekeroog Island (April 2006; CH_4 March 2006). DIC concentrations were calculated using TA and pH.

Concentrations of Cl^- vary around 500 mM in the entire depth profile with a minimum concentration of 480 mM at 0.75 m depth. Consequently, no subterranean fresh water contribution of the nearby mainland influences the salinity at the sampling site. The pH values vary between 7.8 in the upper part of the sediment and 6.9 at 5 m depth.

Nitrate pore water concentrations are below 1 μM except at 5 cm depth where a concentration of 5.6 μM is determined. In contrast, sea water of the study area shows higher NO_3^- concentrations ranging from about 80 μM at the beginning of April to about 5 μM in May and June 2006 (Grunwald et al., 2007). The slightly elevated NO_3^- pore water concentration at 5 cm depth is either due to sea water introduced into the sediment, bioirrigation and/or nitrification. The generally low NO_3^- pore water concentrations imply that sea water NO_3^- introduced into surface sediments is rapidly denitrified.

Sulphate concentrations are close to the sea water value of 26 mM (at salinity 31 in the Wadden Sea) in the upper part of the sediment, followed by a decrease in SO_4^{2-} concentration. At a sediment depth of 5 m very low concentrations of SO_4^{2-} remain. Sulphate reducers were successfully identified in the study area. Sulphate reduction rates are in the low $\text{nM cm}^{-3} \text{d}^{-1}$ range and reach up to 1 $\mu\text{M cm}^{-3} \text{d}^{-1}$ in surface sediments of the back barrier area of Spiekeroog Island (Böttcher et al., 2000; Wilms et al., 2006b; Wilms et al., 2007). In tidal flats with mixed sand and clay composition, sulphate reduction rates remain in the low $\text{nM cm}^{-3} \text{d}^{-1}$ range even in some metres depth (Wilms et al., 2006b). These values are comparable to sulphate reduction rates determined in other tidal flat systems (Kristensen et al., 2000; Gribsholt and Kristensen, 2003).

Sulphide is the terminal metabolic product of sulphate reduction. In the sediment the concentration of sulphide is influenced by the formation of the iron sulphides FeS and FeS_2 (Howarth and Jørgensen, 1984; Moeslund et al., 1994). In the study area the formation of iron sulphides leads to low sulphide concentrations in the upper metres of the sediment. Modelled sulphide concentrations are higher than measured ones because the process of iron sulphide formation is not implemented in the model setup (Fig. 5.6). Modelling thus confirms the precipitation of iron sulphides. To a small extent sulphide oxidation to sulphate may occur in these layers, too (Thamdrup et al., 1993). Sulphide concentrations do not constantly increase with decreasing sulphate concentrations. At 3 m depth the sulphide concentration is high, although sulphate shows little depletion. This finding cannot be fully explained and is not reproduced in the model setup (Fig. 5.6). It may be due to entrapment of sulphide in or below a less permeable clay-rich sediment layer.

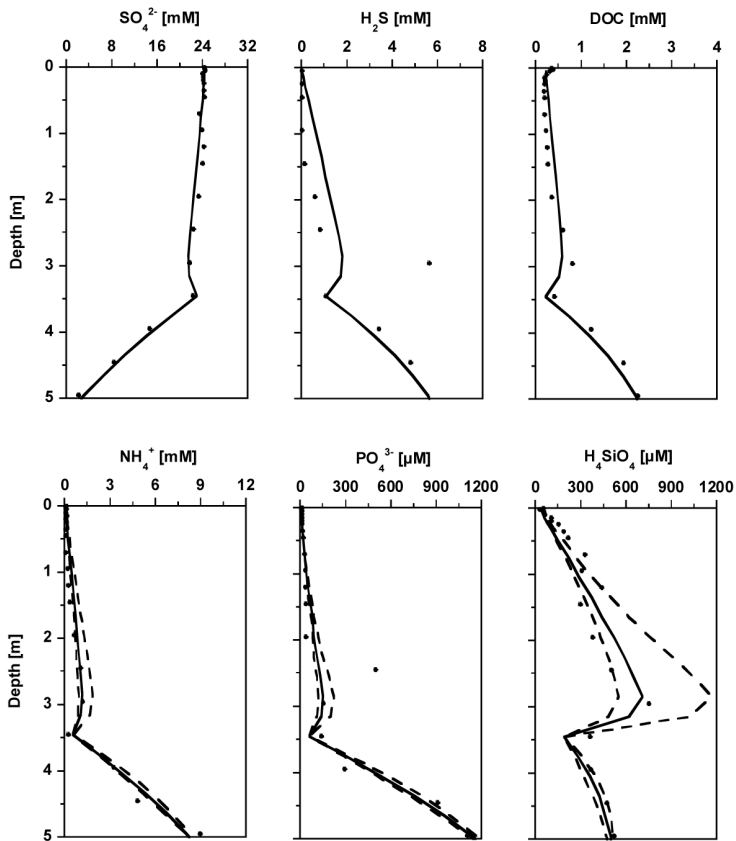


Fig. 5.6. Modelled (continuous line) and measured (points) pore water profiles. Same samples as in Figure 5.3. To test to sensitivity of the pore water profiles to organic matter composition, simulations were conducted with Redfield ratios increased and decreased by 50% (dashed lines).

Methane shows concentrations of about 5 μM at the sediment surface, and increases to about 100 μM at greater depths. Methane concentrations already start to increase in a sediment depth of about 1 m, where high sulphate concentrations are still found. This illustrates the coexistence of sulphate reducers and methanogens (Wilms et al., 2007), and most notably, the upward diffusion of methane from its depth of production below 5 m depth towards the sediment surface.

At the sampling site the sandy sediment surface is covered by ripples leading to advective pore water flow at the sediment surface (Huettel et al., 1996; Huettel and Rusch, 2000). Thus, organic material is easily introduced into the upper layers of the sandy sediments and subsequently degraded aerobically and anaerobically. The degradation products are either used by microorganisms for their metabolism, form part of other biogeochemical reactions or become enriched in pore waters. The enrichment of DOC, NH_4^+ , PO_4^{3-} , and TA with depth reflects the decomposition of organic matter. The increase in H_4SiO_4 concentrations mirrors

the dissolution of biogenic silica. At shallower depths where exchange between pore water and overlying water column occurs, these species show concentrations only slightly higher than in the sea water of the study area (Schnetger et al., 2001; Dellwig et al., 2007a; Grunwald et al., 2007). In the model setup exchange processes between sediment layers of some decimetres depth and the overlying water column are not considered. Therefore, measured concentrations are lower than modelled ones in the upper metre (Fig. 5.6).

5.3.3 Stoichiometry of organic matter degradation

Concentrations of $(\text{SO}_4^{2-})_{\text{Dep}}$ are positively correlated with TA, NH_4^+ , PO_4^{3-} , and DOC. In Fig. 5.7A the correlations are displayed for samples taken in April 2006. To support these results, regression analyses were performed for all samples taken throughout one year from May 2005 until June 2006 (Fig. 5.7B). The ratio of TA: $(\text{SO}_4^{2-})_{\text{Dep}}$ is 1.7 for samples from April 2006 and does only slightly change if all samples analysed during a one year period are taken into account (Table 5.2). This ratio is close to the expected C: $(\text{SO}_4^{2-})_{\text{Dep}}$ ratio of 2, based on Redfield ratios and the assumption that organic matter is degraded by sulphate reduction. Methanogenesis is presumably responsible for organic matter degradation besides sulphate reduction at the study site, however to a much smaller extent. Estimates of the C:N ratio of degraded organic matter are 3.1 regarding samples of April 2006 and 2.8 for samples obtained during the whole sampling period of one year (Table 5.2). The C:P stoichiometry is 76 for samples from April 2006 and 104 for all samples. The modelled C:N and C:P ratios are 3.5 and 77, respectively (Table 5.2).

5.4 Discussion

5.4.1 Terminal metabolic pathways

The oxidation of organic matter in sediments is coupled to electron acceptors, the use of which depends on their reactivity and availability. Aerobic respiration is followed by nitrate reduction, reduction of Mn^{IV} and Fe^{III} oxides, sulphate reduction and finally methanogenesis (Froelich et al., 1979). Based on the availability of SO_4^{2-} compared to other electron acceptors, sulphate reduction contributes largely to anaerobic carbon oxidation in marine subsurface sediments (Jørgensen, 1982).

In this study pore water profiles are used to evaluate the pathways of organic matter degradation in an intertidal flat, with focus on depths exceeding 1 m. At the study site bottom

flow interacting with sediment ripples generates an intrusion of oxygenated water into the sediment surface. The surface layer where organic matter is remineralised aerobically thus extends to some centimetres depth (Billerbeck et al., 2006a). Nitrification, denitrification, and nitrate reduction seem to be closely coupled in the surface sediment leading to low NO_3^- concentrations over the entire depth profile. Assuming that oxygen respiration and denitrification are restricted to the sediment layers containing measurable oxygen and nitrate, these two processes are thus confined to the upper few centimetres of the sediment.

The tight coupling of products of organic matter degradation like NH_4^+ , and PO_4^{3-} with $(\text{SO}_4^{2-})_{\text{Dep}}$ suggests that in anoxic sediment layers the organic matter is mainly degraded by sulphate reduction (Fig. 5.7). Sulphate concentrations remain at a high level down to 3.5 m depth and do attain concentrations close to zero only at 5 m depth. Sulphate reducing bacteria can metabolise labile organic matter when sulphate concentrations are exceeding ~ 1 mM (Alperin et al., 1994). Except at 5 m depth, enough sulphate is thus available as terminal electron acceptor for sulphate reducing bacteria. Pore water advection within the sediment may lead to an underestimation of the sulphate amount reduced in the sediment. The relatively constant sulphate concentrations in the permeable sandy layers down to 2 m depth point towards a replenishment of sulphate by sea water and/or pore water from central parts of the tidal flat. Nevertheless, the general conclusion concerning the importance of sulphate reduction as pathway of anaerobic organic matter degradation remains valid. Weston et al. (2006) drew similar conclusions regarding the relevance of organic matter remineralisation pathways for intertidal creek-bank sediments in Georgia and South Carolina, USA.

A conclusion about the depth where methane is actually being produced can hardly be drawn. Due to concentration gradients and pressure fluctuations induced by tidal cycles, methane will supposedly slowly migrate from its depth of production towards the sediment surface. The main zone of production may thus be located below 5 m depth where sulphate is depleted. In spite of minor methanogenesis occurring in the sediment layers down to 5 m depth, sulphate reduction thus contributes to a large extent to anaerobic organic matter remineralisation. This conclusion is supported by the model results. Depth profiles of sulphate, DOC, and nutrients are reproduced in the model setup where sulphate reduction was assumed to be the anaerobic remineralisation process (Fig. 5.6).

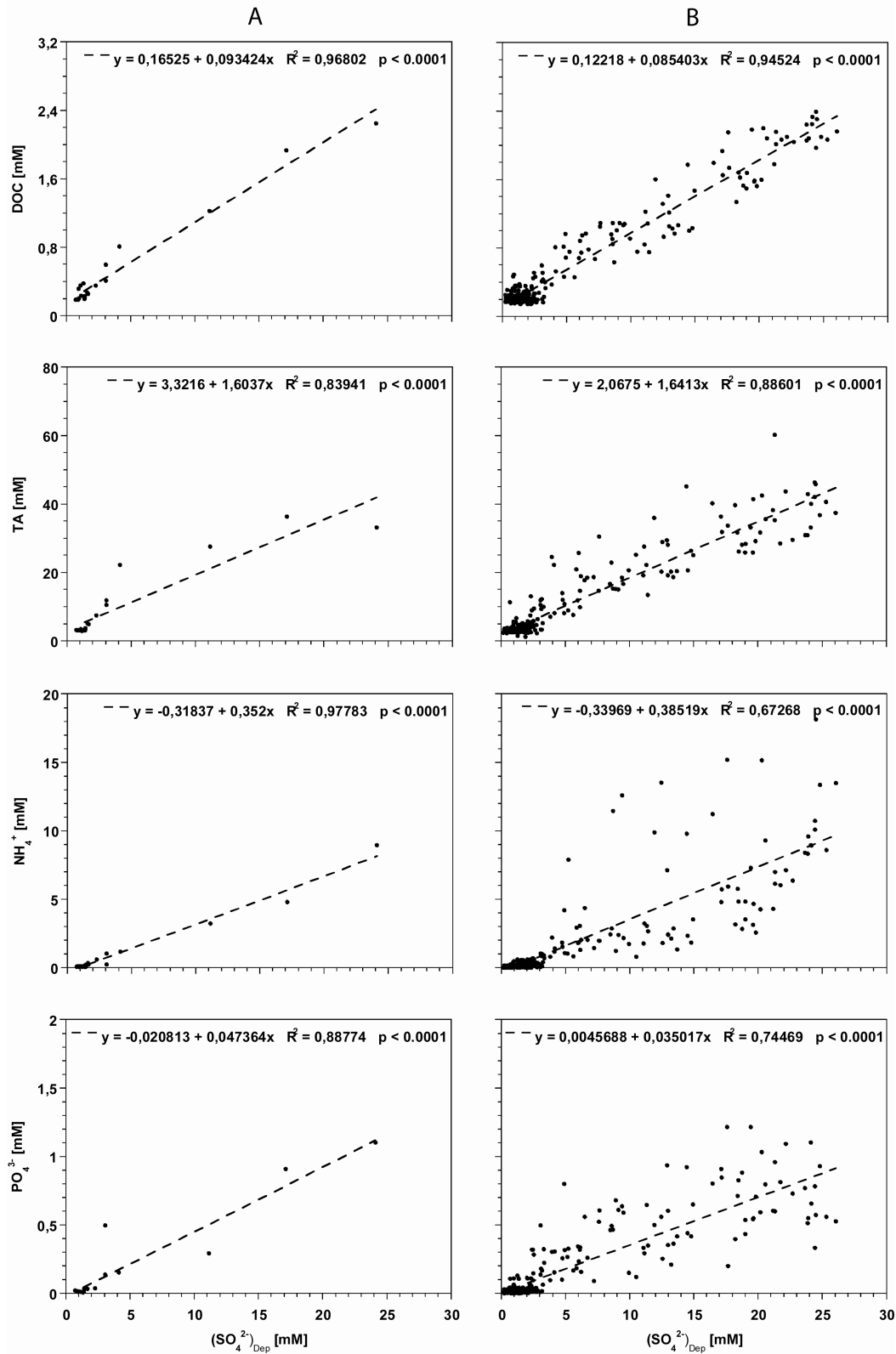


Fig. 5.7. Ratios of DOC, TA, NH_4^+ , and PO_4^{3-} concentrations to $(\text{SO}_4^{2-})_{\text{Dep}}$ concentrations. Best-fit linear regressions are calculated for samples from April 2006 separately (A) and for all samples taken from May 2005 till June 2006 (B).

5.4.2 Organic matter remineralisation

DOC concentrations correlate very well with $(\text{SO}_4^{2-})_{\text{Dep}}$, with maxima in the zone of maximum sulphate depletion (Fig. 5.7). However, it is not evident if this correlation is reflecting a single biogeochemical process involving DOC and SO_4^{2-} . Hydrolysis and fermenting microorganisms could have converted organic matter leading to the production of refractory and labile DOC, whereas the labile part is used by sulphate reducers (Böttcher et al., 1997; Rusch et al., 1998).

The organic matter mineralised at the sampling site is richer in N and P than expected from the Redfield ratio. The C:N and C:P ratios according to Redfield are 6.6 and 106, respectively. Deduced from pore water analyses, the organic matter at our sampling site has a C:N ratio of about 3 and a C:P ratio of 75-106 (Table 5.2). We assume that the regression technique yields valuable results, although certain sediment layers are influenced by advection. Advection mainly occurs in sediment layers above 3 m depth and to a small extent at 3.5 m depth. Regression analyses are however dominated by pore water results from below 3 m depth where a sulphate depletion of more than 4 mM is calculated and advection is of minor importance.

Table 5.2. Stoichiometry during organic matter degradation estimated from slopes of pore water concentrations of total alkalinity TA and sulphate depletion $(\text{SO}_4^{2-})_{\text{Dep}}$ against NH_4^+ and PO_4^{3-} concentrations for samples of April 2006 and for all samples taken from May 2005 till June 2006. The ratios of suspended particulate matter and the ratios derived from modelling pore water profiles are further displayed.

	C: SO_4^{2-}	C:N	C:P
<i>Suspended particulate matter</i>		7.8*	
<i>Sediment April 2005</i>		8.6	
<i>Pore water April 2006</i>			
TA	1.7	3.2	77
$(\text{SO}_4^{2-})_{\text{Dep}}$		3.0	75
<i>Pore water model April 2006</i>		3.5	77
<i>Pore water May 2005 – June 2006</i>			
TA	1.8	2.8	106
$(\text{SO}_4^{2-})_{\text{Dep}}$		2.7	101

* Lunau et al. (2006)

The deviation from the Redfield ratios does not represent a completely unexpected finding as the Redfield ratio is based on average oceanic relationships. In intertidal creek bank sediments of South Carolina and Georgia, USA, C:N ratios down to 3.4 were determined as well (Weston et al., 2006). The results further suggest that organic matter components containing nitrogen are degraded with higher priority. This finding is in accordance with Weston et al. (2006) who found preferential hydrolysis of particulate organic nitrogen relative to particulate organic carbon when organic matter mineralisation rates are high. In our study area suspended particulate matter determined in the open water column has an average C:N ratio of 7.8 (Lunau et al., 2006). This suspended matter is partly incorporated into the sediment and in the following degraded by microorganisms (Huettel et al., 1996; Huettel and Rusch, 2000; Rusch and Huettel, 2000). The C:N ratio of about 3 calculated based on metabolic products in pore water is thus lower than the ratio determined for suspended particulate matter in the open water column suggesting preferential degradation of nitrogen containing compounds in the sediment. The C:N ratio of 8.6 determined for the organic matter in the sediment supports this hypothesis because it reflects an enrichment of carbon in sedimentary organic matter compared to suspended particulate matter.

Anaerobic oxidation of methane may occur in the sediment to a certain degree (K. Bischof, pers. commun.). Anaerobic oxidation of methane consumes sulphate (Hensen et al., 2003) which would have lead to an overestimation of the respiratory sulphate reduction. However, reducing the calculated sulphate depletion would result in even lower C:N ratios. Furthermore, ratios estimated from sulphate depletion and total alkalinity are similar suggesting that anaerobic oxidation of methane is unimportant in the upper 5 m of the sediment.

Modelling our pore water profiles results in C:N and C:P ratios similar to those calculated by regression analysis (Table 5.2). In the model the unexpectedly high PO_4^{3-} concentration at 2.5 m depth is disregarded. The exclusion of this PO_4^{3-} concentration in the model setup seems to be of minor importance as a regression analysis of $(\text{SO}_4^{2-})_{\text{Dep}}$ against PO_4^{3-} without the PO_4^{3-} concentration at 2.5 m depth does not result in a significantly different C:P ratio. The estimations of C:N and C:P ratios by regression analysis are thus supported by the model results. In simulations Redfield ratios were increased and decreased by 50% to test the sensitivity of the depth profiles to Redfield composition (Fig. 5.6) Due to the relative proximity of the advective and reactive layer, the pore water profiles of NH_4^+ , PO_4^{3-} and H_4SiO_4 are somewhat insensitive to variable Redfield ratios. This limits its usability for validating the applicability of the regression technique but the robustness of the resulting pore water profiles supports the hypothesis of the advective layer.

5.4.3 Pore water profiles

Pore water depth profiles are controlled by biogeochemical, sedimentological, and hydrological processes. In general, sulphate, DOC, nutrients, total alkalinity, methane, and sulphide show either an increase or decrease with depth depending on whether the species are consumed or produced during organic matter remineralisation (Fig. 5.5). Despite the dynamic sedimentological conditions in the study area, the general depth profiles determined in the relatively young intertidal flat sediments of some metres depth are comparable to those of deep marine surface sediments (Sholkovitz, 1973; Canfield et al., 1993a,b; Thamdrup and Canfield, 1996; Mäkelä and Tuominen, 2003).

At the study site concentration gradients do not always increase or decrease continuously with depth. At depths exceeding 3.5 m sulphate shows a stronger depletion with depth than in the overlying sediment layers, whereas DOC, ammonium and phosphate exhibit a more pronounced enrichment. This is probably due to a displacement of the tidal flat margin. Within 14 years the eastern tidal flat margin of the Janssand was displaced about 100 m to the east (B.W. Flemming pers. comm.) suggesting that the sampling site may formerly have been located at the tidal flat margin in contrast to its recent position 75 m away from the low tide water line. In the study area tidal flat margins show a high microbial activity, especially near the low water line, resulting in high nutrient concentrations (Billerbeck et al., 2006a). Sediments at depths exceeding 4 m which show enrichments in nutrients and DOC thus probably formed part of the former tidal flat margin.

In permeable sediments pore water depth profiles may be further influenced by pore water advection. In several studies advection processes were described in tidal flat sediments (Whiting and Childers, 1989; Howes and Goehringer, 1994; Billerbeck et al., 2006a,b; Wilson and Gardner, 2006). All these studies were carried out close to tidal flat margins where at low tide a hydraulic gradient is generated between the pore water level in the tidal flat and the water level in the tidal creek. There are evidences that advection occurs in specific sediment depths at our sampling site. For example, NH_4^+ shows an unexpected low concentration at 3.5 m depth. The sediment is lithologically composed of layers with different porosities and permeabilities. At 3.5 m depth a sediment layer which is more permeable than the layers above and below promote water flow. In the sediment core this permeable layer is geochemically identified as a sandy layer below 3 m depth owing to its high SiO_2 content. The depth of the permeable layer in the sediment core does not exactly match the depth of low NH_4^+ concentrations at the pore water sampling site due to slight compression of the sediment core during vibration coring. The NH_4^+ depth profile thus implies that NH_4^+ concentrations at

3.5 m depth are influenced by deep pore water advection. The NH_4^+ minimum at 3.5 m depth may be caused via channelled pore water flow from central parts of the sand flat where average NH_4^+ concentrations of about 0.4 mM are determined down to 3.5 m depth. DOC and total alkalinity further show lower concentrations at 3.5 m depth compared to intervals above and below. In the model setup the shape of the pore water profiles is well reproduced when non-local transport is implemented in the model as surrogate process for advection at 3.5 m depth. The only exceptions are the sulphide concentration at 3 m depth and the PO_4^{3-} concentration at 2.5 m depth. The model results thus support the hypothesis that pore water exchange processes are influenced by advection besides diffusion.

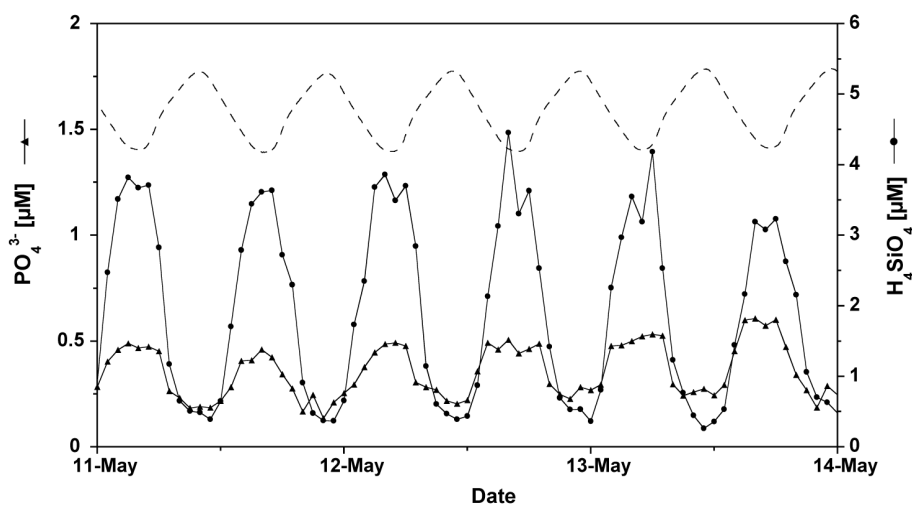


Fig. 5.8. Sea water PO_4^{3-} and H_4SiO_4 concentrations determined at a monitoring station in the back barrier area of Spiekeroog Island in May 2006. The dashed line indicates the tidal variations of the sea water level.

At tidal flat margins pore water flow generated by a hydraulic gradient may lead to the release of pore waters from creekbanks. This may have an impact on the chemistry of the overlying water column. In the back barrier area of Spiekeroog Island, PO_4^{3-} and H_4SiO_4 sea water concentrations vary depending on the state of the tidal cycle with higher concentrations being determined at low tide (Fig. 5.8). In the study area concentrations in deep pore water are 10 to 1000 times higher than in sea water (Liebezeit et al., 1996; Schnetger et al., 2001; Grunwald et al., 2007). Pore water seepage at the tidal flat margin thus may explain increases in PO_4^{3-} and H_4SiO_4 concentrations in sea water during low tide. Our pore water concentrations determined several metres afar from the low tide water line do not completely equal those of seeping pore waters at the tidal flat margin. However, the results of our study

give first insights into deep pore waters, which may be horizontally transported towards the tidal flat margin where they seep out of the sediment. Close to the low tide water line at the tidal flat margin where most of the pore water seeps are found, the oxic layer of the sediment surface is very thin or even lacking. This suggests that the seeping pore waters may chemically only be slightly modified before entering the overlying water column.

Fresh water, which occasionally flows into the back barrier area at low tide via a flood gate, may additionally represent a nutrient source. At the flood gate of Neuharlingersiel (Fig. 5.1) the average PO_4^{3-} and H_4SiO_4 concentrations determined in 2002 and 2003 were 4 μM and 110 μM , respectively (at salinities about 1). Fresh water concentrations are lower than deep pore water concentrations (Fig. 5.5) and fresh water does not flow into the back barrier area during every low tide. Fresh water thus presumably releases a smaller amount of nutrients into the back barrier area compared to pore water.

5.5 Conclusions

Biogeochemical processes are for the first time described in tidal flat sediments of some metres depth. Despite the dynamic sedimentological conditions in the study area, the general depth profiles obtained in the relatively young intertidal flat sediments of some metres depth are comparable to those determined in deep marine surface sediments. Lithological and hydrological conditions however exert influence on sulphate, DOC, and nutrient pore water profiles. In some sediment layers advective flow occurs besides diffusive transport. Due to the hydraulic gradient generated at tidal flat margins during low tide between the pore water level and the water level in the tidal creek, pore waters rich in remineralisation products are transported towards the tidal flat margin. The release of these nutrient-rich pore waters at creekbanks may account for the increase in sea water nutrient concentrations in the study area during low tide.

Sulphate reduction has been identified as the most important pathway for anaerobic organic matter remineralisation. Pore water concentrations of sulphate, ammonium, and phosphate have been used to elucidate the composition of organic matter degraded in the sediment. The calculated C:N and C:P ratios are below the Redfield ratio. Preferential hydrolysis of particulate organic nitrogen relative to particulate organic carbon may explain the low C:N ratios of about 3. Model results support the results concerning the composition of remineralised organic matter and the importance of sulphate reduction as the dominant anaerobic remineralisation process.

Acknowledgements

The authors would like to thank Malte Groh for his valuable assistance during all sampling campaigns and Carola Lehnert and Eleonore Gründken for their assistance during laboratory work. Furthermore, we wish to thank the TERRAMARE Research Centre for providing transportation to the sampling site by boat and especially Helmo Nicolai for his help regarding technical questions. We thank Joris M. Gieskes for his critical reading of a previous version of this manuscript. Finally, we thank the Associate editor R.K. Wieder and two anonymous reviewers for their comments, which greatly improved the manuscript. We gratefully acknowledge the financial support by the German Science Foundation (DFG, BR 775/14-4) within the framework of the Research Group 'BioGeoChemistry of Tidal Flats' (FOR 432/2).

6 Trace metal dynamics in the water column and pore waters in a temperate tidal system: Response to the fate of algae derived organic matter

Kowalski, N., Dellwig, O., Beck, M., Grunwald, M., Fischer, S., Piepho, M., Riedel, T., Freund, H., Brumsack, H.-J., Böttcher, M. E.

This chapter has been published 2009 in *Ocean Dynamics* 59, 333-350.

Abstract

Tidal and seasonal behaviour of the redox-sensitive trace metals Mn, Fe, Mo, U, and V have been investigated in the open water column and shallow pore waters of the back barrier tidal flats of the island of Spiekeroog (Southern North Sea) in 2002 and 2007. The purpose was to study the response of trace metal cycles on algae blooms, which are assumed to cause significant changes in the redox-state of the entire ecosystem. Trace metal data were complemented by measurements of nutrients and enumeration of algae cells in 2007.

Generally, Mn and V show a tidal cyclicity in the water column with maximum values during low tide which is most pronounced in summer due to elevated microbial activity in the sediments. Mo and U behave almost conservatively throughout the year with slightly increasing levels towards high tide. Exceptions are observed for both metals after summer algae blooms. Thus, the seasonal behaviour of the trace metals appear to be significantly influenced by productivity in the water column as the occurrence of algae blooms is associated with an intense release of organic matter (e.g. transparent exopolymer particles, TEP) thereby forming larger organic-rich aggregates. Along with elevated temperatures in summer the deposition of such aggregates favours microbial activity within the surface sediments and release of DOC, nutrients, and trace metals (Mn, Mo, and V) during the degradation of the aggregates. Additionally, pronounced reducing conditions lead to the reduction of Mn(IV)-oxides and Fe(III)-(oxihydr)oxides, thereby releasing formerly scavenged compounds as V and phosphate. Therefore, pore water profiles show significant enrichments in trace metals especially from July to September. Finally, the trace metals are released to the open water column via draining pore waters (esp. Mo, Mn, and V) and/or fixed in the sediment as sulphides (Fe, Mo) and bound to organic matter (U).

Non-conservative behaviour of Mo in oxygenated seawater, first observed in the investigation area by Dellwig et al. (2007b), was shown to be a recurrent phenomenon which is closely coupled to bacterial activity after the breakdown of algae blooms. In addition to the postulated fixation of Mo in oxygen-depleted micro-zones of the aggregates or by freshly formed organic matter, a direct removal of Mo from the water column by reduced sediment surfaces may also play an important role.

6.1 Introduction

The back barrier tidal flats of the East-Frisian island chain form the transition zone between the terrestrial and marine realm (Fig. 6.1). Such ecosystems are subject to pronounced dynamics caused by distinct tidal and seasonal changes of physical, chemical, and biological parameters significantly influencing biogeochemical element cycles (e.g. de Jonge et al., 1993; Raabe et al., 1997; van Beusekom et al., 1999; Philippart et al., 2000; van Beusekom and de Jonge, 2002; de Beer et al., 2005; Lunau et al., 2006; Dellwig et al. 2007a,b). Especially redox-sensitive trace metals like Mn or Mo are promising candidates for reflecting variations in bioproductivity and microbial activity. Dellwig et al. (2007a), for instance, investigated the tidal and seasonal behaviour of Mn in the water column of the study area and reported a strong relationship between water column signatures and microbial activity within the underlying sediments. Additionally, Bosselmann et al. (2003), Dellwig et al. (2007a,b), and Beck et al. (2008a) found pronounced dynamics of redox-sensitive trace metals in the top sediments which appear to be controlled by redox stratification and deposition of detrital inorganic matter.

As a consequence of the different electro-chemistry of redox-sensitive trace metals their response to changing redox conditions varies. While U, Mo, and V occur as soluble oxyanions in oxygenated seawater, Mn is only soluble under reducing conditions (e.g. Morris, 1975; Collier, 1985; Burdige, 1993; Shiller, 1997; von Langen et al., 1997; Statham et al., 1998). The trace metals can be stabilized in the dissolved phase by complexation with inorganic (carbonate, chloride, phosphate, and sulphate) or organic ligands (fulvic, humic acids). They further can be removed from the water column by “scavenging” on organic (Hoffman and Fletcher, 1981) or inorganic particles (Goldberg, 1954; Balistrieri et al., 1981), assimilation by organisms (Cole et al., 1993) or co-precipitation with minerals (e.g. sulphides, Huerta-Diaz and Morse, 1992). Hence, the response of trace metals in the open water column and the pore waters to changing redox conditions should provide information about the state of the investigated ecosystem.

The major aim of this contribution is to draw attention to the response of selected redox-sensitive trace metals (Mn, Mo, U, V, Fe) to changes in bioproductivity. Therefore, tidal and seasonal characteristics of trace metals in the open water column and in the pore waters of surface sediments were investigated during several sampling campaigns in the back barrier tidal flats of the island of Spiekeroog (NW Germany). In 2007 trace metal dynamics are accomplished by measurements of nutrients, sulphur species, and algae cell numbers.

6.2 Geochemistry of selected redox-sensitive trace metals

In oxic sea water *uranium* (U) behaves conservatively as soluble U(VI) carbonate complex but can be reduced enzymatically by microorganisms (Lovley et al., 1991, 1993) leading to insoluble U(IV) (uranyl). Additionally, U shows a strong tendency towards complexation with organic matter (Klinkhammer and Palmer, 1991).

Molybdenum (Mo) occurs as soluble molybdate anion (MoO_4^{2-}) in oxygenated seawater and is generally assumed to behave conservatively, i.e. it follows salinity (Bruland, 1983; Collier, 1985). However, some deviations from conservative behaviour have been reported by several authors for various ecosystems. For instance, Head and Burton (1970) and Cole et al. (1993) observed Mo removal from oxic estuarine waters which was explained by plankton assimilation and adsorption on organic matter. Yamazaki and Gohda (1990) also suggested that organic Mo capture by biological activity could be responsible for Mo depletion in shallow coastal and oceanic waters. Such association of Mo with particulate organic matter was earlier mentioned by Szilagyi (1967) and Nissenbaum and Swaine (1976). As a further process of Mo removal from the water column, Berrang and Grill (1974) explained decreasing Mo values in the water column of Saanich Inlet by Mo scavenging via freshly formed MnO_x phases. More recently, Tuit and Ravizza (2003) observed both Mo enrichment and depletion in the equatorial Pacific. The authors suggested a strong relationship between Mo and cyanobacteria growth. Dellwig et al. (2007b) reported extreme Mo depletion in coastal waters of the Southern North Sea and postulated Mo fixation in oxygen-depleted micro-zones of large aggregates and/or scavenging by freshly formed organic matter. In sulphidic waters, however, MoO_4^{2-} is sequentially transformed to particle-reactive thiomolybdates (Erickson and Helz, 2000) which are predominantly captured by iron sulphides (Vorlicek and Helz, 2002; Helz et al., 2004; Vorlicek et al., 2004) or particulate organic matter. Thus, molybdenum removal by anoxic or even euxinic sediments by sulphide-organic matter-Mo interactions presumably forms the ultimate process for Mo burial (Helz et al., 1996; McManus et al., 2002; Algeo and Lyons, 2006; Neubert et al., 2008).

Variations of *vanadium* (V) are also linked to salinity but with a slight salinity-independent surface depletion in ocean waters. V occurs in three oxidation states: As V(V) forming soluble oxyanions, e. g. H_2VO_4^- and HVO_4^{2-} , and under reducing conditions as V(IV), forming the oxocation VO(II) (vanadyl), and V(III). Reduction of V(V) is assumed to be caused by sulphide (Wehrli and Stumm, 1989; Wanty and Goldhaber, 1992) leading to particle-reactive species which precipitate as oxyhydroxides (Wehrli and Stumm, 1989) or form stable complexes with humic acids (Szalay and Szilagyi, 1967).

Reactive *iron* (Fe) occurs under oxic conditions as Fe(III)-(oxyhydr)oxides and can be reduced chemically by sulphide (Poulton, 2003) or enzymatically by Fe(III)- and sulphate-reducing bacteria to Fe^{2+} (Lovley et al., 1993). Depending on the availability of reactive iron the reduction of Fe(III) in a sulphide-containing system results in the formation of Fe-sulphide minerals like Fe-monosulfides and pyrite (e.g. Berner, 1984; Canfield, 1989; Canfield et al., 1992).

Due to the slow oxidation rate, dissolved *manganese* (Mn^{2+}) is relatively stable in oxic waters, e.g. as chloro-complexes (Roitz et al., 2002). Bacterially catalysed or photochemical Mn^{2+} oxidation leads to precipitation of Mn-oxides (Emerson et al., 1982; Anbar and Holland, 1992; Nico et al., 2002) which have the ability to trap other trace metals by “scavenging“ (e.g. Feely et al., 1983; Koschinsky et al., 2003). Suboxic and anoxic conditions favour microbial reduction of Mn(IV) (Burdige and Nealson, 1985) thereby releasing scavenged trace metals. Recently, Trouwborst et al. (2006) reported the occurrence of Mn^{3+} in the suboxic zone of the Black Sea water column as an important intermediate during bacterial oxidation of Mn^{2+} .

6.3 Geographical Setting

The Wadden Sea system of the Southern North Sea extends over a length of 450 km from Den Helder (Netherlands) in the West to Esbjerg (Denmark) in the North. The development of the coastal area started about 7500 BP with the Holocene sea-level rise. The mesotidal regime of the East Frisian Wadden Sea (tidal amplitude: 2.2 to 2.8 m) formed a complex system of barrier islands and back barrier tidal flats (Streif, 1990). Deep inlet channels between the islands enable water and material exchange with the open North Sea.

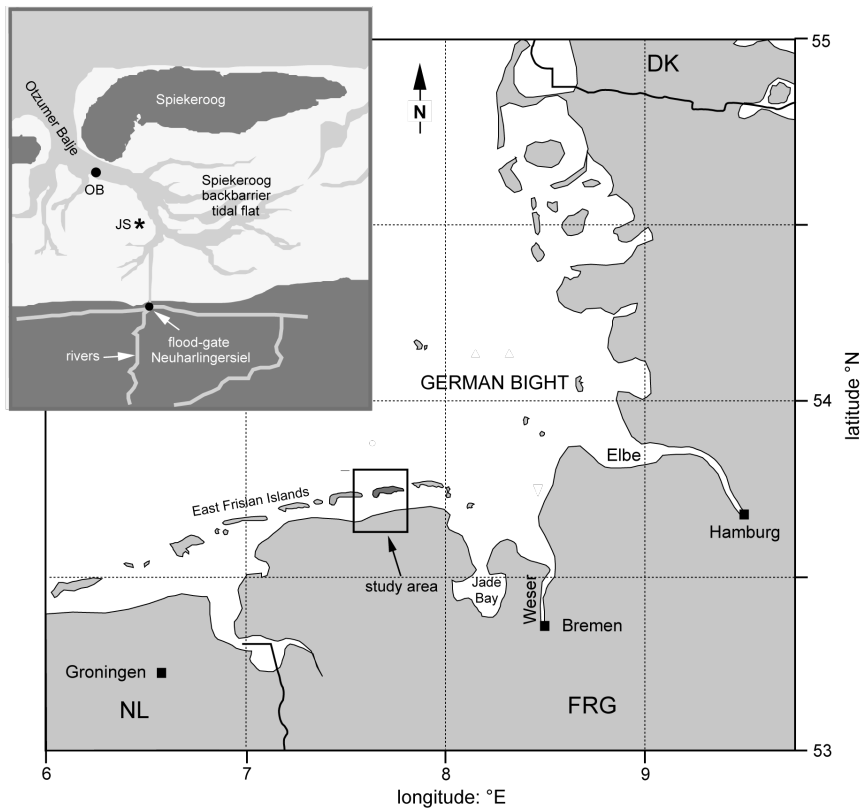


Fig. 6.1. Map of the study area showing the back barrier tidal flats of Spiekeroog island, Wadden Sea (NW Germany). The detailed map presents sampling sites in the tidal inlet (Otzumer Balje, OB) and on the Janssand tidal flat (JS).

Sampling sites of this work are located in the back barrier tidal flat of the island of Spiekeroog which is situated in the East Frisian Wadden Sea of NW Germany (Fig. 6.1). Surface water samples were taken in the tidal inlet between the islands of Spiekeroog and Langeoog (Otzumer Balje, OB) near a time series station located at position $53^{\circ}45'01.00''\text{N}$, $7^{\circ}40'16.30''\text{E}$ (Grunwald et al., 2007). Sampling of pore waters and sediments was carried out on the Janssand (JS), a sand flat (position $53^{\circ}43'57.72''\text{N}$, $7^{\circ}41'17.00''\text{E}$) which becomes exposed during low tide (Fig. 6.1). The high permeability of sandy sediments enables advective pore water transport which leads to more effective organic matter degradation and nutrient release whereas processes in muddy sediments often are more influenced by diffusion (Billerbeck et al., 2006a; Franke et al., 2006).

6.4 Material and Methods

6.4.1 Sampling

In 2002, surface water samples for the analysis of dissolved and particulate matter were taken during four cruises aboard R/V “Senckenberg” at position OB (Fig. 6.1). Depending on suspended particulate matter (SPM) concentrations, 0.15 to 1.25 L of water were filtered through pre-weighed Millipore Isopore[®] membrane filters (0.45 µm polycarbonate (PC), for multi-element analyses) and Whatman glass microfibre filters GF/F (0.7 µm glass fibre [GF], for TC and TIC analyses). Filters were rinsed with purified water, dried at 60°C for 48 h and re-weighed for the determination of total SPM. Samples for the analysis of dissolved metals were directly taken with pre-cleaned PE-syringes and 0.45 µm SFCA syringe filters. These samples were acidified with HNO₃ (supra pure, Merck) to 1 % (v/v) and stored in pre-cleaned PE-bottles. Tidal creek water samples (five samples for each cruise) were also directly taken with syringes. Pore waters were sampled with portable lances. The samples were subsequently treated in the same way as the seawater samples.

In 2007, sampling of seawater and suspended particulate matter (SPM) from the upper 1 metre of the water column was performed with a multi water sampler (Hydro-Bios, Kiel, Germany) aboard of R/V “Navicula” (Carl von Ossietzky University, Oldenburg). Pore water was sampled with an in-situ pore water sampler which is permanently installed in the tidal flat sediments and reaches a maximum depth of 5 metres (Beck et al., 2007). This communication only focuses on pore water from the uppermost metre. For data from deeper parts of the sediment column the authors refer to Beck et al. (2008a,c).

Seawater and pore water samples were rinsed through 0.45 µm SFCA syringe filters. Samples for metal analyses were acidified to 1 % (v/v) with HNO₃ (supra pure, Merck). For determination of hydrogen sulphide (H₂S) 2 ml of filtered sample were fixed in a PE vial with 100 µl of 5 % zinc acetate solution.

For SPM determination during the campaigns in 2007, 0.5 to 1.5 L seawater was filtered through pre-weighed PC filters (Millipore Isopore membrane filters, 0.4 µm pore size). After rinsing the filters with approx. 100 ml purified water they were dried at 60° C for 48 h.

6.4.2 Geochemical analysis

For analysis of particulate metals the PC filters were completely digested with an acid mixture of HNO₃, HClO₄ and HF in a PDS-6 pressure digestion system (Loftfields

Analytical Solutions) at 180° C for 6 h and measured by ICP-OES (Thermo, iCAP 6300 Duo). A more detailed description of these procedures is given by Dellwig et al. (2007). Water samples were measured using ICP-OES (Thermo, iCAP 6300 Duo) and HR-ICP-MS (Thermo Finnigan, Element 1 and 2). For ICP-MS measurements the samples were diluted 25-fold according to the method published by Rodushkin and Ruth (1997) and 2-fold for ICP-OES.

Sulphide was determined after the method described by Cline (1969). A diamine reagent (N, N-dimethyl-p-phenylenediamine sulphate and ferric chloride diluted in hydrochloric acid) was added to a sample aliquot. After a reaction time of 20 min the absorbance was measured photometrically (Analytik Jena AG, Specord 40) at a wavelength of 670 nm. Sulphate was also determined by photometry (wavelength 450 nm) after the method described by Tabatabai (1974) using aliquots from ZnAc fixed samples after centrifugation.

DOC was measured by temperature catalytic oxidation (Analytik Jena AG, multi N/C 3000 analyser) using K-hydrogenphthalate for external calibration.

Photometric measurements of the nutrients phosphate, ammonium and silica in pore waters were performed using the methods described by Grasshoff et al. (1999). Determination of total alkalinity followed the method described by Sarazin et al. (1999). Silica in surface water was determined by automated nutrient analysers installed at the time series station and based on a loop-flow reactor and loop-flow analysis technique. A detailed description of the time series station and the nutrient analyzer setup can be found in Grunwald et al. (2007).

6.4.3 Phytoplankton count

For phytoplankton cell count seawater samples (2.5 L) were filtered through plankton nets with 10 µm mesh size. The cells were preserved by the addition of Lugol's solution and stored in PE bottles at 4°C. Phytoplankton cells were enumerated according to the method by Utermöhl (1958). Aliquots of the concentrated samples were stored over night in 10 ml chambers to enable sedimentation of the cells. Analyses were performed with an inversion microscope (Zeiss Axiovert 100), and the cells were counted in 2 or 3 diametrical transects across the whole chamber. 200-fold magnification was used to identify species with high abundances and small cell size, afterwards 100-fold magnification was used for species with small abundance and large cell size.

6.5 Results and discussion

6.5.1 Influence of algae blooms on tidal flat sediments

The Wadden Sea is subject to drastic short-term changes due to the general influence of the tidal regime and changes in primary production, mainly by microalgae. The occurrence of algae blooms during spring and summer leads to an intense consumption of nutrients and subsequently a high production of biomass in the water column. Figure 6.2 shows phytoplankton cell counts and the corresponding variations in silica from April until the end of August 2007. Cell numbers of diatoms increase distinctly during mid of April reflecting the onset of the spring bloom. The time offset of about 2 weeks which is obvious between decreasing silica concentrations and increasing diatom cells in April has methodological reasons as only diatoms larger than 10 μm were sampled. Therefore, the apparent beginning of the bloom is delayed due to the exclusion of smaller cell sizes in the present sampling protocol (Heike Simon, personal communication). On the basis of these diatom counts the bloom lasted for about two weeks and was paralleled by elevated numbers of *Phaeocystis* species. During breakdown of the spring bloom, which is caused by the reduced availability of nutrients in the open water column, the values of silica increased again and showed some fluctuations afterwards. In early June, a second diatom bloom occurred which lasted for about ten days in the study area. A significant increase in silica values marks the breakdown of this second bloom in mid June. In the following time-period only slight changes in diatom numbers and some variations in silica occurred.

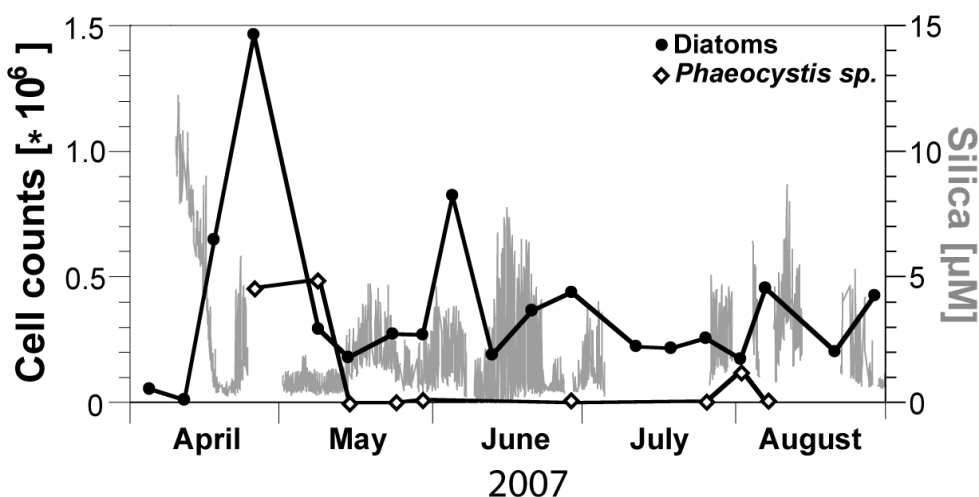


Fig. 6.2. Silica concentrations and diatom cell counts in the water column of the Spiekeroog island back barrier area in 2007.

An important consequence of algae lysis is the pronounced release of DOC (Dellwig et al., 2007b) and nutrients (Martens and Elbrächter, 1997) to the water column. Thus, high amounts of organic compounds like TEP (transparent exopolymer particles) are released. In contrast to the spring bloom when microbial activity is comparatively low, the microbial biomass decomposition is much more intense during the summer months (Dellwig et al., 2007b) resulting in the production of sticky carbohydrates which colligate suspended inorganic and organic particles in the water column thereby forming larger aggregates (Passow, 2002; Chen et al., 2005). The resulting aggregates hydraulically behave differently and sinking velocities resemble of coarser grained material. Therefore, significant amounts of aggregates are deposited on the tidal flat sediments forming a fluffy layer of organic-rich material on the sediment surface (Chang et al., 2006a). Subsequently, the deposited organic-rich aggregates are incorporated into the upper first centimetres of the sediment by tidal forces (Rusch and Huettel, 2000; Billerbeck et al., 2006a). These coupled processes result in a supply of freshly formed and readily degradable marine organic matter to the sediments. Along with increasing temperature in summer, the organic matter input leads to elevated activity of microorganisms in the upper sediment layer (Böttcher et al., 1999; Bosselmann et al., 2003).

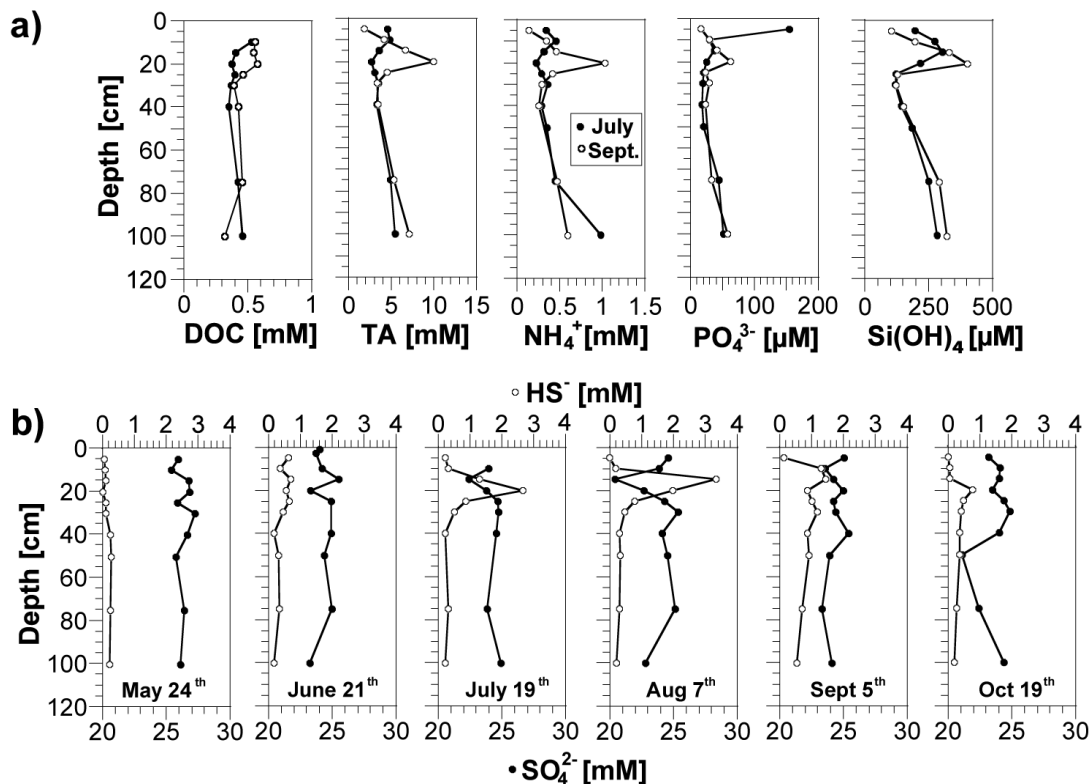


Fig. 6.3. Concentrations of a) DOC, TA, ammonium, phosphate, and silica, and b) hydrogen sulphide and sulphate in the pore waters at site JS in 2007.

In the pore water profiles, DOC, total alkalinity (TA), ammonium, and phosphate (Fig. 6.3a), which represent products of organic matter degradation, are clearly enriched as seen in the depth interval of around 20 cm after the summer bloom when comparing data from July and September 2007. Along with the increase in HS^- and parallel decreasing SO_4^{2-} values in July and August 2007 (Fig. 6.3b), these enrichments can be explained by elevated microbial activity, which is favoured by the organic matter input after the algae bloom breakdown in June.

In contrast, elevated phosphate values in September are most likely caused by dissolution of Fe(III)-(oxyhydr)oxides due to pronounced reducing conditions in the sediments during late summer. Iron phases are known to adsorb PO_4^{3-} during formation, which are again released when solid phases are reduced (e.g. van Raaphorst and Kloosterhuis, 1994).

The variations of silica in the pore waters are less pronounced as dissolution of diatom frustules is a relatively slow process which seems to occur throughout the entire year, resulting in an almost constant release of silica out of the sediment (Beck et al., 2008c). Thus, increasing concentrations of silica after collapsing algae blooms (Fig. 6.2) are more likely the result of advective pore water release (Billerbeck et al., 2006a; Beck et al., 2008a,c) and reduced consumption rather than decomposition of diatoms within the water column. While the lysis of algae cells is a comparatively fast process, their frustules are stable for longer time periods, are therefore deposited on the sediment surface and enter slightly deeper layers due to tidal forces (e.g. Rusch and Huettel, 2000).

Overall, algae- and temperature-induced increases in microbial activity in the water column and especially in the top sediment layers lead to a shift of redox conditions in the sediment and reduces the thickness of the oxic sediment surface layer. An example of such extreme changes in sedimentary redox conditions is the formation of anoxic sediment surfaces where sulphidic pore waters are drained out of the sediment (e.g. Böttcher et al., 1998, 1999; Böttcher, 2003). Upward advective pore water flow has been shown to be promoted by near surface methane formation.

The data presented so far reveal intense interactions between water column and sedimentary processes. Thus, seasonal variations in the top sediments are remarkably influenced by bioproductivity in the open water column. The following chapters provide an insight into the interaction of both reservoirs with respect to selected redox-sensitive trace metals.

6.5.2 Uranium

The data from the Wadden Sea cruises in 2002 (site OB) show a general depletion of dissolved U (Fig. 6.4) when compared with the level in ocean waters (14 nM; Ku et al., 1977; Maeda and Windom, 1982).

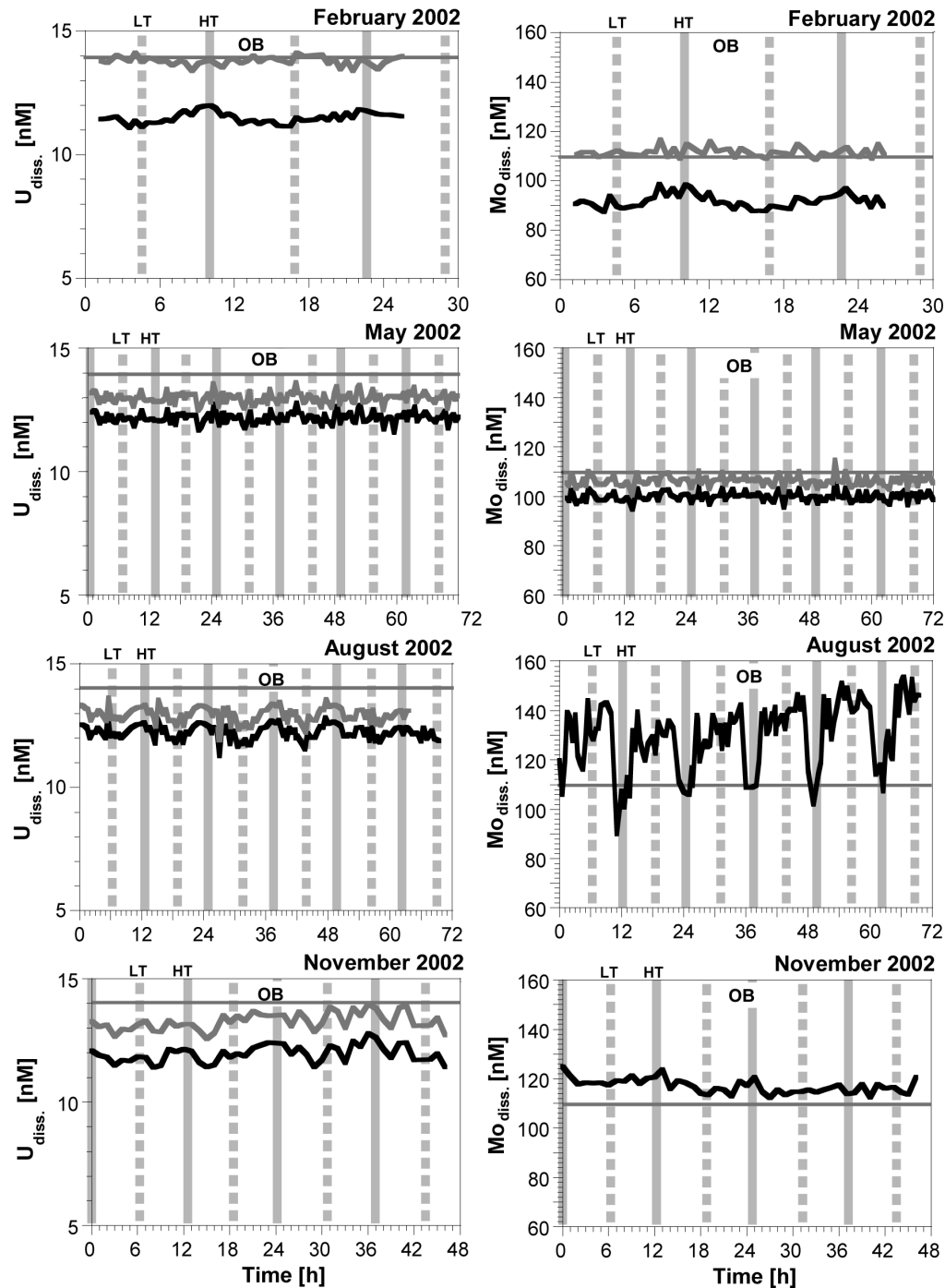


Fig. 6.4. Seasonal variations of dissolved U and Mo in the water column of the Spiekeroog island back barrier area in 2002. Data presented in blue colour are normalized to offshore salinity. The grey line denotes the North Atlantic value; the vertical grey lines mark high tide (HT) and the dashed line low tide (LT).

Table 6.1. Average values and range (in parentheses) of salinity, SPM, POC, and dissolved and particulate trace metals in the Wadden Sea and in freshwater flowing into the back barrier area via flood-gates in Neuharlingersiel in 2002.

	Wadden Sea				freshwater (flood-gate)	
	January	May	August	November	winter	summer
salinity	27.2 (26.3 -28.4)	30.9 (30.8-31.0)	31.2 (31.0-31.3)	29.5 (29.0-30.2)	1.7 (0.5-3.8)	2.1 (0.5-3.8)
DOC [mM]	0.24 (0.19 -0.29)	0.21 (0.18-0.28)	0.21 (0.17-0.25)	0.21 (0.18-0.25)	1.3 (0.9-1.8)	1.2 (0.8-2.4)
Mn _{diss.} [μ M]	0.07 (0.02 -0.16)	0.28 (0.07-0.58)	0.63 (0.14-1.1)	0.07 (0.01 -0.16)	4.0 (2.2-6.3)	4.1 (0.8-8.4)
Mo _{diss.} [nM]	92 (86-100)	100 (95-105)	131 (94-155)	115 (110-121)	11 (6-19)	11 (4-19)
Fe _{diss.} [μ M]	—	—	—	—	11 (6.5-19)	10 (0.1-31)
U _{diss.} [nM]	11.4 (10.8-12.0)	12.2 (11.6 -12.8)	12.2 (11.3-12.9)	12.0 (11.4 -14.5)	2.2 (0.9-4.2)	1.6 (0.7-4.0)
V _{diss.} [nM]	36 (28-43)	34 (28 -43)	53 (37-70)	32 (28-36)	45 (16-90)	86 (49-164)
SPM [mg l^{-1}]	62 (28-43)	12 (3.1-47)	8.4 (2.6-46)	45 (12-104)	24 (8.2-38)	37 (9.2-84)
POC [%]	3.6 (2.6-4.0)	5.2 (1.3 -12)	4.3 (2.5-8.5)	4.2 (3.3-4.8)	8.6 (7.3-11)	13 (7.8-20)
Mn _{part.} [mg kg^{-1}]	763 (657-838)	1105 (626 -3923)	1289 (676-1846)	903 (434-1046)	471 (333-687)	2273 (698-5772)
Mo _{part.} [mg kg^{-1}]	2.7 (1.6-7.4)	9.9 (1.1-8.3)	19 (4.6-83)	2.2 (1.6-4.7)	2.6 (1.6-4.3)	2.8 (0.9-9.5)
Fe _{part.} [%]	3.6 (3.4-3.8)	2.9 (1.7-4.7)	2.8 (1.3-3.5)	3.7 (3.3-4.0)	8.3 (4.7-13)	7.0 (3.5-12)
U _{part.} [mg kg^{-1}]	2.9 (2.5-3.3)	1.9 (1.3-3.0)	2.0 (0.9-3.1)	2.1 (1.7-2.4)	2.2 (1.8-2.6)	1.5 (0.9-2.1)
V _{part.} [mg kg^{-1}]	133 (109-155)	100 (52-141)	98 (45-150)	125 (114-155)	153 (104-182)	136 (80-184)

In a first approximation this difference is caused by the lower salinity in the Wadden Sea as the freshwater from continental run-off contributes only minor amounts of U (Table 6.1). Dissolved U shows a tidal pattern with maximum concentrations during high tide for most of the cruises. A normalisation to North Sea salinity smoothes the tidal pattern in February 2002 and moves all data points close to the ocean value (Fig. 6.4). In contrast, during the cruises in May and August 2002 when salinity was distinctly higher and almost constant over the entire tidal cycles (Table 6.1), the normalized U concentrations increase only slightly and the general pattern remains unaffected. This finding contradicts a strictly conservative behaviour. Hence, the tidal variation of U in summer must be caused by other processes. Moreover, the depletion of U in the water column especially during low tide must be linked to processes like fixation of U within anoxic parts of the tidal flat sediments (Klinkhammer and Palmer, 1991; Shaw et al., 1994). This assumption is in accordance with measurements in August 2002 of pore waters and tidal creek waters draining out of the sediment during low tide, which are depleted in U (Fig. 6.5).

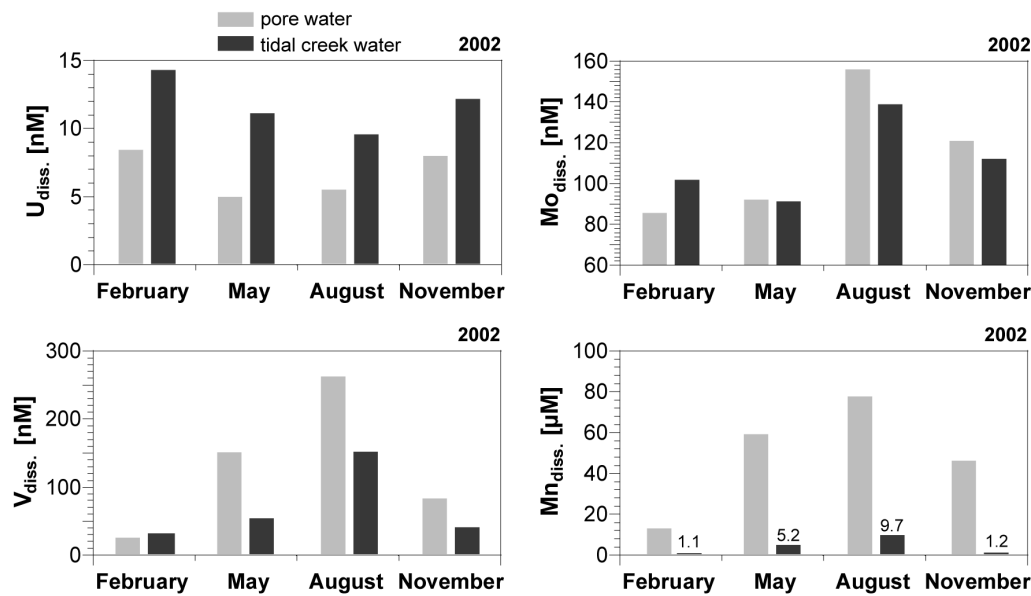


Fig. 6.5. Seasonal variations of dissolved U, Mo, V, and Mn in pore waters and tidal creek waters in 2002.

In the time series of 2007, U normalized to salinity shows a slight seasonal variation in the water column with depletion phases in April/May and June (Fig. 6.6) which is probably due to the breakdown of algae blooms and U sorption on organic particles. In 2002 U enrichment on SPM was insignificant (Fig. 6.7) but is probably masked by the geogenic background of U ($3.0 \mu\text{g g}^{-1}$; Wedepohl, 1971)). In pore waters uranium is generally depleted in comparison to the water column due to a fast fixation in the sediment caused by complexation with organic matter and microbial reduction (e. g. Klinkhammer and Palmer, 1991; Lovley et al., 1991, 1993). While the pore water shows depletion at 5 cm depth higher concentrations occur at 10 to 25 cm depth with values around 5-6 nM from April to June (Fig. 6.8a). This behaviour is in agreement with investigations carried out by Morford et al. (2007). In addition, these authors found typical enrichments in the uppermost centimetres (0-5 cm), due to diffusion from the open water column into the sediment. Such a pattern is not reflected here as the first sampling occurred at 5 cm depth.

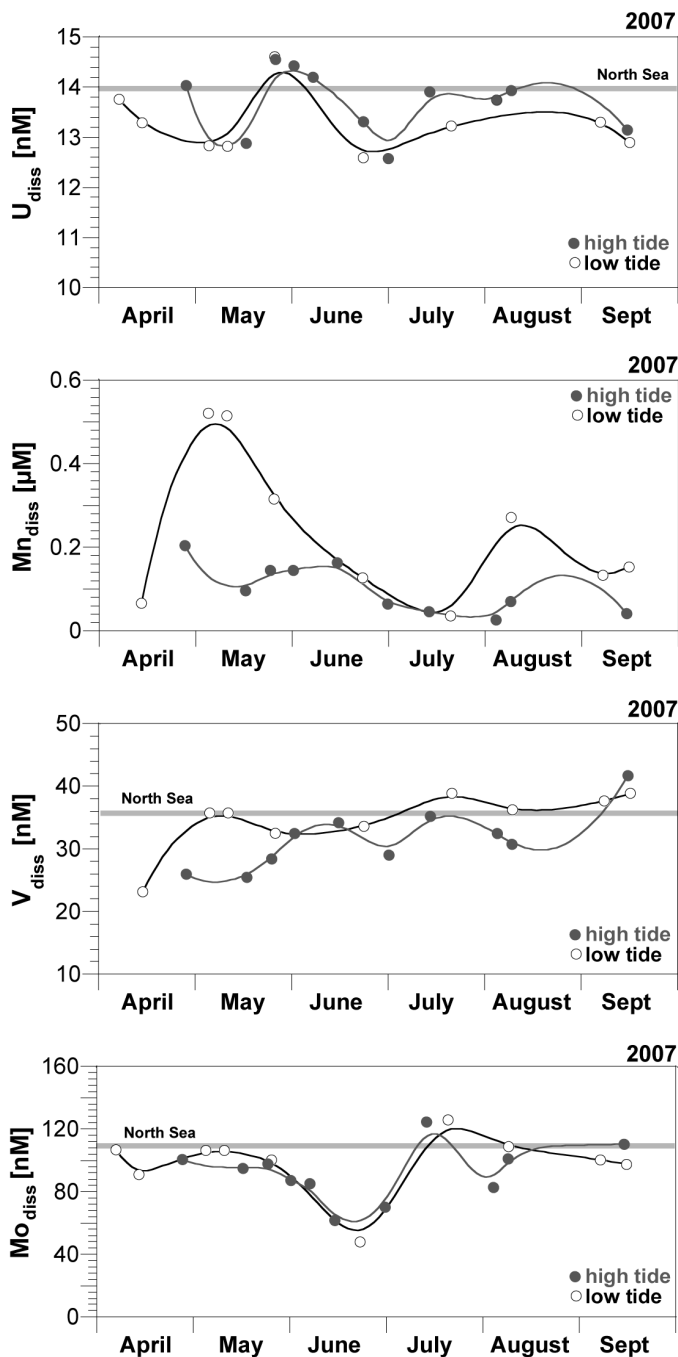


Fig. 6.6. Concentrations of dissolved U, Mn, V, and Mo in the water column of the Spiekeroog island back barrier area from April to September 2007. The grey line denotes the North Sea value.

In July an enrichment of U with respect to deeper parts of the profile is seen at 5 to 10 cm sediment depth. This enrichment increases to a maximum value of almost 12 nM in August (Fig. 6.8a). This behaviour could be the result of release from organic matter during its degradation and mineralization. Additionally, U release from reduced Fe(III)-

(oxyhydr)oxides could also be responsible for the U enrichment in the uppermost sediment layers. In August 2007 the U concentrations in the water column reach the seawater value (Fig. 6.6) most likely due to U release from sediments.

In the depth interval from 15 to 20 cm U is removed from the pore water by reduction. This depth coincides with the depth of highest iron (Fe^{2+}) concentrations. The conformity of uranium reduction depth with reduction depth of iron was also described by Cochran et al. (1986), Zheng et al. (2002) and Morford et al. (2005) confirming the investigation results of Lovely et al. (1991) who found that U(VI) reduction is coupled with Fe(III) reducing bacteria. U which is released during Fe(III)-(oxyhydr)oxide reduction may be directly fixed in the sediment.

6.5.3 Iron

In April 2007 dissolved iron shows elevated values of up to $88 \mu\text{M}$ in the pore water of the uppermost sediment layer (Fig. 6.8b), which is probably caused by intense reduction after the algae bloom in spring. Anoxic conditions may prevail during this period but with a presumably limited occurrence of sulphide (no sulphide measurements are available for April). Additionally, complexation with organic ligands favours solubility of Fe as shown by Luther et al. (1996). In the salt marshes of the island of Langeoog, Kolditz et al. (2009) observed Fe enrichments and complexation by organic compounds in an anoxic system without any significant sulphate reduction.

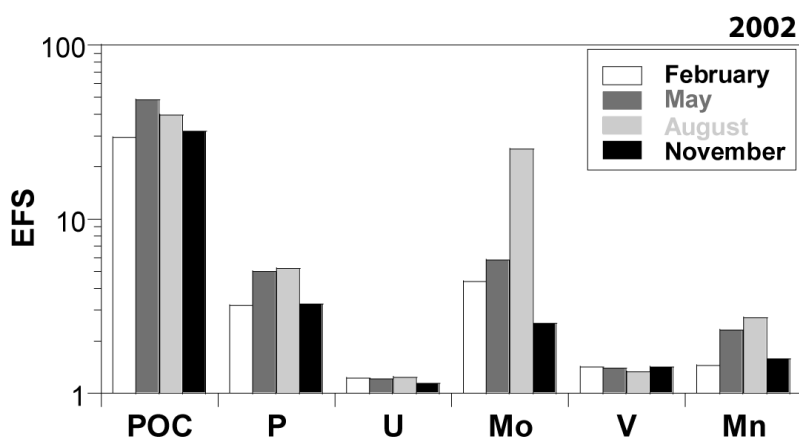


Fig. 6.7. Seasonal variation of enrichment factors (EFS) for particulate organic matter (POC), P, U, Mo, V, and Mn of suspended particulate matter in 2002.

With increasing temperature the onset of sulphide production is assumed to occur from May to July leading to Fe fixation in the sediment as FeS. Temperature has been shown to be

one of the two major drivers for microbial sulphate reduction in the intertidal sands (Al-Raei et al., 2009). Although less pronounced, Fe^{2+} concentrations increase again in August and reach a maximum value of 28 μM . Along with organic-rich aggregates deposited in the surface sediment Fe(III)-(oxihydr)oxides are transferred to the sediment where they may be reduced by sulphide. The Fe(III) content of sinking aggregates is close to the geogenic background as seen in the enrichment factors (EF) of SPM of 1.1 (4.83 $\mu\text{g g}^{-1}$; Wedepohl, 1971). However, leaching experiments carried out by Hinrichs et al. (2002) showed that more than 40 % of reactive Fe is adsorbed to nearshore SPM. As a further source, Fe(III)-(oxihydr)oxides, which were formed in the surface sediments under oxic conditions in the winter months, are reduced when anoxic conditions reach the uppermost sediment layers in summer. Below a sediment depth of about 15 cm Fe^{2+} is effectively removed from the pore water throughout the year due to the reaction with sulphide. Especially in July and August this depth interval is highly enriched in sulphide (Fig. 6.8).

Phosphate which is adsorbed to FeOOH as insoluble Fe(III)-phosphate complexes (Krom and Berner, 1980; Matthiesen et al., 2001) is released together with Fe^{2+} which explains the high PO_4^{3-} enrichment in the pore water in September (Fig. 6.3). Thus, within the water column, phosphate shows continuously increasing values after a significant depletion during the algae bloom in April and May (Fig. 6.9). In October maximum values are reached which are almost 50 % higher than concentrations before the algae bloom which is caused by PO_4^{3-} release from the sediment.

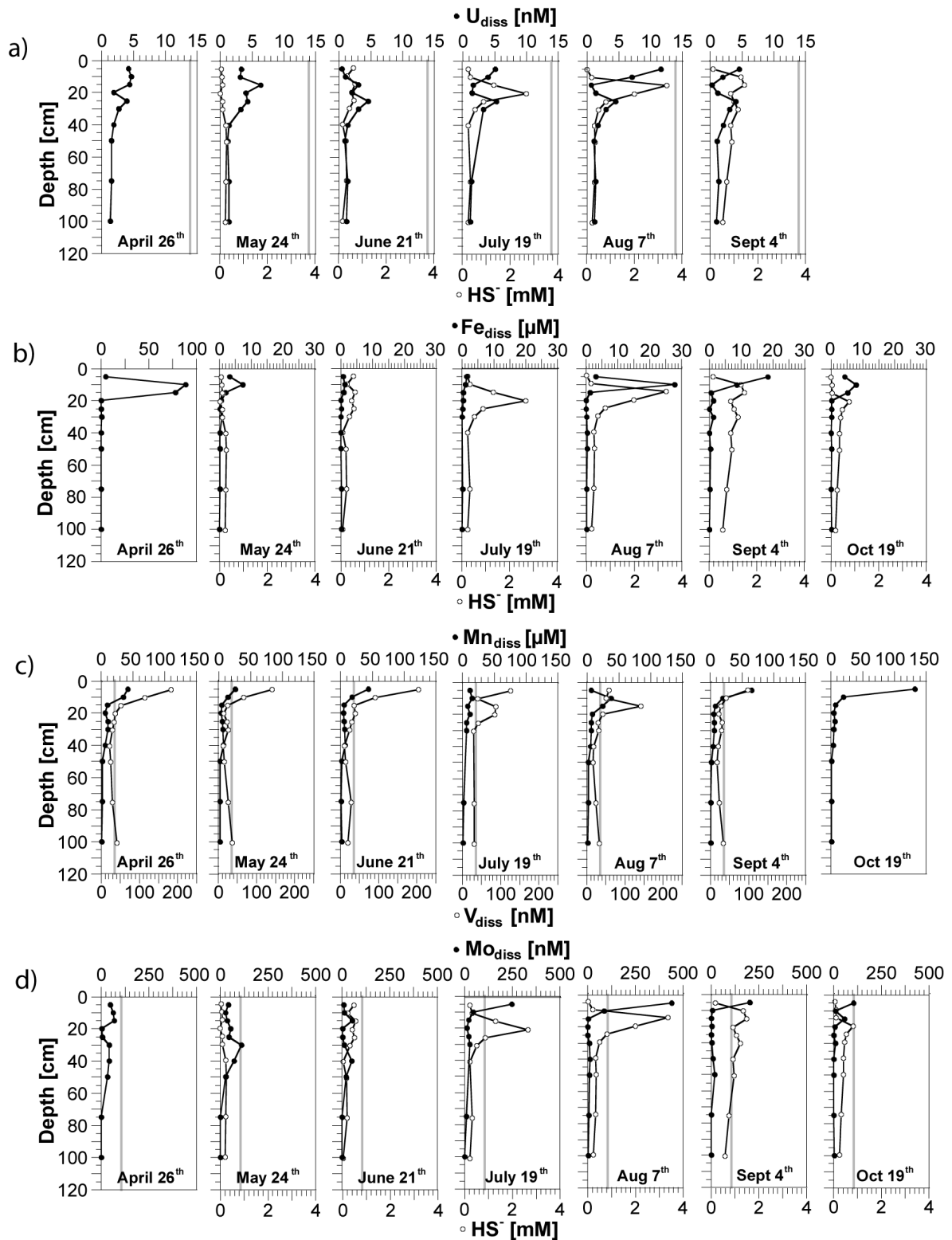


Fig. 6.8. Concentrations of dissolved a) U and HS^- , b) Fe (please note the different scale for Fe_{diss} in April) and HS^- , c) Mn and V, and d) Mo and HS^- in the pore waters of site JS from April to October 2007. The grey lines mark the North Sea values of the trace metals.

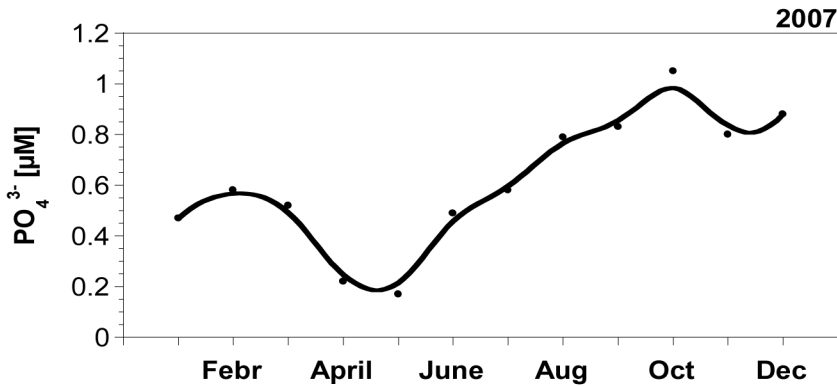


Fig. 6.9. Phosphate concentrations in the water column of the Spiekeroog island back barrier area in 2007 (monthly average).

6.5.4 Manganese

Mn concentrations are more than an order of magnitude higher in the Wadden Sea than in the open North Sea or the North Atlantic (Tappin et al., 1995; Shiller, 1997; Slomp et al., 1997; Dellwig et al., 2007a). In comparison to other trace metals tidal and seasonal variations are most pronounced for Mn. During all cruises in 2002 a tidal cyclicity of Mn is visible with values being ca. 5 times higher during low tide compared to high tide. Seasonal differences were obvious with concentrations generally increasing from winter to summer by a factor of 10 (Fig. 6.10). Such elevated Mn levels have been almost exclusively explained by release from anoxic sediments during spring and summer while freshwater inputs may only contribute to certain amounts during high precipitation periods in autumn and winter (Dellwig et al., 2007b). However, considering the concentrations of Mn in pore waters and tidal creek waters (Fig. 6.5) the level of Mn released from the sediment is distinctly smaller when compared with the other trace metals. This difference can be attributed to oxidation effects close to the sediment-water interface leading to partial retention of Mn in the surface layer. Nevertheless, Mn values in tidal creek waters are still enriched when compared with the open water column (Fig. 6.10). For a more detailed description of the behaviour of Mn in the study area the authors refer to Dellwig et al. (2007b) and Bosselmann et al. (2003).

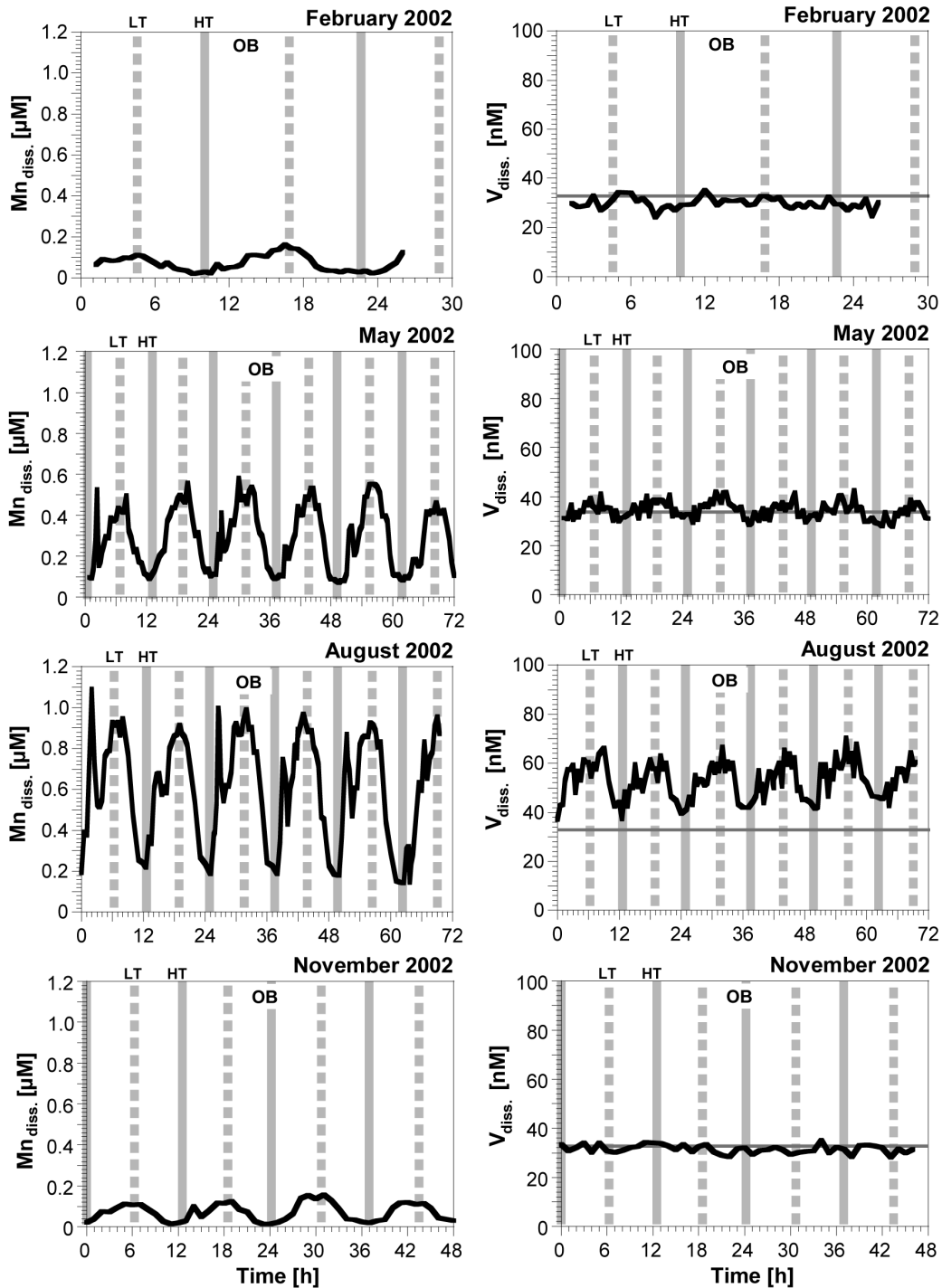


Fig. 6.10. Seasonal variations of dissolved Mn and V in the water column of the Spiekeroog island back barrier area in 2002. The vertical grey line marks high tide (HT) and the dashed line low tide (LT). The horizontal grey lines in the V plots denote the North Atlantic value.

In the time series of 2007 the above mentioned tidal differences are clearly visible with distinctly higher values at low tide (Fig. 6.6). Furthermore, seasonal variations are obvious especially at low tide with two maxima in April/May (max. $0.59 \mu\text{M}$) and in August

(max. 0.26 μM). Mn-oxides precipitated at the sediment surface or freshly formed in the sediment during the winter months are reduced in spring and summer when the reduction zone for Mn(IV) moves upwards in the sediment leading to seasonal differences in the pore water composition.

From April to June Mn^{2+} is enriched in the uppermost pore waters with values ranging from 26 to 44 μM at 5 cm depth (Fig. 6.8c). In July dissolved manganese is depleted which is possibly caused by an exhaustion of the sediment in reducible Mn. The concentrations decrease to 12 μM at 5 cm depth (16 μM at 10 cm). This decrease is also obvious in surface water values (Fig. 6.6). From mid June to beginning of August a phase of depletion occurs with values around 0.07 μM at low tide. However, the water column already shows Mn depletion in June whereas in the shallow pore waters Mn^{2+} enrichment is still visible. Exhaustion of Mn^{2+} in the pore water is apparently not the only reason for Mn^{2+} depletion in the water column. In addition, elevated microbial Mn^{2+} oxidation in the water column may also cause depletion of dissolved Mn, thereby leading to enrichments of Mn on SPM (Nico et al., 2002). This hypothesis is confirmed by SPM data from 2002 which show a general increase of particulate Mn from winter towards summer (Fig. 6.7). Additionally, data from June 2007 (not shown) reveal a clear Mn enrichment with an EFS value of 2.5. Depletion in dissolved Mn may further be due to accumulation of Mn-oxides by *Phaeocystis* sp. as reported by Lubbers et al. (1990). However, data of 2007 do not show a pronounced increase of *Phaeocystis* sp. cell numbers (Fig. 6.2) during the period of Mn^{2+} depletion.

In August, pore water concentrations increase again to 38 μM (at 10 cm depth) and to 65 μM (at 5 cm depth) in September and finally reach a value of 132 μM (at 5 cm depth) in October. SPM data of August 2002 show a significant Mn enrichment (Fig. 6.7; Dellwig et al., 2007a) which is also confirmed by the data from 2007 showing a 3-fold Mn enrichment in August. After the summer algae bloom Mn-oxides are deposited along with organic-rich aggregates at the sediment surface replenishing the Mn reservoir in the sediment. Consequently, microbial reduction of Mn-oxides leads to a significant release of Mn^{2+} into the pore water, followed by Mn^{2+} diffusion from the surface sediment into the open water column, which causes an increasing Mn^{2+} level in the water column (Fig. 6.6).

6.5.5 Vanadium

During the Wadden Sea cruises in February and November 2002 dissolved V concentrations are close to the value in the North Atlantic (33-36 nM; Huizinga and Kester, 1982; Middelburg et al., 1988). In contrast to dissolved Mo and U tidal cyclicality is less

pronounced for the winter samples (Fig. 6.10), as the freshwater, which is contributed to the Wadden Sea via the flood gates in Neuharlingersiel, contains slightly higher levels of dissolved V (flood gate in winter: 45 nM, Table 6.1). During spring and summer a pronounced tidal cyclicity is obvious with elevated values during low tide especially in August 2002. Such increase requires an additional element source, thus freshwater (flood-gate summer: 86 nM) as well as pore water input have to be considered. Although the V concentration of freshwater is about 2-fold higher in summer, this source is insufficient to cause the observed vanadium increase in the surface waters of the back barrier area (Dellwig et al., 2007a). Therefore pore waters draining out of the sediments during low tide are the more likely source as seen in Figure 6.5 which shows elevated concentrations of V in pore water and tidal creek waters.

The similarity between the tidal patterns of V and Mn in spring and summer indicates a coupling of V to the Mn cycle although their redox chemistry is different (Fig. 6.10). Shiller and Mao (1999) reported a complex behaviour for V in two estuaries of the Louisiana shelf. The authors observed both, the loss of V from open Gulf water to oxygen-depleted shelf sediments as well as release of V from the sediments. This initially contradictory finding was explained by up- and downward diffusion of V released from particles at the sediment surface. A similar process might be of importance for V enrichments in tidal creeks during summer. Oxidation of dissolved Mn and Fe in the water column of the Wadden Sea leads to the formation of oxy-hydroxide phases and concomitant scavenging of certain trace metals like Co, Mo, and also V (e.g. Goldberg, 1954; Craig, 1974; Balistrieri et al., 1981). SPM does not show seasonal variations or significant V enrichment (Fig. 6.7) because the high geogenic background of V ($130 \mu\text{g g}^{-1}$; Wedepohl, 1971) possibly covers influences caused by dissolved-particulate transfer reactions. When the particles impinge the tidal flat sediment surface and reach the anoxic zone oxy-hydroxides are reduced and trace metals will be released to the pore water (e.g. Callender and Bowser, 1980; Klinkhammer, 1980; Klinkhammer et al., 1982; Sawlan and Murray, 1983). A fraction of the released V may remain mobile due to complexation by organic ligands (Brumsack and Gieskes, 1983) and may, therefore, be able to escape from the pore water system into the water column via advective processes induced by the tides (Fig. 6.10).

In the 2007 time series, vanadium shows less significant variations with concentrations lying around the usual seawater level (Fig. 6.6). However, similarities to Mn are visible with maximum values in April/May followed by a slight depletion in May and June, which is possibly due to effective V scavenging by freshly formed Mn-oxides. In July, V values exceed the North Sea value whereby V increases earlier than Mn, a relation which probably

can be explained by processes in the pore water, e. g. V release from degraded organic matter (Szalay and Szilagyi, 1967).

In the pore water system, V shows highest concentrations in the uppermost centimetres of the sediment (Fig. 6.8c) with values ranging between 165 and 204 nM from April to June, which is clearly above the seawater level. By contrast, in July the concentrations start to decline in the top centimetres and decrease to a value of 57 nM in August. After this short depletion phase V increases again and reaches a value of 93 nM in September, possibly caused by reduction of MnO_x phases as reported for instance by Morford et al. (2005).

However, a slight V enrichment in the pore water of the uppermost sediment is still visible in July while Mn is distinctly depleted. Therefore, a V release from organic matter is suggested for the enrichment. Cheshire et al. (1977) described vanadium binding in solid phase by sorption to organic substances. During organic matter degradation vanadium is released increasing the pore water concentrations and finally the sea water concentrations, which may explain the elevated V concentrations in the water column in July.

6.5.6 Molybdenum

Figure 6.4 presents the seasonal and tidal variability of dissolved Mo for the Wadden Sea cruises in 2002. Like U, dissolved Mo reveals a conservative tidal pattern in February 2002 with maximum concentrations at high tide when the influence of North Sea water is most pronounced. Again, a normalisation to a salinity of 35 psu leads to concentrations close to the North Atlantic value (Morris, 1975) and smoothes tidal patterns. Conspicuous is the complete change in behaviour of Mo in August 2002 (Dellwig et al., 2007a), with Mo showing a tidal cyclicality with maximum values during low tide (Fig. 6.4). As a certain increase of dissolved Mo in tidal creek waters was also observed in August 2002 (Fig. 6.5) tidal flat sediments have to be considered as a significant source. Such a process would imply less pronounced reducing conditions in the sediments, enabling the release of Mo due to oxidation of sulphidic compounds via tidal pumping. However, this is rather improbable due to the occurrence of partly anoxic sediment surfaces in the summer months. Therefore, a complexation with organic ligands is more likely to cause Mo stabilization in this sulphidic environment.

Figure 6.6 shows the trend of Mo in the water column in 2007. From April to May dissolved Mo shows conservative behaviour with values ranging between 92 and 107 nM at salinities between 30 and 32 psu. At the end of May the Mo concentration starts to decrease

until a minimum value of 49 nM is reached in June, without any changes in salinity. In the following time a fast increase of Mo is observed which even exceeds the usual seawater level (107 nM; Morris, 1975; Collier, 1985) in July (126 nM, Fig. 6.6). Again a slight decrease to a value of 83 nM is seen at the beginning of August followed by a further increase to 100 nM (Fig. 6.6). These findings are in agreement with recently published results by Dellwig et al. (2007b). The authors observed a decrease in dissolved Mo down to 30 nM in the same area in 2005. During both years this decrease in Mo coincided with collapsing algae blooms as deduced from the ratio of phaeopigments and chlorophyll *a* in 2005 (Dellwig et al., 2007b) and decreasing numbers of diatom cells parallel to increasing silica values in June 2007 (Fig. 6.2). During the spring bloom no depletion was observed in 2005 and 2007 which emphasizes the importance of bacterial activity. In spring, bacterial cell numbers are still as low as in the winter months and their activity is limited by lower temperatures. In contrast, elevated temperature in the summer months favours bacterial activity as seen in increasing numbers of bacteria cells (Dellwig et al., 2007b).

Assimilatory uptake of Mo by cyanobacteria (N_2 fixation) or phytoplankton (NO_3^- fixation) can be ruled out to cause such a distinct Mo decrease in the water column. Cyanobacteria do not occur in the water column of the study area and the diatom abundance is too low during the phase of Mo depletion due to breakdown of the diatom bloom. Furthermore, Mo uptake is inhibited by the high sulphate concentrations in the study area (Cole et al., 1986, 1993).

Scavenging of Mo during bacterial oxidation of Mn^{2+} may be an effective process for Mo removal (e.g. Berrang and Grill, 1974; Barling and Anbar, 2004; Wasylenki et al., 2008). This assumption is underlined by simultaneously increasing EFS values of Mo and Mn from winter to summer (Fig. 6.7). Dellwig et al. (2007b), on the other hand, did not observe a clear relation between the behaviour of Mo and Mn during detailed investigations in the study area in 2005. Therefore, the authors assumed fixation of Mo in oxygen depleted micro-zones on aggregates, which are favoured by elevated microbial activity during breakdown of algae blooms. However, Ploug et al. (1997) for instance did not observe any sulphide in anoxic areas of aggregates which is required for Mo fixation in aggregates. The authors assumed that short persistence of anoxic conditions limits slow-growing sulphate reducers.

Another possibility is the complexation by freshly formed organic matter during the breakdowns of summer phytoplankton blooms (Dellwig et al., 2007b). This assumption is supported by the fact that particulate matter is generally enriched in Mn during summer, whereas enrichments of Mo are only observed during time periods of high bioproductivity.

Furthermore, the formation of large areas with reduced sediment surfaces (Böttcher et al., 1999) may be a temporal and local sink for Mo in sulphidic sediments (Erickson and Helz, 2000). This assumption is confirmed by data from 2002 showing significant Mo depletion ($\text{Mo}_{\text{diss.}} 29 \text{ nM}$) in the water above such a sulphidic sediment surface. Nevertheless, an unusual expansion of reduced sediment surfaces as reported by Böttcher et al. (1999) was not observed during the investigation period.

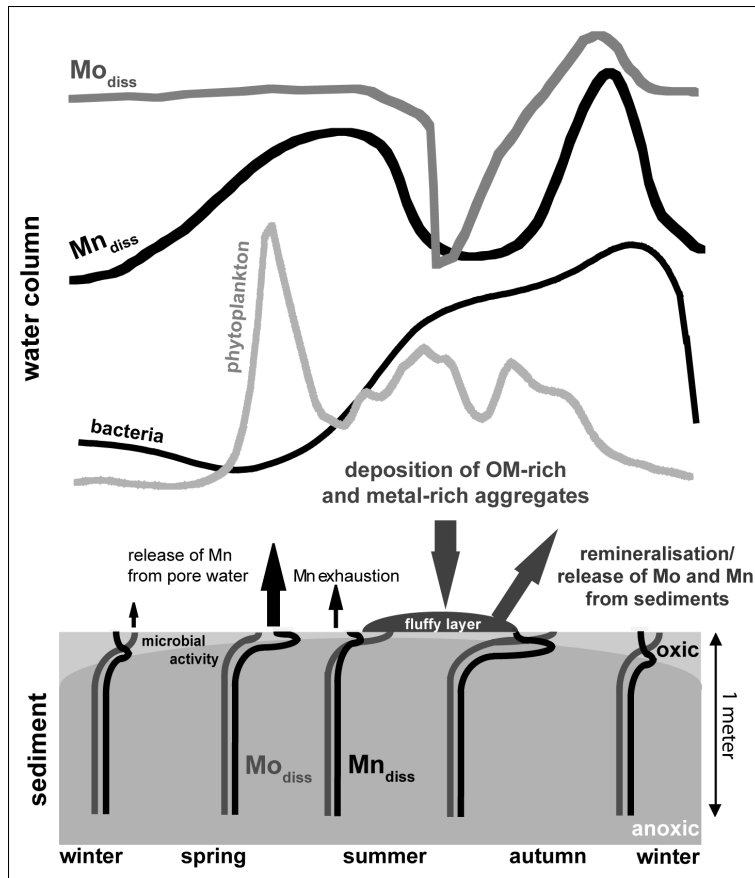


Fig. 6.11. Conceptual model (modified after Dellwig et al., 2007b) showing Mn and Mo dynamics in the water column and pore waters resulting from a pronounced benthic-pelagic coupling. Seasonal fluctuations of phytoplankton growth significantly influence the trace metal budget in the water column and shallow pore waters. Schematic water column trends and pore water profiles illustrate the seasonal variations of Mn (black lines) and Mo (dark grey lines) dynamics due to pelagic and benthic coupling. The general pore water trends are adapted to the scale of the present investigations.

The pore water generally shows Mo depletion compared to the usual seawater value (Fig. 6.8d). At depths below 50 cm Mo is effectively removed from the dissolved phase by sulphide. After the Mo depletion in the water column the Mo level increases significantly in

the uppermost pore waters from 246 nM in July 2007 to a maximum value of 440 nM in August 2007, thus exceeding the seawater level by a factor of 4. In contrast, below a sediment depth of 10 to 15 cm Mo still shows the typical depletion due to fixation in the presence of sulphide. Elevated Mo values in the pore waters may be caused by deposition and subsequent microbial mineralization of Mo-rich aggregates (Dellwig et al., 2007a). Additionally, reduction of Mn-oxides from impinged aggregates can also cause release of formerly scavenged Mo. In September 2007, the Mo concentrations in the uppermost pore waters still have a value of 204 nM (Fig. 6.8d) although sulphide is present. The finding is probably due to sulphide concentration below the switching point between the geochemical states MoO_4^{2-} and MoS_4^{2-} , which was found by Erickson & Helz (2000) to be close to 11 μM $\text{H}_2\text{S}(aq.)$. In October 2007 the Mo concentrations decrease to 104 nM reaching again the sea water value.

6.6 Conclusions

During sampling campaigns in 2002 and 2007 samples were taken from the open water column and from shallow pore waters of the back barrier tidal flats of the island of Spiekeroog (Southern North Sea). It was the aim to investigate tidal and seasonal variations of the redox-sensitive trace metals Mn, Fe, Mo, U, and V and their response to biological activity.

Water column signatures of redox-sensitive trace metals (Mo, Mn, U, and V) are significantly influenced by changes in bioproductivity. Pelagic and benthic coupling is triggered by enhanced biomass production in the open water column. Organic matter produced during algae blooms is deposited via aggregates and incorporated into the sediments. Increasing microbial activity in summer leads to significant release of DOC, metabolites, and trace metals during degradation of the aggregates. Most pronounced dynamics in the open water column are seen for Mn showing maximum values during low tide when Mn-rich pore waters drain out of the sediments. Exhaustion and replenishing periods in the surface sediments cause distinct seasonal differences of the Mn level in the water column. V behaves similar to Mn due to scavenging by freshly formed MnO_x while U shows only slight water column depletion especially in summer, most likely due to fixation in anoxic sediments.

Non-conservative behaviour of Mo in the open water column has been evidenced recurrently, after breakdown of summer algae blooms. It remains unclear whether this phenomenon is caused by scavenging of Mo by MnO_x , interactions with organic matter, and/or sedimentary uptake. However, Mo enrichments in shallow pore waters during summer indicate Mo removal from the water column and transfer into surface sediments.

This benthic-pelagic coupling of the investigated ecosystem is summarized in the conceptual model shown in Figure 6.11. The model illustrates the behaviour of Mo and Mn in the water column and upper sediments as a response to biological, geochemical and sedimentological processes. Future investigations will have to consider benthic flux measurements to elucidate the quantitative impact of different processes on benthic-pelagic coupling. The determination of exchange rates will show the importance of Wadden Sea sediments as temporal trace metal sources or sinks.

Acknowledgements

The authors would like to thank Malte Groh (Argonauta, Wildeshausen), Helmo Nicolai, and Waldemar Siewert (ICBM-Terramare, Wilhelmshaven) for their assistance during the sampling campaigns. We thank Conny Lenz and Vera Winde (IOW, Rostock) for their support during sampling and laboratory work. Furthermore, we would like to thank Thomas Badewien (University of Oldenburg) for providing salinity data of the monitoring station. This manuscript significantly benefited from comments and constructive suggestions by Tim Lyons and one anonymous reviewer. We wish to thank Jürgen Rullkötter for coordinating the research group and for editorial support.

The study is integrated in the Research Group “BioGeoChemistry of Tidal Flats” (FOR 432/2) and is funded by the Deutsche Forschungsgemeinschaft (BO 1584/4, BR 775/14-4) and Leibniz Institute for Baltic Sea Research.

7 General conclusions and perspectives

It was demonstrated that a continuous nutrient and methane analysis of surface waters on a time-series station is feasible in a highly dynamic area like the Wadden Sea of the German Bight. Autonomous direct measurements do not require sample storage or treatment such as preservation. The high frequency of determination allowed acquisition of concentration variations down to a tidal resolution, which enabled to investigate even short-term concentration characteristics. The online availability of in-situ data of the time-series station is suitable for planning of ship-based sampling campaigns focussed on questions related to the development and breakdown of plankton blooms. Additionally, these data helped to verify mathematical models describing the complex Wadden Sea system and to perform budget calculations for nutrient and methane export from this area.

Methane measurements in the Southern North Sea revealed a general super-saturation with respect to the atmospheric partial pressure. Elevated concentrations in the coastal areas decreased with distance from shore. Thus, estuaries, rivers, and tidal flats turned out to be a source for CH₄ for the German Bight. The concentration pattern of methane in the tidal flat area, determined at the time-series station, evinced a tidal periodicity with maximum values during low tide. Lower concentrations at high tide are mainly caused by degassing processes as well as dilution with methane-poor offshore waters. Estimates of methane sources showed that freshwater contributed via the flood-gate represents a minor fraction of the tidal flat budget. In contrast, pore water forms the major source for methane, generated by biogeochemical remineralisation processes in anaerobic deeper sediments. Despite the recurrent tidal forces the periodical pattern as well as the concentration level of methane in the back barrier area is heavily influenced by strong winds. Cross-correlation calculations revealed an anti-correlation of wind speed and methane concentration. Two different approaches of model based calculations showed that methane contribution of the tidal flat systems to the German Bight is in the same order of magnitude as those of major rivers. Thus, back barrier tidal areas have to be taken into account for methane budgets of marine systems.

Nutrients (silica, phosphate, nitrite, nitrate) in surface water were determined hourly from April 2006 at a time-series station. Silica concentrations were governed by assimilation by diatoms leading to low concentrations in spring and summer. Due to remineralisation of diatom frustules within the sediments accompanied by lower assimilation rates, silica concentrations increased towards autumn with highest values in winter. In contrast, phosphate is not only affected by biological dynamics, but may be trapped by ferric oxyhydroxides in oxygenated sediments, as well. When sediments become anoxic, phosphate is desorbed from

ferric oxyhydroxides and released into the open water column, leading to highest phosphate concentrations in late summer. Nitrite plus nitrate concentrations are highest in winter months, mainly controlled by river discharge.

Nutrient patterns at a tidal resolution revealed a different behaviour for silica, phosphate, and nitrite plus nitrate. Silica revealed a consistent relation to the tidal state with higher concentrations at low tide throughout the year. However, the tidally driven pattern of phosphate is most pronounced in summer. For nitrite plus nitrate a distinct tidal pattern could be observed in autumn, while the remaining seasons reveal a slight or even no coupling to the tide.

Model simulations by an ecological tidal model (EcoTiM) emphasised that freshwater contribution is negligible for the nutrient budget, whereas pore waters form the main source of nutrients in the tidal flat area. Modelling furthermore indicated that dissolved inorganic nutrients are exported from the tidal flat area in an order of magnitude like the sum of the German rivers Elbe, Weser, and Ems. Thus, tidal flat areas play a major role in supplying nutrients to the German Bight and have to be considered in budget calculations besides riverine nutrient discharge.

Investigations of biogeochemical processes in pore waters down to 5 m sediment depth identified sulphate reduction as the most important pathway for anaerobic organic matter remineralisation. Concentrations of sulphate, ammonium, and phosphate in pore waters have been used to elucidate the composition of organic matter degraded in the sediment. The calculated C:N and C:P ratios were below the Redfield ratio. Preferential hydrolysis of particulate organic nitrogen relative to particulate organic carbon could explain the low C:N ratios of about 3.

Due to the hydraulic gradient generated at tidal flat margins during low tide, pore waters rich in remineralisation products are transported advectively towards the tidal flat margin. These findings support the aforementioned conclusion that pore waters account for the increase in sea water nutrient and methane concentration during low tide.

Sampling campaigns in 2002 and 2007 showed that water column signatures of redox-sensitive trace metals (Mo, Mn, U, V) are significantly influenced by changes in bioproductivity. Most pronounced dynamics in the open water column were identified for Mn with maximum concentrations during low tide, due to contribution of Mn-rich pore waters. Seasonal differences of the Mn level in the water column are caused by exhaustion and replenishing periods in the surface sediments. The pattern of V was similar to Mn, due to scavenging by freshly formed MnO_x. In contrast, U shows only slight water column depletion especially in summer, most likely due to fixation in anoxic sediments.

A recurrent non-conservative behaviour of the redox-sensitive trace metal Mo in the open water column has been evidenced after breakdown of summer algae blooms. However, it remains unclear whether this phenomenon is caused by scavenging of Mo by MnO_x , interactions with organic matter, and/or sedimentary uptake. Nevertheless, Mo enrichments in shallow pore waters during summer indicate Mo removal from the water column and transfer into surface sediments.

Perspectives

Besides the application for monitoring of processes in coastal waters, long-time data are needed in a high resolution to review the applicability of mathematical models for the study area. The results of model simulations in the studies emphasised the necessity of an additional sampling site in the coastal area beyond the islands, since these boundary conditions are an essential parameter for mathematical modelling, as they have a major impact on exchange processes of the tidal flat areas with the North Sea. Thus, it could be recommended to install a time-series station at the 10 m water depth line beyond the island of Langeoog to determine continuously physical, meteorological, biological, and chemical parameters in water masses entering the back barrier area. Hence, the results of model simulations in order to tidal and seasonal dynamics as well as budget estimations can be improved. It has to be considered, whether a permanent time-series station or whether a displaceable buoy, which provides the opportunity to change the position dependent upon the prevailing task, turns out to be the feasible instrument.

Additionally, further investigations will have to consider benthic fluxes to elucidate the quantitative impact of biogeochemical as well as physical processes on benthic-pelagic coupling. The determination of sediment/water exchange rates will ascertain the importance of Wadden Sea sediments as temporal sources or sinks for trace metals, nutrients, and further contributors to biogeochemical transformation processes.

It could have been demonstrated, that continuous measurements are essential for determination of processes occurring in tidal flat areas, since weekly or monthly sampling intervals do not comprise the high dynamics in this area. Only if aforementioned information is available, mathematical models can highly be improved and thereby act as a useful tool to predict the response of tidal flat areas on climate change aftermath like sea level rise and increasing temperatures.

8 References

- Al-Raei, A., Bosselmann, K., Böttcher, M., Hespeneide, B., and Tauber, F., 2009. Seasonal dynamics of microbial sulfate reduction in temperate intertidal surface sediments: controls by temperature and organic matter. *Ocean Dynamics* 59, 351-370.
- Algeo, T.J., and Lyons, T.W., 2006. Mo-total organic carbon covariation in modern anoxic marine environments: Implications for analysis of paleoredox and paleohydrographic conditions. *Paleoceanography* 21,
- Alperin, M.J., Albert, D.B., and Martens, C.S., 1994. Seasonal variations in production and consumption rates of dissolved organic carbon in an organic-rich coastal sediment. *Geochimica et Cosmochimica Acta* 58, 4909-4930.
- Anbar, A.D., and Holland, H.D., 1992. The photochemistry of manganese and the origin of banded iron formations. *Geochimica et Cosmochimica Acta* 56, 2595-2603.
- Antia, N.J., McAllister, C.D., Parsons, T.R., Stephens, K., and Strickland, J.D.H., 1963. Further measurements of primary production using a large-volume plastic sphere. *Limnology and Oceanography* 8, 166-183.
- Arakawa, A., and Lamb, V.R., 1977. Computational design of the basic dynamical processes of the UCLA general circulation model. *Methods in Computational Physics* 17, 173-265.
- Atkinson, M.J., and Smith, S.V., 1983. C:N:P ratios of benthic marine plants. *Limnology and Oceanography* 28, 568-574.
- Baldock, J.A., Masiello, C.A., Gelinas, Y., and Hedges, J.I., 2004. Cycling and composition of organic matter in terrestrial and marine ecosystems. *Marine Chemistry* 92, 39-64.
- Balistrieri, L., Brewer, P.G., and Murray, J.W., 1981. Scavenging residence times of trace metals and surface chemistry of sinking particles in the deep ocean. *Deep-Sea Research Part a-Oceanographic Research Papers* 28, 101-121.
- Bange, H.W., Bartell, U.H., Rapsomanikis, S., and Andreae, M.O., 1994. Methane in the Baltic and North Seas and a Reassessment of the Marine Emissions of Methane. *Global Biogeochemical Cycles* 8, 465-480.
- Bange, H.W., 2006. Nitrous oxide and methane in European coastal waters. *Estuarine, Coastal and Shelf Science* 70, 361-374.
- Baretta-Bekker, J.G., and Baretta, J.W. (Eds), 1997. Special issue: European regional seas ecosystem model II

- Barling, J., and Anbar, A.D., 2004. Molybdenum isotope fractionation during adsorption by manganese oxides. *Earth and Planetary Science Letters* 217, 315-329.
- Barnes, J., and Owens, N.J.P., 1998. Denitrification and nitrous oxide concentrations in the Humber estuary, UK, and adjacent coastal zones. *Marine Pollution Bulletin* 37, 247-260.
- Bartlett, K.B., Crill, P.M., Sass, R.L., Harriss, R.C., and Dise, N.B., 1992. Methane Emissions from Tundra Environments in the Yukon-Kuskokwim Delta, Alaska. *Journal of Geophysical Research-Atmospheres* 97, 16645-16660.
- Beare, D.J., Batten, S., Edwards, M., and Reid, D.G., 2002. Prevalence of boreal Atlantic, temperate Atlantic and neritic zooplankton in the North Sea between 1958 and 1998 in relation to temperature, salinity, stratification intensity and Atlantic inflow. *Journal of Sea Research* 48, 29-49.
- Beck, M., Dellwig, O., Kolditz, K., Freund, H., Liebezeit, G., Schnetger, B., and Brumsack, H.J., 2007. In situ pore water sampling in deep intertidal flat sediments. *Limnology and Oceanography-Methods* 5, 136-144.
- Beck, M., Dellwig, L., Schnetger, B., and Brumsack, H.J., 2008a. Cycling of trace metals (Mn, Fe, Mo, U, V, Cr) in deep pore waters of intertidal flat sediments. *Geochimica et Cosmochimica Acta* 72, 2822-2840.
- Beck, M., Dellwig, O., Holstein, J.M., Grunwald, M., Liebezeit, G., Schnetger, B., and Brumsack, H.J., 2008b. Sulphate, dissolved organic carbon, nutrients and terminal metabolic products in deep pore waters of an intertidal flat. *Biogeochemistry* 89, 221-238.
- Beck, M., Dellwig, O., Liebezeit, G., Schnetger, B., and Brumsack, H.J., 2008c. Spatial and seasonal variations of sulphate, dissolved organic carbon, and nutrients in deep pore waters of intertidal flat sediments. *Estuarine Coastal and Shelf Science* 79, 307-316.
- Becker, G.A., 1990. Die Nordsee als physikalisches System. In: Lozán J.L., Lenz W., Rachor E., Watermann B., and von Westernhagen H. (Eds), *Warnsignale aus der Nordsee*. Verlag Paul Parey, Berlin; Hamburg, p 11-27.
- Behrends, B., and Liebezeit, G., 1999. Particulate amino acids in Wadden Sea waters -- seasonal and tidal variations. *Journal of Sea Research* 41, 141-148.
- Bendschneider, K., and Robinson, R.J., 1952. A New Spectrophotometric Method for the Determination of Nitrite in Sea Water. *Journal of Marine Research* 11, 87-96.
- Bergamaschi, B.A., Tsamakis, E., Keil, R.G., Eglinton, T.I., Montlucon, D.B., and Hedges, J.I., 1997. The effect of grain size and surface area on organic matter, lignin and

- carbohydrate concentration, and molecular compositions in Peru Margin sediments. *Geochimica et Cosmochimica Acta* 61, 1247-1260.
- Berner, R.A., 1973. Phosphate removal from sea water by adsorption on volcanogenic ferric oxides. *Earth and Planetary Science Letters* 18, 77-86.
- Berner, R.A., 1984. Sedimentary pyrite formation: An update. *Geochimica et Cosmochimica Acta* 48, 605-615.
- Berrang, P.G., and Grill, E.V., 1974. The Effect of Manganese Oxide scavenging on Molybdenum in Saanich Inlet, British Columbia. *Marine Chemistry* 2, 125-148.
- Bhaskar, P.V., Grossart, H.P., Bhosle, N.B., and Simon, M., 2005. Production of macroaggregates from dissolved exopolymeric substances (EPS) of bacterial and diatom origin. *Fems Microbiology Ecology* 53, 255-264.
- Bianchi, M., Marty, D., Teyssie, J.L., and Fowler, S.W., 1992. Strictly Aerobic and Anaerobic-Bacteria Associated with Sinking Particulate Matter and Zooplankton Fecal Pellets. *Marine Ecology-Progress Series* 88, 55-60.
- Billerbeck, M., Werner, U., Polerecky, L., Walpersdorf, E., deBeer, D., and Huettel, M., 2006a. Surficial and deep pore water circulation governs spatial and temporal scales of nutrient recycling in intertidal sand flat sediment. *Marine Ecology-Progress Series* 326, 61-76.
- Billerbeck, M., Werner, U., Bosselmann, K., Walpersdorf, E., and Huettel, M., 2006b. Nutrient release from an exposed intertidal sand flat. *Marine Ecology-Progress Series* 316, 35-51.
- Billerbeck, M., Røy, H., Bosselmann, K., and Huettel, M., 2007. Benthic photosynthesis in submerged Wadden Sea intertidal flats. *Estuarine, Coastal and Shelf Science* 71, 704-716.
- Blackford, J.C., 2002. The influence of microphytobenthos on the northern Adriatic ecosystem: A modelling study. *Estuarine Coastal and Shelf Science* 55, 109-123.
- Boetius, A., Ravenschlag, K., Schubert, C.J., Rickert, D., Widdel, F., Gieseke, A., Amann, R., Jørgensen, B.B., Witte, U., and Pfannkuche, O., 2000. A marine microbial consortium apparently mediating anaerobic oxidation of methane. *Nature* 407, 623-626.
- Böhnecke, G., 1922. Salzgehalt und Strömungen in der Nordsee. Humboldt-Universität, Berlin.
- Bosselmann, K., Böttcher, M.E., Billerbeck, M., Walpersdorf, E., Theune, A., de Beer, D., Huettel, M., Brumsack, H.-J., and Jørgensen, B.B., 2003. Iron-sulfur-manganese dynamics in intertidal surface sediments of the North Sea. *Forschungszentrum Terramare - Berichte* 12, 32-35.

- Böttcher, M.E., Rusch, A., Höpner, T., and Brumsack, H.J., 1997. Stable sulfur isotope effects related to local intense sulfate reduction in a tidal sandflat (southern North Sea): Results from loading experiments. *Isotopes in Environmental and Health Studies* 33, 109-129.
- Böttcher, M.E., Oelschlager, B., Höpner, T., Brumsack, H.J., and Rullkötter, J., 1998. Sulfate reduction related to the early diagenetic degradation of organic matter and "black spot" formation in tidal sandflats of the German Wadden Sea (southern North Sea): stable isotope ($C-13$, $S-34$, $O-18$) and other geochemical results. *Organic Geochemistry* 29, 1517-1530.
- Böttcher, M.E., Oelschlager, B., Höpner, T., Brumsack, H.J., and Rullkötter, J., 1999. Isotopendiskriminierung ($^{34}S/^{32}S$, $^{13}C/^{12}C$) im Zusammenhang mit dem Auftreten großflächiger anoxischer Sedimentoberflächen im Rückseitenwatt der Insel Baltrum (südliche Nordsee). *Zeitschriftenblatt für Geologie und Päläontologie Teil 1*, 1063-1075.
- Böttcher, M.E., Hespeneide, B., Llobet-Brossa, E., Beardsley, C., Larsen, O., Schramm, A., Wieland, A., Böttcher, G., Berninger, U.G., and Amann, R., 2000. The biogeochemistry, stable isotope geochemistry, and microbial community structure of a temperate intertidal mudflat: an integrated study. *Continental Shelf Research* 20, 1749-1769.
- Böttcher, M.E., 2003. Schwarze Flecken und Flächen im Wattenmeer. In: Lozán J.L., Rachor E., Reise K., Sündermann J., and von Westernhagen H. (Eds), *Warnsignale aus der Nordsee & Wattenmeer – Eine aktuelle Umweltbilanz*. Blackwell-Verlag, Berlin, p 193-195.
- Böttcher, M.E., Hespeneide, B., Brumsack, H.-J., and Bosselmann, K., 2004. Stable isotope biogeochemistry of the sulfur cycle in modern marine sediments: I. Seasonal dynamics in a temperate intertidal sandy surface sediment. *Isotopes in Environmental and Health Studies* 40, 267-283.
- Boudreau, B.P., 1992. A kinetic model for microbial organic-matter decomposition in marine sediments. *Fems Microbiology Ecology* 102, 1-14.
- Boudreau, B.P., 1997. *Diagenetic models and their implications*. Springer, Berlin.
- Brasse, S., Reimer, A., Seifert, R., and Michaelis, W., 1999. The influence of intertidal mudflats on the dissolved inorganic carbon and total alkalinity distribution in the German Bight, southeastern North Sea. *Journal of Sea Research* 42, 93-103.
- Brockmann, U.H., Laane, R.W.P.M., and Postma, J., 1990. Cycling of nutrient elements in the North Sea. *Netherlands Journal of Sea Research* 26, 239-264.

- Broecker, H.C., Petermann, J., and Siems, W., 1978. Influence of Wind on Co₂-Exchange in a Wind-Wave Tunnel, Including Effects of Monolayers. *Journal of Marine Research* 36, 595-610.
- Broecker, H.C., and Siems, W., 1984. The role of bubbles for gas transfer from water to air at higher windspeeds: Experiments in the wind-wave facility in Hamburg. In: Brutsaert W., and Jirka G.H. (Eds), *Gas Transfer at Water Surfaces*. Reidel, D., Hingham, Mass., p 229-238.
- Broecker, W.S., and Peng, T.H., 1982. *Tracers in the Sea*. Eldigio Press, Lamont-Doherty Geological Observatory, Palisades, N.Y.
- Bruland, K.W., Knauer, G.A., and Martin, J.H., 1978a. Cadmium in northeast Pacific waters. *Limnology and Oceanography* 23, 618-625.
- Bruland, K.W., Knauer, G.A., and Martin, J.H., 1978b. Zinc in north-east Pacific water. *Nature* 271, 741-743.
- Bruland, K.W., 1983. Trace elements in seawater. *Chemical Oceanography* 8, 157-220.
- Bruland, K.W., Rue, E.L., Smith, G.J., and DiTullio, G.R., 2005. Iron, macronutrients and diatom blooms in the Peru upwelling regime: brown and blue waters of Peru. *Marine Chemistry* 93, 81-103.
- Brumsack, H.J., and Gieskes, J.M., 1983. Interstitial water trace-metal chemistry of laminated sediments from the Gulf of California, Mexico. *Marine Chemistry* 14, 89-106.
- Bugna, G.C., Chanton, J.P., Cable, J.E., Burnett, W.C., and Cable, P.H., 1996. The importance of groundwater discharge to the methane budgets of nearshore and continental shelf waters of the northeastern Gulf of Mexico. *Geochimica et Cosmochimica Acta* 60, 4735-4746.
- Burdige, D.J., and Nealson, K.H., 1985. Microbial manganese reduction by enrichment cultures from coastal marine sediments. *Applied and Environmental Microbiology* 50, 491-497.
- Burdige, D.J., 1993. The Biogeochemistry of Manganese and Iron Reduction in Marine-Sediments. *Earth-Science Reviews* 35, 249-284.
- Cadée, G.C., 1996. Accumulation and sedimentation of *Phaeocystis globosa* in the Dutch Wadden Sea. *Journal of Sea Research* 36, 321-327.
- Caetano, M., Falcao, M., Vale, C., and Bebianno, M.J., 1997. Tidal flushing of ammonium, iron and manganese from inter-tidal sediment pore waters. *Marine Chemistry* 58, 203-211.

- Callender, E., and Bowser, C.J., 1980. Manganese and copper geochemistry of interstitial fluids from manganese nodule-rich pelagic sediments of the Northeastern Equatorial Pacific-Ocean. *American Journal of Science* 280, 1063-1096.
- Cameron, T.D.J., Stoker, M.S., and Long, D., 1987. The history of Quaternary sedimentation in the UK sector of the North Sea Basin. *Journal of the Geological Society* 144, 43-58.
- Cammen, L.M., 1991. Annual Bacterial Production in Relation to Benthic Microalgal Production and Sediment Oxygen-Uptake in an Intertidal Sandflat and an Intertidal Mudflat. *Marine Ecology-Progress Series* 71, 13-25.
- Canfield, D.E., 1989. Reactive iron in marine sediments. *Geochimica et Cosmochimica Acta* 53, 619-632.
- Canfield, D.E., Raiswell, R., and Bottrell, S., 1992. The reactivity of sedimentary iron minerals toward sulfide. *American Journal of Science* 292, 659-683.
- Canfield, D.E., Thamdrup, B., and Hansen, J.W., 1993a. The anaerobic degradation of organic matter in Danish coastal sediments: Iron reduction, manganese reduction, and sulphate reduction. *Geochimica et Cosmochimica Acta* 57, 3867-3883.
- Canfield, D.E., Jørgensen, B.B., Fossing, H., Glud, R., Gundersen, J., Ramsing, N.B., Thamdrup, B., Hansen, J.W., Nielsen, L.P., and Hall, P.O.J., 1993b. Pathways of organic carbon oxidation in three continental margin sediments. *Marine Geology* 113, 27-40.
- Caperon, J., Schell, D., Hirota, J., and Laws, E., 1979. Ammonium excretion rates in Kaneohe Bay, Hawaii, measured by a ¹⁵N isotope dilution technique. *Marine Biology* 54, 33-40.
- Chang, T.S., Joerdel, O., Flemming, B.W., and Bartholomä, A., 2006a. The role of particle aggregation/disaggregation in muddy sediment dynamics and seasonal sediment turnover in a back-barrier tidal basin, East Frisian Wadden Sea, southern North Sea. *Marine Geology* 235, 49-61.
- Chang, T.S., Bartholomä, A., and Flemming, B.W., 2006b. Seasonal dynamics of fine-grained sediments in a back-barrier tidal basin of the German Wadden Sea (Southern North Sea). *Journal of Coastal Research* 22, 328-338.
- Chang, T.S., Flemming, B.W., Tilch, E., Bartholomä, A., and Wöstmann, R., 2006c. Late Holocene stratigraphic evolution of a back-barrier tidal basin in the East Frisian Wadden Sea, southern North Sea: transgressive deposition and its preservation potential. *Facies* 52, 329-340.
- Charette, M.A., and Sholkovitz, E.R., 2006. Trace element cycling in a subterranean estuary: Part 2. Geochemistry of the pore water. *Geochimica et Cosmochimica Acta* 70, 811-826.

- Chen, M.S., Wartel, S., and Temmerman, S., 2005. Seasonal variation of flocculation characteristics on tidal flats, the Scheldt estuary. *Hydrobiologia* 540, 181-195.
- Cheng, T., Hammond, D.E., Berelson, W.M., Hering, J.G., and Dixit, S., 2009. Dissolution kinetics of biogenic silica collected from the water column and sediments of three Southern California borderland basins. *Marine Chemistry* 113, 41-49.
- Cheshire, M.V., Berrow, M.L., Goodman, B.A., and Mundie, C.M., 1977. Metal distribution and nature of some Cu, Mn and V complexes in humic and fulvic acid fractions of soil organic matter. *Geochimica et Cosmochimica Acta* 41, 1131-1138.
- Chow, D.T.W., and Robinson, R.J., 1953. Forms of silicate available for colorimetric determination. *Analytical Chemistry* 25, 646-648.
- Christensen, J.P., 1994. Carbon export from continental shelves, denitrification and atmospheric carbon dioxide. *Continental Shelf Research* 14, 547-576.
- Christiansen, C., Volund, G., Lund-Hansen, L.C., and Bartholdy, J., 2006. Wind influence on tidal flat sediment dynamics: Field investigations in the Ho Bugt, Danish Wadden Sea. *Marine Geology* 235, 75-86.
- Cicerone, R.J., and Oremland, R.S., 1988. Biogeochemical aspects of atmospheric methane. *Global Biogeochemical Cycles* 2, 299-327.
- Cline, J.D., 1969. Spectrophotometric determination of hydrogen sulfide in natural waters. *Limnology and Oceanography* 14, 454-458.
- Cochran, J.K., Carey, A.E., Sholkovitz, E.R., and Surprenant, L.D., 1986. The Geochemistry of Uranium and Thorium in Coastal Marine-Sediments and Sediment Pore Waters. *Geochimica et Cosmochimica Acta* 50, 663-680.
- Cole, J.J., Howarth, R.W., Nolan, S.S., and Marino, R., 1986. Sulfate Inhibition of Molybdate Assimilation by Planktonic Algae and Bacteria - Some Implications for the Aquatic Nitrogen-Cycle. *Biogeochemistry* 2, 179-196.
- Cole, J.J., Lane, J.M., Marino, R., and Howarth, R.W., 1993. Molybdenum Assimilation by Cyanobacteria and Phytoplankton in Fresh-Water and Salt-Water. *Limnology and Oceanography* 38, 25-35.
- Colijn, F., 1982. Light absorption in the waters of the Ems-Dollard estuary and its consequences for the growth of phytoplankton and microphytobenthos. *Netherlands Journal of Sea Research* 15, 196-216.
- Colijn, F., and de Jonge, V.N., 1984. Primary Production of Microphytobenthos in the Ems-Dollard Estuary. *Marine Ecology-Progress Series* 14, 185-196.
- Colijn, F., and Cadée, G.C., 2003. Is phytoplankton growth in the Wadden Sea light or nitrogen limited? *Journal of Sea Research* 49, 83-93.

- Colijn, F., and van Beusekom, J.E.E., 2004. Effect of eutrophication on phytoplankton productivity and growth in the Wadden Sea. In: Wilson J.G. (Ed), *The Intertidal Ecosystem: The Value of Ireland's Shores*. Royal Irish Academy, Dublin, p 58–68.
- Collier, R.W., 1985. Molybdenum in the Northeast Pacific-Ocean. *Limnology and Oceanography* 30, 1351-1354.
- Craig, H., 1974. Scavenging model for trace-elements in deep sea. *Earth and Planetary Science Letters* 23, 149-159.
- Crutzen, P.J., and Zimmermann, P.H., 1991. The Changing Photochemistry of the Troposphere. *Tellus Series a-Dynamic Meteorology and Oceanography* 43, 136-151.
- D'Andrea, A.F., Aller, R.C., and Lopez, G.R., 2002. Organic matter flux and reactivity on a South Carolina sandflat: The impacts of porewater advection and macrobiological structures. *Limnology and Oceanography* 47, 1056-1070.
- Dando, P.R., Austen, M.C., Burke, R.A., Kendall, M.A., Kennicutt, M.C., Judd, A.G., Moore, D.C., Ohara, S.C.M., Schmaljohann, R., and Southward, A.J., 1991. Ecology of a North-Sea Pockmark with an Active Methane Seep. *Marine Ecology-Progress Series* 70, 49-63.
- de Beer, D., Wenzhofer, F., Ferdelman, T.G., Boehme, S.E., Huettel, M., van Beusekom, J.E.E., Böttcher, M.E., Musat, N., and Dubilier, N., 2005. Transport and mineralization rates in North Sea sandy intertidal sediments, Sylt-Romo Basin, Wadden Sea. *Limnology and Oceanography* 50, 113-127.
- de Jonge, V.N., and Postma, H., 1974. Phosphorus compounds in the Dutch wadden sea. *Netherlands Journal of Sea Research* 8, 139-153.
- de Jonge, V.N., Essink, K., and Boddeke, R., 1993. The Dutch Wadden Sea - a changed ecosystem. *Hydrobiologia* 265, 45-71.
- de Jonge, V.N., and Colijn, F., 1994. Dynamics of Microphytobenthos Biomass in the Ems Estuary. *Marine Ecology-Progress Series* 104, 185-196.
- de Angelis, M.A., and Lilley, M.D., 1987. Methane in Surface Waters of Oregon Estuaries and Rivers. *Limnology and Oceanography* 32, 716-722.
- de Angelis, M.A., and Scranton, M.I., 1993. Fate of Methane in the Hudson River and Estuary. *Global Biogeochemical Cycles* 7, 509-523.
- de Angelis, M.A., and Lee, C., 1994. Methane Production During Zooplankton Grazing on Marine-Phytoplankton. *Limnology and Oceanography* 39, 1298-1308.
- Delafontaine, M.T., Bartholomä, A., Flemming, B.W., and Kurmis, R., 1996. Volume-specific dry POC mass in surficial intertidal sediments: a comparison between biogenic muds and adjacent sand flats. *Senckenbergiana maritima* 26, 167-178.

- Dellwig, O., Hinrichs, J., Hild, A., and Brumsack, H.J., 2000. Changing sedimentation in tidal flat sediments of the southern North Sea from the Holocene to the present: a geochemical approach. *Journal of Sea Research* 44, 195-208.
- Dellwig, O., Böttcher, M.E., Lipinski, M., and Brumsack, H.J., 2002. Trace metals in Holocene coastal peats and their relation to pyrite formation (NW Germany). *Chemical Geology* 182, 423-442.
- Dellwig, O., Bosselmann, K., Kölsch, S., Hentscher, M., Hinrichs, J., Böttcher, M.E., Reuter, R., and Brumsack, H.J., 2007a. Sources and fate of manganese in a tidal basin of the German Wadden Sea. *Journal of Sea Research* 57, 1-18.
- Dellwig, O., Beck, M., Lemke, A., Lunau, M., Kolditz, K., Schnetger, B., and Brumsack, H.J., 2007b. Non-conservative behaviour of molybdenum in coastal waters: Coupling geochemical, biological, and sedimentological processes. *Geochimica et Cosmochimica Acta* 71, 2745-2761.
- Dick, S., Brockmann, U., van Beusekom, J., Fabiszisky, B., George, M., Hentschke, U., Hesse, K., Mayer, B., Nitz, T., Pohlmann, T., Poremba, K., Schaumann, K., Schönfeld, W., Starke, A., Tillmann, U., and Weide, G., 1999. Exchange of matter and energy between the Wadden Sea and the coastal waters of the German Bight- Estimations based on numerical simulations and field measurements. *Ocean Dynamics* 51, 181-219.
- Dippner, J.W., 1984. Ein Strömungs- und Öldrifftmodell für die Deutsche Bucht. *Veröffentlichungen des Instituts für Meeresforschung in Bremerhaven Supplement* 8, 193.
- Dortch, Q., 1982. Effect of growth conditions on accumulation of internal nitrate, ammonium, amino acids, and protein in three marine diatoms. *Journal of Experimental Marine Biology and Ecology* 61, 243-264.
- Duwe, K.C., and Hewer, R.R., 1982. Ein semiimplizites Gezeitenmodell für Wattgebiete. *Deutsche hydrographische Zeitschrift* 35, 223-238.
- Ebenhöh, W., Kohlmeier, C., and Radford, P.J., 1995. The benthic biological submodel in the European regional seas ecosystem model. *Netherlands Journal of Sea Research* 33, 423-452.
- Ebenhöh, W., Hamberg, F., and Kohlmeier, C., 1996. The benthic nutrient module. In: Radford P. (Ed), *The Modules of the European Regional Seas Ecosystem Model II* 1993-1996

- Ebenhöh, W., Kohlmeier, C., Baretta, J.W., and Flöser, G., 2004. Shallowness may be a major factor generating nutrient gradients in the Wadden Sea. *Ecological Modelling* 174, 241-252.
- Egge, J.K., and Aksnes, D.L., 1992. Silicate as Regulating Nutrient in Phytoplankton Competition. *Marine Ecology-Progress Series* 83, 281-289.
- Egge, J.K., 1998. Are diatoms poor competitors at low phosphate concentrations? *Journal of Marine Systems* 16, 191-198.
- Ehhalt, D., Prather, M., Dentener, F., Derwent, R., Dlugokencky, E., Holland, E., Isaksen, I., Katima, J., Kirchhoff, V., Matson, P., Midgley, P., and Wang, M., 2001. Atmospheric Chemistry and Greenhouse Gases. In: Houghton J.T., Ding Y., Griggs D.J., Noguer M., Linden P.J.v.d., Dai X., Maskell K., and Johnson C.A. (Eds), *Climate Change 2001: The Scientific Basis Contribution of Working Group I to the Third Assessment Report of the Intergovernmental Panel on Climate Change* Cambridge University Press, Cambridge, United Kingdom and New York, NY, USA, p 241-287.
- Ehlers, J., 1994. Geomorphologie und Hydrologie des Wattenmeeres. In: Lozan J.L., Rachor E., Von Westernhagen H., and Lenz W. (Eds), *Warnsignale aus dem Wattenmeer*. Blackwell Wissenschaftsverlag, Berlin, p 1-11.
- Ehrenhauss, S., Witte, U., Janssen, F., and Huettel, M., 2004. Decomposition of diatoms and nutrient dynamics in permeable North Sea sediments. *Continental Shelf Research* 24, 721-737.
- Einsele, W., 1938. Über chemische und kolloidchemische Vorgänge in Eisen-Phosphat-Systemen unter limnochemischen und limnogeologischen Gesichtspunkten. *Archiv für Hydrobiologie* 33, 361-387.
- Emerson, S., Kalthorn, S., Jacobs, L., Tebo, B.M., Nealson, K.H., and Rosson, R.A., 1982. Environmental oxidation rate of manganese(II): bacterial catalysis. *Geochimica et Cosmochimica Acta* 46, 1073-1079.
- Engel, H., 1995. Die Hydrologie der Weser. In: Gerken B., and Schirmer M. (Eds), *Limnologie aktuell, Vol 6 Die Weser*. Gustav Fischer Verlag, Stuttgart, p 3-14.
- Erickson, B.E., and Helz, G.R., 2000. Molybdenum(VI) speciation in sulfidic waters: Stability and lability of thiomolybdates. *Geochimica et Cosmochimica Acta* 64, 1149-1158.
- Essink, K., Dettmann, C., Farke, H., Laursen, K., Luerßen, G., Marencic, H., and Wiersinga, W. (Eds), 2005. *Wadden Sea Quality Status Report 2004*. Wadden Sea Ecosystem No. 19. Trilateral Monitoring and Assessment Group. Common Wadden Sea Secretariat, Wilhelmshaven, Germany,

- Feely, R.A., Massoth, G.J., Paulson, A.J., and Gendron, J.F., 1983. Possible evidence for enrichment of trace-elements in the hydrous manganese oxide phases of suspended matter from an urbanized embayment. *Estuarine Coastal and Shelf Science* 17, 693-708.
- FGG-Weser, 2008. Flussgebietsgemeinschaft Weser. Available from <http://www.fgg-weser.de>, Hildesheim
- Flemming, B., and Ziegler, K., 1995. High resolution grain size distribution patterns and textural trends in the back barrier environment of Spiekeroog Island (Southern North Sea). *Senckenbergiana maritima* 26, 1-24.
- Flemming, B.W., and Davis, J., R. A., 1994. Holocene evolution, morphodynamics and sedimentology of the Spiekeroog Barrier island system (southern North Sea). *Senckenbergiana maritima* 24, 117-155.
- Flemming, B.W., and Nyandwi, N., 1994. Land reclamation as a cause of fine-grained sediment depletion in back barrier tidal flats (southern North Sea). *Netherlands Journal of Aquatic Ecology* 28, 299-307.
- Fong, P., Donohoe, R.M., and Zedler, J.B., 1993. Competition with Macroalgae and Benthic Cyanobacterial Mats Limits Phytoplankton Abundance in Experimental Microcosms. *Marine Ecology-Progress Series* 100, 97-102.
- Forster, P., Ramaswamy, V., Artaxo, P., Berntsen, T., Betts, R., Fahey, D.W., Haywood, J., Lean, J., Lowe, D.C., Myhre, G., Nganga, J., R. Prinn, Raga, G., Schulz, M., and Dorland, R.V., 2007. Changes in Atmospheric Constituents and in Radiative Forcing. In: Solomon S., Qin D., Manning M., Chen Z., Marquis M., Averyt K.B., M.Tignor, and Miller H.L. (Eds), *Climate Change 2007: The Physical Science Basis Contribution of Working Group I to the Fourth Assessment Report of the Intergovernmental Panel on Climate Change*. Cambridge University Press, Cambridge, United Kingdom and New York, NY, USA
- Franke, U., Polerecky, L., Precht, E., and Huettel, M., 2006. Wave tank study of particulate organic matter degradation in permeable sediments. *Limnology and Oceanography* 51, 1084-1096.
- Froelich, P.N., Klinkhammer, G.P., Bender, M.L., Luedtke, N.A., Heath, G.R., Cullen, D., Dauphin, P., Hammond, D., Hartman, B., and Maynard, V., 1979. Early oxidation of organic matter in pelagic sediments of the eastern equatorial Atlantic: suboxic diagenesis. *Geochimica et Cosmochimica Acta* 43, 1075-1090.

- Fung, I., John, J., Lerner, J., Matthews, E., Prather, M., Steele, L.P., and Fraser, P.J., 1991. 3-Dimensional Model Synthesis of the Global Methane Cycle. *Journal of Geophysical Research-Atmospheres* 96, 13033-13065.
- Garcia, M.L., and Masson, M., 2004. Environmental and geologic application of solid-state methane sensors. *Environmental Geology* 46, 1059-1063.
- Gittel, A., Mußmann, M., Sass, H., Cypionka, H., and Könneke, M., 2008. Identity and abundance of active sulfate-reducing bacteria in deep tidal flat sediments determined by directed cultivation and CARD-FISH analysis. *Environmental Microbiology* 10, 2645-2658.
- Glibert, P.M., 1982. Regional studies of daily, seasonal and size fraction variability in ammonium remineralisation. *Marine Biology* 70, 209-222.
- Goldberg, E.D., 1954. Marine geochemistry I. Chemical scavengers of the sea. *Journal of Geology* 62, 249-265.
- Goldman, J.C., Dennett, M.R., and Frew, N.M., 1988. Surfactant Effects on Air Sea Gas-Exchange under Turbulent Conditions. *Deep-Sea Research Part a-Oceanographic Research Papers* 35, 1953-1970.
- Grant, B.R., 1971. Variation in silicate concentration at Port Hacking station, Sydney, in relation to phytoplankton growth. *Australian Journal of Marine and Freshwater Research* 22, 49-&.
- Grasshoff, K., Kremling, K., Ehrhardt, M., 1999. *Methods of Seawater Analysis*. 3rd Edition. Wiley - VCH, Weinheim, New York, Chichester, Brisbane, Singapore, Toronto.
- Gribsholt, B., and Kristensen, E., 2003. Benthic metabolism and sulfur cycling along an inundation gradient in a tidal *Spartina anglica* salt marsh. *Limnology and Oceanography* 48, 2151-2162.
- Grossart, H.P., Brinkhoff, T., Martens, T., Duerselen, C., Liebezeit, G., and Simon, M., 2004. Tidal dynamics of dissolved and particulate matter and bacteria in a tidal flat ecosystem in spring and fall. *Limnology and Oceanography* 49, 2212-2222.
- Grunwald, M., Dellwig, O., Liebezeit, G., Schnetger, B., Reuter, R., and Brumsack, H.-J., 2007. A novel time-series station in the Wadden Sea (NW Germany): First results on continuous nutrient and methane measurements. *Marine Chemistry* 107, 411-421.
- Grunwald, M., Dellwig, O., Beck, M., Dippner, J.W., Freund, J.A., Kohlmeier, C., Schnetger, B., and Brumsack, H.-J., 2009. Methane in the southern North Sea: Sources, spatial distribution and budgets. *Estuarine, Coastal and Shelf Science* 81, 445-456.

- Gunnars, A., and Blomqvist, S., 1997. Phosphate exchange across the sediment-water interface when shifting from anoxic to oxic conditions an experimental comparison of freshwater and brackish-marine systems. *Biogeochemistry* 37, 203-226.
- Hagmeier, E., and Bauerfeind, E., 1990. Phytoplankton. In: Lozán J.L., Lenz W., Rachor E., Watermann B., and Westernhagen H.v. (Eds), *Warnsignale aus der Nordsee - Wissenschaftliche Fakten*. Paul Parey, Berlin, p 102-111.
- Hamberg, F., 1996. CEMoS, eine Programmierumgebung zur Simulation komplexer Modelle., Carl von Ossietzky Universität Oldenburg.
- Head, P.C., and Burton, J.D., 1970. Molybdenum in some ocean and estuarine waters. *Journal of the Marine Biological Association of the UK* 50, 439-448.
- Heip, C.H.R., Goosen, N.K., Herman, P.M.J., Kromkamp, J., Middelburg, J.J., and Soetaert, K., 1995. Production and consumption of biological particles in temperate tidal estuaries. In, *Oceanography and Marine Biology - an Annual Review*, Vol 33, p 1-149.
- Helder, W., 1974. The cycle of dissolved inorganic nitrogen compounds in the Dutch wadden sea. *Netherlands Journal of Sea Research* 8, 154-173.
- Helmcke, J.G., 1954. Die Feinstruktur der Kieselsäure und ihre physiologische Bedeutung in Diatomeenschalen. *Naturwissenschaften* 41, 254-255.
- Helz, G.R., Miller, C.V., Charnock, J.M., Mosselmans, J.F.W., Patrick, R.A.D., Garner, C.D., and Vaughan, D.J., 1996. Mechanism of molybdenum removal from the sea and its concentration in black shales: EXAFS evidence. *Geochimica et Cosmochimica Acta* 60, 3631-3642.
- Helz, G.R., Vorlicek, T.P., and Kahn, M.D., 2004. Molybdenum scavenging by iron monosulfide. *Environmental Science & Technology* 38, 4263-4268.
- Hensen, C., Zabel, M., Pfeifer, K., Schwenk, T., Kasten, S., Riedinger, N., Schulz, H.D., and Boettius, A., 2003. Control of sulfate pore-water profiles by sedimentary events and the significance of anaerobic oxidation of methane for the burial of sulfur in marine sediments. *Geochimica et Cosmochimica Acta* 67, 2631-2647.
- Herbert, R.A., 1999. Nitrogen cycling in coastal marine ecosystems. *Fems Microbiology Reviews* 23, 563-590.
- Hickel, W., Mangelsdorf, P., and Berg, J., 1993. The human impact in the German Bight: Eutrophication during three decades (1962–1991). *Helgoland Marine Research* 47, 243-263.

- Hinrichs, J., Dellwig, O., and Brumsack, H.J., 2002. Lead in sediments and suspended particulate matter of the German Bight: natural versus anthropogenic origin. *Applied Geochemistry* 17, 621-632.
- Hoffman, S.J., and Fletcher, W.K., 1981. Organic matter scavenging of copper, zinc, molybdenum, iron and manganese, estimated by a sodium-hypochlorite extraction (pH 9.5). *Journal of Geochemical Exploration* 15, 549-562.
- Hoselmann, C., and Streif, H., 2004. Holocene sea-level rise and its effect on the mass balance of coastal deposits. *Quaternary International* 112, 89-103.
- Hovland, M., Judd, A.G., and Burke, R.A., 1993. The global flux of methane from shallow submarine sediments. *Chemosphere* 26, 559-578.
- Howarth, M.J., Dyer, K.R., Joint, I.R., Hydes, D.J., Purdie, D.A., Edmunds, H., Jones, J.E., Lowry, R.K., Moffat, T.J., Pomroy, A.J., and Proctor, R., 1994. Seasonal cycles and their spatial variability. In: Charnock H., Dyer K.R., Huthnance J.M., Liss P.S., Simpson J.H., and Tett P.B. (Eds), *Understanding the North Sea System*. Chapman & Hall, London (Chapter 2)
- Howarth, R.W., and Jørgensen, B.B., 1984. Formation of S-35-Labeled Elemental Sulfur and Pyrite in Coastal Marine-Sediments (Limfjorden and Kysing Fjord, Denmark) During Short-Term (So₄²⁻-)S-35 Reduction Measurements. *Geochimica et Cosmochimica Acta* 48, 1807-1818.
- Howes, B.L., and Goehring, D.D., 1994. Porewater Drainage and Dissolved Organic-Carbon and Nutrient Losses through the Intertidal Creekbanks of a New-England Salt-Marsh. *Marine Ecology-Progress Series* 114, 289-301.
- Huerta-Diaz, M.A., and Morse, J.W., 1992. Pyritization of trace metals in anoxic marine sediments. *Geochimica et Cosmochimica Acta* 56, 2681-2702.
- Huettel, M., Ziebis, W., and Forster, S., 1996. Flow-induced uptake of particulate matter in permeable sediments. *Limnology and Oceanography* 41, 309-322.
- Huettel, M., Ziebis, W., Forster, S., and Luther, G.W., 1998. Advective transport affecting metal and nutrient distributions and interfacial fluxes in permeable sediments. *Geochimica et Cosmochimica Acta* 62, 613-631.
- Huettel, M., and Rusch, A., 2000. Transport and degradation of phytoplankton in permeable sediment. *Limnology and Oceanography* 45, 534-549.
- Huettel, M., Røy, H., Precht, E., and Ehrenhauss, S., 2003. Hydrodynamical impact on biogeochemical processes in aquatic sediments. *Hydrobiologia* 494, 231-236.
- Huizinga, D., L., and Kester, D.R., 1982. The distribution of vanadium in the Northwestern Atlantic Ocean. *EOS* 63, 990.

- Jähne, B., Munnich, K.O., Bosinger, R., Dutzi, A., Huber, W., and Libner, P., 1987. On the Parameters Influencing Air-Water Gas-Exchange. *Journal of Geophysical Research-Oceans* 92, 1937-1949.
- Jahnke, R.A., Alexander, C.R., and Kostka, J.E., 2003. Advective pore water input of nutrients to the Satilla River Estuary, Georgia, USA. *Estuarine Coastal and Shelf Science* 56, 641-653.
- Jansen, S., Walpersdorf, E., Werner, U., Billerbeck, M., Böttcher, M., and de Beer, D., 2009. Functioning of intertidal flats inferred from temporal and spatial dynamics of O₂, H₂S and pH in their surface sediment. *Ocean Dynamics* 59, 317-332.
- Jensen, H.S., Mortensen, P.B., Andersen, F.O., Rasmussen, E., and Jensen, A., 1995. Phosphorus cycling in a coastal marine sediment, Aarhus Bay, Denmark. *Limnology and Oceanography* 40, 908-917.
- Jensen, K.M., Jensen, M.H., and Kristensen, E., 1996. Nitrification and denitrification in Wadden Sea sediments (Konigshafen, Island of Sylt, Germany) as measured by nitrogen isotope pairing and isotope dilution. *Aquatic Microbial Ecology* 11, 181-191.
- Johannsen, A., Dähnke, K., and Emeis, K., 2008. Isotopic composition of nitrate in five German rivers discharging into the North Sea. *Organic Geochemistry* 39, 1678-1689.
- Jones, R.D., 1991. Carbon-Monoxide and Methane Distribution and Consumption in the Photic Zone of the Sargasso Sea. *Deep-Sea Research Part a-Oceanographic Research Papers* 38, 625-635.
- Jørgensen, B.B., 1982. Mineralization of Organic-Matter in the Sea Bed - the Role of Sulfate Reduction. *Nature* 296, 643-645.
- Kamatani, A., and Riley, J.P., 1979. Rate of dissolution of diatom silica walls in seawater. *Marine Biology* 55, 29-35.
- Kamatani, A., 1982. Dissolution rates of silica from diatoms decomposing at various temperatures. *Marine Biology* 68, 91-96.
- Karl, D.M., and Tilbrook, B.D., 1994. Production and transport of methane in oceanic particulate organic-matter. *Nature* 368, 732-734.
- Kelley, C.A., Martens, C.S., and Ussler, W., 1995. Methane Dynamics across a Tidally Flooded Riverbank Margin. *Limnology and Oceanography* 40, 1112-1129.
- Kim, G., and Hwang, D.W., 2002. Tidal pumping of groundwater into the coastal ocean revealed from submarine Rn-222 and CH₄ monitoring. *Geophysical Research Letters* 29.
- Klinkhammer, G., Heggie, D.T., and Graham, D.W., 1982. Metal diagenesis in oxic marine sediments. *Earth and Planetary Science Letters* 61, 211-219.

- Klinkhammer, G.P., 1980. Early diagenesis in sediments from the Eastern Equatorial Pacific, II. Pore water metal results. *Earth and Planetary Science Letters* 49, 81-101.
- Klinkhammer, G.P., and Palmer, M.R., 1991. Uranium in the oceans - Where it goes and why. *Geochimica et Cosmochimica Acta* 55, 1799-1806.
- Kohlmeier, C., 2004. Modellierung des Spiekerooger Rückseitenwatts mit einem gekoppelten Euler-Lagrange-Modell auf der Basis von ERSEM. Dissertation, Carl von Ossietzky Universität Oldenburg.
- Kohlmeier, C., and Ebenhöf, W., 2007. Modelling the ecosystem dynamics and nutrient cycling of the Spiekeroog back barrier system with a coupled Euler-Lagrange model on the base of ERSEM. *Ecological Modelling* 202, 297-310.
- Kohlmeier, C., and Ebenhöf, W., 2009. Modelling the biogeochemistry of a tidal flat ecosystem with EcoTiM. *Ocean Dynamics* 59, 393-415.
- Kolditz, K., Dellwig, O., Barkowski, J., Beck, M., Freund, H., and Brumsack, H.-J., 2009. Salt marsh restoration: Effects of de-embankment on pore water geochemistry. *Journal of Coastal Research*, in press.
- Koschinsky, A., Winkler, A., and Fritsche, U., 2003. Importance of different types of marine particles for the scavenging of heavy metals in the deep-sea bottom water. *Applied Geochemistry* 18, 693-710.
- Kourtidis, K., Kioutsioukis, I., McGinnis, D.F., and Rapsomanikis, S., 2006. Effects of methane outgassing on the Black Sea atmosphere. *Atmospheric Chemistry and Physics* 6, 5173-5182.
- Kowalski, N., Dellwig, O., Beck, M., Grunwald, M., Fischer, S., Piepho, M., Riedel, T., Freund, H., Brumsack, H.-J., and Böttcher, M., 2009. Trace metal dynamics in the water column and pore waters in a temperate tidal system: response to the fate of algae-derived organic matter. *Ocean Dynamics* 59, 333-350.
- Kristensen, E., Bodenbender, J., Jensen, M.H., Rennenberg, H., and Jensen, K.M., 2000. Sulfur cycling of intertidal Wadden Sea sediments (Konigshafen, Island of Sylt, Germany): sulfate reduction and sulfur gas emission. *Journal of Sea Research* 43, 93-104.
- Krom, M.D., and Berner, R.A., 1980. Adsorption of phosphate in anoxic marine sediments. *Limnology and Oceanography* 25, 797-806.
- Ku, T.L., Knauss, K.G., and Mathieu, G.G., 1977. Uranium in open ocean - Concentration and isotopic composition. *Deep-Sea Research* 24, 1005-1017.

- Kuwae, T., Kibe, E., and Nakamura, Y., 2003. Effect of emersion and immersion on the porewater nutrient dynamics of an intertidal sandflat in Tokyo Bay. *Estuarine Coastal and Shelf Science* 57, 929-940.
- Lacroix, G., Ruddick, K., Gypens, N., and Lancelot, C., 2007. Modelling the relative impact of rivers (Scheldt/Rhine/Seine) and Western Channel waters on the nutrient and diatoms/Phaeocystis distributions in Belgian waters (Southern North Sea). *Continental Shelf Research* 27, 1422-1446.
- Langner-van Voorst, I., and Höpner, T., 1996. Horizontal and vertical inhomogeneity of nutrient concentrations in porewater of an intertidal sandflat (Gröninger Plate, Rückseitenwatt von Spiekeroog, südliche Nordsee). *Senckenbergiana maritima* 26, 179-194.
- Lelieveld, J., Crutzen, P.J., and Bruhl, C., 1993. Climate Effects of Atmospheric Methane. *Chemosphere* 26, 739-768.
- Lemke, A., Lunau, M., Stone, J., Dellwig, O., and Simon, M., 2009. Spatio-temporal dynamics of suspended matter properties and bacterial communities in the back-barrier tidal flat system of Spiekeroog Island. *Ocean Dynamics* 59, 277-290.
- Lenhart, H.-J., and Pätsch, J., 2001. Daily nutrient loads of the European continental rivers for the years 1977-1998. *Berichte aus dem Zentrum für Meeres- und Klimaforschung; Reihe B: Ozeanographie*, No 40, 146pp.
- Lenhart, H.J., Radach, G., and Ruardij, P., 1997. The effects of river input on the ecosystem dynamics in the continental coastal zone of the North Sea using ERSEM. *Journal of Sea Research* 38, 249-274.
- Lewin, J.C., 1961. The dissolution of silica from diatom walls. *Geochimica et Cosmochimica Acta* 21, 182-198.
- Lewin, J.C., 1962. Silicification. In: Lewin R.A. (Ed), *Physiology and Biochemistry of Algae*. Academic Press, New York, p 445-455.
- Lewis, E., and Wallace, D.W.R., 1998. Program developed for CO₂ system calculations. ORNL/CDIAC-105. Carbon Dioxide Information Analysis Center, Oak Ridge National Laboratory, U.S. Department of Energy, Oak Ridge, Tennessee
- Liebezeit, G., Behrends, B., and Kraul, T., 1996. Variability of nutrients and particulate matter in back barrier tidal flats of the East Frisian Wadden Sea. *Senckenbergiana maritima* 26, 195-202.
- Lillington, J.N., 1981. A Vector Upstream Differencing Scheme for Problems in Fluid-Flow Involving Significant Source Terms in Steady-State Linear-Systems. *International Journal for Numerical Methods in Fluids* 1, 3-16.

- Llobet-Brossa, E., Rossello-Mora, R., and Amann, R., 1998. Microbial community composition of Wadden Sea sediments as revealed by fluorescence in situ hybridization. *Applied and Environmental Microbiology* 64, 2691-2696.
- Loebl, M., Dolch, T., and van Beusekom, J.E.E., 2007. Annual dynamics of pelagic primary production and respiration in a shallow coastal basin. *Journal of Sea Research* 58, 269-282.
- Loebl, M., Colijn, F., van Beusekom, J.E.E., Baretta-Bekker, J.G., Lancelot, C., Philippart, C.J.M., Rousseau, V., and Wiltshire, K.H., 2009. Recent patterns in potential phytoplankton limitation along the Northwest European continental coast. *Journal of Sea Research* 61, 34-43.
- Lohse, L., Malschaert, J.F.P., Slomp, C.P., Helder, W., and Vanraaphorst, W., 1993. Nitrogen Cycling in North-Sea Sediments - Interaction of Denitrification and Nitrification in Offshore and Coastal Areas. *Marine Ecology-Progress Series* 101, 283-296.
- Lomstein, E., Jensen, M.H., and Sorensen, J., 1990. Intracellular NH_4^+ and NO_3^- Pools Associated with Deposited Phytoplankton in a Marine Sediment (Aarhus Bight, Denmark). *Marine Ecology-Progress Series* 61, 97-105.
- Long, D., Laban, C., Streif, H., Cameron, T.D.J., and Schuttenhelm, R.T.E., 1988. The Sedimentary Record of Climatic Variation in the Southern North Sea. *Philosophical Transactions of the Royal Society of London Series B-Biological Sciences* 318, 523-537.
- Lovley, D.R., Phillips, E.J.P., Gorby, Y.A., and Landa, E.R., 1991. Microbial reduction of uranium. *Nature* 350, 413-416.
- Lovley, D.R., Roden, E.E., Phillips, E.J.P., and Woodward, J.C., 1993. Enzymatic iron and uranium reduction by sulfate-reducing bacteria. *Marine Geology* 113, 41-53.
- Lubbers, G.W., Gieskes, W.W.C., Delcastilho, P., Salomons, W., and Bril, J., 1990. Manganese accumulation in the high pH microenvironment of *Phaeocystis* sp. (Haptophyceae) colonies from the North Sea *Marine Ecology-Progress Series* 59, 285-293.
- Lunau, M., Lemke, A., Dellwig, O., and Simon, M., 2006. Physical and biogeochemical controls of microaggregate dynamics in a tidally affected coastal ecosystem. *Limnology and Oceanography* 51, 847-859.
- Luther, G.W., III., Shellenbarger, P.A., and Brendel, P.J., 1996. Dissolved organic Fe(III) and Fe(II) complexes in salt marsh porewaters. *Geochimica et Cosmochimica Acta* 60, 951-960.

- Madigan, M.T., Martinko, J.M., and Parker, J., 2003. Brock Biology of Microorganisms. Pearson Education Inc., Upper Saddle River, NJ.
- Maeda, M., and Windom, H.L., 1982. Behavior of uranium in 2 estuaries of the southeastern United-States. *Marine Chemistry* 11, 427-436.
- Magni, P., and Montani, S., 2006. Seasonal patterns of pore-water nutrients, benthic chlorophyll a and sedimentary AVS in a macrobenthos-rich tidal flat. *Hydrobiologia* 571, 297-311.
- Mäkelä, K., and Tuominen, L., 2003. Pore water nutrient profiles and dynamics in soft bottoms of the northern Baltic Sea. *Hydrobiologia* 492, 43-53.
- Marencic, H., Essink, K., Kellermann, A., and Eskildsen, K., 2005. Introduction. In Wadden Sea quality status report 2004 In: Essink K., Dettmann C., Farke H., Laursen K., Lüerßen G., Marencic H., and Wiersinga W. (Eds), Wadden Sea ecosystem No 19 Trilateral monitoring and assessment group. Common Wadden Sea Secretariat (CWSS), Wilhelmshaven, Germany, p 11-25.
- Marinero, G., Etiope, G., Gasparoni, F., Calore, D., Cenedese, S., Furlan, F., Masson, M., Favali, F., and Blandin, J., 2004. GMM - a gas monitoring module for long-term detection of methane leakage from the seafloor. *Environmental Geology* 46, 1053-1058.
- MARNET, 2008. Marines Umweltmessnetz in Nord- und Ostsee. <http://www.bsh.de/de/Meeresdaten/Beobachtungen/MARNET-Messnetz/index.jsp>. Bundesamt für Seeschifffahrt und Hydrographie (BSH), Hamburg, Hamburg, Germany
- Martens, P., 1989. On Trends in Nutrient Concentration in the Northern Wadden Sea of Sylt. *Helgoländer Meeresuntersuchungen* 43, 489-499.
- Martens, P., and Elbrächter, M., 1997. Zeitliche und räumliche Variabilität der Mikronährstoffe und des Phytoplanktons im Sylt-Rømø Wattenmeer. In: Gätje C., and Reise K. (Eds), *Ökosystem Wattenmeer - Austausch-, Transport- und Stoffumwandlungsprozesse*. Springer-Verlag, Heidelberg, Berlin, p 65-79.
- Marty, D.G., 1993. Methanogenic Bacteria in Seawater. *Limnology and Oceanography* 38, 452-456.
- Matthiesen, H., Leipe, T., and Laima, M., 2001. A new experimental setup for studying the formation of phosphate binding iron oxides in marine sediments. Preliminary results. *Biogeochemistry* 52, 79-92.
- Mayer, L.M., 1994. Relationships between mineral surfaces and organic carbon concentrations in soils and sediments. *Chemical Geology* 114, 347-363.

- McManus, J., Nagler, T.F., Siebert, C., Wheat, C.G., and Hammond, D.E., 2002. Oceanic molybdenum isotope fractionation: Diagenesis and hydrothermal ridge-flank alteration. *Geochemistry Geophysics Geosystems* 3,
- Merlivat, L., and Memery, L., 1983. Gas-Exchange across an Air-Water-Interface - Experimental Results and Modeling of Bubble Contribution to Transfer. *Journal of Geophysical Research-Oceans and Atmospheres* 88, 707-724.
- Middelburg, J.J., Hoede, D., Vandersloot, H.A., Vanderweijden, C.H., and Wijkstra, J., 1988. Arsenic, Antimony and Vanadium in the North-Atlantic Ocean. *Geochimica et Cosmochimica Acta* 52, 2871-2878.
- Middelburg, J.J., Klaver, G., Nieuwenhuize, J., Wielemaker, A., deHaas, W., Vlug, T., and vanderNat, J., 1996. Organic matter mineralization in intertidal sediments along an estuarine gradient. *Marine Ecology-Progress Series* 132, 157-168.
- Middelburg, J.J., Nieuwenhuize, J., Iversen, N., Høgh, N., De Wilde, H., Helder, W., Seifert, R., and Christof, O., 2002. Methane distribution in European tidal estuaries. *Biogeochemistry* 59, 95-119.
- Moeslund, L., Thamdrup, B., and Jørgensen, B.B., 1994. Sulfur and Iron Cycling in a Coastal Sediment - Radiotracer Studies and Seasonal Dynamics. *Biogeochemistry* 27, 129-152.
- Morford, J.L., Emerson, S.R., Breckel, E.J., and Kim, S.H., 2005. Diagenesis of oxyanions (V, U, Re, and Mo) in pore waters and sediments from a continental margin. *Geochimica et Cosmochimica Acta* 69, 5021-5032.
- Morford, J.L., Martin, W.R., Kalnejais, L.H., Francois, R., Bothner, M., and Karle, I.M., 2007. Insights on geochemical cycling of U, Re and Mo from seasonal sampling in Boston Harbor, Massachusetts, USA. *Geochimica et Cosmochimica Acta* 71, 895-917.
- Morris, A.W., and Riley, J.P., 1963. The determination of nitrate in sea water. *Analytica Chimica Acta* 29, 272-279.
- Morris, A.W., 1975. Dissolved molybdenum and vanadium in Northeast Atlantic Ocean. *Deep-Sea Research* 22, 49-54.
- Morris, A.W., Mantoura, R.F.C., Bale, A.J., and Howland, R.J.M., 1978. Very Low Salinity Regions of Estuaries - Important Sites for Chemical and Biological Reactions. *Nature* 274, 678-680.
- Murphy, J., and Riley, J.P., 1962. A modified single solution method for the determination of phosphate in natural waters. *Analytica Chimica Acta* 26, 31-&.

- Murray, L.G., Mudge, S.M., Newton, A., and Icely, J.D., 2006. The effect of benthic sediments on dissolved nutrient concentrations and fluxes. *Biogeochemistry* 81, 159-178.
- Nelson, D.M., Treguer, P., Brzezinski, M.A., Leynaert, A., and Queguiner, B., 1995. Production and dissolution of biogenic silica in the ocean: Revised global estimates, comparison with regional data and relationship to biogenic sedimentation. *Global Biogeochemical Cycles* 9, 359-372.
- Neubert, N., Nagler, T.F., and Böttcher, M.E., 2008. Sulfidity controls molybdenum isotope fractionation into euxinic sediments: Evidence from the modern Black Sea. *Geology* 36, 775-778.
- Nico, P.S., Anastasio, C., and Zasoski, R.J., 2002. Rapid photo-oxidation of Mn(II) mediated by humic substances. *Geochimica et Cosmochimica Acta* 66, 4047-4056.
- Nies, H., 1990. Radioaktive Substanzen. In: Lozán J.L., Lenz W., Rachor E., Watermann B., and von Westernhagen H. (Eds), *Warnsignale aus der Nordsee*. Verlag Paul Parey, Berlin; Hamburg, p 87-100.
- Niewöhner, C., Hensen, C., Kasten, S., Zabel, M., and Schulz, H.D., 1998. Deep sulfate reduction completely mediated by anaerobic methane oxidation in sediments of the upwelling area off Namibia. *Geochimica et Cosmochimica Acta* 62, 455-464.
- Nissenbaum, A., and Swaine, D.J., 1976. Organic matter-metal interactions in recent sediments: the role of humic substances. *Geochimica et Cosmochimica Acta* 40, 809-816.
- Nixon, S.W., Oviatt, C.A., and Hale, S.S., 1976. Nitrogen regeneration and the metabolism of coastal marine bottom communities. In: Anderson J.M., and Mcfadyen A. (Eds), *The role of terrestrial and aquatic organisms in decomposition processes*. Blackwell Scientific, Oxford, p 269-283.
- Nixon, S.W., 1990. Marine Eutrophication - a Growing International Problem. *Ambio* 19, 101-101.
- Oremland, R.S., Miller, L.G., and Whiticar, M.J., 1987. Sources and flux of natural gases from Mono Lake, California. *Geochimica et Cosmochimica Acta* 51, 2915-2929.
- OSPAR Commission, 2000. Quality Status Report 2000. Region II - Greater North Sea, OSPAR Commission, London, 136 + XIII pp.
- Paasche, E., 1973. Silicon and the ecology of marine plankton diatoms. I. *Thalassiosira pseudonana* (*Cyclotella nana*) grown in a chemostat with silicate as limiting nutrient. *Marine Biology* 19, 117-126.

- Passow, U., 2002. Production of transparent exopolymer particles (TEP) by phyto- and bacterioplankton. *Marine Ecology-Progress Series* 236, 1-12.
- Pätsch, J., and Kühn, W., 2008. Nitrogen and carbon cycling in the North Sea and exchange with the North Atlantic--A model study. Part I. Nitrogen budget and fluxes. *Continental Shelf Research* 28, 767-787.
- Patton, C.J., and Crouch, S.R., 1977. Spectrophotometric and Kinetics Investigation of Berthelot Reaction for Determination of Ammonia. *Analytical Chemistry* 49, 464-469.
- Peeters, J.C.H., Haas, H., Peperzak, L., and Wetsteyn, L., 1991. Limiting factors for phytoplankton in the North Sea. *Water Science and Technology* 24, 261-267.
- Pethick, J., 1984. *An Introduction to Coastal Geomorphology*. Edward Arnold, London.
- Philippart, C., Beukema, J., Cadée, G., Dekker, R., Goedhart, P., van Iperen, J., Leopold, M., and Herman, P., 2007. Impacts of Nutrient Reduction on Coastal Communities. *Ecosystems* 10, 96-119.
- Philippart, C.J.M., Cadee, G.C., van Raaphorst, W., and Riegman, R., 2000. Long-term phytoplankton-nutrient interactions in a shallow coastal sea: Algal community structure, nutrient budgets, and denitrification potential. *Limnology and Oceanography* 45, 131-144.
- Ploug, H., Kuhl, M., Buchholz-Cleven, B., and Jørgensen, B.B., 1997. Anoxic aggregates - an ephemeral phenomenon in the pelagic environment? *Aquatic Microbial Ecology* 13, 285-294.
- Postma, H., 1954. Hydrography of the Dutch Wadden Sea. *Archives Néerlandaises de Zoologie* 10, 405-511.
- Postma, H., 1961. Transport and accumulation of suspended matter in the Dutch Wadden Sea. *Netherlands Journal of Sea Research* 1, 148-180.
- Postma, H., 1981. Exchange of materials between the North Sea and the Wadden Sea. *Marine Geology* 40, 199-213.
- Poulton, S.W., 2003. Sulfide oxidation and iron dissolution kinetics during the reaction of dissolved sulfide with ferrihydrite. *Chemical Geology* 202, 79-94.
- Precht, E., and Huettel, M., 2003. Advective pore-water exchange driven by surface gravity waves and its ecological implications. *Limnology and Oceanography* 48, 1674-1684.
- Precht, E., Franke, U., Polerecky, L., and Huettel, M., 2004. Oxygen dynamics in permeable sediments with wave-driven pore water exchange. *Limnology and Oceanography* 49, 693-705.
- Precht, E., and Huettel, M., 2004. Rapid wave-driven advective pore water exchange in a permeable coastal sediment. *Journal of Sea Research* 51, 93-107.

- Pulliam, W.M., 1993. Carbon-Dioxide and Methane Exports from a Southeastern Floodplain Swamp. *Ecological Monographs* 63, 29-53.
- Raabe, T.U., Brockmann, U.H., Dürselen, C.D., Krause, M., and Rick, H.J., 1997. Nutrient and plankton dynamics during a spring drift experiment in the German Bight. *Marine Ecology-Progress Series* 156, 275-288.
- Radach, G., and Pätsch, J., 2007. Variability of continental riverine freshwater and nutrient inputs into the North Sea for the years 1977-2000 and its consequences for the assessment of eutrophication. *Estuaries and Coasts* 30, 66-81.
- Redfield, A.C., 1958. The biological control of chemical factors in the environment. *American Scientist* 46, 205-222.
- Rehder, G., Keir, R.S., Suess, E., and Pohlmann, T., 1998. The multiple sources and patterns of methane in North Sea waters. *Aquatic Geochemistry* 4, 403-427.
- Reid, P.C., Lancelot, C., Gieskes, W.W.C., Hagmeier, E., and Weichart, G., 1990. Phytoplankton of the North Sea and its dynamics: A review. *Netherlands Journal of Sea Research* 26, 295-331.
- Reise, K., 2005. Coast of change: habitat loss and transformations in the Wadden Sea. *Helgoland Marine Research* 59, 9-21.
- Reuter, R., Badewien, T., Bartholomä, A., Braun, A., Lübben, A., and Rullkötter, J., 2009. A hydrographic time series station in the Wadden Sea (southern North Sea). *Ocean Dynamics* 59, 195-211.
- Rodushkin, I., and Ruth, T., 1997. Determination of trace metals in estuarine and sea-water reference materials by high resolution inductively coupled plasma mass spectrometry. *Journal of Analytical Atomic Spectrometry* 12, 1181-1185.
- Roitz, J.S., Flegal, A.R., and Bruland, K.W., 2002. The biogeochemical cycling of manganese in San Francisco Bay: Temporal and spatial variations in surface water concentrations. *Estuarine Coastal and Shelf Science* 54, 227-239.
- Roulet, N., Moore, T., Bubier, J., and Lafleur, P., 1992a. Northern Fens - Methane Flux and Climatic-Change. *Tellus Series B-Chemical and Physical Meteorology* 44, 100-105.
- Roulet, N.T., Ash, R., and Moore, T.R., 1992b. Low Boreal Wetlands as a Source of Atmospheric Methane. *Journal of Geophysical Research-Atmospheres* 97, 3739-3749.
- Røy, H., Lee, J.S., Jansen, S., and de Beer, D., 2008. Tide-driven deep pore-water flow in intertidal sand flats. *Limnology and Oceanography* 53, 1521-1530.
- Rupert, D., Aden, L., and Maarfeld, S., 2004. Ermittlung von Abflüssen über Siel und Pumpmengen in Ostfriesland. *Niedersächsischer Landesbetrieb für Wasserwirtschaft*

- und Küstenschutz, Betriebsstelle Aurich, Geschäftsbereich 3, Quantitative Hydrologie, p 101.
- Rusch, A., Topken, H., Böttcher, M.E., and Hopner, T., 1998. Recovery from black spots: results of a loading experiment in the Wadden Sea. *Journal of Sea Research* 40, 205-219.
- Rusch, A., Huettel, M., and Forster, S., 2000. Particulate Organic Matter in Permeable Marine Sands--Dynamics in Time and Depth. *Estuarine, Coastal and Shelf Science* 51, 399-414.
- Rusch, A., and Huettel, M., 2000. Advective particle transport into permeable sediments - evidence from experiments in an intertidal sandflat. *Limnology and Oceanography* 45, 525-533.
- Rusch, A., Forster, S., and Huettel, M., 2001. Bacteria, diatoms and detritus in an intertidal sandflat subject to advective transport across the water-sediment interface. *Biogeochemistry* 55, 1-27.
- Rusch, A., Huettel, M., Reimers, C.E., Taghon, G.L., and Fuller, C.M., 2003. Activity and distribution of bacterial populations in Middle Atlantic Bight shelf sands. *Fems Microbiology Ecology* 44, 89-100.
- Rusch, A., Huettel, M., Wild, C., and Reimers, C.E., 2006. Benthic oxygen consumption and organic matter turnover in organic-poor, permeable shelf sands. *Aquatic Geochemistry* 12, 1-19.
- Rutgers van der Loeff, M.M., van Es, F.B., Helder, W., and de Vries, R.T.P., 1981. Sediment water exchanges of nutrients and oxygen on tidal flats in the EMS-Dollard estuary. *Netherlands Journal of Sea Research* 15, 113-129.
- Ryther, J.H., Menzel, D.W., Hulburt, E.M., Lorenzen, C.J., and Corwin, N., 1971. Production and utilization of organic matter in Peru Coastal Current. *Investigacion Pesquera* 35, 43-&.
- Sarazin, G., Michard, G., and Prevot, F., 1999. A rapid and accurate spectroscopic method for alkalinity measurements in sea water samples. *Water Research* 33, 290-294.
- Sass, R.L., Fisher, F.M., Harcombe, P.A., and Turner, F.T., 1990. Methane Production And Emission in a Texas Rice Field. *Global Biogeochemical Cycles* 4, 47-68.
- Sawlan, J.J., and Murray, J.W., 1983. Trace metal remobilization in the interstitial waters of red clay and hemipelagic marine sediments. *Earth and Planetary Science Letters* 64, 213-230.
- Schlesinger, W.H., 1997. *Biogeochemistry: An Analysis of Global Change*. 2nd edition. Academic Press, San Diego, CA.

- Schnetger, B., Hinrichs, J., Dellwig, O., Shaw, T., and Brumsack, H.-J., 2001. The significance of radionuclides and trace elements in a back barrier tidal area: results from the German Wadden Sea. In: Inaba J., Hisamatsu S., and Ohtsuka Y. (Eds), *Distribution and Speciation of Radionuclides in the Environment Proceedings of the International Workshop on Distribution and Speciation of Radionuclides in the Environment*, Rokkasho, Aomori, Japan, October 2000, p 99-106.
- Schoemann, V., de Baar, H.J.W., de Jong, J.T.M., and Lancelot, C., 1998. Effects of phytoplankton blooms on the cycling of manganese and iron in coastal waters. *Limnology and Oceanography* 43, 1427-1441.
- Scranton, M.I., and McShane, K., 1991. Methane Fluxes in the Southern North-Sea - the Role of European Rivers. *Continental Shelf Research* 11, 37-52.
- Seitzinger, S., and Giblin, A., 1996. Estimating denitrification in North Atlantic continental shelf sediments. *Biogeochemistry* 35, 235-260.
- Shaw, T.J., Sholkovitz, E.R., and Klinkhammer, G., 1994. Redox dynamics in the Chesapeake Bay: The effect on sediment/water uranium exchange. *Geochimica et Cosmochimica Acta* 58, 2985-2995.
- Shiller, A.M., and Boyle, E.A., 1991. Trace elements in the Mississippi River Delta outflow region: Behavior at high discharge. *Geochimica et Cosmochimica Acta* 55, 3241-3251.
- Shiller, A.M., 1996. The effect of recycling traps and upwelling on estuarine chemical flux estimates. *Geochimica et Cosmochimica Acta* 60, 3177-3185.
- Shiller, A.M., 1997. Manganese in surface waters of the Atlantic Ocean. *Geophysical Research Letters* 24, 1495-1498.
- Shiller, A.M., and Mao, L.J., 1999. Dissolved vanadium on the Louisiana Shelf: effect of oxygen depletion. *Continental Shelf Research* 19, 1007-1020.
- Shinn, J.A., 1941. *A Practical Handbook of Seawater Analysis*. Fisheries Research Board Canadian Bulletin, Canada.
- Sholkovitz, E., 1973. Interstitial Water Chemistry of Santa Barbara Basin Sediments. *Geochimica et Cosmochimica Acta* 37, 2043-2073.
- Slomp, C.P., Van der Gaast, S.J., and Van Raaphorst, W., 1996. Phosphorus binding by poorly crystalline iron oxides in North Sea sediments. *Marine Chemistry* 52, 55-73.
- Slomp, C.P., Malschaert, J.F.P., Lohse, L., and Van Raaphorst, W., 1997. Iron and manganese cycling in different sedimentary environments on the North Sea continental margin. *Continental Shelf Research* 17, 1083-1117.

- Smetacek, V., and Passow, U., 1990. Spring bloom initiation and Sverdrup's critical-depth model. *Limnology and Oceanography* 35, 228-234.
- Smith, S.V., and Hollibaugh, J.T., 1993. Coastal Metabolism and the Oceanic Organic-Carbon Balance. *Reviews of Geophysics* 31, 75-89.
- Soetaert, K., Middelburg, J.J., Heip, C., Meire, P., Van Damme, S., and Maris, T., 2006. Long-term change in dissolved inorganic nutrients in the heterotrophic Scheldt estuary (Belgium, The Netherlands). *Limnology and Oceanography* 51, 409-423.
- Sørensen, J., Christensen, D., and Jørgensen, B.B., 1981. Volatile Fatty-Acids and Hydrogen as Substrates for Sulfate-Reducing Bacteria in Anaerobic Marine Sediment. *Applied and Environmental Microbiology* 42, 5-11.
- Stanev, E.V., Wolff, J.-O., Burchard, H., Bolding, K., and Flöser, G., 2003. On the circulation in the East Frisian Wadden Sea: numerical modelling and data analysis. *Ocean Dynamics* 53, 27-51.
- Stanev, E.V., Flemming, B.W., Bartholomä, A., Staneva, J.V., and Wolff, J.-O., 2007. Vertical circulation in shallow tidal inlets and back-barrier basins. *Continental Shelf Research* 27, 798-831.
- Staneva, J., Stanev, E.V., Wolff, J.-O., Badewien, T.H., Reuter, R., Flemming, B., Bartholomä, A., and Bolding, K., 2009. Hydrodynamics and sediment dynamics in the German Bight. A focus on observations and numerical modelling in the East Frisian Wadden Sea. *Continental Shelf Research* 29, 302-319.
- Statham, P.J., Yeats, P.A., and Landing, W.M., 1998. Manganese in the eastern Atlantic Ocean: processes influencing deep and surface water distributions. *Marine Chemistry* 61, 55-68.
- Stevens, H., Brinkhoff, T., and Simon, M., 2005. Composition of free-living, aggregate-associated and sediment surface-associated bacterial communities in the German Wadden Sea. *Aquatic Microbial Ecology* 38, 15-30.
- Stolte, W., McCollin, T., Noordeloos, A.A.M., and Riegman, R., 1994. Effect of nitrogen source on the size distribution within marine phytoplankton populations. *Journal of Experimental Marine Biology and Ecology* 184, 83-97.
- Streif, H., 1990. *Das ostfriesische Wattenmeer. Nordsee, Inseln, Watten und Marschen.* Gebrüder Borntraeger, Berlin.
- Strickland, J.D.H., and Parsons, T.R., 1968. Determination of reactive nitrate. In: *A Practical Handbook of Seawater Analysis.* In, *A Practical Handbook of Seawater Analysis.* Fisheries Research Board of Canada Bulletin, Canada, p 71-75.

- Szalay, A., and Szilagyi, M., 1967. Association of vanadium with humic acids. *Geochimica et Cosmochimica Acta* 31, 1-6.
- Szilagyi, M., 1967. Sorption of molybdenum by humus preparations. *Geochemistry International* 4, 1165-1167.
- Tabatabai, M.A., 1974. Determination of sulphate in water samples. *Sulphur Institute Journal* 10, 11-13.
- Tappin, A.D., Millward, G.E., Statham, P.J., Burton, J.D., and Morris, A.W., 1995. Trace-Metals in the Central and Southern North-Sea. *Estuarine Coastal and Shelf Science* 41, 275-323.
- Thamdrup, B., Finster, K., Hansen, J.W., and Bak, F., 1993. Bacterial disproportionation of elemental sulfur coupled to chemical reduction of iron or manganese. *Applied and Environmental Microbiology* 59, 101-108.
- Thamdrup, B., and Canfield, D.E., 1996. Pathways of carbon oxidation in continental margin sediments off central Chile. *Limnology and Oceanography* 41, 1629-1650.
- The Common Wadden Sea Secretariat (CWSS), 2009. <http://www.waddensea-secretariat.org/>
- Tillmann, U., Hesse, K.J., and Colijn, F., 2000. Planktonic primary production in the German Wadden Sea. *Journal of Plankton Research* 22, 1253-1276.
- Townsend, D.W., Cammen, L.M., Holligan, P.M., Campbell, D.E., and Pettigrew, N.R., 1994. Causes and consequences of variability in the timing of spring phytoplankton blooms. *Deep Sea Research Part I: Oceanographic Research Papers* 41, 747-765.
- Trouwborst, R.E., Clement, B.G., Tebo, B.M., Glazer, B.T., and Luther, G.W., 2006. Soluble Mn(III) in suboxic zones. *Science* 313, 1955-1957.
- Tuit, C.B., and Ravizza, G., 2003. The marine distribution of molybdenum, 13th Annual VM Goldschmidt Conference, Kurashiki, Japan, p A495-A495.
- Turner, R.E., Rabalais, N.N., Justic, D., and Dortch, Q., 2003. Global patterns of dissolved N, P and Si in large rivers. *Biogeochemistry* 64, 297-317.
- Umweltbundesamt (Ed) 2004. Gesamtsynthese Ökosystemforschung Wattenmeer. Zusammenfassender Bericht zu Forschungsergebnissen und Systemschutz im deutschen Wattenmeer. UBAFBNr 000190, Förderkennzeichen 296 85 905. Selbstverlag, Berlin, 481 pp.
- Upstill-Goddard, R.C., Barnes, J., Frost, T., Punshon, S., and Owens, N.J.P., 2000. Methane in the southern North Sea: Low-salinity inputs, estuarine removal, and atmospheric flux. *Global Biogeochemical Cycles* 14, 1205-1217.
- Upstill-Goddard, R.C., 2006. Air-sea gas exchange in the coastal zone. *Estuarine, Coastal and Shelf Science* 70, 388-404.

- Utermöhl, H., 1958. Zur Vervollkommnung der quantitativen Phytoplankton-Methodik. *Mitteilungen Internationale Vereinigung Theoretische und Angewandte Limnologie* 9, 1-38.
- van Bennekom, A.J., Krijgsman-Van Hartingsveld, E., Van der Veer, G.C.M., and Van Voorst, H.F.J., 1974. The seasonal cycles of reactive silicate and suspended diatoms in the Dutch Wadden Sea. *Netherlands Journal of Sea Research* 8, 174-207.
- van Bennekom, A.J., and Wetsteijn, F.J., 1990. The winter distribution of nutrients in the Southern Bight of the North Sea (1961-1978) and in the estuaries of the scheldt and the rhine/meuse. *Netherlands Journal of Sea Research* 25, 75-87.
- van Beusekom, J.E.E., and de Jonge, V., 1997. Transformation of phosphorus in the wadden sea: Apatite formation. *Ocean Dynamics* 49, 297-305.
- van Beusekom, J.E.E., and de Jonge, V.N., 1998. Retention of phosphorus and nitrogen in the Ems estuary. *Estuaries* 21, 527-539.
- van Beusekom, J.E.E., Brockmann, U., Hesse, K., Hickel, W., Poremba, K., and Tillmann, U., 1999. The importance of sediments in the transformation and turnover of nutrients and organic matter in the Wadden Sea and German Bight. *Ocean Dynamics* 51, 245-266.
- van Beusekom, J.E.E., Fock, H., de Jong, F., Diel-Christiansen, S., and Christiansen, B., 2001. Wadden Sea Specific Eutrophication Criteria. Wadden Sea Ecosystem No. 14. Common Wadden Sea Secretariat, Wilhelmshaven, Germany,
- van Beusekom, J.E.E., and de Jonge, V.N., 2002. Long-term changes in Wadden Sea nutrient cycles: importance of organic matter import from the North Sea. *Hydrobiologia* 475, 185-194.
- van Beusekom, J.E.E., 2005. A historic perspective on Wadden Sea eutrophication. *Helgoland Marine Research* 59, 45-54.
- van Beusekom, J.E.E., and Reise, K., 2008. Long-term ecological change in the northern Wadden Sea. *Helgoland Marine Research* 62, 1-2.
- van Beusekom, J.E.E., and Diel-Christiansen, S., 2009. Global change and the biogeochemistry of the North Sea: the possible role of phytoplankton and phytoplankton grazing. *International Journal of Earth Sciences* 98, 269-280.
- van der Nat, F.J., and Middelburg, J.J., 2000. Methane emission from tidal freshwater marshes. *Biogeochemistry* 49, 103-121.
- van der Zee, C., and Chou, L., 2005. Seasonal cycling of phosphorus in the southern bight of the North Sea. *Biogeosciences* 2, 27-42.
- van Raaphorst, W., and Kloosterhuis, H.T., 1994. Phosphate sorption in superficial intertidal sediments. *Marine Chemistry* 48, 1-16.

- van Raaphorst, W., and de Jonge, V.N., 2004. Reconstruction of the total N and P inputs from the IJsselmeer into the western Wadden Sea between 1935-1998. *Journal of Sea Research* 51, 109-131.
- Villbrandt, M., Hild, A., and Dittmann, S., 1999. Biogeochemical processes in tidal flat sediments and mutual interactions with macrobenthos. In: Dittmann S. (Ed), *The Wadden Sea Ecosystem*. Springer-Verlag, p 95-132.
- Volkenborn, N., Polerecky, L., Hedtkamp, S.I.C., van Beusekom, J.E.E., and de Beer, D., 2007. Bioturbation and bioirrigation extend the open exchange regions in permeable sediments. *Limnology and Oceanography* 52, 1898-1909.
- von Langen, P.J., Johnson, K.S., Coale, K.H., and Elrod, V.A., 1997. Oxidation kinetics of manganese (II) in seawater at nanomolar concentrations. *Geochimica et Cosmochimica Acta* 61, 4945-4954.
- Vorliceck, T.P., and Helz, G.R., 2002. Catalysis by mineral surfaces: Implications for Mo geochemistry in anoxic environments. *Geochimica et Cosmochimica Acta* 66, 3679-3692.
- Vorliceck, T.P., Kahn, M.D., Kasuya, Y., and Helz, G.R., 2004. Capture of molybdenum in pyrite-forming sediments: Role of ligand-induced reduction by polysulfides. *Geochimica et Cosmochimica Acta* 68, 547-556.
- Vosjan, J.H., 1974. Sulphate in water and sediment of the Dutch Wadden Sea, 8. *Netherlands Journal of Sea Research*
- Walther, F., 1972. Zusammenhänge zwischen der Größe der ostfriesischen Seegaten mit ihren Wattgebieten sowie den Gezeiten und Strömungen. *Jahresbericht 1971, Forschungsstelle für Insel- und Küstenschutz, Norderney Bd.23*.
- Wanninkhof, R., 1992. Relationship between Wind-Speed and Gas-Exchange over the Ocean. *Journal of Geophysical Research-Oceans* 97, 7373-7382.
- Wanty, R.B., and Goldhaber, M.B., 1992. Thermodynamics and kinetics of reactions involving vanadium in natural systems: Accumulation of vanadium in sedimentary rocks. *Geochimica et Cosmochimica Acta* 56, 1471-1483.
- Ward, B.B., Kilpatrick, K.A., Novelli, P.C., and Scranton, M.I., 1987. Methane Oxidation and Methane Fluxes in the Ocean Surface-Layer and Deep Anoxic Waters. *Nature* 327, 226-229.
- Wasylenki, L.E., Rolfe, B.A., Weeks, C.L., Spiro, T.G., and Anbar, A.D., 2008. Experimental investigation of the effects of temperature and ionic strength on Mo isotope fractionation during adsorption to manganese oxides. *Geochimica et Cosmochimica Acta* 72, 5997-6005.

- Wedepohl, K.H., 1971. Environmental influence on the chemical composition of shales and clays. In: Ahrens L.H., Press F., Runcorn S.K., and Urey H.C. (Eds), *Physics and Chemistry of the Earth*. Pergamon, Oxford, p 305-333.
- Wehrli, B., and Stumm, W., 1989. Vanadyl in natural waters - Adsorption and hydrolysis promote oxygenation. *Geochimica et Cosmochimica Acta* 53, 69-77.
- Werner, U., Billerbeck, M., Polerecky, L., Franke, U., Huettel, M., van Beusekom, J.E.E., and de Beer, D., 2006. Spatial and temporal patterns of mineralization rates and oxygen distribution in a permeable intertidal sand flat (Sylt, Germany). *Limnology and Oceanography* 51, 2549-2563.
- Weston, N.B., Porubsky, W.P., Samarkin, V.A., Erickson, M., Macavoy, S.E., and Joye, S.B., 2006. Porewater stoichiometry of terminal metabolic products, sulfate, and dissolved organic carbon and nitrogen in estuarine intertidal creek-bank sediments. *Biogeochemistry* 77, 375-408.
- Whiting, G.J., and Childers, D.L., 1989. Subtidal Advective Water Flux as a Potentially Important Nutrient Input to Southeastern USA Saltmarsh Estuaries. *Estuarine Coastal and Shelf Science* 28, 417-431.
- Wiesenburg, D.A., and Guinasso, N.L., Jr., 1979. Equilibrium Solubilities of Methane, Carbon-Monoxide, and Hydrogen in Water and Sea-Water. *Journal of Chemical and Engineering Data* 24, 356-360.
- Wilms, R., Sass, H., Köpke, B., Köster, H., Cypionka, H., and Engelen, B., 2006a. Specific bacterial, archaeal, and eukaryotic communities in tidal-flat sediments along a vertical profile of several meters. *Applied and Environmental Microbiology* 72, 2756-2764.
- Wilms, R., Köpke, B., Sass, H., Chang, T.S., Cypionka, H., and Engelen, B., 2006b. Deep biosphere-related bacteria within the subsurface of tidal flat sediments. *Environmental Microbiology* 8, 709-719.
- Wilms, R., Sass, H., Köpke, B., Cypionka, H., and Engelen, B., 2007. Methane and sulfate profiles within the subsurface of a tidal flat are reflected by the distribution of sulfate-reducing bacteria and methanogenic archaea. *Fems Microbiology Ecology* 59, 611-621.
- Wilson, A.M., and Gardner, L.R., 2006. Tidally driven groundwater flow and solute exchange in a marsh: Numerical simulations. *Water Resources Research* 42,
- Wiltshire, K.H., and Manly, B.F.J., 2004. The warming trend at Helgoland Roads, North Sea: Phytoplankton response. *Helgoland Marine Research* 58, 269-273.
- Wiltshire, K.H., Malzahn, A.M., Wirtz, K., Greve, W., Janisch, S., Mangelsdorf, P., Manly, B.F.J., and Boersma, M., 2008. Resilience of North Sea phytoplankton spring bloom

- dynamics: An analysis of long-term data at Helgoland Roads. *Limnology and Oceanography* 53, 1294-1302.
- Wirtz, K.W., 2003. Control of biogeochemical cycling by mobility and metabolic strategies of microbes in the sediments: an integrated model study. *Fems Microbiology Ecology* 46, 295-306.
- Withers, P.J.A., and Jarvie, H.P., 2008. Delivery and cycling of phosphorus in rivers: A review. *Science of The Total Environment* 400, 379-395.
- Yamazaki, H., and Gohda, S., 1990. Distribution of dissolved molybdenum in the Seto Inland Sea, the Japan Sea, the Bering Sea and the Northwest Pacific-Ocean. *Geochemical Journal* 24, 273-281.
- Zheng, Y., Anderson, R.F., van Geen, A., and Fleisher, M.Q., 2002. Remobilization of authigenic uranium in marine sediments by bioturbation. *Geochimica et Cosmochimica Acta* 66, 1759-1772.
- Ziebis, W., Huettel, M., and Forster, S., 1996. Impact of biogenic sediment topography on oxygen fluxes in permeable seabeds. *Marine Ecology-Progress Series* 140, 227-237.

Acknowledgements / Danksagung

Ich möchte mich bei allen bedanken, die mir während der Zeit meiner Doktorarbeit zur Seite standen und zum Gelingen dieser Arbeit beigetragen haben.

Prof. Dr. H.-J. Brumsack ermöglichte mir, in seiner Arbeitsgruppe an den hier dargestellten interessanten und vielfältigen Themen zu arbeiten und gab mir jederzeit die Freiheit und das Vertrauen, Ideen eigenverantwortlich umzusetzen. Für die fortwährende Unterstützung und interessanten Diskussionen bin ich ihm sehr dankbar.

Prof. Dr. J. Rullkötter möchte ich für die Leitung der Forschergruppe „BioGeoChemie des Watts“, in deren Rahmen diese Arbeit entstanden ist, und für die Bereitschaft zur Erstellung des Zweitgutachtens danken.

Mein besonderer Dank gilt Olaf Dellwig, der durch stetige Diskussion und konstruktive Kritik maßgeblich zum Gelingen dieser Arbeit beigetragen hat. Danke auch für die interessanten zahlreichen Schiffseinsätze, die wir zusammen mit anderen Mitgliedern der Forschergruppe erlebt haben.

Bernhard (Barnie) Schnetger danke ich für seine unermüdliche Diskussionsbereitschaft bei analytischen Fragestellungen.

Ich danke allen Mitarbeitern der Arbeitsgruppe Mikrobiogeochemie für die schöne Zeit am ICBM. Danke Eleonore (Eli) Gründken, Carola Lehnert und Martina Wagner für die Hilfsbereitschaft im Labor und Alexander (Josi) Josefowicz für das unkomplizierte und schnelle Erfüllen von Literaturwünschen. Melanie Beck danke ich für die Betreuung der Nährstoffmessungen nach meinem Ausscheiden aus dem ICBM.

Waldemar Siewert danke ich für die Weiterführung der Wartungsarbeiten auf der Messstation.

Danke auch an die Arbeitsgruppe Meeresphysik, die mich bei den Arbeiten auf der Messstation unterstützt haben.

Mein Dank gilt auch Friedhelm Schroeder und seiner gesamten Arbeitsgruppe bei der GKSS. Sie gaben mir die Möglichkeit, diese Arbeit fertig zu stellen.

Nicht zuletzt möchte ich meinen Eltern für die große Unterstützung während der gesamten Zeit herzlich danken.

Diese Arbeit wurde von der Deutschen Forschungsgemeinschaft (DFG) in Rahmen der „Forschergruppe BioGeoChemie des Watts“ (FOR 432) gefördert.

Curriculum vitae

Name: Maik Grunwald
Geburtsdatum: 02. Juni 1972
Geburtsort: Cloppenburg
Staatsangehörigkeit: deutsch
Familienstand: ledig

Schulbildung

1978 – 1979 Grundschule, Cloppenburg
1979 – 1982 Grundschule, Barßel
1982 – 1984 Orientierungsstufe, Barßel
1984 – 1991 Albertus-Magnus-Gymnasium, Friesoythe

Studium

1991 – 2002 Studium der Chemie (Diplom)
an der Carl von Ossietzky Universität Oldenburg
Diplom: 18. Dezember 2002
Thema der Diplomarbeit: *„Anorganisch-geochemische
Charakterisierung von Auftriebsedimenten der Chilenischen Küste“*

seit April 2003 Promotionsstudium an der Fakultät für Mathematik und
Naturwissenschaften der Carl von Ossietzky Universität Oldenburg

Berufstätigkeit

04/2003 – 12/2006 Wissenschaftlicher Mitarbeiter in der Arbeitsgruppe
„Mikrobiogeochemie“, ICBM

04/2007 – 10/2007 Wissenschaftliche Hilfskraft in der Arbeitsgruppe
„Mikrobiogeochemie“, ICBM

seit 11/2007 Wissenschaftlicher Mitarbeiter in der Arbeitsgruppe „in-situ-
Verfahren“ beim GKSS Forschungszentrum Geesthacht, Institut für
Küstenforschung

Erklärung

Hiermit versichere ich, dass ich die vorliegende Arbeit selbstständig angefertigt und keine anderen als die angegebenen Quellen und Hilfsmittel verwendet habe. Zusätzlich erkläre ich, dass diese Dissertation weder in ihrer Gesamtheit noch in Teilen einer anderen wissenschaftlichen Hochschule zur Begutachtung in einem Promotionsverfahren vorliegt oder vorgelegen hat.

Geesthacht, im Juni 2009

Maik Grunwald